UC Irvine
UC Irvine Electronic Theses and Dissertations

Title

Investigations of Nickel-Catalyzed Coupling Reactions: Development of New Methods and Structure-Reactivity Relationships

Permalink

https://escholarship.org/uc/item/2c07q1gz

Author

Herbert, Claire Anna

Publication Date

2024

Peer reviewed|Thesis/dissertation

eScholarship.org Powered by the California Digital Library
University of California

UNIVERSITY OF CALIFORNIA,
IRVINE

Investigations of Nickel-Catalyzed Coupling Reactions: Development of New Methods and Structure-Reactivity Relationships

DISSERTATION

submitted in partial satisfaction of the requirements
for the degree of

DOCTOR OF PHILOSOPHY

in Chemistry

by

Claire A. Herbert

Dissertation Committee:
Professor Elizabeth R. Jarvo, Chair
Professor Suzanne A. Blum
Professor Scott D. Rychnovsky

2024

Chapter 1 © 2023 American Chemical Society
Chapter 2 © 2021 MDPI
Chapter 3 © 2022 American Chemical Society
All other materials @ 2024 Claire A. Herbert

DEDICATION

To

My Dadi

TABLE OF CONTENTS

	Page
LIST OF FIGURES	v
LIST OF TABLES	vi
LIST OF SCHEMES	vii
ACKNOWLEDGEMENTS	ix
VITA	xi
ABSTRACT OF THE DISSERTATION	xiv
CHAPTER 1: Nickel-Catalyzed Stereoselective Coupling Reactions of Benzylic and Alkyl Alcohol Derivatives	
1.1 Introduction	1
1.2 Stereospecific Reactions of Alcohol Derivatives	4
1.3 Stereoablative Reactions of Alcohol Derivatives	17
1.4 Multivariable Control of Mechanism of Oxidative Addition	22
1.5 Conclusion	25
CHAPTER 2: Nickel-catalyzed Kumada Cross-Coupling Reaction of Benzylic Sulfonamides	
2.1 Introduction	27
2.2 Results and Discussion	31
2.2.1 Optimization of the Nickel-catalyzed Kumada Cross-Coupling Reaction	31
2.2.2 Evaluation of Substrate Scope for the Kumada XC Reaction	33
2.2.3 Synthesis of Diarylmethane	36
2.2.4 Proposed Mechanism of Kumada XC Reaction	37
2.3 Conclusion	38
2.4 Experimental Results	39
2.4.1 General Procedures	39
2.4.2 General Nickel-Catalyzed Kumada Cross-Coupling Reaction Procedures	40
2.4.2.1 Method A: Nickel-Catalyzed Kumada Cross-Coupling Reaction	40
2.4.2.2 Preparation of Grignard Reagent	41
2.4.2.3 Synthesis of ((R)-BINAP)NiCl2	41
2.4.3 Characterization Data for Ring-Opening Kumada Cross-Coupled Products	42
2.4.4 General Procedures for Synthesis of Starting Materials	48
2.4.4.1 Method B: Condensation Reaction	48
2.4.4.2 Method C: Fe-Catalyzed Formal [4+2] Cycloaddition	49
2.4.4.3 Method D: Pd/C Reduction of Alkenes	49
2.4.4.4 Method E: TFA Mediated Aza-Prins Cyclization	49
2.4.4.5 Method F: Alkylation of Secondary Alcohol	50
2.4.5 Synthesis and Characterization of Sulfonamide Starting Materials	51

CHAPTER 3: Synthesis of Vicinal Carbocycles by Intramolecular Nickel-Catalyzed Cross-Electrophile Coupling Reaction
3.1 Introduction 60
3.2 Results 63
3.2.1 Optimization 63
3.2.2 Evaluation of Substrate Scope 65
3.2.3 Mechanism 66
3.3 Conclusion 68
3.4 Experimental Details 68
3.4.1 General Procedures 68
3.4.2 Conjunctive XEC Reaction Procedures 70
3.4.2.1 Method A: Nickel-Catalyzed Conjunctive XEC Reaction 70
3.4.2.2 Preparation of Grignard Reagent 71
3.4.3 Characterization Data for Conjunctive XEC Reaction Products 71
3.4.4 General Procedures for the Synthesis of Dimesylate Starting Materials 75
3.4.4.1 Method B: Pd-Catalyzed Heck Reaction 75
3.4.4.2 Method C: Preparation of Grignard Reagent 76
3.4.4.3 Method D: Nucleophilic Grignard Addition in Aldehyde 76
3.4.4.4 Method E: Ozonolysis of Terminal Alkenes 77
3.4.4.5 Method F: Preparation of Wittig Salt 3.16 77
3.4.4.6 Method G: Wittig Reaction 78
3.4.4.7 Method H: Mesylation Reaction 78
3.4.5 Synthesis and Characterization of Dimesylate Starting Materials 79

CHAPTER 4: Structure Reactivity-Relationships of Nickel-Catalyzed Cross-Coupling Reactions
4.1 Introduction 91
4.2 Results 99
4.3 Conclusion 105
4.4 Experimental Details 105
4.4.1 General Procedures 106
4.4.2 General Procedures for Nickel-Catalyzed Open-Shell Suzuki XC Reactions 106
4.4.2.1 Method A: Nickel-Catalyzed Open-Shell Suzuki XC Reaction of Alkyl Bromides and Iodides 106
4.4.2.2 Method B: Nickel-Catalyzed Open-Shell Suzuki XC Reaction of Alkyl Chlorides 107
4.4.3 Representative Reactions 108
4.4.3.1 Representative Reaction of 4-Bromopiperidine with Phenyl Boronic Acid 108
4.4.3.2 Representative Reaction of 4-chloropiperidine with Phenyl Boronic Acid 108
4.4.4 Tables with Nickel-Catalyzed Open-Shell Suzuki XC Reaction Data 109

APPENDIX: ^{1}H, ^{13}C, ^{1}F, COSY, and NOE NMR Spectra 116

LIST OF FIGURES

Page

Figure 1.1 Harnessing Readily Available Electrophiles for XC and XEC 2

Figure 1.2 Nickel-catalyzed Stereospecific XC of Benzylic Ethers 5

Figure 1.3 Key Design Principle: Rapid Access to Starting Materials from Commercially Available Aldehydes and Olefins 12

Figure 1.4 Multi-variable Control in Nickel-catalyzed Reactions 24

Figure 2.1 Proposed Mechanism of Kumada XC Reaction 38

Figure 3.1 Medicinally Relevant Carbocycles 62

Figure 3.2 Scope of Nickel-Catalyzed Conjunctive XEC Reaction 65

Figure 4.1 Mechanisms of nickel-catalyzed oxidative addition 92

Figure 4.2 Nickel-catalyzed XC Reactions (a) Open-shell reactions that utilize nitrogen-based ligands (b) Closed-shell reactions that utilize phosphorous-based ligands 94

Figure 4.3 Reactions employing P vs. N Ligand-Based Control (a) Activation of aryl halides via Ni^{I}/Ni^{II} or Ni^{I}/Ni^{III} in trifluoromethylthiolation reactions (b) Electroreductive XEC reaction facilitated by phosphine/nitrogen ligand exchange 96

Figure 4.4 Control of open- and closed-shell pathways with phosphine and nitrogen-based ligands 97

Figure 4.5 Phosphine and Nitrogen-based ligands selected for their reported efficacy in nickel-catalyzed XC reactions 101

Figure 4.6 Phosphine vs. Nitrogen Ligand-based Reactivity Trends in Open- and Closed-Shell Suzuki Reactions 105

LIST OF TABLES

Page

Table 2.1 Optimization of the Kumada XC Reaction 32

Table 2.2 Scope of Kumada XC Reaction with Acyclic Sulfonamides 34

Table 3.1 Optimization of Conjunctive XEC Reaction 64

Table 4.1 Reactivity of Secondary Alkyl Bromide in Open-Shell Suzuki Reactions with Phosphine and Nitrogen-Based Ligands 102

Table 4.2 Reactivity of Secondary Alkyl Iodide in Open-Shell Suzuki Reactions with Phosphine and Nitrogen-Based Ligands 103

Table 4.3 Reactivity of Secondary Alkyl Chloride in Open-Shell Suzuki Reactions with Phosphine and Nitrogen-Based Ligands 104

Table 4.4 Open-Shell Suzuki XC Reaction with 4-Bromopiperidine and Phenyl Boronic Acid 110

Table 4.5 Open-Shell Suzuki XC Reaction with 4-Bromopiperidine and Trifluoromethylphenyl Boronic Acid 111

Table 4.6 Open-Shell Suzuki XC Reaction with 4-Iodopiperidine and Phenyl Boronic Acid 112

Table 4.7 Open-Shell Suzuki XC Reaction with 4-Iodopiperidine and Trifluoromethylphenyl Boronic Acid 113

Table 4.8 Open-Shell Suzuki XC Reaction with 4-Chloropiperidine Phenyl Boronic Acid 114

Table 4.9 Open-Shell Suzuki XC Reaction with 4-Chloropiperidine and p-Tolyl Boronic Acid 115

LIST OF SCHEMES

Page

Scheme 1.1 Stereospecific Kumada Coupling Reactions of Benzylic Ethers 6

Scheme 1.2 Stereospecific Kumada Coupling Reaction of Cyclic Ethers 7

Scheme 1.3 Stereospecific XC Reactions of Alkyl Alcohol Derivatives 8

Scheme 1.4 Leaving Group Stability as a Predictor for Stereospecific OA 9

Scheme 1.5 XEC as a Strategy to Overcome of Challenges of Intramolecular XC 11

Scheme 1.6 Representative XEC Reactions of Benzylic and Allylic Ethers and Benzylic Sulfonamides 12

Scheme 1.7 Investigation of Stereochemical Outcomes of of XEC Reaction 13

Scheme 1.8 Activation of Benzylic Esters for Reductive C(sp3)–C(sp2) Coupling Reactions 14

Scheme 1.9 Comparison of Mechanisms for Kumada-type XC and XEC Reactions Using Grignard Reagent 15

Scheme 1.10 Domino Reaction of Alkynylpiperidines 16

Scheme 1.11 Stereoconvergent XEC Reactions of 1,3-dimesylates 18

Scheme 1.12 In-situ Conversion of Readily Accessible 1,3-Diols to Cyclopropanes 18

Scheme 1.13 Mechanistic Investigation of XEC of 1,3-Dimesylates 19

Scheme 1.14 Zn-mediated Synthesis of Cyclopropanes from Complex 1,3-Diols 20

Scheme 1.15 Synthesis of Vicinal Carbocycles from Alkyl Dimesylates 21

Scheme 1.16 Allylic Difluorides as Intramolecular Coupling Partners 22

Scheme 1.17 Probing Ligand-Based Control of Chemoselectivity 25

Scheme 2.1 C–O vs. C–N Activation 28

Scheme 2.2 Activation of Benzylic Sulfonamides via Ring Strain 29

Scheme 2.3 Activation of Benzylic Sulfonamides via Charged Salts 30

Scheme 2.4 Proposed Kumada XC Reaction of Benzylic Amine Derivatives 31

Scheme 2.5 Synthesis of Aryl Piperidines for Kumada XC Reaction 35

Scheme 2.6	Scope of Kumada XC Reaction	36
Scheme 2.7	Synthesis of Diarylmethane via Kumada XC Reaction	37
Scheme 3.1	Prior Art: Conjunctive XEC Reactions	61
Scheme 3.2	In-situ conversion of alkyl mesylates to alkyl iodides	63
Scheme 3.3	Control Reaction with Single Alkene Diastereomer	66
Scheme 3.4	Control reaction with no nickel catalyst	67
Scheme 3.5	Proposed Mechanism	67
Scheme 3.6	General Synthesis of Dimesylate Starting Material	79
Scheme 4.1	Evaluation of P vs. N-Based Ligand Control in Nickel-Catalyzed Suzuki Reactions	98
Scheme 4.2	Previously developed open- and closed-shell Suzuki reactions	100

ACKNOWLEDGEMENTS

Chapter 1 of this dissertation is a reprint of the material as it appears in "Nickel-Catalyzed Stereoselective Coupling Reactions of Benzylic and Alkyl Alcohol Derivatives" in *Accounts of Chemical Research*, used with permission from the American Chemical Society (CC-BY 4.0). The coauthor listed in this publication is Elizabeth R. Jarvo. Portions of Chapter 2 of this dissertation are an adaptation of the material as it appears in "Nickel-Catalyzed Kumada Cross-Coupling Reactions of Benzylic Sulfonamides" in *Molecules*, used with permission from MDPI (CC-BY 4.0). The coauthors listed in this publication are Kirsten A. Hewitt, Alissa C. Matus, and Elizabeth R. Jarvo. Portions of Chapter 3 of this dissertation are an adaptation of the material as it appears in "Synthesis of Vicinal Carbocycles by Intramolecular Nickel-Catalyzed Conjunctive Cross-Electrophile Coupling Reaction" in *Organic Letters*, used with permission from the American Chemical Society (CC-BY 4.0). The coauthors listed in this publication are Kirsten A. Hewitt and Elizabeth R. Jarvo. Elizabeth R. Jarvo directed and supervised research which forms the basis for the dissertation.

First and foremost, I would like to thank Professor Elizabeth R. Jarvo for the opportunity to conduct research in her laboratory. I would not be the scientist I am today without her mentorship. While I have significantly deepened my knowledge of synthetic and organometallic chemistry throughout my time in the Jarvo group perhaps the most important thing I have learned from Liz is how to be an effective leader. I hope to replicate her kindness, honesty, and wisdom throughout the rest of my career.

I would like to thank the faculty and staff that serve the UCI chemistry department. Specifically, I am grateful for the support of the members of my thesis committee, Professor Suzanne A. Blum and Professor Scott D. Rychnovsky who have provided wonderful insight and engaging conversations about my chemistry over the years. I am grateful to Dr. Phil Dennison and Dr. Suvrajit Sengupta for their care of the NMR facilities without which many of my experiments would not be possible. I would like to thank Dr. Felix Grun and Dr. Benjamin Katz for maintaining the many mass spectrometers I have used throughout my graduate work. In particular, I am grateful for everything they have taught me about GC-MS, which enabled a great deal of our structure-reactivity relationship studies.

I am incredibly grateful for the friendship and mentorship that members of the Jarvo lab have provided me over the last five years. Dr. Kirsten Hewitt, who I met on my very first day at UCI during my summer rotation in the Jarvo group, taught me everything I didn't know about working in an organometallic laboratory from proper Schlenk technique to glovebox use, to the "right" way to run a flash column. I am incredibly lucky to have you as a mentor and friend. Professor Taylor Thane, who I have learned so much from both professionally and personally and who continues to be a bright source of positivity when I need it the most. To Dr. Patricia Lin and Nadia Hirbawi, I could not have asked for better lab mates to start and end this degree with. To Anjali Bardhan, the first graduate student I mentored, I could not have asked for a better partner to join SRR. I hope you have learned as much from me as I have learned from you. To Erin Eason, being mentored by a stressed-out fifth year graduate student is not easy. Thank you for your patience and the laughter you have brought me in my last year. And finally, to Vincent Chen Chen, my first undergraduate mentee, it has been such a pleasure to watch you grow as a synthetic chemist throughout your time in this the Jarvo group, thank you for all the joy and positivity you have brought our group.

I would like to acknowledge several mentors who have significantly impacted my education and career as a chemist both before and throughout my time at UCI. Joining the laboratory of Professor Daniel P. Becker at Loyola made a pivotal impact on my experiential education. I am extremely grateful to both Dr. Becker and my first mentor in the Becker Lab, Dr. Tahirah K. Heath who was so patient as I was first learning how to conduct research. Lastly, I would like to thank Dr. Jason R. Abbott for his mentorship and encouragement during my time at AbbVie and throughout the last few years of my graduate career.

Finally, I am incredibly grateful to the countless friends and family that have supported me through graduate school, you know who you are. And to the folks that have supported me since day one, Mom, Dad, Cameron, and Connor, I am so lucky to have you four as my family.

VITA

Claire A. Herbert

EDUCATION

2019–2024	Doctor of Philosophy in Chemistry, University of California, Irvine
2015–2019	Bachelor of Science in Chemistry, Loyola University Chicago

RESEARCH EXPERIENCE

2019–2024	Doctoral Research (University of California, Irvine) *Investigations of Nickel-Catalyzed Coupling Reactions: Development of New Methods and Structure-Reactivity Relationships* Advisor: Elizabeth R. Jarvo
2022	Internship (AbbVie Inc.) *DNA-Encoded Library Synthesis*
2016–2019	Undergraduate Research (Loyola University Chicago) *Synthesis of DapE Inhibitors as Novel Antibiotics* Advisor: Daniel P. Becker
2018	Internship (Regis Technologies Inc.) *Process Research*

FIELD OF STUDY

Organic Chemistry

AWARDS AND HONORS

2024	Chemistry Graduate Dissertation Fellowship – University of California, Irvine
2019	ACS Undergraduate Award in Inorganic Chemistry – Loyola University Chicago
2019	Fr. Morrissey Medal – Loyola University Chicago
2017–2019	Mulcahy Scholars Research Fellowship – Loyola University Chicago
2018–2019	Louis Glunz Family Regis Scholarship – Loyola University Chicago
2017	ACS Undergraduate Award in Analytical Chemistry – Loyola University Chicago
2017	Provost Research Fellowship – Loyola University Chicago

PUBLICATIONS

Herbert, C. A.; Bardhan, A. S.; Eason, E. M.; Jarvo, E. R. Structure-Reactivity Relationships of Nickel-Catalyzed Suzuki Reactions. *Manuscript in preparation.*

Herbert, C. A.; Jarvo, E. R. Nickel-Catalyzed Stereoselective Coupling Reactions of Benzylic and Alkyl Alcohol Derivatives. *Acc. Chem. Res.* 2023, *56*, 3313–3324.

Hewitt, K.A.; Herbert, C. A.; Jarvo, E. R. Synthesis of Vicinal Carbocycles by Intramolecular Nickel-Catalyzed Conjunctive Cross-Electrophile Coupling Reaction. *Org. Lett.* 2022, *24*, 6093–6098.

Hewitt, K. A.; Herbert, C. A.; Matus, A. C.; Jarvo, E. R. Nickel-Catalyzed Kumada Cross-Coupling Reactions of Benzylic Sulfonamides. *Molecules* 2021, *26*, 5947.

DiPuma, T.; Thabthimthong, T.; Kelley, E. H.; Konczak, K.; Beulke, M.; Herbert, C.; Habeeb Mohammad, T. S.; Starus, A.; Nocek, B.; Olsen, K. W.; Holz, R. C.; Becker, D. P. Tetrazole-based inhibitors of the bacterial enzyme N-succinyl-L,L-2,6-diaminopimelic acid desuccinylase as potential antibiotics. *Bioorg. Med. Chem. Lett.* **2023**, *83*, 129177.

Heath,T. K; Lutz M.R; Reidl C. T; Guzman, E. R.; Herbert, C. A.; Nocek, B. P.; Holz, R. C.; Olsen, K. W.; Ballicora, M. A.; Becker, D. P. Practical Spectrophotometric Assay for the dapE-Encoded N-Succinyl-L,L-Diaminopimelic Acid Desuccinylase, a Potential Antibiotic Target. *PLOS ONE* 2018, *13* (4).

CONFERENCE PRESENTATIONS

Herbert, C. A.; Hewitt, K. A.; Bardhan, A. S.; Eason, E. M.; Matus, A. C.; Jarvo, E. R. "Investigations of Nickel-Catalyzed Coupling Reactions: Development of New Methods and Structure-Reactivity Relationships." Presented at the Amgen Women in Chemistry Graduate Student Symposium, Thousand Oaks, California, March 2024 (poster presentation).

Herbert, C. A.; Hewitt, K. A.; Jarvo, E. R. "Nickel-Catalyzed Reactions of C(sp3)–O Electrophiles." Presented at the American Chemical Society National Meeting, San Francisco, California, August 2023 (oral presentation).

Herbert, C. A.; Hewitt, K. A.; Jarvo, E. R. "Synthesis of Vicinal Carbocycles by Intramolecular Nickel-Catalyzed Conjunctive Cross-Electrophile Coupling Reaction." Presented at the Division of Organic Chemistry Graduate Research Symposium, Bozeman, Montana, July 2023 (poster presentation).

Herbert, C. A.; Hewitt, K. A.; Jarvo, E. R. "Synthesis of Vicinal Carbocycles by Intramolecular Nickel-Catalyzed Conjunctive Cross-Electrophile Coupling Reaction." Presented at the Empowering Women in Organic Chemistry Conference, Thousand Oaks, California, June 2023 (poster presentation).

Herbert, C. A.; Hewitt, K. A.; Matus, A. C.; Jarvo, E. R. "Nickel-Catalyzed Kumada Cross-Coupling Reactions of Benzylic Sulfonamides." Presented at the American Chemical Society National Meeting, Chicago, Illinois, August 2022 (oral presentation).

Herbert, C. A.; Hewitt, K. A.; Matus, A. C.; Jarvo, E. R. "Nickel-Catalyzed Kumada Cross-Coupling Reactions of Benzylic Sulfonamides." Presented at the American Chemical Society National Meeting, virtual, August 2021 (oral presentation).

Herbert, C. A.; Hewitt, K. A.; Matus, A. C.; Jarvo, E. R. "Nickel-Catalyzed Kumada Cross-Coupling Reactions of Benzylic Sulfonamides." Presented at the Empowering Women in Organic Chemistry Conference, virtual, June 2021 (poster presentation).

Herbert, C. A.; Hewitt, K. A.; Matus, A. C.; Jarvo, E. R. "Nickel-Catalyzed Kumada Cross-Coupling Reactions of Benzylic Sulfonamides." Presented at the American Chemical Society National Meeting, virtual, March 2021 (poster presentation).

Herbert, C. A.; Heath, T. K.; Becker, D. P. "Synthesis of DapE Inhibitors as Novel Antibiotics." Presented at the Loyola University Chicago LUROP Symposium, Chicago, Illinois, April 2019 (poster presentation).

Herbert, C. A.; Heath, T. K.; Becker, D. P. "Synthesis of DapE Inhibitors as Novel Antibiotics." Presented at the Loyola University Chicago LUROP Symposium, Chicago, Illinois, April 2018 (poster presentation).

TEACHING EXPERIENCE

2019-2022	Honors/Majors Organic Chemistry Laboratory (University of California, Irvine) Organic Chemistry Laboratory (University of California, Irvine) Advanced Organic Chemistry (University of California, Irvine) Organic Chemistry Lecture (University of California, Irvine)

LEADERSHIP AND OUTREACH

2021, 2023	SoCal Undergraduate Research Symposium Graduate Student Coordinator
2021–2023	Iota Sigma Pi Activities Coordinator
2021–2023	ChemUnity Mentor
2020–2021	Chemistry Peer Mentoring Program Recruitment Representative
2020–2021	Iota Sigma Pi Socical Media/Marketing Chair
2019–2022	Chemistry Outreach Program Volunteer

AFFILIATIONS

2018–present	Alpha Sigma Nu
2019–present	American Chemical Society
2019–present	Iota Sigma Pi

ABSTRACT OF THE DISSERTATION

Investigations of Nickel-Catalyzed Coupling Reactions: Development of New Methods and Structure-Reactivity Relationships

By

Claire A. Herbert

Doctor of Philosophy in Chemistry

University of California, Irvine, 2024

Professor Elizabeth R. Jarvo, Chair

Development of new reactions for the introduction of C(sp^3) centers is a key challenge in synthetic and medicinal chemistry. Cross-coupling (XC) and cross-electrophile coupling (XEC) reactions provide a robust platform for the introduction of these motifs. Traditional cross-coupling chemistry, for which Suzuki, Heck, and Negishi were awarded the Nobel prize in 2010 was developed using palladium catalysts. Since the initial development of these reactions, remarkable strides have been made in the palladium catalyzed coupling of C(sp^2) centers. However, there is an increased interest in developing new reactions which couple C(sp^3) centers. Nickel catalysts play a key role in this development because these catalysts offer unique properties suited to the challenge of activating C(sp^3) coupling partners. Nickel is more electropositive than palladium which allows it to activate weaker electrophiles. Nickel can also readily access the 0, +1, +2, and +3 oxidation states which facilitates both one- and two-electron mechanistic pathways. However, while the unique reactivity of nickel catalysts in both XC and XEC reactions has been observed, the mechanistic features of these reactions remain poorly understood.

The work described herein will address the both the development of new nickel-catalyzed reactions for C(sp3) coupling and the investigation of ligand-based structure reactivity relationships of nickel catalysts. Chapter one will introduce background on our group's prior work

developing stereospecific and stereoablative methods for the synthesis of new C–C bonds with nickel catalysis. A description will be provided for how our group has addressed synthetic challenges in constructing C(sp^3)-rich frameworks by harnessing alkyl alcohol derivatives. We will also describe how through this work we uncovered aspects of nickel-catalyzed XC and XEC mechanisms. Finally we address our ongoing work evaluating the relationship between phosphine and nitrogen-based ligands and nickel-catalysts and the observed effects on reactivity in nickel-catalyzed reactions.

In chapter two, the development of a nickel-catalyzed Kumada cross-coupling reaction will be presented. In this work, benzylic sulfonamides undergo cross-coupling with methyl and aryl Grignard reagents to form new C(sp^3)–C(sp3) and C(sp3)–C(sp2) bonds. This work provides a method to access 1,3-acyclic fragments in high diastereomeric ratios from commercially available aryl aldehydes. We hypothesize that this reaction proceeds through a stereospecific polar oxidative addition into the C–N bond.

In chapter three, the development of a nickel-catalyzed conjunctive XEC reaction of alkyl dimesylates will be presented. In this work we present a method in which alkyl mesylates tethered through an alkyl chain to an olefin, undergo a nickel-catalyzed cyclization to afford vicinal carbocycles. This method provides access to complex cyclic fragments in one synthetic step from acyclic starting materials. Mechanistic studies demonstrate that the reaction proceeds via alkyl iodides which are formed in situ from Grignard reagent. The reaction proceeds through stereoablative halogen atom abstraction to initiate cyclization.

In chapter four, the relationship between the one- and two-electron pathways discussed in the previous chapters and ligand identity will be described. An analysis of nickel-catalyzed open- and closed-shell Suzuki XC reactions will be presented. We will provide data demonstrating how

phosphine and nitrogen-based ligands influence the product outcomes in open- and closed-shell reactions. This demonstration of multivariable control is important for both our understanding of the mechanisms for nickel-catalyst reactions as well as the development of new methods.

Chapter 1

Nickel-Catalyzed Stereoselective Coupling Reactions of Benzylic and Alkyl Alcohol Derivatives

1.1 Introduction

Introduction and control of C(sp^3) stereogenic centers is a key challenge in synthetic and medicinal chemistry.[1] Strategies for late-stage functionalization will have the highest impact if they engage common functional groups.[2] We envisioned that transforming the C–O bonds of alkyl alcohol derivatives to C–C bonds, via coupling reactions, would be potentially impactful due to the natural abundance of alkyl alcohols as well as access through the versatile methods available for their synthesis (Figure 1.1A). In an analysis of reported natural products, alkyl alcohols were determined to have the highest frequency of all functional groups, found in over 60% of natural products.[3,4] They also appear frequently in medicinal agents.[5] For example, alkyl alcohols are present in 60 of the 200 highest-selling small-molecule pharmaceuticals.[6] Furthermore, there are many stereoselective reactions for preparation of secondary alcohols as single enantiomers and diastereomers. This wide availability of complex alkyl alcohols makes them attractive as potential alkyl coupling partners in cross-coupling (XC) and cross-electrophile coupling reactions (XEC).

---

[1] Portions of this chapter have been published in Accounts of Chemical Research: Herbert, C. A.; Jarvo, E. R. *Acc. Chem. Res.* **2023**, *56*, 3313–3324.
[2] Shugrue, C. R.; Miller, S. J. *Chem. Rev. 117*, 18, 11894–11951.
[3] Ertl, P.; Schuhmann, T. A. *J. Nat. Prod.* **2019**, *82*, 1258–1263.
[4] McGrath, N. A.; Birchacek, M.; Njardarson, J. T. *J. Chem. Educ.* **2010**, *87*, 12, 1358–1349.
[5] Cramer, J.; Sager, C. P.; Ernst, B. *J. Med. Chem.* **2019**, *62*, 8915–8930.
[6] See reference 4.

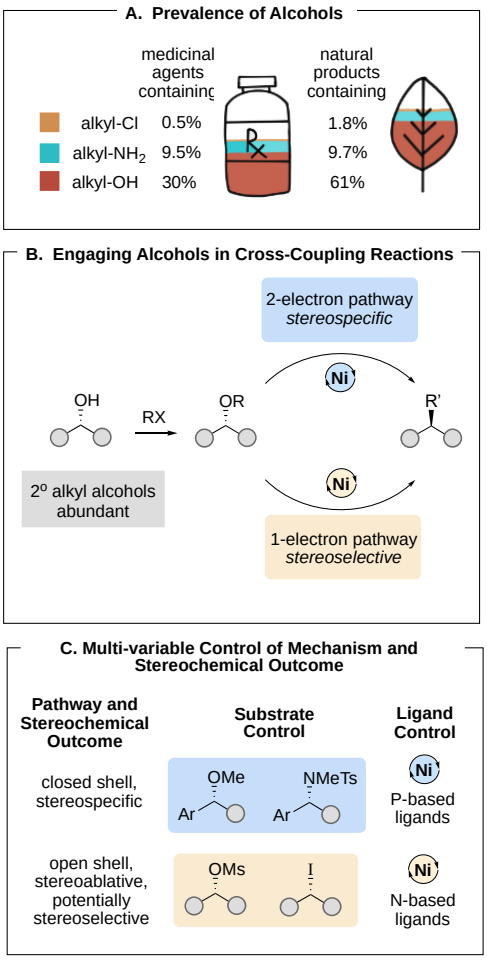


Figure 1.1 Harnessing Readily Available Electrophiles for XC and XEC

One obvious challenge of engaging alkyl alcohols as electrophilic coupling partners is the activation of the strong C(sp^3)–O bond for oxidative addition. Our group is focused on developing nickel-catalyzed reactions with suitable electrophiles that can be accessed through simple synthetic manipulations to weaken the C–O bond. To this end we have developed nickel-catalyzed transformations of ethers, esters, carbamates, lactones, and sulfonates to C(sp^3)–C(sp^2) and C(sp^3)–C(sp^3) coupled products, through traditional cross-coupling, cross-electrophile coupling, and cascade reactions. In contrast to palladium catalysts more commonly employed in aryl coupling reactions, nickel catalysts are generally more reactive toward sluggish oxidative addition (OA) and

less prone to deleterious β-hydride elimination.[7] Indeed, for the transformations described here, nickel catalysts are successful while palladium catalysts often provide primarily recovered starting material or undesired byproducts.

The reactions that we have developed include both stereospecific and stereoablative coupling reactions, reflecting the diverse range of elementary steps available with nickel catalysts (Figure 1.1B).[8] In the stereospecific pathway, typically observed with C(sp^3)–O electrophiles, a two-electron S_N2-like oxidative addition initiates the reaction. With numerous methods for the synthesis of enantioenriched alcohols, a stereospecific oxidative addition is highly advantageous since the stereochemical information of the starting materials is preserved, and cross-coupled products are produced with high enantiospecificity. Alternatively, reactions may proceed via a stereoablative pathway. Stereoablative reactions are typically observed with C(sp^3)–X (X = I, Br, Cl) electrophiles. Oxidative addition proceeds through halogen atom abstraction (XAT) to generate an alkyl radical which can subsequently recombine with nickel to form an organonickel intermediate. This pathway allows for stereoconvergent reactions, such as diastereoselective reactions with starting materials containing pendant stereogenic centers and enantioselective reactions in the presence of a chiral ligand. Our group has developed both stereospecific and stereoconvergent reactions. In the stereospecific reactions of benzylic ethers, esters, and carbamates, we observe either net inversion or retention at the C(sp^3) center. In reactions of alkyl mesylates, we observe rapid conversion to the alkyl iodides in situ and stereoablative reaction of the C(sp^3) center in the presence of nickel catalysts.

[7] Tasker, S. Z.; Standely, E. A.; Jamison, T. A. *Nature* **2014**, *509*, 299–309.
[8] Lucas, E. L.; Jarvo, E. R. *Nat. Rev. Chem.* **2017**, *1*, 65.

Given the potential for mechanisms with very different selectivity profiles, a challenge to design selective nickel-catalyzed alkyl coupling reactions and define the key features guiding selectivity is presented (Figure 1.1C). Factors which favor one pathway for oxidative addition over the other remain elusive because little experimental evidence directly compares reactions that proceed through alternative pathways. However, understanding the reaction features which control these pathways would be useful for reaction design and analysis of nickel-catalyzed XC and XEC reactions. Identity of the leaving group (–OR or –NTsR vs –I, –Br, or –Cl) is a critical factor in determining whether the reaction progresses through a stereospecific or stereoablative oxidative addition: ethers, esters, and sulfonamides favor two-electron oxidative addition and halides favor one-electron halogen atom abstraction. While the electrophile plays an important role in pathway differentiation, the role of the ligand is also crucial. A typical ligand screen for nickel-catalyzed reactions can include a wide variety of phosphines, imines, amines, and N-heterocyclic carbenes. However, detailed analysis of ligand effects is typically restricted to a subset of closely related ligands. A broader understanding of the ligand influence in shunting nickel-catalyzed reactions toward open- or closed-shell intermediates is still under investigation.

In this chapter, we present the developments our group has made in stereospecific and stereoselective reactions using nickel catalysts. Our work demonstrates stereoselective couplings of $C(sp^3)$–$C(sp^3)$ and $C(sp^3)$–$C(sp^2)$ centers in the context of cross-coupling, cross-electrophile coupling, and cascade reactions. We also discuss our progress toward defining catalyst features that control the mechanism of oxidative addition.

1.2 Stereospecific Reactions of Alcohol Derivatives.

To develop strategies for synthesis of $C(sp^3)$ stereogenic centers from alcohol derivatives, we chose to first examine benzylic ethers as cross-coupling (XC) partners. Compared to

unfunctionalized alkyl alcohols, benzylic carbinols have the advantage that oxidative addition is accelerated by ligation of the arene moiety to generate a π-benzylnickel complex.[9] We established stereospecific Kumada, Negishi, and Suzuki-type coupling reactions (Figure 1.2A). These results are consistent with two-electron concerted oxidative addition, with no open-shell intermediates. Hand in hand with reaction development, we challenged each new reaction in syntheses of compounds bearing medicinal chemistry motifs, including diaryl alkanes and triarylmethanes (Figure 1.2B).

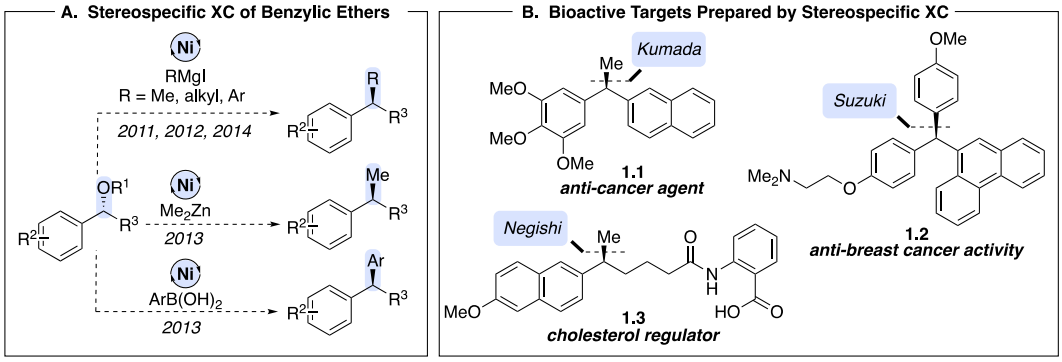


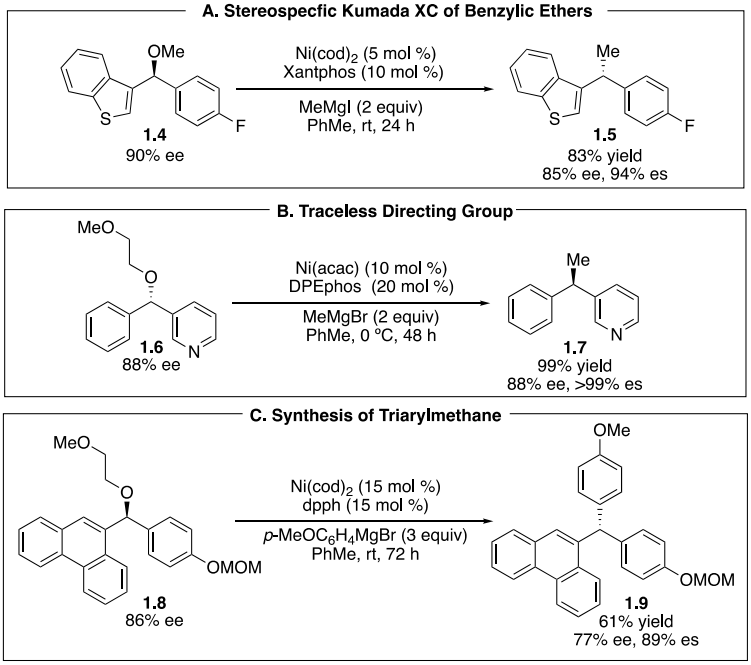
Figure 1.2 Nickel-catalyzed Stereospecific XC of Benzylic Ethers

We first harnessed the C–O bond of benzylic ethers in stereospecific Kumada-type coupling reactions with MeMgI (Scheme 1.1A).[10] In the presence of $Ni(cod)_2$ and bidentate phosphine ligands, enantioenriched benzylic ethers are cleanly converted to enantioenriched products with inversion at the benzylic stereogenic center. The reaction was optimized to suppress the β-hydride elimination pathway which produced styrene byproducts that were found to inhibit the nickel catalyst. To demonstrate the synthetic utility of the transformation, it was applied in the synthesis of bioactive diarylmethanes. One limitation was the requirement for activation of the C–

[9] Su, B.; Cao, Z.-C.; Shi, Z.-J. *Acc. Chem. Res.* **2015**, *48*, 3, 886–896.
[10] Taylor, B. L. H.; Swift, E. C.; Waetzig, J. D.; Jarvo, E. R. *J. Am. Chem. Soc.* **2011**, *133*, 389–391.

O bond by inclusion of an extended aromatic system or heterocycle, reflecting the ability of the arene to coordinate to the low-valent nickel intermediates. Employing substrates with simple benzylic ethers resulted in recovery of starting material, likely due to challenging oxidative addition. This hurdle was overcome by development of a traceless directing group to expand the scope of the reaction to include simple arenes (Scheme 1.1B).[11] This strategy also enabled access to enantioenriched triarylmethane scaffolds such as **1.9**, demonstrated as part of the synthesis of anti-breast-cancer agent **1.2** (Scheme 1.1C).[12] Notably, the Watson group has also shown stereospecific activation of benzylic and allylic pivalates in Suzuki-type coupling reactions.[13]

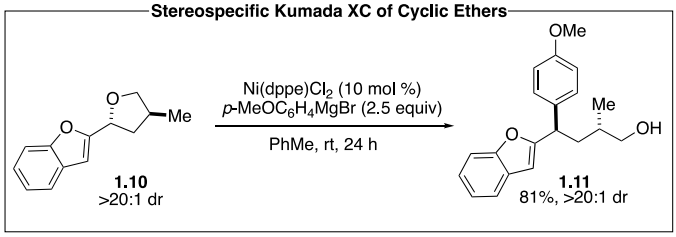
Scheme 1.1. Stereospecific Kumada Coupling Reactions of Benzylic Ethers



[11] Greene, M.A.; Yonova, I. M.; Williams, F. J.; Jarvo, E. R. *Org. Lett.* **2012**, *14*, 16, 4293–4296.
[12] Taylor, B. L. H.; Harris, M. R.; Jarvo, E. R. *Angew. Chem. Int. Ed.* **2012**, *51,* 7790–7793.
[13] (a) Zhou, Q.; Srinivas, H. D.; Dasgupta, S.; Watson, M. P. *J. Am. Chem. Soc*. **2013**, *135*, 3307–3310. (b) Srinivas, H. D.; Zhou, Q.; Watson, M. P. *Org. Lett.* **2014**, *16*, 3596–3599. (c) Zhou, Q.; Srinivas, H. D.; Zhang, S.; Watson, M. P. *J. Am. Chem. Soc.* **2016**, *138*, 11989–11995. (d) Cobb, K. M.; Rabb-Lynch, J. M.; Hoerrner, M. E.; Manders, A.; Zhou, Q.; Watson, M. P. *Org. Lett.* **2017**, *19*, 4355–4358. (e) Xu, J.; Bercher, O. P.; Watson, M. P. *J. Am. Chem. Soc.* **2021**, *143*, 8608–8613.

Stereospecific reactions of cyclic ethers provide further support for robust catalyst control of configuration in nickel-catalyzed activation of C–O bonds, as well as synthetic access to stereochemically-rich acyclic fragments. Tetrahydropyran and tetrahydrofuran derivatives are readily available from the corresponding aldehydes and can be synthesized as single diastereomers. These scaffolds undergo ring-opening XC to engage the benzylic C–O bond in the presence of nickel catalysts to afford acyclic coupled products in high dr (Scheme 1.2).[14] Reactions proceed cleanly with inversion at the reactive center, with no catalyst match or mismatch with respect to additional stereogenic centers.

Scheme 1.2. Stereospecific Kumada Coupling Reaction of Cyclic Ethers

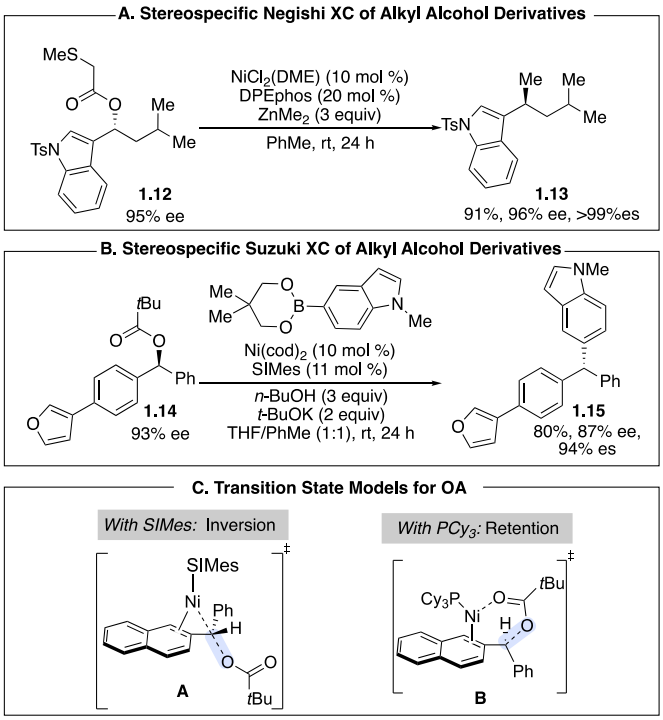


Our laboratory has developed coupling reactions of C–O electrophiles with transmetallating agents such as boronic esters and organozinc reagents that have broad functional group tolerance. As with the Kumada-type coupling reaction to synthesize triaryl methanes, a traceless directing group was employed to activate the C–O bond towards oxidative addition for the Negishi-type coupling (Scheme 1.3A). In this work, the 2-methoxyethyl ether directing group employed for the Kumada-type reaction was ineffective, but the 2-(methylthio)ester afforded the desired Negishi-type coupled product in high yield and enantiospecificity.[15] A stereospecific

[14] Tollefson, E. J.; Dawson, D. D.; Osborne, C. A.; Jarvo, E. R. *J. Am. Chem. Soc.* **2014**, *136*, 14951–14958.
[15] Wisniewska, H. M.; Swift, E. C.; Jarvo, E. R. *J. Am. Chem. Soc.* **2013**, *135*, 9083–9090.

Suzuki coupling of benzylic carbamates and benzylic pivalates with aryl boronic esters was also developed (Scheme 1.3B). Interestingly, in this reaction the choice of ligand dictates whether the reaction occurs with retention or inversion at the benzylic center.[16] Computational studies performed in collaboration with the Houk and Hong laboratories demonstrated that when SIMes ligand was employed, oxidative addition of the nickel catalyst proceeds via backside attack on the pivalate leaving group leading to net inversion in the Suzuki product (Scheme 1.3C, transition state **A**). However, when PCy_3 ligand is employed, coordination of the pivalate leaving group to the nickel catalyst directs oxidative addition via a cyclic transition state that occurs with retention (Scheme 1.3C, transition state **B**).[17]

Scheme 1.3. Stereospecific XC Reactions of Alkyl Alcohol Derivatives

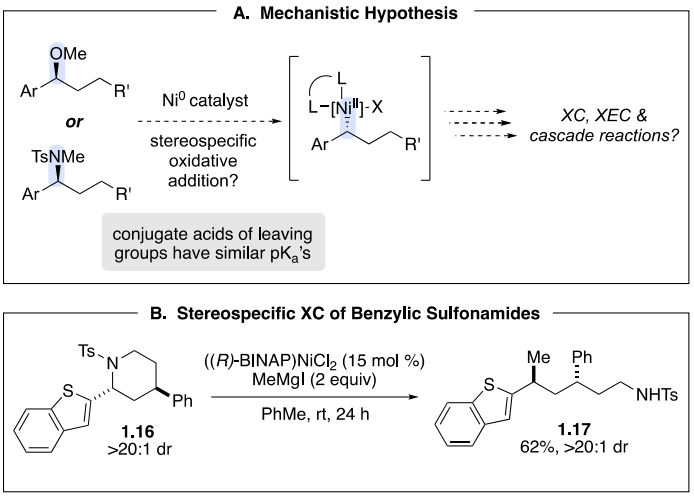


[16] Harris, M. R.; Hanna, E. L.; Greene, M. A.; Moore, C. E.; Jarvo, E. R. *J. Am. Chem. Soc.* **2013**, *135*, 3303–3306.
[17] Zhang, S.-Q.; Taylor, B.L. H.; Ji, C.-L.; Gao, Y.; Harris, M. R.; Hanna, L. E.; Jarvo, E.R.; Houk, K. N.; Hong, X. *J. Am. Chem. Soc.* **2017**, *139*, 12994–13005.

As we learned more about the mechanisms of these reactions, we determined that oxidative addition is frequently the rate-determining step of the catalytic cycle. In the case of Kumada-type coupling reactions of benzylic ethers, oxidative addition is accelerated by coordination of Lewis-acidic magnesium salts.[18,19] We were inspired by analogy to traditional S_N2 and S_N2' reactions and sought to determine whether the guiding principles that helped design substitution reactions could also be instructive in the context of cross-coupling. In particular, we wanted to probe whether leaving groups that have conjugate acids with similar pKa's would behave similarly in a coupling reaction, cementing the importance of the S_N2-like oxidative addition. Sulfonamides have similar pKa's to alcohols, and therefore we hypothesized that they would react similarly to ethers (Scheme 1.4A). Indeed, under the same reaction conditions employed for ethers, sulfonamides and sulfonyl piperidines such as **1.16** underwent ring-opening Kumada-type coupling with clean inversion at the benzylic center (Scheme 1.4B).[20, 21]

Scheme 1.4. Leaving Group Stability as a Predictor for Stereospecific OA

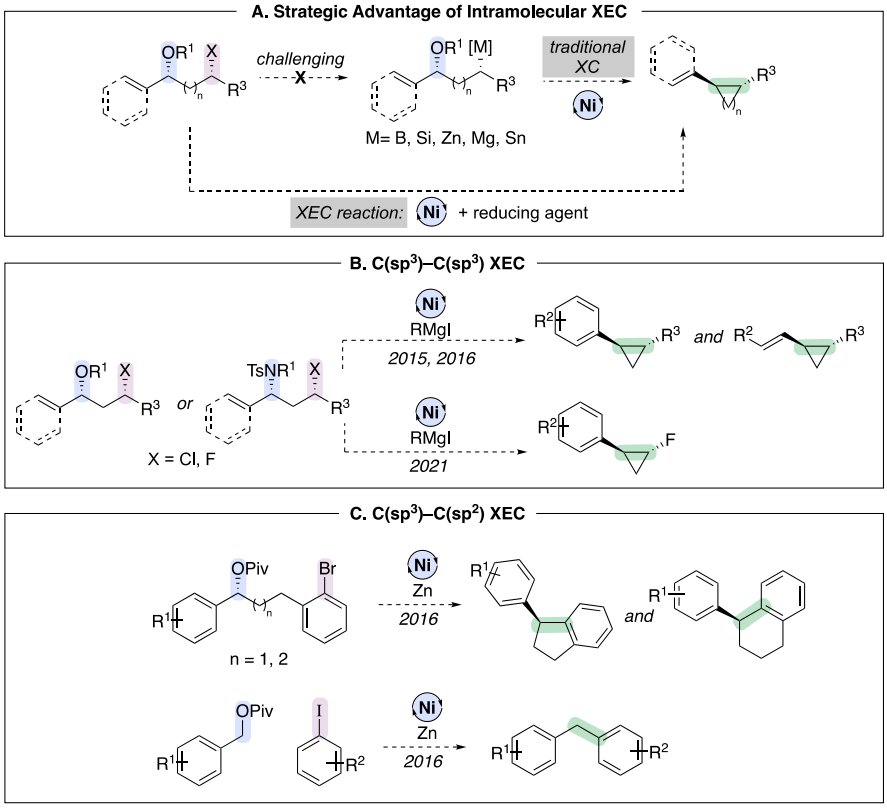
[18] Chen, P.-P.; Lucas, E. L.; Greene, M. A.; Zhang, S.; Tollefson, E. J.; Erickson, L. E.; Taylor, B. L.; Jarvo, E. R.; Hong, X. *J. Am. Chem. Soc.* **2019**, *141*, 5835−5855.
[19] Felkin, H.; Swierczewski, G. *Tetrahedron Lett.* **1972**, *15*, 1433–1436.
[20] Hewitt, K. A.; Herbert, C. A.; Matus, A. C.; Jarvo, E. R. *Molecules*, **2021**, *26*(19), 5947.
[21] More activated amine derivatives, such as aziridines, trimethylammonium and pyridinium salts, also undergo nickel-catalyzed XC. See: (a) Huang, C.-Y.; Doyle, A. G. *J. Am. Chem. Soc.* **2012**, *134*, 9541–9544. (b) Maity, P.; Shacklady-McAtee, D. M.; Yap, G. P. A.; Sirianni, E. R.; Watson, M. P. *J. Am. Chem. Soc.* **2013**, *135*, 280–285. (c) Basch, C. H.; Liao, J.; Xu, J.; Piane, J. J.; Watson, M. P. *J. Am. Chem. Soc.* **2017**, *139*, 5313–5316.



We hypothesized that a broad range of multi-step reactions could be initiated by stereospecific oxidative addition. One such application was in cross-electrophile coupling (XEC) reactions employing benzylic ethers, esters and sulfonamides. Our early efforts focused on intramolecular reactions, where a benzylic electrophile was tethered to a second electrophile, for ring-forming and annulation reactions (Scheme 1.5A). Such transformations demonstrate the potential benefit of XEC over XC, since XEC eliminates the challenge of transforming one electrophile to an organometallic reagent while tethered to a second electrophile. Despite this, intramolecular variants of XEC reactions have and continue to be significantly underrepresented as compared to intermolecular XEC.[22] We developed a series of stereospecific C(sp^3)–C(sp^3) coupling reactions that generate cyclopropanes (Scheme 1.5B) and C(sp^3)–C(sp^2) coupling reactions that generate indanes and tetralins (Scheme 1.5C).[23] Reactions were also expanded to include intermolecular arylation of benzylic esters.

[22] Yan, C. S.; Peng, Y.; Xu, X. B.; Wang, Y. W. *Chem. Eur. J.* **2012**, *18*, 6039–6048. (b) Xue, W.; Xu, H.; Liang, Z.; Qian, Q.; Gong, H. *Org. Lett.* **2014**, *16*, 4984–4987.
[23] Konev, M. O.; Hanna, L. E; Jarvo, E. R. *Angew. Chem. Int. Ed.* **2016**, *55*, 6730–6733

Scheme 1.5. XEC as a Strategy to Overcome of Challenges of Intramolecular XC



One challenge with intramolecular reactions was ensuring that starting material syntheses were practical, such that the XEC strategy could be competitive with alternative approaches towards similar carbocycles. We sought to employ starting materials that were readily available, ideally in a single step from commercial aldehydes or olefins (Figure 1.3A). For cyclopropane synthesis, we required synthetic access to 3-haloethers and sulfonamides, which was achieved by Prins, aza-Prins, and photochemical reactions (Figure 1.3B-D).

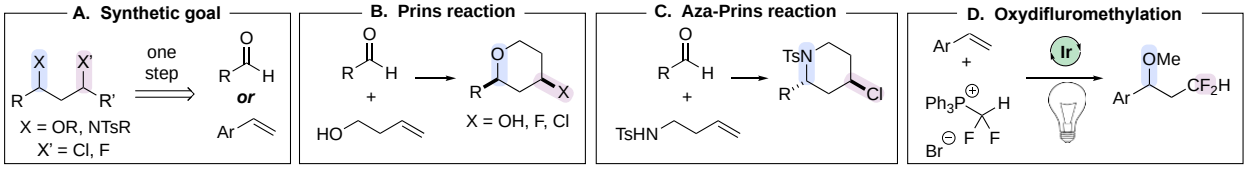
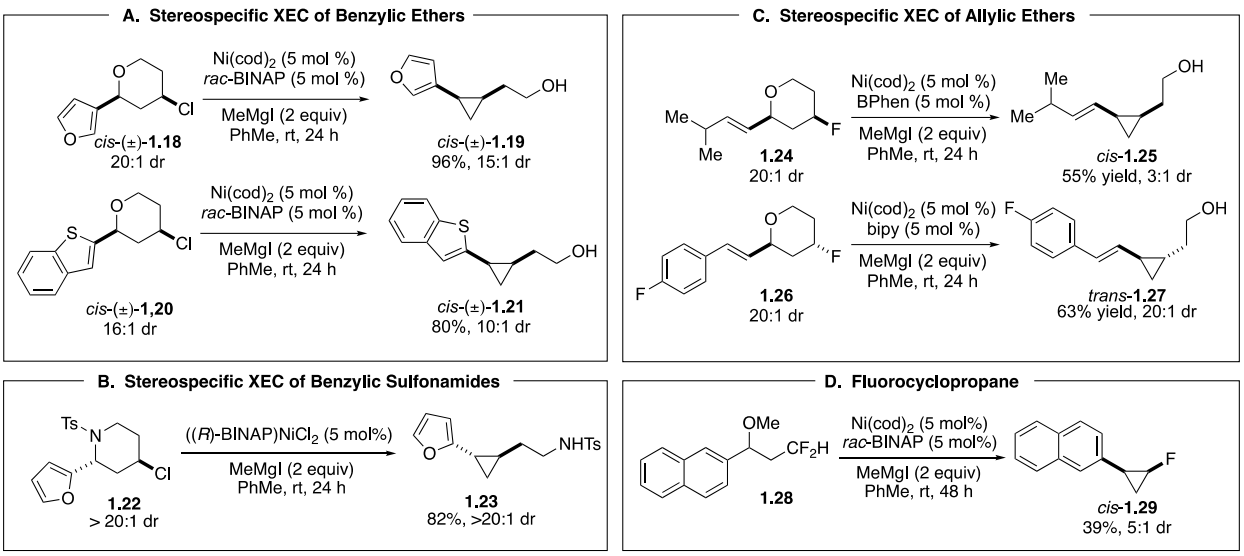


Figure 1.3. Key Design Principle: Rapid Access to Starting Materials from Commercially Available Aldehydes and Olefins.

Representative XEC reactions are shown in Scheme 1.6. Benzylic ethers and sulfonamides underwent smooth transformation in ring-contraction reactions of 4-chlorotetrahydropyrans and piperidines to afford cyclopropanes (Scheme 1.6A and B).[24] Interestingly, the optimal reaction conditions were identical to the conditions for Kumada-type coupling, however in this case the Grignard reagent served as the net reducing agent for the catalyst and was not incorporated into the reaction product. Allylic ethers also participated in intramolecular XEC reactions, including coupling with pendant alkyl fluorides (Scheme 1.6C).[25] Transformations were stereospecific with respect to both alkyl electrophiles, providing robust and predictable access to either diastereomer of substituted cyclopropanes. Inspired by the success of engaging an alkyl fluoride, we challenged the reaction with an intramolecular XEC reaction of geminal difluorides (Scheme 1.6D).[26] Substrates such as **1.28** underwent intramolecular XEC to provide highly strained fluorocyclopropanes.

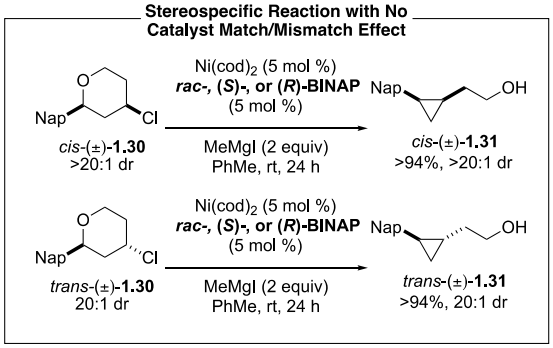
Scheme 1.6. Representative XEC Reactions of Benzylic and Allylic Ethers and Benzylic Sulfonamides.

[24] (a) Tollefson, E. J.; Erickson, L. W.; Jarvo, E. R. *J. Am. Chem. Soc.* **2015**, *137*, 9760–9763. (b) Lucas, E. L.; Hewitt, K. A.; Chen, P. -P.; Castro, A. J.; Hong, X.; Jarvo, E. R. *J. Org. Chem.* **2020**, *85,* 1775–1793.
[25] Erickson, L. W.; Lucas, E. L.; Tollefson, E. J.; Jarvo, E. R. *J. Am. Chem. Soc.* **2016**, *138*, 14006–14011.
[26] Lucas, E. L.; McGinnis, T. M.; Castro, A. J.; Jarvo, E. R. *Synlett* **2021**, *32*, 1525–1530.



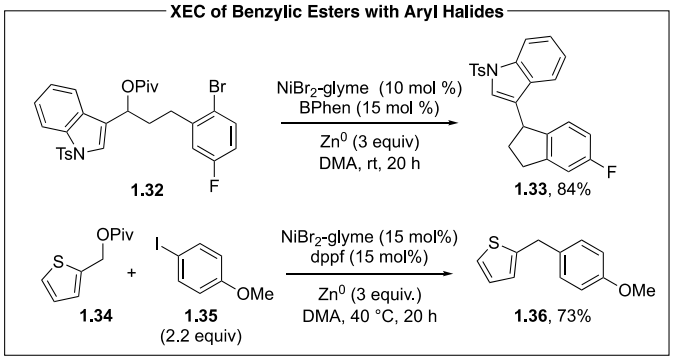
We were curious about the stereochemical outcomes of these transformations. In the XEC reactions where BINAP was employed as a ligand, match-mismatch experiments were conducted to probe the catalyst effects on the diastereoselectivity of the reactions. A representative test case is shown in Scheme 1.7. We found that the *cis*-tetrahydropyran **1.30** cleanly converts to *cis*-cyclopropane **1.31** while the other diastereomer, *trans*-tetrahydropyran **1.30** affords *trans*-cyclopropane **1.31**, irrespective of the enantiomer of ligand. Therefore, we do not observe a catalyst match-mismatch effect for this substrate, consistent with our observations across a range of other enantioenriched substrates in XC and XEC reactions.

Scheme 1.7. Investigation of Stereochemical Outcomes of of XEC Reaction



We further expanded intramolecular XEC into the synthesis of 5- and 6-membered rings by tethering benzylic esters to aryl halides (Scheme 1.8).[27] This reaction provided a new synthesis of indanes and tetralins. It also translated well as a template for intermolecular $C(sp^2)$–$C(sp^3)$ coupling reactions (Scheme 1.8). The mechanism is currently under investigation and is anticipated to be significantly different than $C(sp^3)$–$C(sp^3)$ couplings, due to the sp^2-hybridization of one of the electrophilic carbons.

Scheme 1.8. Activation of Benzylic Esters for Reductive $C(sp^3)$–$C(sp^2)$ Coupling Reactions

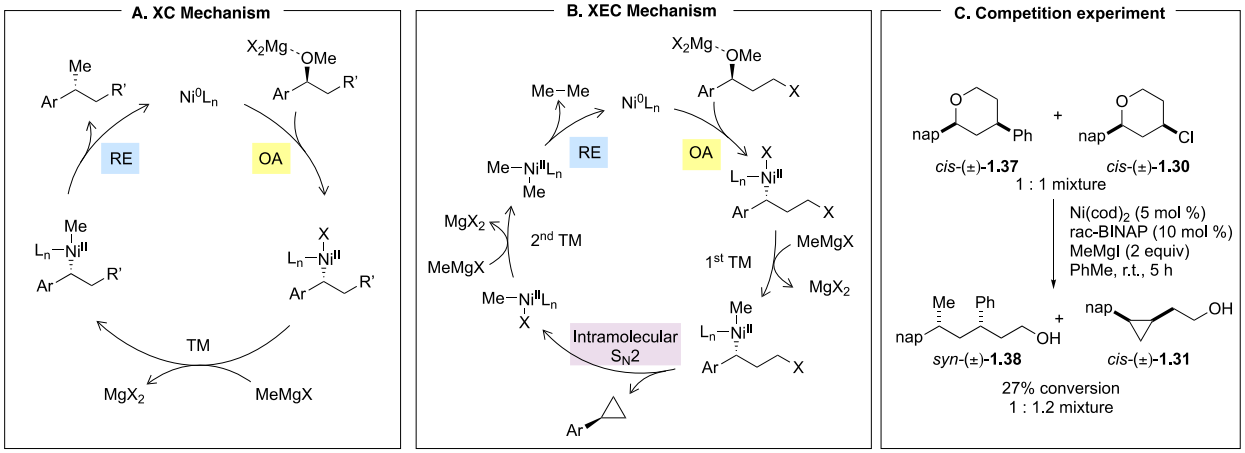


As part of reaction development, we interrogated the mechanisms of each transformation, with a particular focus on $C(sp^3)$–$C(sp^3)$ XC and XEC reactions. Key features of important elementary steps, delineated in the context of Kumada-type reactions, translated cleanly to the mechanisms of more complex reactions including Csp^3–Csp^3 XEC reactions employing Grignard reagents (Scheme 1.9A and B).[28,29] In particular, oxidative addition (OA) is a key step that controls the stereospecific reaction outcome. Experimental and theoretical investigations underscored that, for both the XC and XEC reactions, this elementary step initiates both catalytic cycles, is accelerated

[27] See reference 23.
[28] See reference 18.
[29] Zhang, S.-Q.; Hong, X. Mechanism and Selectivity Control in Ni- and Pd-Catalyzed Cross-Couplings Involving Carbon-Oxygen Bond Activation. *Acc. Chem. Res.* **2021**, *54*, 2158–2171.

by Lewis acidic magnesium salts, proceeds with inversion at the benzylic stereogenic center, and has a barrier height of approximately 20 kcal/mol.[30] Both mechanisms also involve a reductive elimination (RE) step that regenerates the nickel(0) catalyst from the nickel(II) intermediate, and the barrier height is often calculated to be within a few kcal/mol of the oxidative addition. A competition experiment was used to support the mechanistic similarity of the oxidative addition step and that this step initiates both catalytic cycles (Scheme 1.9C). Subjecting an equimolar mixture of 4-phenyltetrahydropyran **1.37** and 4-chlorotetrahydropyran **1.30** to Grignard reagent in the presence of nickel catalyst resulted in formation of a 1:1.2 mixture of Kumada-type and cyclopropane products. This result is consistent with the proposal that both catalytic cycles are initiated by virtually identical oxidative addition events.

Scheme 1.9. Comparison of Mechanisms for Kumada-type XC and XEC Reactions Using Grignard Reagent



For XEC reactions of 1,3-dielectrophiles, we have determined that the new C–C bond of the cyclopropane is formed via a stereospecific intramolecular S_N2-type reaction. Importantly, this mechanism does not correlate to those commonly reported for other XEC reactions, including the

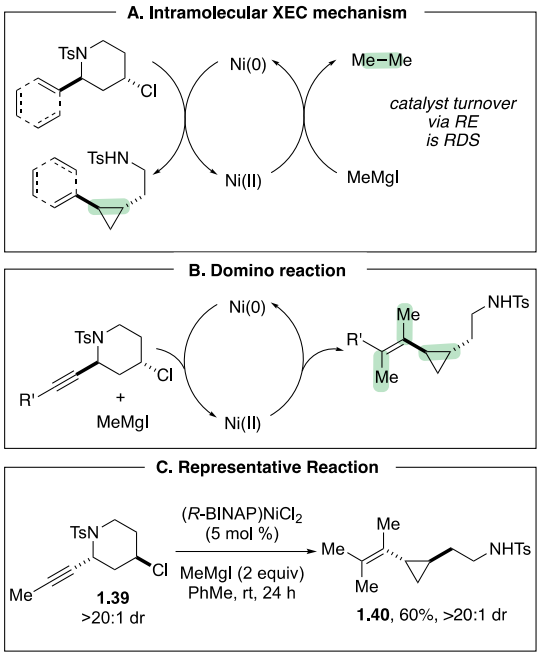
[30] See reference 18.

sequential reduction and radical chain mechanisms proposed for intermolecular XEC reactions. [31] Sequential reduction and radical chain mechanisms typically involve two net OA events (via polar or radical intermediates), four oxidation states of the catalyst [Ni(0), Ni(I), Ni(II) and Ni(III) intermediates], and the C–C bond of the product is generated by reductive elimination.[32] Our mechanism involves only one OA event and only two catalyst oxidation states [Ni(0) and Ni(II) intermediates].

We hypothesized, based on our mechanistic evidence, that the resting state for intramolecular XEC reaction is a nickel(II) intermediate[33], providing an opportunity to further engage the catalyst in additional C–C bond forming steps (Scheme 1.10A). We have established a domino reaction of 2-alkynylpiperidines, which accomplishes ring contraction of the 4-chloropiperidine moiety as well as dicarbofunctionalization of the alkyne moiety (Scheme 1.10B and C).[34] This reaction is similar to our other XEC reactions as we hypothesize that the first step is oxidative addition of the activated C–N bond.

Scheme 1.10. Domino Reaction of Alkynylpiperidines

[31] For mechanisms of intermolecular XEC reactions, see: (a) Knappke, C. E. I.; Grupe, S.; Gärtner, D.; Corpet, M.; Gosmini, C.; von Wangelin, A. J. *Chem. Eur. J.* **2014**, *20*, 6828–6842. (b) Everson, D. A.; Shrestha, R.; Weix, D. J. *J. Am. Chem. Soc.* **2010**, *132*, 920–921. (c) Cherney, A. H.; Reisman, S. E. *J. Am. Chem. Soc.* **2014**, *136*, 14365.
[32] For a discussion of the common mechanisms of XEC reactions, see: Weix, D. J. *Acc*. *Chem. Res.* **2015**, *48*, 6, 1767–1775.
[33] Dawson, D. D.; Oswald, V. F.; Borovik, A. S.; Jarvo, E. R. *Chem. Eur. J*. **2020**, *26*, 3044–3048.
[34] Hewitt, K. A.; Xie, P.-P.; Thane, T. A.; Hirbawi, N.; Zhang, S.-Q.; Matus, A. C.; Lucas, E. L.; Hong, X. ; Jarvo, E. R. *ACS Catal*. **2021**, *11*, 14369–14380.



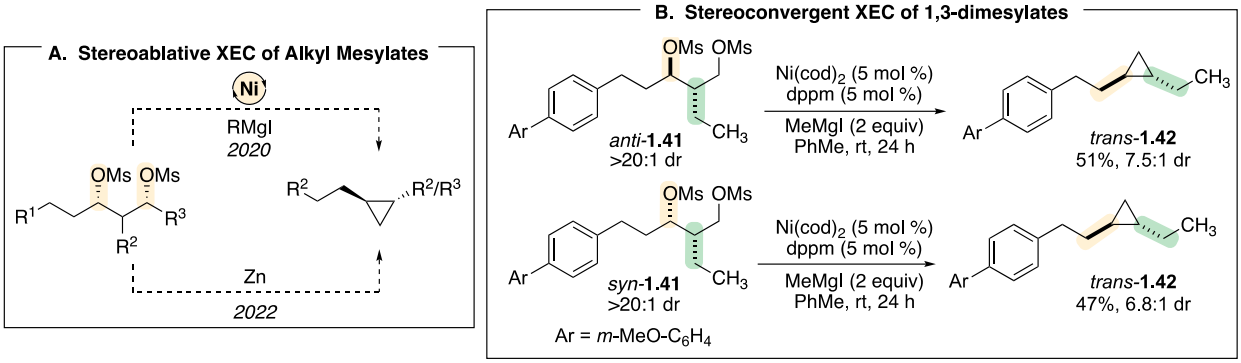
1.3 Stereoablative Reactions of Alcohol Derivatives.

In order to engage a broader range of substrates, we sought alternative methods for activation of alkyl alcohols. For benzylic and allylic ethers, ligation by the arene or olefin facilitates the oxidative addition step, and a π-benzylnickel intermediate is generated, such that a poor leaving group (typically alkoxide) is tolerated. To approach less activated alkyl substrates, where ligation is not possible and subsequent organonickel complexes are not stabilized by conjugation, we examined a series of activating groups. Our group first demonstrated this concept in an intramolecular XEC reaction of 1,3-dimesylates (Scheme 1.11A).[35] Under similar reaction conditions to those employed with benzylic ethers, in the presence of a nickel catalyst and stoichiometric Grignard reagent, 1,3-dimesylates such as **1.41** are converted to cyclopropanes. Notably, the reaction is stereoablative with respect to the secondary mesylate center, with both

[35] Sanford, A. B.; Thane, T. A.; McGinnis, T. M.; Chen, P.-P.; Hong, X.; Jarvo, E. R. *J. Am. Chem. Soc.* **2020**, *142*, 5017–5023.

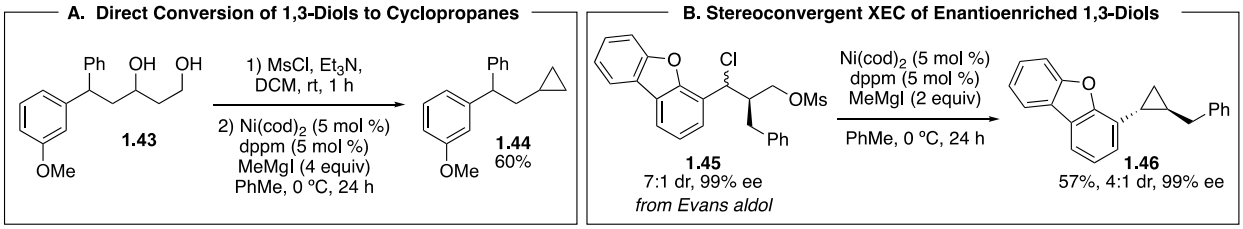
diastereomers of dimesylate **1.41** providing *trans*-cyclopropane **1.42** as the major product (Scheme 1.11B).

Scheme 1.11. Stereoconvergent XEC Reactions of 1,3-dimesylates



We developed the scope of this reaction to include a broad range of alkyl 1,3-diols, including establishing one-pot conditions for direct conversion of 1,3-diols to cyclopropanes (Scheme 1.12A). A significant benefit of this reaction is that starting materials can be prepared by enantioselective aldol reactions, providing straightforward access to enantioenriched cyclopropanes (Scheme 1.12B). For example, an Evans aldol reaction was employed to prepare enantioenriched mesylate **1.45**. Subsequent nickel-catalyzed XEC reaction proceeded to provide the desired *trans*-cyclopropane **1.46** in 99% ee.

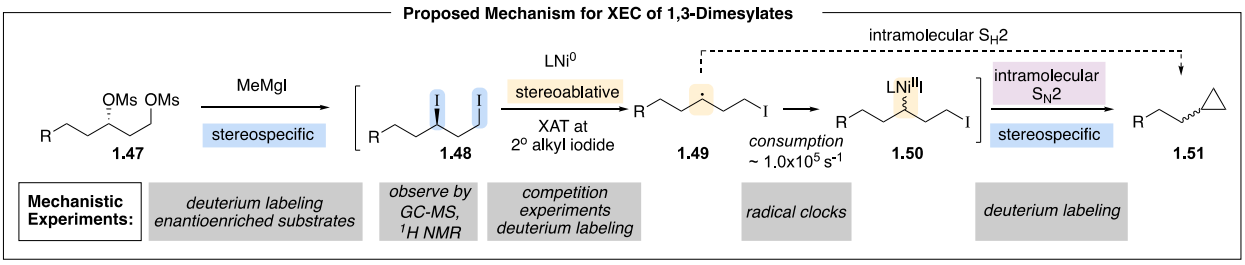
Scheme 1.12. In-situ Conversion of Readily Accessible 1,3-Diols to Cyclopropanes



To better understand and further develop this reactivity manifold, we have examined the mechanism of the reaction.[36] We determined that, in addition to serving as the terminal reductant, the Grignard reagent serves as a source of nucleophilic iodide and transforms dimesylate **1.47** to diiodide **1.48** in situ in a stereospecific S_N2 step.[37] Subsequent XAT of the secondary alkyl iodide generates an alkyl radical (**1.49**) that rapidly epimerizes.[38,39] Based on radical clock experiments, this radical is consumed at a rate competitive to 5-exo-trig cyclization. Secondary radical **1.49** can be captured to generate organonickel(II) complex **1.50**. Based on analysis with deuterium-labeled substrates, subsequent stereospecific ring closure provides cyclopropane **1.51**, proceeding with inversion at the primary electrophilic center (Scheme 1.13). Computational results are consistent with formation of organonickel complex **1.50**, however, direct S_H2 cyclization of secondary radical **1.49** is also possible. Since both pathways are expected to be stereospecific and proceed with inversion at the electrophilic carbon, we have not yet been able to distinguish between these two mechanisms experimentally.

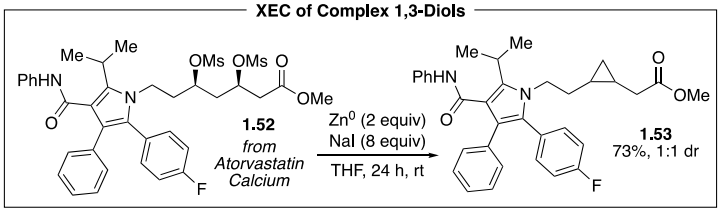
Scheme 1.13. Mechanistic Investigation of XEC of 1,3-Dimesylates

[36] (a) See reference 35. (b) Chen, P.-P.; McGinnis, T. M.; Lin, P. C.; Hong, X.; Jarvo, E. R. *ACS Catal*. **2023**, *13*, 5472–548.
[37] Hirbawi, N.; Lin, P. C.; Jarvo, E. R. *J. Org. Chem.* **2022**, *87*, 12352–12369.
[38] (a) Griller, D.; Ingold, K. U.; Krusic, P. J.; Fischer, H. *J. Am. Chem. Soc*. **1978**, *100*, 21, 6750–6752. (b) Hoffmann, R. W. *Chem. Soc. Rev.* **2003**, *32*, 225–230.
[39] For representative studies of nickel-mediated XAT, see: (a) Kehoe, R.; Mahadevan, M.; Manzoor, A.; McMurray, G.; Wienefeld, P.; Baird, M. C.; Budzelaar, P. H. M. *Organometallics* **2018**, *37*, 2450–2467. (b) Diccianni, J. B.; Katigbak, J.; Hu, C.; Diao, T. *J. Am. Chem. Soc*. **2019**, *141*, 1788–1796. (c) Greaves, M. E.; Ronson, T. O.; Maseras, F.; Nelson, D. J. *Organometallics* **2021**, *40*, 12, 1997–2007.



In order to improve the functional group compatibility of the XEC reaction, we sought to replace the unusual reducing agent, MeMgI, with a metal powder such as Zn or Mn, which are more commonly employed in related XEC reactions.[40] After evaluation of a series of reaction conditions, we determined that zinc powder, in the absence of a nickel catalyst, was capable of transforming dimesylates to cyclopropanes (Scheme 1.14).[41] Critical to the reaction was addition of stoichiometric quantities of an iodide salt, NaI, consistent with formation of alkyl iodides in situ as key intermediates. With these reaction conditions, we can engage a range of substrates bearing sensitive functional groups including a series derived from statins.

Scheme 1.14. Zn-mediated Synthesis of Cyclopropanes from Complex 1,3-Diols

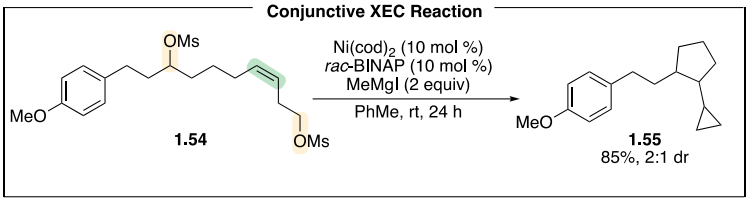


With an understanding of the key steps of the mechanism that allow for activation of the alkyl mesylate and formation of an alkyl radical, we also sought to employ this reactivity manifold for complex ring formation. A series of dimesylates, separated by pendant olefins, underwent

[40] See reference 29.
[41] McGinnis, T. M.; Thane, T. A.; Jarvo, E. R. *Org. Lett.* **2022**, *24*, 30, 5619–5623.

smooth cascade reactions to afford vicinal carbocycles such as **1.55** (Scheme 1.15).[42] These reactions proceed with modest diastereomeric ratios consistent with radical intermediates.

Scheme 1.15. Synthesis of Vicinal Carbocycles from Alkyl Dimesylates

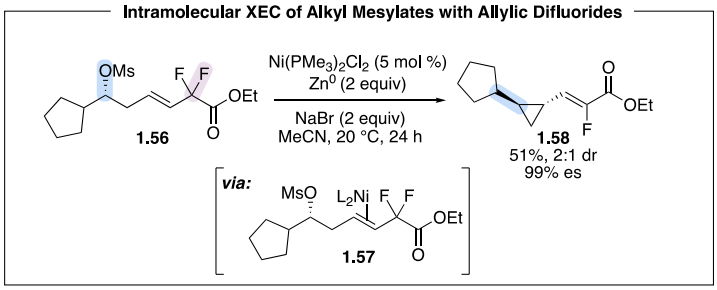


To further the scope and reactivity parameters of intramolecular XEC reactions, we sought to pair an alkyl mesylate with a different electrophile, as we had accomplished in the stereospecific series (e.g., Scheme 1.6). We hypothesized that allylic difluorides could serve as a suitable coupling partners. Upon subjection to the reaction conditions, we were pleased to see that mesylate **1.56** underwent nickel-catalyzed transformation to the desired fluorinated vinylcyclopropane **1.58** (Scheme 1.16).[43] During reaction optimization, we recognized that this transformation was significantly different than the XEC of 1,3-dimesylates. For example, in the presence of zinc as the reducing agent, the nickel catalyst was still required. In addition, iodide salts were detrimental to the reaction and bromide salts provided higher yields and fewer byproducts. Furthermore, we were surprised to observe that the reaction was enantiospecific and occurred cleanly with inversion at the alkyl mesylate. This result rules out a mechanism which involves formation of an alkyl radical intermediate. Experimental mechanistic investigations and theoretical computations performed by the Hirschi laboratory were consistent with formation of a stable olefin complex (**1.57**) that precedes oxidative addition. Indeed, low-valent nickel catalysts are known to have a

[42] Hewitt, K. A.; Herbert, C. A.; Jarvo, E. R. *Org. Lett.* **2022**, *24*, 32, 6093–6098.
[43] Lin, P. C.; Joshi, C.; McGinnis, T. M.; Chandra Mallojjala, S.; Sanford, A. B.; Hirschi, J. S.; Jarvo, E. R. *ACS Catal.* **2023**, *13*, 7, 4488–4499.

strong affinity for electron-poor alkenes.[44] These results underscore the continued mechanistic ambiguity associated with development of new nickel-catalyzed reactions.

Scheme 1.16. Allylic Difluorides as Intramolecular Coupling Partners



1.4 Multivariable Control of Mechanism of Oxidative Addition.

One challenge for the future of the field of nickel-catalyzed coupling reactions is reliable and predictive understanding of features that control the reactivity of nickel catalysts. Future reaction development is more fruitful when it can be guided by straightforward principles that are predictive toward reaction yield and stereochemical outcome. Indeed, mechanistic analysis in the context of palladium coupling reactions provided guidelines for ligand selection that propelled the field and contributed to a wide range of researchers embracing and employing XC reactions.[45] When compared to palladium catalysts, the possibilities for ligand-based mechanistic control are even greater with nickel catalysts due to their propensity to participate in a broader range of elementary steps. Therefore, delineating design principles that can favor certain pathways could be even more impactful.

---

[44] (a) Giovannini, R.; Studemann, T.; Dussin, G.; Knochel, P. *Angew. Chem. Int. Ed.* **1998**, *37*, 17, 2387–2390. (b) Estrada, J. G.; Williams, W. L.; Ting, S. I.; Doyle, A. G. *J. Am. Chem. Soc.* **2020**, *142,* 19, 8928–8937.
[45] (a) Hartwig, J. F. *Inorg. Chem.* **2007**, *46*, 1936–1947. (b) Littke, A. F.; Fu, G. C. *Angew. Chem. Int. Ed.* **1998**, *37*, 3387–3388. (c) Barder, T. E.; Walker, S. D.; Martinelli, J. R.; Buchwald, S. L. *J. Am. Chem. Soc.* **2005**, *127*, 4685–4696.

A design feature that was of interest to us was the control of the mechanism of oxidative addition for C(sp^3)-hybridized electrophilic carbons. Oxidative addition may occur by a two-electron reaction that mirrors a traditional S_N2 reaction and occurs with inversion. Alternatively, oxidative addition may proceed via one-electron steps via formation of an alkyl radical. The one-electron pathways are stereoablative, since the alkyl radical racemizes (or epimerizes) rapidly.[46,47] For transformations that construct new C(sp^3) stereogenic centers, favoring one mechanism for oxidative addition is critical in controlling the overall stereochemical outcome of the reaction.

Based on a broad range of XC and XEC reactions, we hypothesized that two variables control the mechanism of oxidative addition with alkyl electrophiles (Figure 1.4). The first, and most obvious, is the structure of the substrate, and in particular, the identity of the leaving group. The second feature appeared less obvious. Based on our analysis of literature examples as well as unpublished work from our own laboratory, we hypothesized that the ligand also played a role in determining whether oxidative addition proceeded smoothly and by which mechanism. In particular, we hypothesized that phosphine-based ligands tend to provide facile S_N2-type oxidative addition, while nitrogen-based (pyridyl, oxazoline, imidazoline, and amine-type) ligands tend to facilitate one-electron reactions that generate alkyl radicals (Figure 1.4). It is important to note that while the oxidation state of the catalyst is thought to differ between these modes of oxidative addition – nickel(0) complexes are thought to undergo two-electron oxidative addition while nickel(I) complexes are more prone to one-electron reactions – choice of precatalyst cannot reliably control the oxidation state of the active catalyst. Rapid redox reactions occur in situ, such

[46] (a) See reference 35. (b) See reference 36(b).
[47] Stille, J.K.; Cowell, A. B. *J. Organomet. Chem.* **1977**, *124*, 253–261.

that the oxidation state of the active complex may not match that of the precatalyst.[48,49,50] We have demonstrated that for certain reactions, nickel(0), nickel(I) and nickel(II) precatalysts all rapidly generate nickel(0) in situ, and are indistinguishable from a kinetic perspective.[51] Therefore, the oxidation state of the precatalyst will not provide predictive control over the oxidative addition mechanism. However, we hypothesized that the identity of the ligand could indeed favor intermediates of certain oxidation states, as well as influence the barrier heights for key elementary steps.

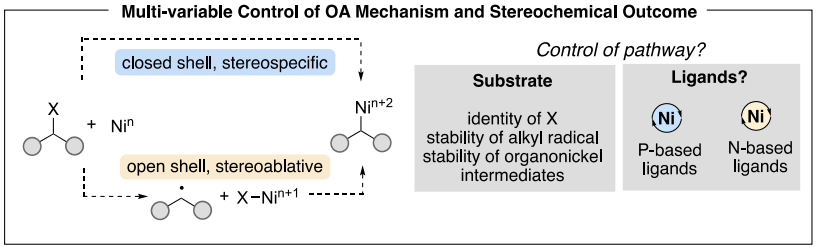


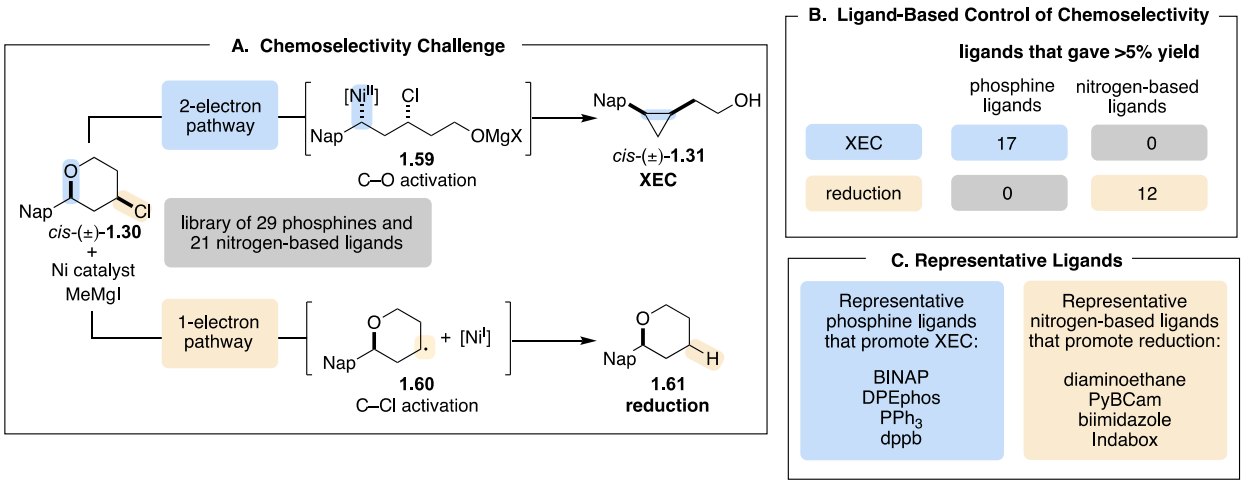
Figure 1.4. Multi-variable Control in Nickel-catalyzed Reactions

We sought a control reaction to test our hypothesis, where the catalyst would have the opportunity to engage in one- or two-electron pathways with a single substrate under a single set of reaction conditions. Divergent reactions of tetrahydropyran **1.30** provided this test reaction (Scheme 1.17A).[52] This substrate presents two electrophilic functional groups, a benzylic ether and an alkyl chloride. Alternatively, oxidative addition of the benzylic ether, which proceeds via a two-electron, S_N2-like transition state, leads to formation of cyclopropane **1.31** as the product. Oxidative addition of the alkyl chloride was established to proceed by XAT and formation of the

[48] Jahn, U. Topics in Current Chemistry, vol 320.; Springer, 2011; pp 323–451.
[49] For seminal studies, see: Morrell, D. G.; Kochi, J. *J. Am. Chem. Soc.* **1975**, *97*, 7262.
[50] Tamaru, Y. Modern Organonickel Chemistry. Wiley-VCH, 2005.
[51] See reference 18.
[52] Thane, T. A.; Jarvo, E. R. *Org. Lett.* **2022**, *24*, 5003–5008.

alkyl radical **1.60** leads to formation of reduced product **1.61**. Therefore, subjecting tetrahydropyran **1.30** to standard reaction conditions and varying the ligand would interrogate the ability of ligands to promote one reaction manifold over the other.

Scheme 1.17. Probing Ligand-Based Control of Chemoselectivity



We examined a series of fifty ligands, including many that are commonly employed in XC and XEC reactions. A selection of monodentate and bidentate phosphines, as well as nitrogen-based ligands including bipy derivatives and diamines, were incorporated. Interestingly, across the fifty ligands, only phosphine ligands provided >5% yield of the cyclopropane XEC product **1.31**, resulting from two-electron oxidative addition (Scheme 1.17B and C). In contrast, significant amounts of reduced tetrahydropyran **1.61** were only observed when nitrogen-based ligands were employed. These results are consistent with ligand-based control of electrophile preference and mechanism of oxidative addition. Further studies are ongoing to determine the generality of this trend and uncover the rationale that underlies the divergent reactivity preferences.

1.5 Conclusion

In this chapter we have highlighted our laboratory's contributions to the field of nickel-catalyzed XC and XEC reactions. We have demonstrated activation of benzylic C–O bonds in stereospecific Kumada, Suzuki, and Negishi-type $C(sp^3)$–$C(sp^3)$ XC reactions and adapted those principles to the development of new XEC reactions. By activation of alkyl alcohols as the corresponding mesylates we established stereoconvergent intramolecular XEC reactions of 1,3-diols. The methods developed and mechanistic analysis of the reaction pathways increases the potential for application of alkyl alcohol derivatives as electrophiles for XC and XEC reactions. Finally, we have begun to investigate the reaction features which differentiate stereospecific from stereoablative oxidative addition pathways and established that there is an interplay between multiple variables including leaving group and ligand structures. Specifically, comparison of phosphine-based versus nitrogen-based ligands demonstrates that they play a distinct role in facilitating formation of closed- versus open-shell intermediates. Future challenges for the field include continued development new $C(sp^3)$–$C(sp^3)$ bond-forming reactions for late-stage functionalization of alcohols. For example, intramolecular reactions that generate a range of ring sizes (e.g., from 1,4-diols, 1,5-diols and 1,6-diols) would provide exciting annulation strategies that would have profound impact on the conformations of complex diols. Expansion to include intermolecular, cross-selective reactions of two diols would also be an important step forward for functionalization (e.g., methylation) as well as fragment coupling. From a mechanistic perspective, further definition of the key features of multivariable control in nickel-catalyzed XC and XEC reactions will be critical in improving our understanding of the factors that underlie reactivity and our ability to predict and design new selective catalytic transformations.

Chapter 2

Nickel-catalyzed Kumada Cross-Coupling Reaction of Benzylic Sulfonamides

2.1 Introduction

In 2010 Richard Heck, Ei-Ichi Negishi, and Akira Suzuki were awarded the Nobel Prize in chemistry for their work developing palladium-catalyzed cross-coupling chemistry.[1] In the decades since this work was first pioneered, cross-coupling reactions have become a ubiquitous tool in the synthetic chemist's arsenal for C–C bond formation. Traditional cross-coupling reactions such as the Suzuki, Negishi, and Heck reactions were developed using palladium as the transition metal catalyst.[2] Later work demonstrated that many of these same transformations can be accomplished with nickel catalysts.[3] During this time, two nickel-catalyzed cross-coupling reactions with Grignard reagents were developed independently by Kumada and Corriu. Kumada subsequently investigated the scope and selectivity of these reactions, leading to widespread applications of "Kumada-type" reactions.[4]

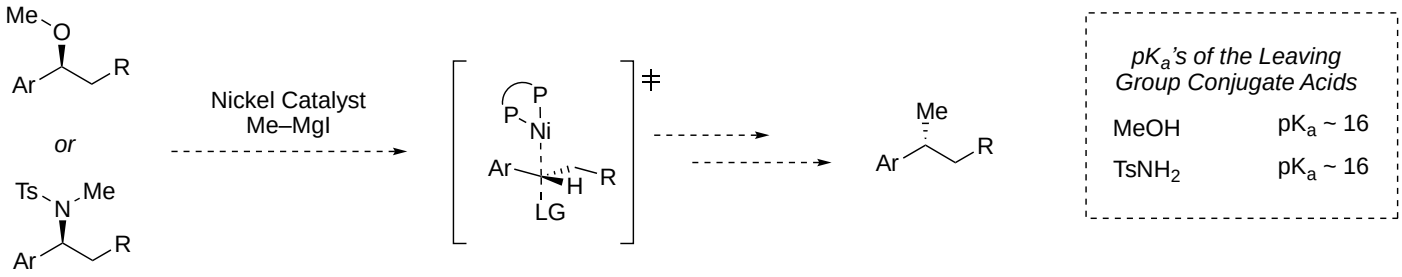
Initial Kumada coupling reactions demonstrated remarkable selectivity in coupling of alkyl and aryl Grignard reagents with aryl, vinyl, and even alkyl halogenated electrophiles.[5,6] In

[1] Portions of this chapter have been published in Molecules: Hewitt, K. A.; Herbert, C. A.; Matus, A. C.; Jarvo, E. R. *Molecules* **2021**, *26*, 5947–5971.
[2] (a) Miyaura, N.; Suzuki, A. *J. Chem. Soc., Chem. Commun.* **1979**, 866–867. (b) Miyaura, N.; Yamada, K.; Suzuki, A. *Tet. Lett.* **1979**, 3437–3440. (c) Miyaura, N.; Yanagi, T.; Suzuki, A. *Synth. Commun.* **1981**, *11*, 513–519. (d) Baba, S.; Negishi, E. *J. Am. Chem. Soc.* **1976**, *98*, 6729–6731. (e) King, A. O.; Okukado, N.; Negishi, E. *J. Chem. Soc., Chem. Commun.* **1977**, 683–684. (f) Heck, R. F. *J. Am. Chem. Soc.* **1968**, *90*, 5518–5516. (g) Mizoroki, T.; Mori, K.; Ozaki, A. *Bull. Chem. Soc. Jpn.* **1971**, *44*, 581.
[3] (a) Han, F. -S. *Chem. Soc. Rev.* **2013**, *42*, 5270–5298. (b) Phapale, V. B.; Cárdenas, D. J. *Chem. Soc. Rev.* **38**, 1598–1607. (c) Bhakta, S.; Ghosh, T. *Adv. Synth. Catal.* **2020**, *362*, 5257–5274. (d) Alisha, M.; Philip, R. M.; Anilkumar, G. *Eur. J. Org. Chem.* **2022**, e202101384.
[4] Cherney, A. H.; Kadunce, N. T.; Reisman, S. E. *Chem. Rev.* **2015**, 115, 9587–9652.
[5] (a) Corriu, R. J. P.; Masses, J. P.; *J. S. C. Chem. Comm.* **1972**, 144. (b) Tamao, K.; Sumitami, K.; Kumada, M. *J. Am. Chem. Soc*. **1972**, *94*, 4374–4376. (c) Tamao, K.; Kiso, Y.; Sumitami, K.; Kumada, M. *J. Am. Chem. Soc.* **1972**, *94*, 9268–9269.
[6] Tamao, K.; Sumitami, K.; Kumada, M. *J. Am. Chem. Soc*. **1972**, *94*, 4374–4376.

following years, synthetic chemists have explored the array of electrophiles that can be activated in Kumada coupling reactions.

For example, our group has previously developed stereospecific Kumada XC reactions that proceed through nickel-catalyzed oxidative addition into C–O bonds. In this work, methyl, alkyl, and cyclic ethers were found to undergo Kumada-type coupling with methyl and aryl Grignard reagents.[7] Inspired the C–O activation of C(sp^3) electrophiles, we were interested in exploring the translation of this reactivity to a C–N C(sp^3) electrophile. We hypothesized that a sulfonamide could have a similar leaving group ability due to the similarity in basicity between the ether leaving group and a tosyl amine (Scheme 2.1).

Scheme 2.1. C–O vs. C–N Activation.

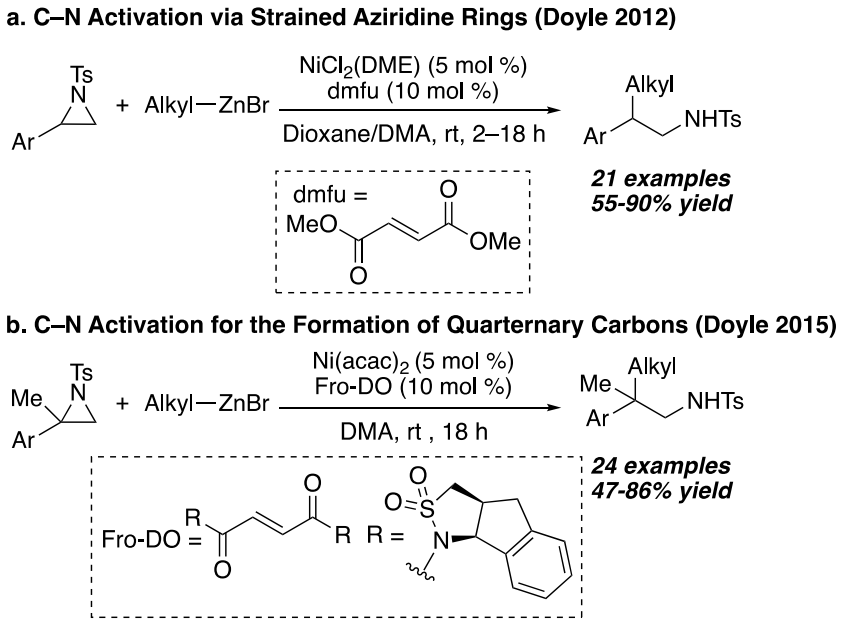


Previous synthetic strategies that have been used to activate benzylic amine derivatives elegantly incorporate the C–N bond into a synthetic intermediate that is primed for oxidative addition. For example, strained aziridine rings have been found to undergo oxidative addition with Ni(0) and Ni(II) complexes.[8] The Doyle group has harnessed this reactivity in catalytic Negishi

[7] (a) Taylor, B. L. H.; Swift, E. C.; Waetzig, J. D.; Jarvo, E. R. J. *Am. Chem. Soc.* **2011**, *133*, 389−391. (b) Greene, M. A.; Yonova, I. M.; Williams, F. J.; Jarvo, E. R. *Org. Lett.* **2012**, *14* (16), 4293−4296. (c) Taylor, B. L. H.; Harris, M. R.; Jarvo, E. R. *Angew. Chem., Int. Ed.* **2012**, *51*, 7790−7793. (d) Tollefson, E. J.; Dawson, D. D.; Osborne, C. A.; Jarvo, E. R. *J. Am. Chem. Soc.* **2014**, *136*, 14951−14958.
[8] Lin, B. L.; Clough, C. R.; Hillhouse, G. L.; *J. Am. Chem. Soc.* **2002**, *124*, 2890–2891.

reactions of styrenyl aziridine rings.[9] They propose that oxidative addition affords an azametallacyclobutane intermediate, first reported by Hillhouse[10] and subsequent reductive elimination is aided by the coordination of an electron deficient olefin (Scheme 2.2). While this reaction is highly regieoselective, one limitation to this work is the lack of stereocontrol. While future efforts from the Doyle group were directed at developing enantioselective variants of these reactions, they note that few methods are available for the asymmetric synthesis of styrenyl aziridines and they observe erosion of ee when enantioenriched aziridines are subjected to the reaction conditions.

Scheme 2.2. Activation of Benzylic Sulfonamides via Ring Strain.

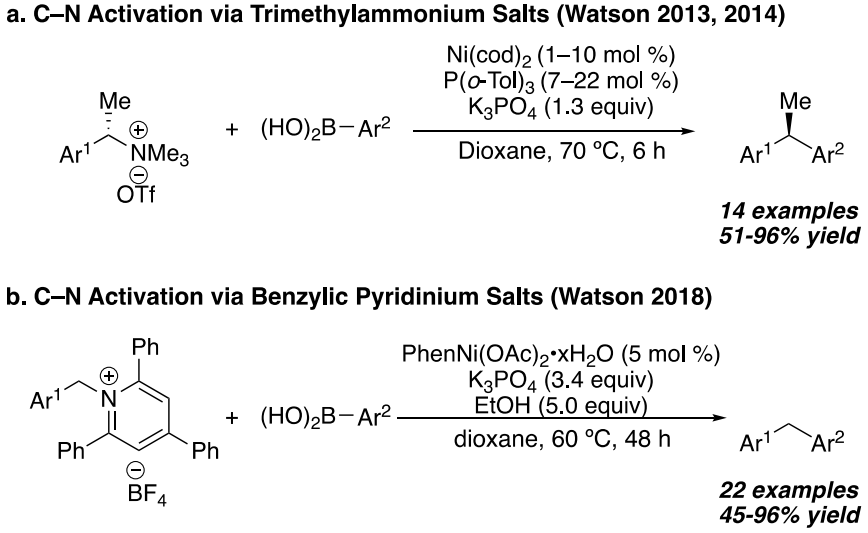


In an alternative synthetic strategy, the Watson group activated benzylic amine derivatives for stereospecific nickel-catalyzed XC. This method activates the amine via a charged salt. Initial

[9] (a) Huang, C.–Y.; Doyle, A.G. *J. Am. Chem. Soc*. **2012**, *134*, 9541−9544. (b) Huang, C.–Y.; Doyle, A.G. *J. Am. Chem. Soc*. **2015**, *137*, 5638−5641.
[10] See reference 8.

efforts weakened the C–N bond via alkylation of tertiary benzylic amines to afford trimethyl ammonium salts.[11] These benzylic ammonium triflates were found to readily undergo enantiospecific Suzuki-type XC reactions with aryl and vinyl boronic acids (Scheme 2.3). The Watson group has also harnessed this method of electronic C–N activation in nickel-catalyzed Suzuki XC reactions by converting benzylic amine derivatives into Katritzky salts.[12] Interestingly, while the authors hypothesized that the trimethylammonium salts proceed through an S_N2-type oxidative addition with the nickel-catalyst, they propose that the reactions with the Katritzky salts proceed through stabilized benzylic radical intermediates.[13]

Scheme 2.3. Activation of Benzylic Sulfonamides via Charged Salts.



While these methods highlight the clever use of both electronic and strain activation of C–N bonds, we set out to develop a stereospecific XC method with less activated benzylic amine

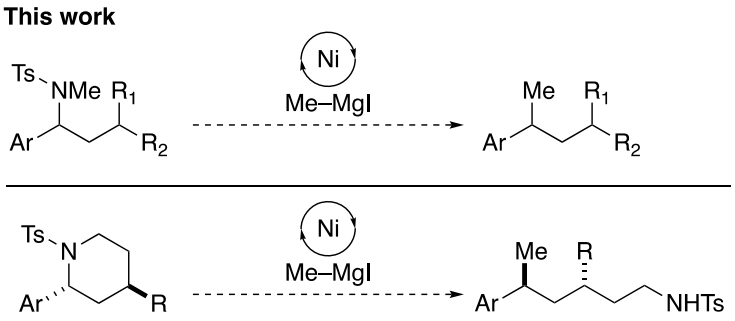
[11] (a) Maity, P.; Shacklady-McAtee, D. M.; Yap, G. P. A.; Sirianni, E. P.; Watson, M. P. *J. Am. Chem. Soc.* **2012**, *135*, 280–285. (b) Shacklady-McAtee, D. M.; Roberts, K. M.; Basch, C. H.; Song, Y.-G.; Watson, M. P. *Tetrahedron* **2014**, *70*, 4257–4763.

[12] (a) Liao, J.; Guan, W.; Boscoe, B. P.; Tucker, J. W.; Tomlin, J. W.; Garnsey, M. R.; Watson, M. P. *Org. Lett.* **2018**, *20*, 3030–3033. (b) Guan, W.; Liao, J.; Watson, M. P. *Synthesis* **2018**, *50*, 3231–3237.

[13] (a) Basch, C. H.; Liao, J.; Xu, J.; Piane, J. J.; Watson, M. P. *J. Am. Chem. Soc.* **2017**, *139*, 5313–5316. (b) Tcyrulnikov, S.; Cai, Q.; Twitty, J. C.; Xu, J.; Atifi, A.; Bercher, O. P.; Yap, G. P. A.; Rosenthal, J.; Watson, M. P.; Kozlowski, M. C. *ACS Catal.* **2021**, *11*, 8456–8466.

derivatives (Scheme 2.4). We were especially interested in developing a method that could achieve $C(sp^3)$–$C(sp^3)$ coupling of a benzylic amine derivative. To do this, we chose to focus on benzylic sulfonamides as coupling partners because of their prevalence in medicinal agents, making this method attractive for late-stage functionalization of complex molecules.[14] We hypothesized that MeMgI would serve as an amenable coupling partner as it is easily prepared, relatively stable, and would allow for the facile installation of a methyl group. We have demonstrated that these nickel-catalyzed Kumada-type coupling reactions proceed in modest yields with both cyclic and acyclic sulfonamides. In contrast to previously developed work that proceeds through strained aziridine rings or charged Katritzky salts we have established a $C(sp^3)$–$C(sp^3)$ XC method with unstrained, uncharged benzylic amine derivatives which proceeds through a stereospecific pathway.

Scheme 2.4. Proposed Kumada XC Reaction of Benzylic Amine Derivatives.



2.2 Results and Discussion

2.2.1 Optimization of the Nickel-catalyzed Kumada Cross-Coupling Reaction

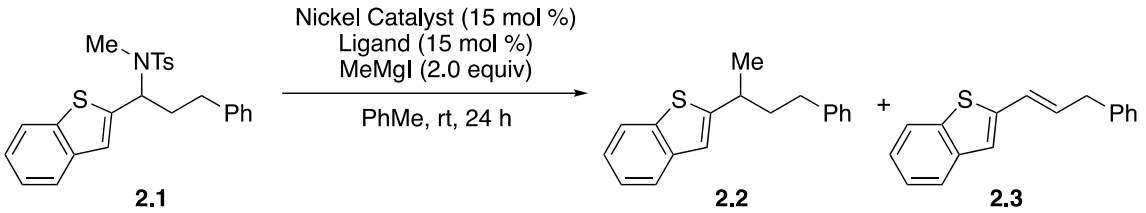
We began the optimization of the Kumada reaction on benzylic sulfonamide **2.1** (Table 2.1).[15] We initially focused our efforts on conditions that proved fruitful for the Kumada

[14] Ilardi, E. A.; Vitaku, E.; Njardarson, J. T. *J. Med. Chem.* **2014**, *57*, 2832–2842.
[15] Hewitt, K. A.; Herbert, C. A.; Matus, A. C.; Jarvo, E. R. *Molecules*, **2021**, *26*, 5947.

reactions of benzylic ethers. In our group's previous development of nickel-catalyzed Kumada reactions of benzylic ethers, $Ni(cod)_2$ precatalyst and *rac*-BINAP ligand efficiently provided cross-coupled product (entry 1).[16] These conditions afforded the desired Kumada coupled product **2.2** in a 25% yield with 19% recovered starting material (RSM), and 10% of styrene **2.3**, likely formed through the β-hydride elimination pathway. Increasing the catalyst loading added a slight increase in yield, but with a significant increase in undesired formation of **2.3** (entry 2). We next screened a series of ligands including bidentate phosphines, NHC, and a phenanthroline derivative (entries 3–7). However, only one of these ligands, SiMes·BF_4 exhibited activation of the sulfonamide electrophile (entry 6), albeit in significantly lower yield. Finally, we turned to an alternative precatalyst (entry 8). Inspired by previous work performed by our lab activating benzylic sulfonamides in cross-electrophile coupling (XEC) reactions, we employed an ((*R*)-BINAP)$NiCl_2$ precatalyst and were delighted to observe formation of Kumada product **2.2** in 54%.[17] We proceeded with this catalyst as the optimal conditions for the Kumada coupling reaction.

Table 2.1. Optimization of the Kumada XC Reaction[18]

[16] See reference 7(d).
[17] Lucas, E. L.; Hewitt, K. A.; Chen, P. -P.; Castro, A. J.; Hong, X.; Jarvo, E. R. *J. Org. Chem.* **2020**, *85*, 1775–1793.
[18] Optimization performed by Dr. Kirsten Hewitt.



2.1 **2.2** **2.3**

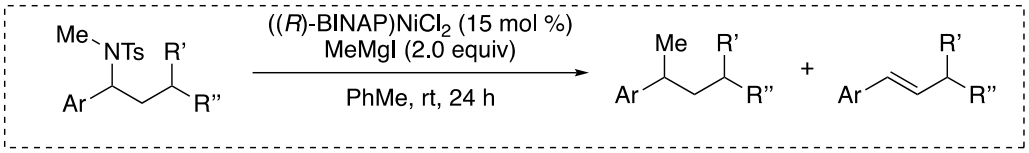
Entry	*Nickel Catalyst*	*Ligand*	*Yield 2.2 (%)[a]*	*Yield 2.3 (%)[a]*	*RSM 2.1 (%)[a]*
1[b]	$Ni(cod)_2$	*rac*-BINAP	25	10	19
2	$Ni(cod)_2$	*rac*-BINAP	34	30	7
3	$Ni(cod)_2$	DPEPhos	42	20	0
4	$Ni(cod)_2$	Xantphos	0	<5	37
5	$Ni(cod)_2$	dppe	0	<5	65
6	$Ni(cod)_2$	SiMes•BF_4	12	0	86
7	$Ni(cod)_2$	BPhen	0	0	61
8	((*R*)-BINAP)$NiCl_2$	–	54	40	0

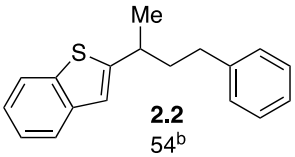
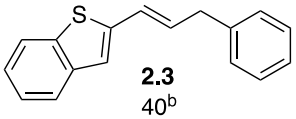
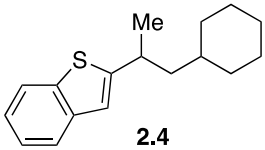
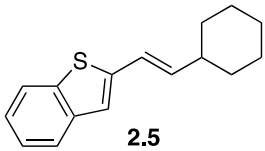
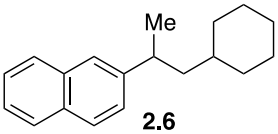
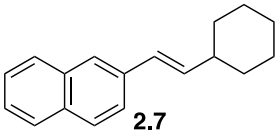
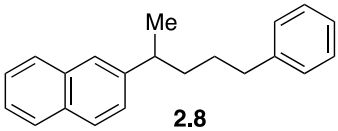
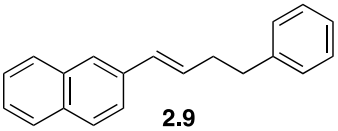
[a]Yields of **2.2** and **2.3** and recovered starting material (RSM) determined by ^1H NMR based on comparison to PhTMS as internal standard. [b]5 mol % $Ni(cod)_2$

2.2.2 Evaluation of Substrate Scope for the Kumada XC Reaction

With the optimized conditions in hand, we set about evaluating the scope of the Kumada XC reaction with acyclic benzylic sulfonamides. We hypothesized that branching at the β-position could potentially destabilize the conformation necessary for β-hydride elimination, thereby hindering the undesired pathway. We were pleased to see that this was indeed the case with substrates **2.4** and **2.6**. Surprisingly though, substrate **2.8**, which contained no β-branching performed best in the reaction affording the Kumada product in an 84% yield with just 13% **2.9**.

Table 2.2. Scope of Kumada XC Reaction with Acyclic Sulfonamides[19]



Yield Kumada Product (%)	*Yield Styrene (%)*
 **2.2** 54[b]	 **2.3** 40[b]
 **2.4** 48[a]	 **2.5** 30[b]
 **2.6** 69[b]	 **2.7** 22[b]
 **2.8** 84[b]	 **2.9** 13[b]

[a] Isolated Yield. [b] Yield determined by ^{1}H NMR based on comparison to PhTMS as internal standard.

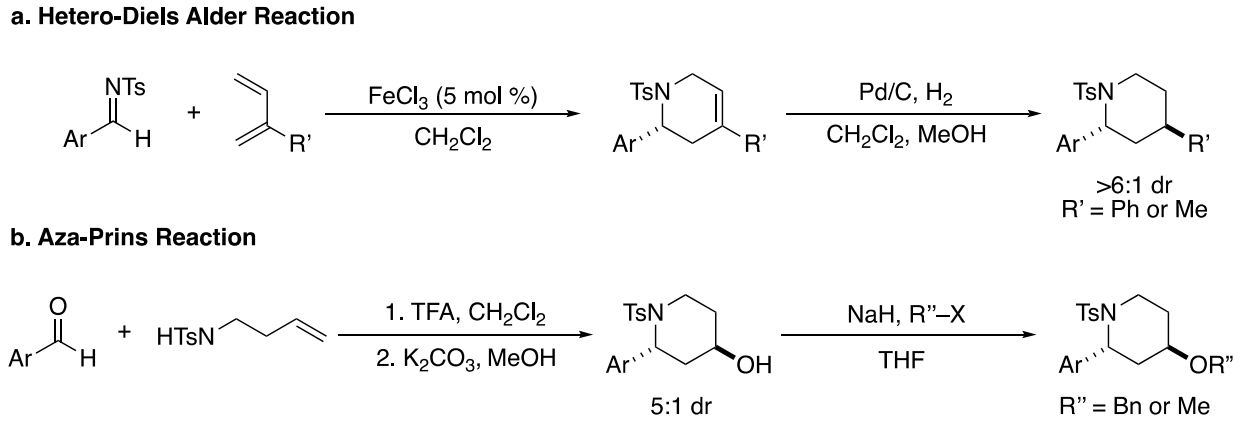
While we were excited by the demonstrated activation of these benzylic sulfonamides, there were two key features of the reaction we were still looking to optimize. The first was the presence of by-products formed through β-hydride elimination pathway which we hypothesized could potentially be dampened in the presence of more conformationally constricted substrates. The second facet we wanted to explore was the introduction of stereocontrol to the reaction. In an effort to optimize these two elements, we turned to aryl

[19] Substrates **2.4**, **2.6** and **2.8** were synthesized by Dr. Alissa Matus. Substrate **2.2** was synthesized by Dr. Kirsten Hewitt.

piperidines. We hypothesized that if we were going through a stereospecific mechanism, we could potentially make these poly-ketide-like fragments with 1,3 stereocenters upon ring opening. We synthesized these aryl piperidines in relatively high dr, affording separable diastereomers, using route (**a)** and route (**b)** (Scheme 2.5).

Both synthetic routes start from commercially available aryl aldehydes. In route (**a)**, N-tosyl imines are reacted with 1,3-dienes in a hetero-Diels Alder reaction to afford the unsaturated piperidine. The ring is then reduced under hydrogenation conditions to afford piperidines with phenyl or methyl substitution at the 4 position. In route (**b**), a TFA-mediated Aza-Prins reaction is utilized to afford 4-hydroxypiperidines from aryl aldehydes. Subsequent alkylation affords the protected ethers.

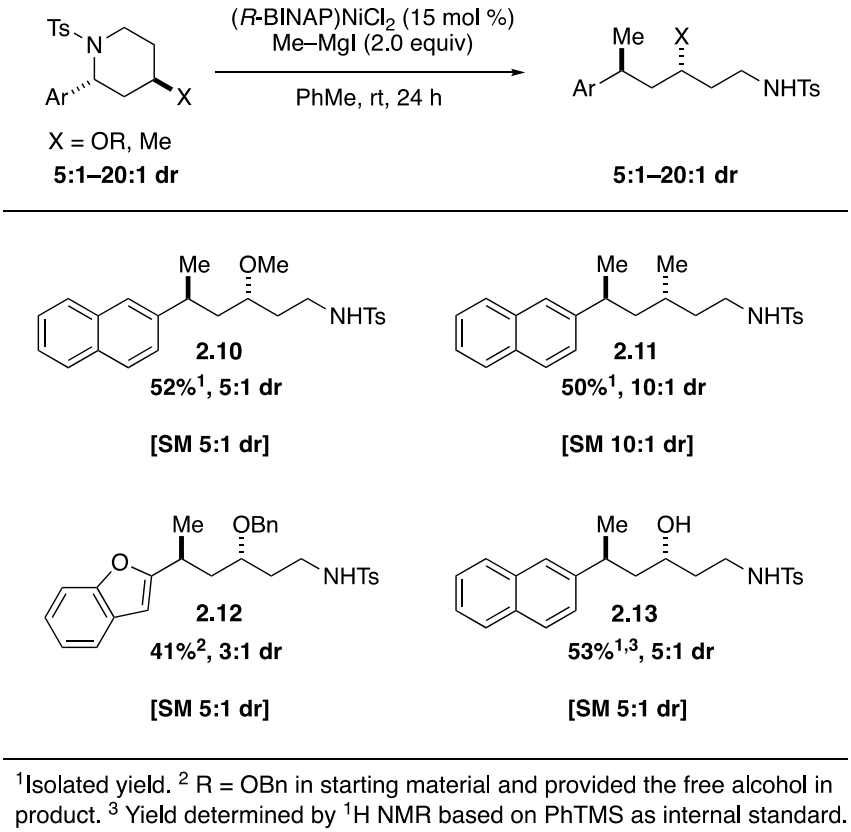
Scheme 2.5. Synthesis of Aryl Piperidines for Kumada XC Reaction.



We examined the scope of the nickel-catalyzed Kumada XC reaction of aryl piperidines with MeMgI (Scheme 2.6). We were pleased to observe that the reaction was tolerant of different aryl groups including heteroaromatic rings (**2.12**). In addition, the reaction was tolerant of both alkyl moieties (**2.11**), as well as alkyl ethers (**2.10, 2.12, 2.13**). Notably, we observed only minimal amounts of styrene by-products formed in the reaction, likely due to the coordination of the

pendant sulfonamide restricting the conformational pathway required for β-hydride elimination. Finally, the scope of the reaction with cyclic sulfonamides demonstrated retention of the diastereomeric ratios in the starting piperidines, indicating that the reaction likely proceeds through a stereospecific pathway.

Scheme 2.6. Scope of Kumada XC Reaction.



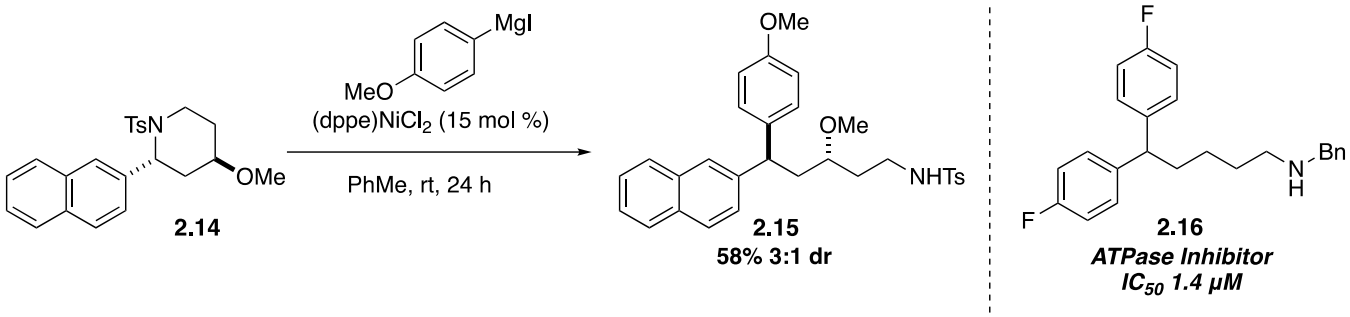
[1]Isolated yield. [2] R = OBn in starting material and provided the free alcohol in product. [3] Yield determined by ^{1}H NMR based on PhTMS as internal standard.

2.2.3 Synthesis of Diarylmethane

With rapid access to the 1,3 acyclic substitution pattern, we were interested in investigating what other structural motifs could be installed at the benzylic position (Scheme 2.7). In particular, we were interested in synthesizing analogues of the ATPase inhibitor **2.16**. To do this, we subjected piperidine **2.14** to modified reaction conditions with 4-methoxyphenyl

magnesium iodide and obtained the Kumada coupled product **2.15** in a 58% yield. This demonstrated access to the diarylmethane motif in just 3 synthetic steps from commercial aldehyde using our nickel-catalyzed Kumada XC method.

Scheme 2.7. Synthesis of Diarylmethane via Kumada XC Reaction



2.2.4 Proposed Mechanism of Kumada XC Reaction

We propose the following mechanism for the nickel-catalyzed Kumada XC reaction of benzylic sulfonamides based on previous experimental work performed by our laboratory and previous computational studies performed by the Hong laboratory.[20,21] We propose that initial reduction of the ((*R*)-BINAP)$NiCl_2$ to the active Ni(0) complex **2.17** is facilitated by the Grignard reagent. The Ni(0) catalyst will then engage the benzylic sulfonamide and undergo oxidative addition to afford the alkyl Ni(II) species **2.18**. We hypothesize that this step proceeds with inversion based on the stereochemical outcomes observed in the reaction. We also hypothesized that the oxidative addition step is rate-determining based on our previous

[20] See reference 17.
[21] Chen, P.-P. Lucas, E. L.; Greene, M. A.; Zhang, Q.-S.; Tollefson, E. J.; Erickson, L. W.; Taylor, B. L. H.; Jarvo, E. R.; Hong, X. *J. Am. Chem. Soc.* **2019**, *141*, 5835–5855.

studies. Following transmetalation with the Grignard reagent, reductive elimination from intermediate **2.19** affords the Kumada coupled product.

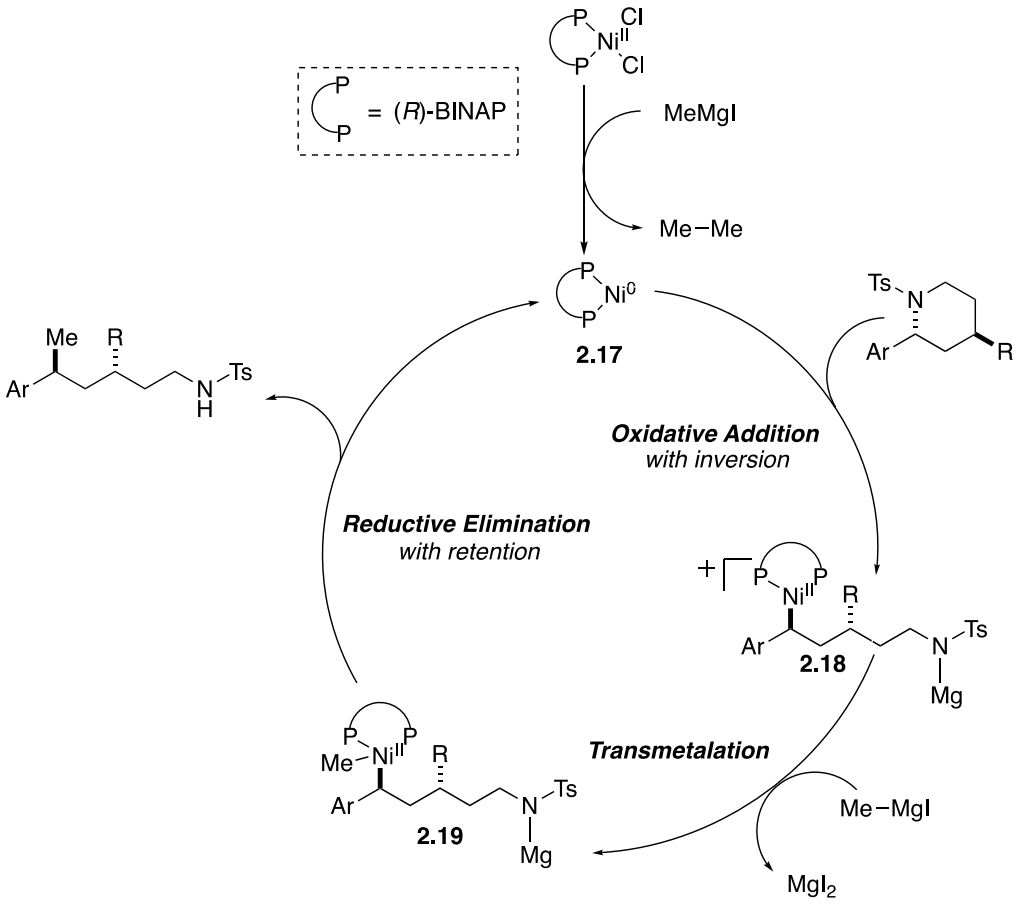


Figure 2.1. Proposed Mechanism of Kumada XC Reaction.

2.3 Conclusion

We have developed a nickel-catalyzed Kumada XC reaction of simple benzylic sulfonamides. In this reaction we provide $C(sp^3)$–$C(sp^3)$ coupled products from both acyclic benzylic sulfonamides and aryl piperidines with methyl magnesium iodide. Reactions of the aryl piperidines were demonstrated to be stereospecific and afford 1,3-acyclic fragments in high dr. This reaction demonstrates the first example of a nickel-catalyzed Kumada coupling of simple benzylic sulfonamides.

2.4 Experimental Details

2.4.1 General Procedures

All reactions were carried out under an atmosphere of N_2, or Ar when noted. All glassware was oven- or flame-dried prior to use. Tetrahydrofuran (THF), diethyl ether (Et_2O), dichloromethane (CH_2Cl_2), and toluene (PhMe) were degassed with Ar and then passed through two 4 X 36 inch columns of anhydrous neutral A-2 alumina (8 X 14 mesh; LaRoche Chemicals; activated under a flow of argon at 350 °C for 12 h) to remove H_2O.[22] All other solvents utilized were purchased anhydrous commercially, or purified as described. ^{1}H NMR spectra were recorded on Bruker DRX-400 (400 MHz ^{1}H, 100 MHz ^{13}C, 376.5 MHz ^{19}F), GN-500 (500 MHz ^{1}H, 125.4 MHz ^{13}C), or CRYO-500 (500 MHz ^{1}H, 125.8 MHz ^{13}C) spectrometers. Proton chemical shifts are reported in ppm (δ) relative to internal tetramethylsilane (TMS, δ 0.00). Data are reported as follows: chemical shift (multiplicity [singlet (s), broad singlet (br s), doublet (d), doublet of doublet (dd), doublet of doublet of doublets (ddd), doublet of doublet of doublet of doublets (dddd), doublet of triplet (dt), doublet of doublet of triplet (ddt), doublet of triplet of doublet (dtd), triplet (t), broad triplet (br t), triplet of doublet (td), triplet of doublet of doublet (tdd), triplet of triplet (tt), quartet (q), quartet of doublet (qd), quartet of doublet of doublets (qdd), quintet (quint), apparent quintet (appar quint), sextet, apparent sextet (appar sextet), multiplet (m)], coupling constants [Hz], integration). Carbon chemical shifts are reported in ppm (δ) relative to TMS with the respective solvent resonance as the internal standard (CDCl3, δ 77.16 ppm). Unless otherwise indicated, NMR data were collected at 25 °C. Infrared (IR) spectra were obtained on a Thermo Scientific Nicolet iS5 spectrometer with an iD5 ATR tip (neat) and are reported in terms of frequency of

[22] Pangborn, A. B.; Giardello, M. A.; Grubbs, R. H.; Rosen, R. K.; Timmers, F. J.. *Organometallics* **1996**, *15*, 1518–1520.

absorption (cm^{-1}). Analytical thin-layer chromatography (TLC) was performed using Silica Gel 60 F_{254} precoated plates (0.25 mm thickness). Visualization was accomplished by irradiation with a UV lamp and/or staining with $KMnO_4$ or CAM. Flash chromatography was performed using SiliaFlash F60 (40–63 μm, 60 Å) from SiliCycle. Automated chromatography was carried out on a Teledyne Isco CombiFlash Rf Plus. Melting points (m.p.) were obtained using a Mel-Temp melting point apparatus and are uncorrected. High resolution mass spectrometry was performed by the University of California, Irvine Mass Spectrometry Center.

Bis(1,5-cyclooctadiene)nickel was purchased from Strem, stored in a glove box freezer (–20 °C) under an atmosphere of N_2 and used as received. All ligands were purchased from Strem or Sigma Aldrich and were stored in a glovebox and used as received. The methylmagnesium iodide was titrated with iodine prior to use.[23] All other chemicals were purchased commercially and used as received, unless otherwise noted.

2.4.2 General Nickel-Catalyzed Kumada Cross-Coupling Reaction Procedures

2.4.2.1 Method A: Nickel-Catalyzed Kumada Cross-Coupling Reaction

In a glovebox, a flame-dried 7 mL vial equipped with a stir bar was charged with sulfonamide substrate (1.0 equiv), nickel precatalyst (15 mol %) and PhMe (0.10–0.20 M in substrate). The Grignard reagent (2.0 equiv) was then added dropwise via a syringe. After 24 h, the reaction was removed from the glovebox, quenched with methanol, filtered through a plug of silica gel eluting with 100% Et_2O and concentrated in vacuo. Phenyltrimethylsilane (PhTMS; 8.6 μL, 0.050 mmol) was added and the yield was determined by ^1H NMR based on comparison to PhTMS as internal standard before purification by column chromatography.

[23] Krasoviskiy, A.; Knochel, P. *Synthesis* **2006**, *5*, 890.

2.4.2.2 Preparation of Grignard Reagent

Under a N_2 atmosphere, a three-neck flask equipped with a stir bar, reflux condenser, and Schlenk filtration apparatus was charged with magnesium turnings (1.1 g, 45 mmol). The flask and magnesium turnings were then flame-dried under vacuum and the flask was back-filled with N_2. Anhydrous Et_2O (7.0 mL) and a crystal of iodine (ca. 2.0 mg) were added to the flask. Freshly distilled iodomethane (1.9 mL, 31 mmol, neat) or 4-iodoanisole (4.7 g, 20. mmol, 6.7 M in Et_2O) was slowly added over 30 min to maintain a gentle reflux. The mixture was stirred for 2 h at room temperature then filtered through the fritted Schlenk filter into a Schlenk flask under N_2 atmosphere. The magnesium turnings were washed with Et_2O (2 X 1.0 mL) then the Schlenk flask was sealed, removed, and placed under an N_2 atmosphere. The resulting methylmagnesium iodide was typically between 2.4 and 3.0 M as titrated by Knochel's method[24] and could be stored, sealed under N_2 atmosphere or in a glovebox, for up to 8 weeks.

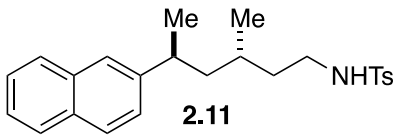
2.4.2.3 Synthesis of ((*R*)-BINAP)$NiCl_2$

This method was adapted from a procedure reported by Jamison.[25] To a flame-dried 50 mL round bottom flask equipped with a stir bar was added $NiCl_2 \cdot 6H_2O$ (0.24 g, 1.0 mmol, 1.0 equiv). The flask was placed under vacuum and flame-dried until nearly all of the nickel compound had turned from emerald green to yellow-orange. Some of the green hexahydrate is necessary for the reaction to proceed. The flask was allowed to cool to room temperature then(*R*)-BINAP (0.62 g, 1.0 mmol, 1.0 equiv) was added. The flask was then equipped with a reflux condenser and was evacuated and backfilled with N_2. Then, the solids were dissolved in MeCN (20 mL, 0.05 M) and the reaction mixture was allowed to reflux for 24 h. Upon completion, the reaction was cooled to

[24] See reference 23.
[25] Standley, E. A.; Smith, S. J.; Müller, P.; Jamison, T. F. *Organometallics* **2014**, *33*, 2012–2018.

room temperature and the black crystalline precipitate was filtered under vacuum to yield a fine black powder (0.53 g, 0.71 mmol, 71% yield).

2.4.3 Characterization Data for Ring-Opening Kumada Cross-Coupled Products



2.11

4-Methyl-N-(3-methyl-5-(naphthalen-2-yl)hexyl)benzenesulfonamide (**2.11**) was prepared according to Method A. The following amounts of reagents were used: piperidine **2.20** (10. mg, 30. μmol, 1.0 equiv), ((*R*)-BINAP)$NiCl_2$ (3.0 mg, 40. μmol, 15 mol %), methylmagnesium iodide (10. uL, 60. μmol, 2.0 equiv, 2.9 M in Et_2O), and PhMe (0.30 mL). Before purification, a ^1H NMR yield of 48% and 10:1 dr was obtained based on comparison to PhTMS as an internal standard. The residue was purified by flash column chromatography (0–15% EtOAc/hexanes) to afford the title compound as a colorless oil (5.4 mg, 14 μmol, 50% yield, 6:1 dr) with a small amount of styrene (0.6 mg, 0.2 μmol, 6%). The ratio of diastereomers was determined by integration of the resonances attributed to amine hydrogen in the ^1H NMR spectrum. The relative configuration of the major **2.11** was assigned based on analogy to a compound that has been previously reported.[26] For clarity, the ^1H NMR and ^{13}C NMR data of the major and minor diastereomers have been tabulated individually.

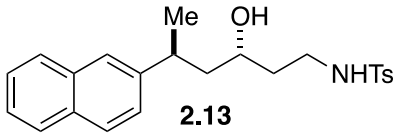
TLC R_f = 0.7 (30% EtOAc/hexanes, stained with CAM); HRMS (TOF MS E+) m/z [M+Na] calcd. for $C_{24}H_{29}NO_2SNa$, 418.1817; found, 418.1830.

Major Diastereomer: ^1H NMR (500 MHz, $CDCl_3$) δ 7.81–7.76 (m, 3H), 7.69 (d, *J* = 8.3 Hz, 2H), 7.6 (s, 1H), 7.47–7.40 (m, 2H), 7.31–7.26 (m, 3H), 4.29 (t, *J* = 5.9 Hz, 1H), 3.03–2.82 (m, 3H), 2.41 (s, 3H), 1.49 (t, *J* = 6.2 Hz, 1H), 1.43–1.46 (m, 1H), 1.30–1.25 (m, 3H), 1.25 (d, *J* =

[26] See reference 7(a) and 7(d).

6.9 Hz, 3H), 0.79 (d, J = 6.5 Hz, 3H); ^{13}C NMR (125.8, $CDCl_3$) δ 145.1, 148.4, 133.7, 132.2, 129.7 (2C), 128.1, 127.6, 127.6, 127.1 (2C), 126.0, 125.6, 125.2, 125.0, 45.6, 41.1, 37.2, 36.5, 29.1, 28.1, 22.1, 21.5, 19.6.

Minor Diastereomer: ^{1}H NMR (500 MHz, $CDCl_3$) δ 7.81–7.76 (m, 3H), 7.69 (d, J = 8.3, 2H), 7.63 (s, 1H), 7.47–7.40 (m, 2H), 7.31–7.26 (m, 3H), 4.39 (t, J = 5.5 Hz, 1H), 3.03–2.82 (m, 3H), 2.41 (s, 3H), 1.49 (t, J = 6.2 Hz, 1H), 1.43–1.46 (m, 1H), 1.30–1.25 (m, 3H), 1.25 (d, J = 6.9 Hz, 3H), 1.08 (d, J = 6.7, 3H); ^{13}C NMR (125.8, $CDCl_3$) δ 145.1, 148.4, 133.7, 132.2, 129.7 (2C), 128.1, 127.6, 127.6, 127.1 (2C), 126.0, 125.7, 125.2, 125.0, 45.6, 41.5, 37.2, 36.5, 29.7, 29.1, 22.1, 21.5, 19.6.



2.13

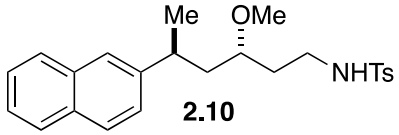
N-(3-hydroxy-5-(naphthalen-2-yl)hexyl)-4-methylbenzenesulfonamide (**2.13**) was prepared according to Method A. The following amounts of reagents were used: piperidine **2.21** (93 mg, 0.20 mmol, 1.0 equiv), ((*R*)-BINAP)$NiCl_2$ (23 mg, 30. μmol, 15 mol%), methylmagnesium iodide (0.14 mL, 0.40 mmol, 2.0 equiv, 2.9 M in Et_2O), and PhMe (2.0 mL). The residue was purified by flash column chromatography (0–15% EtOAc/hexanes) to afford the title compound as a colorless oil (42 mg, 0.11 mmol, 53% yield, 5:1 dr). The ratio of diastereomers was determined by integration of the resonances attributed to amine hydrogen in the ^{1}H

NMR spectrum. The relative configuration of the major **2.13** was assigned based on analogy to ring opened compound **2.11**. For clarity, the ^{1}H NMR and ^{13}C NMR data of the major and minor diastereomers have been tabulated individually.

TLC R_f = 0.5 (30% EtOAc/hexanes, stained with CAM); HRMS (TOF MS E+) m/z [M + Na] calcd. for $C_{23}H_{27}NO_3SNa$, 420.1609; found, 420.1604.

Major Diastereomer: ^{1}H NMR (500 MHz, $CDCl_3$) δ 7.79–7.75 (m, 3H), 7.69 (d, *J* = 8.15 Hz, 2H), 7.59 (s, 1H), 7.43 (appar quint, *J* = 7.44 Hz, 2H), 7.31 (d, *J* = 8.82 Hz, 1H), 7.23 (d, *J* = 8.17 Hz, 2H), 5.27 (t, *J* = 5.55 Hz, 1H), 3.74–3.70 (m, 1H), 3.12–3.06 (m, 1H), 3.01–2.93 (m, 2H), 2.37 (s, 3H), 1.89 (br s, 1H), 1.86–1.80 (m, 1H), 1.72–1.62 (m, 2H), 1.53–1.46 (m, 1H), 1.28 (d, *J* = 7.23 Hz, 3H); ^{13}C NMR (125.8, $CDCl_3$) δ 144.4, 143.3, 136.9, 133.7, 132.3, 129.7 (2C), 128.4, 127.7, 127.6, 127.1 (2C), 126.1, 125.5, 125.0, 124.4, 69.2, 45.9, 40.8, 37.0, 36.0, 22.2, 21.5.

Minor Diastereomer: ^{1}H NMR (500 MHz, $CDCl_3$) δ 7.79–7.75 (m, 3H), 7.65 (d, *J* = 8.14 Hz, 2H), 7.59 (s, 1H), 7.43 (appar quint, *J* = 7.44 Hz, 2H), 7.29 (d, *J* = 8.91 Hz, 1H), 7.19 (d, *J* = 8.05 Hz, 2H), 5.19 (t, *J* = 5.57 Hz, 1H), 3.43–3.39 (m, 1H), 3.12–3.06 (m, 1H), 2.91–2.82 (m, 2H), 2.35 (s, 3H), 1.86–1.80 (m, 1H), 1.76 (br s, 1H), 1.72–1.62 (m, 2H), 1.53–1.46 (m, 1H), 1.29 (d, *J* = 6.40 Hz, 3H); ^{13}C NMR (125.8, $CDCl_3$) δ 143.7, 143.3, 136.8, 133.7, 132.3, 129.7 (2C), 128.4, 127.7, 127.6, 127.1 (2C), 126.1, 125.5, 125.0, 124.4, 68.7, 45.6, 40.8, 36.45, 36.42 23.2, 21.5.



2.10

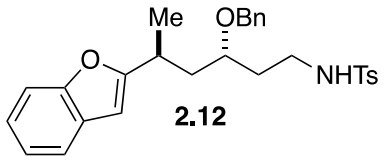
N-(3-methoxy-5-(naphthalen-2-yl)hexyl)-4-methylbenzenesulfonamide (**2.10**) was prepared according to Method A. The following amounts of reagents were used: piperidine **2.14** (58 mg, 0.15 mmol, 1.0 equiv), ((*R*)-BINAP)$NiCl_2$ (15 mg, 20. μmol, 15 mol %), methylmagnesium iodide (0.11 mL, 0.30 mmol, 2.0 equiv, 2.8 M in Et2O), and PhMe (1.5 mL). The residue was purified by flash column chromatography (0–25% EtOAc/hexanes) to afford the title compound as a colorless oil (32 mg, 80. μmol, 52% yield, 5:1 dr). The ratio of diastereomers was determined by integration of the resonances attributed to amine hydrogen in the ^{1}H NMR spectrum. The relative configuration of the major **2.10** was assigned based on analogy to ring opened compound **2.11**.

For clarity, the ^{1}H NMR and ^{13}C NMR data of the major and minor diastereomers have been tabulated individually.

TLC R_f = 0.4 (30% EtOAc/hexanes, stained with CAM); HRMS (TOF MS E+) m/z [M + Na] calcd. for $C_{24}H_{29}NO_3SNa$, 424.1766; found, 434.1775.

Major Diastereomer: ^{1}H NMR (500 MHz, $CDCl_3$) δ 7.81–7.76 (m, 3H), 7.68 (d, *J* = 8.37 Hz, 2H), 7.55 (s, 1H), 7.47–7.40 (m, 2H), 7.29 (dd, *J* = 8.48, 1.70 Hz, 1H), 7.26–7.24 (m, 1H), 7.21 (d, *J* = 7.97 Hz, 1H), 5.11 (t, *J* = 5.53 Hz, 1H), 3.15 (s, 3H), 3.08–2.91 (m, 3H), 2.86 (appar sextet, *J* = 7.37 Hz, 1H), 2.34 (s, 3H), 1.96 (ddd, *J* = 14.3, 8.50, 5.78 Hz, 1H), 1.82–1.76 (m, 1H), 1.58–1.50 (m, 2H), 1.28 (d, *J* = 6.98 Hz, 3H); ^{13}C NMR (125.8, $CDCl_3$) δ 144.1, 143.2, 136.8, 133.6, 132.3, 129.7 (2C), 128.3, 127.7, 127.6, 127.1 (2C), 126.1, 125.4, 125.24, 125.17, 78.4, 56.3, 40.9, 40.5, 36.3, 32.0, 22.9, 21.5.

Minor Diastereomer: ^{1}H NMR (500 MHz, $CDCl_3$) δ 7.81–7.76 (m, 3H), 7.70 (d, *J* = 8.60 Hz, 2H), 7.55 (s, 1H), 7.47–7.40 (m, 2H), 7.29 (dd, *J* = 8.48, 1.70 Hz, 1H), 7.26–7.24 (m, 1H), 7.21 (d, *J* = 7.97 Hz, 1H), 5.03 (t, *J* = 5.52 Hz, 1H), 3.20 (s, 3H), 3.08–2.91 (m, 3H), 2.86 (appar sextet, *J* = 7.37 Hz, 1H), 2.38 (s, 3H), 1.96 (ddd, *J* = 14.3, 8.50, 5.78 Hz, 1H), 1.71–1.66 (m, 1H), 1.47–1.40 (m, 2H), 1.27 (d, *J* = 7.32 Hz, 3H) ^{13}C NMR (125.8, $CDCl_3$) δ 144.2, 143.2, 136.9, 133.6, 132.3, 129.7 (2C), 128.3, 127.7, 127.6, 127.1 (2C), 126.1, 125.52, 125.46, 125.4, 78.4, 56.3, 40.9, 40.5, 36.3, 32.0, 22.9, 21.5.



2.12

N-(5-(benzofuran-2-yl)-3-(benzyloxy)hexyl)-4-methylbenzenesulfonamide (**2.12**) was prepared according to Method A. The following amounts of reagents were used: piperidine **2.22** (78 mg, 0.17 mmol, 1.0 equiv), ((*R*)-BINAP)$NiCl_2$ (22 mg, 30. μmol, 15 mol %), methylmagnesium iodide

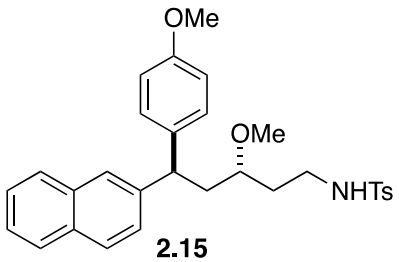
(0.23 mL, 0.68 mmol, 4.0 equiv, 2.9 M in Et2O), and PhMe (1.5 mL). The residue was purified by flash column chromatography (0–15% EtOAc/hexanes) to afford a mixture of the title compound and styrene. To separate the major product and the styrene, a dihydroxylation was performed. The following amounts of reagents were used: AD-mix-β (52 mg, 1.4 g/mmol), *t*-BuOH (1.0 mL), and H_2O (1.0 mL). The residue was purified by flash column chromatography to afford the title compound as a colorless oil. (7.0 mg, 15 μmol, 8.6% yield over two steps, 5:1 dr). The ratio of diastereomers was determined by integration of the resonances attributed to amine hydrogen in the ^{1}H NMR spectrum. The relative configuration of the major **2.12** was assigned based on analogy to ring opened compound **2.11**. When the reaction was performed with 2.0 equivalents of methylmagnesium iodide, a ^{1}H NMR yield of 41% was obtained based on comparison to PhTMS as an internal standard before purification. For clarity, the ^{1}H NMR and ^{13}C NMR data of the major and minor diastereomers have been tabulated individually.

TLC R_f = 0.5 (30% EtOAc/hexanes, stained with CAM); HRMS (TOF MS E+) m/z [M + Na] calcd. for $C_{28}H_{31}NO_4SNa$, 500.1872; found, 500.1861.

Major Diastereomer: ^{1}H NMR (500 MHz, $CDCl_3$) δ 7.64 (d, *J* = 7.9 Hz, 2H), 7.48 (d, *J* = 7.4 Hz, 1H), 7.42 (d, *J* = 7.9 Hz, 1H), 7.27–7.16 (m, 8H), 6.33 (s, 1H), 4.79 (t, *J* = 6.0 Hz, 1H), 4.45 (d, *J* = 11.5 Hz, 1H), 4.31 (d, *J* = 11.4 Hz, 1H), 3.49–3.42 (m, 1H), 3.09–2.95 (m, 3H), 2.38 (s, 3H), 2.12 (appar quint, *J* = 6.9 Hz, 1H), 1.87–1.81 (m, 1H), 1.65–1.54 (m, 3H), 1.29 (d, *J* = 6.9 Hz, 3H); ^{13}C NMR (125.8, $CDCl_3$) δ 162.6, 154.5, 143.3, 137.9, 136.9, 129.7 (2C), 128.5 (2C), 128.1 (2C), 127.9, 127.1 (2C), 123.4, 122.6, 120.5, 110.9, 101.1, 75.0, 70.7, 40.2, 39.1, 32.9, 30.3, 29.7, 21.5, 19.7.

Minor Diastereomer: ^{1}H NMR (500 MHz, $CDCl_3$) δ 7.80 (d, *J* = 7.9 Hz, 2H), 7.75 (d, *J* = 7.7 Hz, 1H), 7.58 (d, *J* = 8.4 Hz, 1H), 7.27–7.16 (m, 8H), 6.25 (s, 1H), 4.79 (t, *J* = 6.0 Hz, 1H),

4.40 (s, 2H), 3.53–3.48 (m, 1H), 3.09–2.95 (m, 3H), 2.73 (appar quint, J = 6.5 Hz, 1H), 2.40 (s, 3H), 1.80–1.77 (m, 1H), 1.65–1.60 (m, 3H), 0.88 (d, J = 7.0 Hz, 3H); ^{13}C NMR (125.8, $CDCl_3$) δ 162.6, 154.5, 143.3, 137.9, 136.9, 129.4 (2C), 128.7 (2C), 128.3 (2C), 127.9, 127.1 (2C), 123.4, 122.6, 120.5, 110.9, 101.4, 75.6, 71.4, 39.9, 39.1, 32.8, 30.5, 29.7, 21.5, 20.2.



2.15

N-3-methoxy-5-(4-methoxyphenyl)-5-(naphthalen-2-yl)pentyl)-4methylbenzenesulfonamide (**2.15**) was prepared according to Method A. The following amounts of reagents were used: piperidine **2.14** (37 mg, 90 μmol, 1.0 equiv), Ni(dppe)Cl_2 (7.0 mg, 10. μmol, 15 mol %), (4-methoxyphenyl)magnesium iodide (0.11 mL, 0.18 mmol, 2.0 equiv, 1.7 M in Et2O), and PhMe (0.90 mL). Before purification, a ^{1}H NMR yield of 56% was obtained based on comparison to PhTMS as an internal standard. The residue was purified by flash column chromatography (0–20% EtOAc/hexanes) to afford the title compound as a yellow oil (26 mg, 50. μmol, 58% yield, 3:1 dr). The ratio of diastereomers was determined by integration of the resonances attributed to methyl hydrogens of the tosyl group in the ^{1}H NMR spectrum. The relative configuration of the major **2.15** was assigned based on analogy to ring opened compound **2.14**. For clarity, the ^{1}H NMR and ^{13}C NMR data of the major and minor diastereomers have been tabulated individually.

TLC R_f = 0.3 (30% EtOAc/hexanes, stained with CAM); HRMS (TOF MS E+) m/z [M + H] calcd. for $C_{30}H_{34}NO_4S$, 504.2209; found, 504.2206.

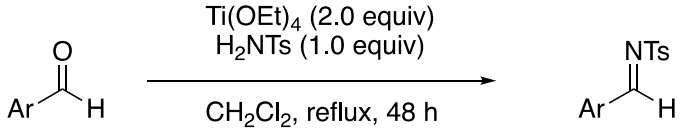
Major Diastereomer: ^{1}H NMR (500 MHz, $CDCl_3$) δ 7.76 (d, J = 7.3 Hz, 2H), 7.70–7.69 (m, 3H), 7.61 (s, 1H), 7.43 (dt, J = 20.4, 7.3 Hz, 2H), 7.29–7.19 (m, 3H), 7.13 (d, J = 8.5 Hz, 2H),

6.81 (d, *J* = 8.6 Hz, 2H), 5.09–5.-5 (m, 1H), 4.12 (t, *J* = 7.8 Hz, 1H), 3.76 (s, 3H), 3.20 (s, 3H), 3.13–3.09 (m, 1H), 3.05–2.97 (m, 2H), 2.30 (s, 3H), 2.25 (appar sext, *J* = 7.3 Hz, 1H), 2.02–1.97 (m, 1H), 1.85–1.80 (m, 1H), 1.58–1.52 (m, 1H); ^{13}C NMR (125.8, $CDCl_3$) δ 158.2, 143.4, 142.4, 136.8, 135.2, 133.6, 129.7 (2C), 129.0 (2C), 128.8, 128.3, 127.8, 127.7, 127.2 (2C), 126.5, 126.2, 125.6, 125.5, 114.1 (2C), 78.0, 56.7, 55.3, 46.5, 40.3, 39.1, 31.8, 21.5.

Minor Diastereomer: ^{1}H NMR (500 MHz, $CDCl_3$) δ 7.76 (d, *J* = 7.3 Hz, 2H), 7.73–7.70 (m, 3H), 7.63 (s, 1H), 7.43 (dt, J = 20.4, 7.3 Hz, 2H), 7.29–7.19 (m, 3H), 7.14 (d, *J* = 7.7 Hz, 2H), 6.81 (d, *J* = 8.8 Hz, 2H), 5.09–5.-5 (m, 1H), 4.12 (t, *J* = 7.8 Hz, 1H), 3.76 (s, 3H), 3.19 (s, 3H), 3.13–3.09 (m, 1H), 3.05–2.97 (m, 2H), 2.35 (s, 3H), 2.25 (appar sext, *J* = 7.3 Hz, 1H), 2.06–2.03 (m, 1H), 1.76–1.78 (m, 1H), 1.58–1.52 (m, 1H); ^{13}C NMR (125.8, $CDCl_3$) δ 158.2, 143.4, 142.0, 136.9, 136.5, 133.6, 129.7 (2C), 129.0 (2C), 128.8, 128.4, 127.8, 127.7, 127.2 (2C), 126.5, 126.2, 125.9, 125.6, 114.1 (2C), 78.0, 56.7, 55.3, 46.5, 40.3, 39.1, 31.9, 21.6.

2.4.4 General Procedures for Synthesis of Starting Materials

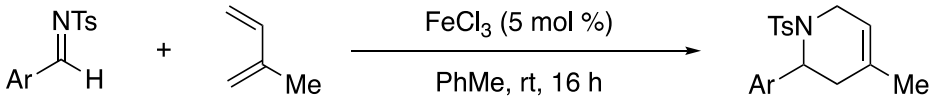
2.4.4.1 Method B: Condensation Reaction



This method was adapted from a procedure reported by Ruano et al.[27] A flame-dried two-neck flask equipped with a stir bar, condenser, septum and N_2 inlet was charged with aldehyde (1.0 equiv), and p-toluenesulfonamide (1.0 equiv) and CH_2Cl_2 (330 mL). Then $Ti(OEt)_4$ (2.0 equiv) was added dropwise. The deep orange solution was brought to reflux (~45 °C) and allowed to stir for 48 h. The solution was cooled to room temperature and was quenched with H_2O. The mixture was vacuum filtered and the filtrate was concentrated in vacuo.

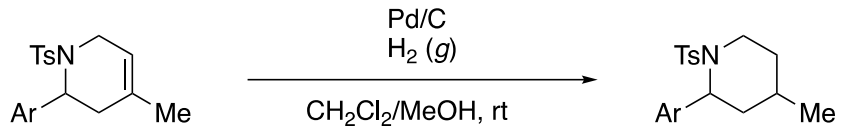
[27] García Ruano, J.L.; Alemán, J.; Belén Cid, M.; Parra, A. *Org. Lett.* **2005**, *7*, 179–182.

2.4.4.2 Method C: Fe-Catalyzed Formal [4+2] Cycloaddition



This method was adapted from a procedure reported by Matsubara.[28] To a flame-dried round-bottom flask equipped with a stir bar was added imine (1.0 equiv), $FeCl_3$ (5.0 mol%), and PhMe (0.1 M). Once the solution was homogenous, diene (2.0 equiv) was added. The reaction mixture was allowed to stir at rt overnight. After completion, the reaction mixture was filtered through a short pad of silica, washed with excess ethyl acetate, and concentrated in vacuo.

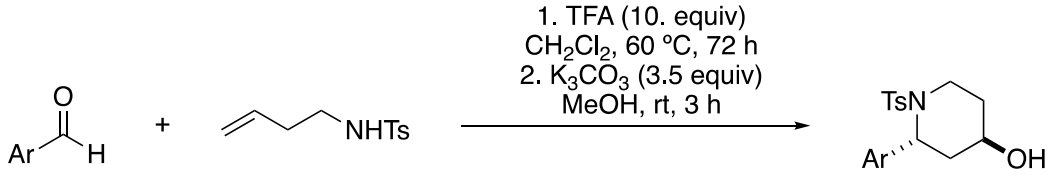
2.4.4.3 Method D: Pd/C Reduction of Alkenes



A flame-dried round-bottom flask with stir bar was charged with palladium on carbon (1.0 mg/3.5 mmol of substrate), flushed with N_2, and capped with septum. Slowly, CH_2Cl_2 was added, until Pd/C was fully submerged. Then MeOH (0.2 M in substrate), and alkene (1.0 equiv) were added. Vacuum was pulled on the flask until the solvent began to bubble, at which point the flask was backfilled with N_2 (X3). An H_2 balloon was added and the reaction mixture was allowed to stir vigorously until complete by ^1H NMR. The balloon was then removed, and the flask was purged with N_2 for 30 min. The septum was removed, and the reaction mixture was filtered through Celite using MeOH (100 mL). The collected solvent was then concentrated in vacuo.

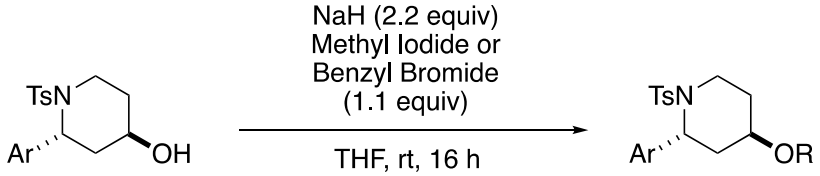
2.4.4.4 Method E: TFA Mediated Aza-Prins Cyclization

[28] Tomifuji, R.; Maeda, K.; Takahashi, T.; Kurahashi, T.; Mastubara, S. *Org. Lett.* **2018**, *20*, 7474–7477.



This method was adapted from a procedure reported by Sabitha.[29][30] To a flame-dried pressure tube equipped with a stir bar was added aldehyde (1.0 equiv), homoallylic sulfonamide (1.1 equiv), and CH_2Cl_2 (0.10 M). Then trifluoroacetic acid (10.0 equiv) was added slowly via syringe. The solution was warmed to 60 °C and allowed to stir for 72 h. The solution was then cooled to rt and quenched with saturated aq. $NaHCO_3$. Then the pH was adjusted to >7 by the addition of Et_3N. The solution was transferred to a separatory funnel, and the aqueous layer was extracted with CH_2Cl_2 (X3). The combined organic layers were washed with brine, dried over Na_2SO_4, filtered and concentrated in vacuo. The residue was then redissolved in MeOH, and K_2CO_3 (3.5 equiv) was added to the flask and the slurry was allowed to stir at rt for 3 h. The solvent was removed under reduced pressure, then H_2O was added, and the residue was transferred to a separatory funnel. The aqueous layer was extracted with EtOAc (X3). layers were washed with brine, dried over Na_2SO_4, filtered, and concentrated in vacuo.

2.4.4.5 Method F: Alkylation of Secondary Alcohol

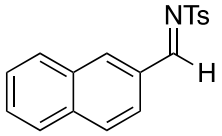


This method was adapted from a procedure reported by Yang.[31] In a glovebox, to a flame-dried round bottom flask equipped with a stir bar was added NaH (2.2 equiv). The flask was

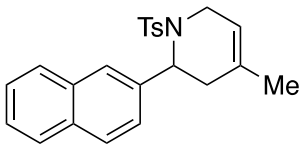
[29] Sabitha, G.; Reddy, N. M.; Prasad, M. N.; Yadav, J. S. *Helv. Chim. Acta* **2009**, *92*, 967–976.
[30] Tollefson, E. J.; Erickson, L. W.; Jarvo, E. R. *J. Am. Chem. Soc.* **2015**, *137*, 9760–9763.
[31] Fu, M.; Chen, L.; Jiang, Y.; Jiang, Z.-X.; Yang, Z. *Org. Lett.* **2016**, *18*, 348–351.

removed from the glovebox and NaH was dissolved in THF (0.2 M). Alcohol (1.0 equiv) was added dropwise as a solution in THF (0.3 M) and the reaction mixture was allowed to stir at rt for 1 h. Methyl iodide or benzyl bromide was then added dropwise to the stirring slurry and the reaction mixture was allowed to stir at rt overnight. The reaction was then quenched with saturated aq. NH_4Cl and extracted with EtOAc (X3). The combined organic layers were washed with brine, dried over Na_2SO_4 and concentrated in vacuo.

2.4.5 Synthesis and Characterization of Sulfonamide Starting Materials



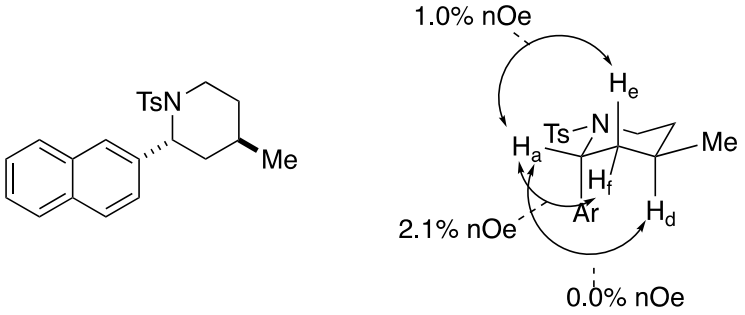
4-Methyl-N-(naphthalen-2-ylmethylene)benzenesulfonamide (**2.23**) was prepared according to Method B. The following amounts of reagents were used: 2-naphthaldehyde (0.31 g, 2.0 mmol, 1.0 equiv), p-toluenesulfonamide (0.34 g, 2.0 mmol, 1.0 equiv), $Ti(OEt)_4$ (0.59 mL, 4.0 mmol, 2.0 equiv), and CH_2Cl_2 (33 mL). The residue was purified by flash column chromatography (0–25% EtOAc/hexanes) to yield the title compound as a pale yellow solid (0.31 g, 1.0 mmol, 50% yield). Analytical data are consistent with literature values.[32] ^{1}H NMR (400 MHz, $CDCl_3$) δ 9.18 (s, 1H), 8.34 (s, 1H), 8.04 (dd, J = 8.6, 1.7 Hz, 1H), 7.98–7.86 (m, 5H), 7.67–7.55 (m, 2H), 7.36 (d, J = 8.0 Hz, 2H), 2.44 (s, 3H).



4-Methyl-2-(naphthalen-2-yl)-1-tosyl-1,2,3,6-tetrahydropyridine (**2.24**) was prepared according to Method C. The following amounts of reagents were used: imine **2.23** (0.31 g, 1.0 mmol, 1.0 equiv),

[32] Syu, S.; Lee, Y.-T.; Jang, Y.-J.; Lin, W. *J. Org. Chem.* **2011**, *76*, 2888–2891.

isoprene (1.5 mL, 15 mmol, 15 equiv), $FeCl_3$ (16 mg, 0.10 mmol, 10. mol %), and PhMe (10. mL, 0.10 M). The residue was purified by flash column chromatography (0–5% EtOAc/hexanes) to afford the title compound as a yellow oil (150 mg, 0.40 mmol, 40% yield). TLC R_f = 0.5 (20% EtOAc/hexanes); ^{1}H NMR (500 MHz, $CDCl_3$) δ 7.78–7.71 (m, 3H), 7.69 (d, *J* = 8.3 Hz, 2H), 7.56 (s, 1H), 7.48–7.40 (m, 3H), 7.20 (d, *J* = 8.1 Hz, 2H), 5.43 (d, *J* = 3.5 Hz, 1H), 5.29 (s, 1H), 4.11 (d, *J* = 18.0 Hz, 1H), 3.35 (d, *J* = 18.1 Hz, 1H), 2.40–2.30 (m, 2H), 2.35 (s, 3H), 1.68 (s, 3H).



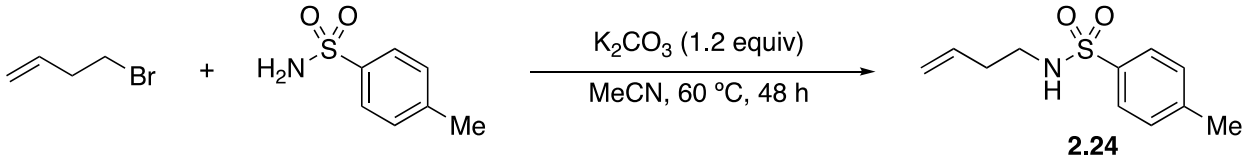
4-Methyl-2-(naphthalen-2-yl)-1-tosylpiperidine (**2.20**) was prepared according to Method D. The following amounts of reagents were used: substrate **2.24** (53 mg, 0.14 mmol, 1.0 equiv), Pd/C (27 mg), CH_2Cl_2 (1.0 mL) and MeOH (1.0 mL). The residue was purified by flash column chromatography (0–10% EtOAc/hexanes) to afford the title compound as a pale yellow oil (9.6 mg, 25 μmol, 18% yield, 6:1 dr trans:cis). The dr was determined based on the integration of the resonances attributed to the benzylic hydrogens in the ^{1}H NMR spectrum. The relative configuration was assigned based on nOe analysis. For clarity, the ^{1}H NMR and ^{13}C NMR data of the major and minor diastereomers have been tabulated individually.

TLC R_f = 0.5 (10% EtOAc/hexanes); HRMS (TOF MS ES+) m/z [M + H] calcd. for $C_{23}H_{26}NO_2S_2$ 380.1684, found 380.1689.

Major Diastereomer: ^{1}H NMR (500 MHz, $CDCl_3$) δ 7.80–7.76 (m, 4H), 7.73–7.71 (m, 1H), 7.63 (s, 1H), 7.46–7.44 (m, 3H), 7.28 (d, *J* = 8.0 Hz, 2H), 5.48 (d, *J* = 4.5 Hz, 1H), 3.96 (d, *J* = 14.4 Hz, 1H), 3.06 (ddd, *J* = 14.0, 13.2, 3.1 Hz, 1H), 2.69 (d, *J* = 25.9 Hz, 1H), 2.42 (s, 3H), 2.30

(d, *J* = 13.3 Hz, 1H), 1.43–1.36 (m, 2H), 0.98 (ddd, *J* = 24.5, 12.4, 4.5 Hz, 1H), 0.82 (d, *J* = 6.5 Hz, 3H); ^{13}C NMR (151 MHz, $CDCl_3$) δ 143.1, 138.8, 136.7, 133.3, 132.3, 129.7 (2C), 128.4, 128.0, 127.5, 127.1 (2C), 126.1, 125.9, 125.8, 125.1, 55.6, 42.0, 36.0, 33.0, 25.3, 22.2, 21.5.

Minor Diastereomer: ^{1}H NMR (500 MHz, $CDCl_3$) δ 7.80–7.76 (m, 4H), 7.73–7.71 (m, 1H), 7.63 (s, 1H), 7.46–7.44 (m, 3H), 7.28 (d, *J* = 8.0 Hz, 2H), 5.25 (d, *J* = 4.9 Hz, 1H), 3.88 (d, *J* = 10.6 Hz, 1H), 3.04–2.98 (m, 1H), 2.42 (s, 3H), 2.38 (d, *J* = 3.86 Hz, 1H), 2.14 (d, *J* = 13.7 Hz, 1H), 1.43–1.36 (m, 2H), 0.79 (d, *J* = 6.5 Hz, 3H), 0.75 (d, *J* = 6.4 Hz, 1H); ^{13}C NMR (151 MHz, $CDCl_3$) δ 143.1, 138.8, 136.7, 133.3, 132.3, 129.6 (2C), 129.3, 128.0, 127.6, 127.1 (2C), 126.1, 125.9, 125.8, 124.0, 55.2, 41.8, 36.0, 33.1, 25.2, 23.3, 21.5.

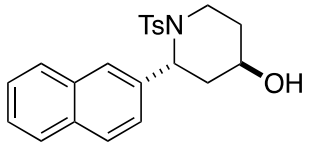


2.24

N-(but-3-en-1-yl)-4-methylbenzenesulfonamide (**2.24**) was prepared according to a procedure reported by Jiang.[33] To a flame-dried flask equipped with a stir bar was added 4-bromo-1-butene (4.1 mL, 40. mmol, 1.0 equiv), p-toluenesulfonamide (6.8 g, 40. mmol, 1.0 equiv), K_2CO_3 (6.6 g, 48 mmol, 1.2 equiv), and MeCN (160 mL). The mixture was heated to 60 °C and allowed to stir for 3 d. The reaction mixture was quenched with saturated NH_4Cl (100 mL) and extracted with EtOAc (3 X 50 mL). The combined organic layers were washed with H2O (50 mL) and brine (50 mL), dried over Na_2SO_4, and concentrated in vacuo. The residue was purified by column chromatography (5–25% EtOAc/hexanes) to afford the title compound as a clear, colorless oil (5.4 g, 24 mmol, 60%). Analytical data are consistent with literature values.[34] ^{1}H NMR: (400 MHz,

[33] Huang, J.; Zheng, J.; Wu, W.; Li, J.; Ma, J.; Ren, Y.; Jiang, H. *J. Org. Chem*. **2017**, *82*, 8191–8198.
[34] See reference 33.

$CDCl_3$) δ 7.76 (d, *J* = 8.2, 2H), 7.30 (d, *J* = 8.1, 2H), 5.63 (ddt, *J* = 17.1, 10.4, 6.8, 1H), 5.11 (br s, 1H), 5.02–4.93 (m, 2H), 2.99 (q, *J* = 6.7, 2H), 2.41 (s, 3H), 2.20 (q, *J* = 6.9, 2 H).



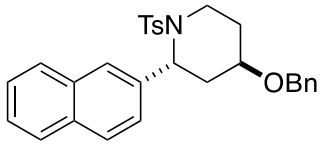
2-(Naphthalen-2-yl)-1-tosylpiperidin-4-ol (**2.25**) was prepared according to Method E. The following amounts of reagents were used: 2-napthaldehyde (0.94 g, 6.0 mmol, 1.0 equiv), homoallylic sulfonamide **2.24** (1.1 mL, 6.0 mmol, 1.0 equiv), TFA (4.6 mL, 60. mmol, 10 equiv), and CH_2Cl_2 (60 mL, 0.10 M). The residue was purified by flash column chromatography (0–30% EtOAc/hexanes) to afford the title compound as an orange solid (0.72 g, 1.8 mmol, 31% yield, 5:1 dr trans:cis). The dr was determined based on the integration of the resonances attributed to the benzylic hydrogens in the 1H NMR spectrum. The relative configuration of the major **2.25** was assigned based on analogy to compound **2.20**. For clarity, the ^{1}H NMR data of the major and minor diastereomers have been tabulated individually.

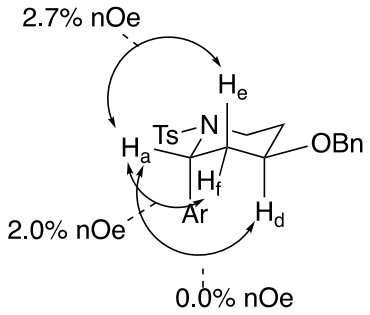
TLC R_f = 0.1 (30% EtOAc/hexanes, stained with CAM); HRMS (TOF MS ES+) m/z [M + H] calcd. for $C_{22}H_{24}NO_3S$ 382.1477, found 382.1483.

Major Diastereomer: ^{1}H NMR (500 MHz, $CDCl_3$) δ 7.79–7.77 (m, 4H), 7.68 (s, 1H), 7.49–7.41 (m, 4H), 7.29 (d, *J* = 8.1 Hz, 2H), 5.54 (d, *J* = 4.5 Hz, 1H), 3.99 (d, *J* = 15.0 Hz, 1H), 3.74 (tt, *J* = 10.9, 7.9 Hz, 1H), 3.03 (td, *J* = 15.3, 2.7 Hz, 1H), 2.63 (dt, *J* = 13.3, 2.0 Hz 1H), 2.43 (s, 3H), 1.70 (br s, 1H), 1.58 (ddd, *J* = 13.6, 11.3, 5.5 Hz, 1H), 1.26–1.18 (m, 2H); ^{13}C NMR (151 MHz, $CDCl_3$) δ 143.5, 138.3, 135.9, 133.3, 132.5, 130.0 (2C), 128.7, 128.0, 127.5, 127.0 (2C), 126.3, 126.2, 125.5, 124.7, 64.7, 55.8, 40.7, 36.2, 33.8, 21.6.

Minor Diastereomer: ^{1}H NMR (500 MHz, $CDCl_3$) δ 7.74–7.70 (m, 4H), 7.63 (s, 1H), 7.60 (d, *J* = 8.3 Hz, 2H), 7.49–7.41 (m, 2H), 7.16 (d, *J* = 8.4 Hz, 2H), 5.10 (t, *J* = 5.1 Hz, 1H), 3.99 (d,

J = 15.0 Hz, 1H), 3.67 (tt, J = 13.4, 4.6 Hz, 1H), 3.03 (td, J = 15.3, 2.7 Hz, 1H), 2.63 (dt, J = 13.3, 2.0 Hz 1H), 2.36 (s, 3H), 1.81–1.73 (m, 1H), 1.67 (br s, 1H), 1.26–1.18 (m, 2H). ^{13}C NMR (151 MHz, $CDCl_3$) δ 143.3, 137.7, 135.9, 133.2, 132.5, 129.6 (2C), 128.7, 128.2, 127.5, 127.2 (2C), 126.3, 126.0, 125.3, 124.8, 65.1, 55.5, 39.0, 37.0, 31.9, 21.5.





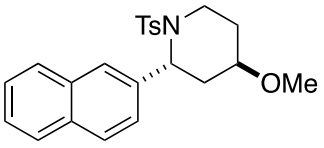
4-(Benzyloxy)-2-(naphthalen-2-yl)-1-tosylpiperidine (**2.21**) was prepared according to Method F. The following amounts of reagents were used: alcohol **2.25** (0.25 g, 0.66 mmol, 1.0 equiv), NaH (63 mg, 2.6 mmol. 4.0 equiv), benzyl bromide (90. µL, 0.73 mmol, 1.1 equiv), and THF (2.3 mL, 0.2 M). The residue was purified by column chromatography (0–10% EtOAc/hexanes) to afford the title compound as a white solid (140 mg, 0.30 mmol, 56% yield, 5:1 dr trans:cis). The dr was determined based on the integration of the resonances attributed to the benzylic hydrogens in the ^{1}H NMR spectrum. The relative configuration was assigned based on nOe analysis. For clarity, the ^{1}H NMR and ^{13}C NMR data of the major and minor diastereomers have been tabulated individually.

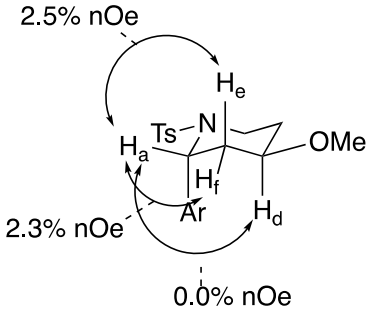
TLC R_f = 0.8 (20% EtOAc/hexanes, stained with CAM); HRMS (TOF MS ES+) m/z [M + Na] calcd. for $C_{29}H_{29}NO_3SNa$ 494.1766, found 494.1758.

Major Diastereomer: ^{1}H NMR (500 MHz, $CDCl_3$) δ 7.80 (d, J = 8.1 Hz, 4H), 7.70 (d, 1H), 7.61 (s, 1H), 7.48–7.45 (m, 3H), 7.32–7.26 (m, 7H), 5.55 (d, J = 3.8 Hz, 1H), 4.50 (d, J = 11.9 Hz, 1H), 4.43 (d, J = 11.9 Hz, 1H), 4.02 (d, J = 14.7 Hz, 1H), 3.52 (tt, J = 10.8 Hz, 1H), 3.04 (td, J = 14.5, 2.5 Hz, 1H), 2.68 (d, J = 13.6 Hz, 1H), 2.43 (s, 3H), 1.80 (d, J = 11.5 Hz, 1H), 1.62 (ddd, J

= 17.7, 11.9, 6.1 Hz, 1H), 1.31–1.34 (m, 1H); ^{13}C NMR (151 MHz, $CDCl_3$) δ 143.4, 138.3, 136.0, 133.2, 132.5, 130.0 (2C), 129.5, 128.6, 128.5 (2C), 128.0, 127.8, 127.7 (2C), 127.5, 127.0 (2C), 126.2, 126.1, 125.5, 124.8, 71.3, 70.2, 55.8, 40.8, 33.4, 30.8, 21.6.

Minor Diastereomer: ^{1}H NMR (500 MHz, $CDCl_3$) δ 7.80 (d, J = 8.1 Hz, 4H), 7.70 (d, 1H), 7.59 (s, 1H), 7.48–7.45 (m, 3H), 7.32–7.26 (m, 2H), 7.15 (d, J = 8.2 Hz, 1H), 7.07 (t, J = 7.6 Hz, 1H), 6.96 (t, J = 7.3 Hz, 2H), 6.69 (d, J = 7.6 Hz, 1H), 5.17 (t, J = 5.1 Hz, 1H), 4.24, 4.20 (ABq, J_{AB} = 12.3 Hz, 2H), 3.80–3.68 (m, 3H), 2.53 (dt, J = 14.4, 9.4 Hz, 1H), 2.35 (s, 3H), 2.06 (ddd, J = 14.3, 5.3, 2.9 Hz, 1H), 1.81–1.80 (m, 2H), 1.31–1.34 (m, 1H); ^{13}C NMR (151 MHz, $CDCl_3$) δ 143.4, 138.4, 136.0, 133.2, 132.5, 130.0 (2C), 129.5, 128.6, 128.5 (2C), 128.0, 127.8, 127.7 (2C), 127.5, 127.19 (2C), 127.16, 125.9, 125.6, 125.2, 71.2, 69.8, 55.8, 39.3, 34.2, 30.8, 21.6.





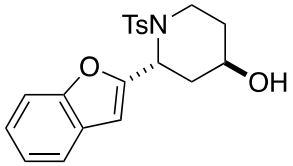
4-Methoxy-2-(naphthalen-2-yl)-1-tosylpiperidine (**2.14**) was prepared according to Method F. The following amounts of reagents were used: alcohol **2.25** (110 mg, 0.30 mmol, 1.0 equiv), NaH (16 mg, 0.67 mmol, 2.2 equiv), methyl iodide (20. L, 0.33 mmol, 1.1 equiv), and THF (1.5 mL, 0.20 M). The residue was purified by column chromatography (0–20% EtOAc/hexanes) to afford the title compound as a pale yellow solid (61 mg, 0.15 mmol, 52% yield, 5:1 dr trans:cis). The dr was determined based on the integration of the resonances attributed to the benzylic hydrogens in the ^{1}H NMR spectrum. The relative configuration was assigned based on nOe analysis. For clarity,

the 1H NMR and 13C NMR data of the major and minor diastereomers have been tabulated individually.

TLC R_f = 0.6 (30% EtOAc/hexanes, stained with CAM); HRMS (TOF MS ES+) m/z [M + Na] calcd. for $C_{23}H_{25}NO_3SNa$ 396.1633, found 396.1636.

Major Diastereomer: ^{1}H NMR (500 MHz, $CDCl_3$) δ 7.83–7.76 (m, 5H), 7.72 (s, 1H), 7.54–7.51 (m, 1H), 7.48–7.46 (m, 2H), 7.29 (d, *J* = 7.9 Hz, 2H), 5.56 (s, 1H), 4.04 (d, *J* = 14.1 Hz, 1H), 3.29 (tt, *J* = 7.4, 3.0 Hz, 1H), 3.25 (s, 3H), 3.09 (t, *J* = 13.1 Hz, 1H), 2.68 (d, *J* = 13.2 Hz, 1H), 2.42 (s, 3H), 1.80 (d, *J* = 11.5 Hz, 1H), 1.53 (td, *J* = 12.2 Hz, 1H), 1.16 (qd, *J* = 11.6, 5.8 Hz, 1H); ^{13}C NMR (151 MHz, $CDCl_3$) δ 143.4, 138.4, 136.1, 133.4, 132.5, 130.0 (2C), 126.7, 128.1, 127.6, 127.0 (2C), 126.3, 126.1, 125.5, 124.7, 73.2, 55.8, 55.5, 40.8, 33.2, 30.2, 21.6.

Minor Diastereomer: ^{1}H NMR (500 MHz, $CDCl_3$) δ 7.83–7.76 (m, 5H), 7.72 (s, 1H), 7.54–7.51 (m, 1H), 7.48–7.46 (m, 2H), 7.29 (d, *J* = 7.9 Hz, 2H), 4.99 (t, *J* = 5.38 Hz, 1H), 3.77–3.71 (m, 1H), 3.60 (dt, *J* = 13.6, 4.6 Hz, 1H), 3.42 (br s, 1H), 3.03 (s, 3H), 2.37–2.29 (m, 1H), 2.33 (s, 3H), 2.02 (d, *J* = 15.2 Hz, 1H), 1.86–1.82 (m, 1H), 1.72–1.68 (m, 1H); ^{13}C NMR (151 MHz, $CDCl_3$) δ 143.0, 138.3, 137.4, 133.1, 132.5, 129.4 (2C), 126.7, 128.0, 127.5, 127.2 (2C), 125.8, 125.7, 125.5, 125.2, 73.5, 56.4, 55.5, 40.0, 34.1, 29.6, 21.5.



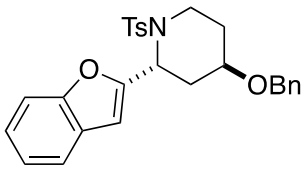
2-(Naphthalen-2-yl)-1-tosylpiperidin-4-ol (**2.26**) was prepared according to Method E. The following amounts of reagents were used: 2-benzofurancarboxaldehyde (0.60 mL, 5.0 mmol, 1.0 equiv), homoallylic sulfonamide **2.24** (0.91 mL, 5.0 mmol, 1.0 equiv), TFA (3.8 mL, 50. mmol, 10 equiv), CH_2Cl_2 (50 mL, 0.10 M). The residue was purified by flash column chromatography (0–50% EtOAc/hexanes) to afford the title compound as an orange solid (0.42 g, 1.1 mmol, 22%

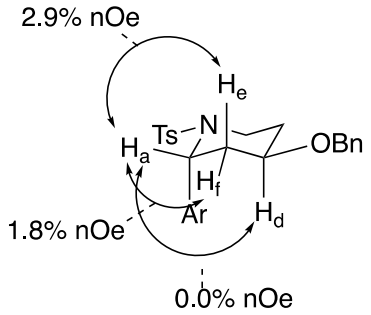
yield, 5:1 dr trans:cis). The dr was determined based on the integration of the resonances attributed to the benzylic hydrogens in the ^{1}H NMR spectrum. The relative configuration was assigned based on analogy to compound **2.20**. For clarity, the 1H NMR data of the major and minor diastereomers have been tabulated individually.

TLC R_f = 0.1 (30% EtOAc/hexanes, stained with CAM).

Major Diastereomer: ^{1}H NMR (500 MHz, $CDCl_3$) δ 7.65 (d, *J* = 8.29 Hz, 2H), 7.46 (dd, *J* = 6.75, 2.12 Hz, 1H), 7.21–7.18 (m, 3H), 7.15 (d, *J* = 8.61 Hz, 2H), 6.49 (t, *J* = 2.0 Hz, 1H), 5.51 (d, *J* = 5.48 Hz, 1H), 3.97–3.90 (m, 2H), 3.23 (td, *J* = 13.5, 2.7 Hz, 1H), 2.51–2.45 (m, 1H), 2.33 (s, 3H), 1.94–1.88 (m, 1H), 1.75 (ddd, *J* = 13.0, 11.6, 5.9 Hz, 1H), 1.53 (d, *J* = 5.0 Hz, 1H), 1.44 (ddd, *J* = 24.1, 12.8, 4.5 Hz, 1H).

Minor Diastereomer: ^{1}H NMR (500 MHz, $CDCl_3$) δ 7.65 (d, *J* = 8.29 Hz, 2H), 7.46 (dd, *J* = 6.75, 2.12 Hz, 1H), 7.21–7.18 (m, 3H), 7.15 (d, *J* = 8.61 Hz, 2H), 6.51 (t, *J* = 1.1 Hz, 1H), 5.33 (d, *J* = 5.6 Hz, 1H), 4.14–4.10 (m, 2H), 3.64 (td, *J* = 10.9, 4.0 Hz, 1H), 2.51–2.45 (m, 1H), 2.32 (s, 3H), 2.12 (ddd, *J* = 14.4, 6.7, 3.3 Hz, 1H), 1.94–1.88 (m, 1H), 1.53 (d, *J* = 5.0 Hz, 1H), 1.44 (ddd, *J* = 24.1, 12.8, 4.5 Hz, 1H).





2-(benzofuran-2-yl)-4-(benzyloxy)-1-tosylpiperidine (**2.22**) was prepared according to method F. The following amounts of reagents were used: alcohol **2.26** (0.15 g, 0.40 mmol, 1.0 equiv), NaH (46 mg, 1.9 mmol, 4.7 equiv), benzyl bromide (52 μL, 0.44 mmol, 1.1 equiv), and THF (3.0 mL, 0.2 M). The residue was purified by column chromatography (0–10% EtOAc/hexanes) to afford

the title compound as a yellow solid (87 mg, 0.19 mmol, 47% yield, 5:1 dr trans:cis). The dr was determined based on the integration of the resonances attributed to the benzylic hydrogens in the ^{1}H NMR spectrum. The relative configuration was assigned based on nOe analysis. For clarity, the ^{1}H NMR and ^{13}C NMR data of the major and minor diastereomers have been tabulated individually.

TLC R_f = 0.8 (30% EtOAc/hexanes, stained with CAM); HRMS (TOF MS ES+) m/z [M + Na] calcd. for $C_{27}H_{27}NO_4SNa$ 484.1559, found 484.1542.

Major Diastereomer: ^{1}H NMR (500 MHz, $CDCl_3$) δ 7.65 (d, *J* = 8.3 Hz, 2H), 7.45, (d, *J* = 8.3 Hz, 1H), 7.30–7.17 (m, 8H), 7.15 (d, *J* = 8.2 Hz, 2H), 6.44 (s, 1H), 5.52 (d, *J* = 5.3 Hz, 1H), 4.49 (s, 2H), 3.94 (d, *J* = 13.7 Hz, 1H), 3.66 (tt, *J* = 11.2, 4.0 Hz, 1H), 3.20 (td, *J* = 13.4, 2.6 Hz, 1H), 2.57 (dt, *J* = 13.2, 1.8 Hz, 1H), 2.32 (s, 3H), 1.97 (d, *J* = 12.3 Hz, 1H), 1.78 (ddd, *J* = 13.0, 11.7, 5.8 Hz, 1H), 1.45 (qd, *J* = 12.8, 4.8 Hz, 1H); ^{13}C NMR (151 MHz, $CDCl_3$) δ 155.3, 154.7, 143.3, 138.2, 137.2, 129.5 (2C), 128.5 (2C), 128.1, 128.0, 127.8, 127.1, 126.9, 124.1, 122.9, 120.9, 111.1, 104.8, 71.8, 70.2, 51.7, 41.4, 34.2, 31.3, 21.5.

Minor Diastereomer: ^{1}H NMR (500 MHz, $CDCl_3$) δ 7.68 (d, *J* = 8.3 Hz, 2H), 7.35, (d, *J* = 4.4 Hz, 1H), 7.30–7.17 (m, 5H), 7.07 (t, *J* = 7.5 Hz, 1H), 6.99 (t, *J* = 7.6, 2H), 6.79 (d, *J* = 7.6 Hz, 2H), 6.42 (s, 1H), 5.36 (d, *J* = 6.4 Hz, 1H), 4.28 (s, 2H), 3.76–3.73 (m, 2H), 3.66 (tt, *J* = 11.2, 4.0 Hz, 1H), 2.70 (d, *J* = 14.1 Hz, 1H), 2.32 (s, 3H), 1.97 (d, *J* = 12.3 Hz, 1H), 1.83 (d, *J* = 13.8 Hz, 1H), 1.72–1.68 (m, 1H); ^{13}C NMR (151 MHz, $CDCl_3$) δ 155.3, 154.7, 143.3, 138.2, 137.2, 129.5 (2C), 128.5 (2C), 128.1, 128.0, 127.8, 127.1, 126.9, 123.6, 122.6, 120.7, 110.9, 103.2, 71.8, 70.0, 49.6, 37.6, 31.0, 29.3, 15.3.

Chapter 3

Synthesis of Vicinal Carbocycles by Intramolecular Nickel-Catalyzed Cross-Electrophile Coupling Reaction

3.1 Introduction

Conjunctive cross-electrophile coupling reactions have emerged as a useful synthetic tool to rapidly build C(sp^3) character in a molecule.[1,2] These reactions, in which an olefin is functionalized with two different electrophilic coupling partners present interesting challenges to achieve chemo-, regio-, and stereoselectivity.[3] Several strategies have been employed to overcome these challenges. In three component reactions, selectivity is typically achieved using electronic differentiation of the electrophiles or an excess of one electrophile (Scheme 3.1a).[4] In two component reactions, selectivity is achieved by tethering one electrophile to the

[1] Portions of this chapter have been published in Organic Letters: Hewitt, K. A.; Herbert, C. A.; Jarvo, E. R. *Org Lett.* **2022**, *24*, 6093–6098.

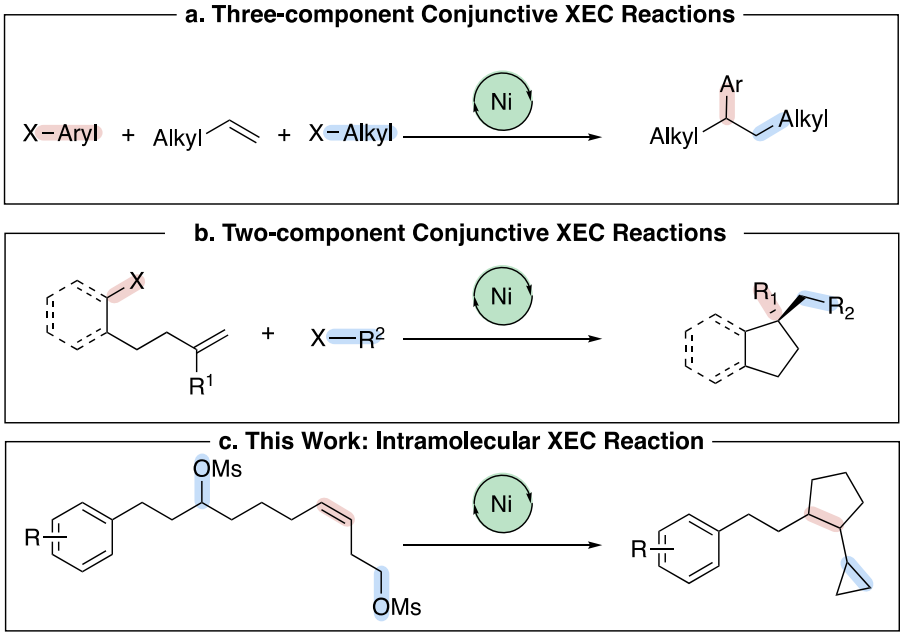
[2] For reviews of conjunctive XC and XEC reactions see: (a) Derosa, J.; Tran, V. T.; van der Puyl, V. A.; Engle, K. M. *Aldrichim. Acta* **2018**, *51*, 21– 32. (b) Zhang, J.-S.; Liu, L.; Chen, T.; Han, L.-B. *Chem. Asian J.* **2018**, *13*, 2277–2291. (c) Qi, X.; Diao, T. *ACS Catal.* **2020**, *10*, 8542– 8556. (d) Derosa, J.; Apolinar, O.; Kang, T.; Tran, V. T.; Engle, K. M. *Chem. Sci.* **2020**, *11*, 4287– 4296. (e) Badir, S. O.; Molander, G. A. *Chem.* **2020**, *6*, 1327–1339. (f) Tu, H.-Y. Zhu, S.; Qing, F.-L.; Chu, L. *Synthesis* **2020**, *52*, 1346–1356. (g) Ping, Y.; Kong, W. *Synthesis* **2020**, *52*, 979–992. (h) Wickham, L. M.; Giri, R. *Acc. Chem. Res.* **2021**, *54*, 3415–3437. (i) Zhu, S.; Zhao, X.; Li, H.; Chu, L. *Chem. Soc. Rev.* **2021**, *50*, 10836–10856. (j) Gao, P.; Niu, Y.-J.; Yang, F.; Guo, L. N.; Duan, X.-H. *Chem. Commun.* **2022**, *58*, 730–746.

[3] For a discussion of conjunctive XEC reaction mechanisms see: (a) Lin, Q.; Diao, T. *J. Am. Chem. Soc.* **2019**, *141*, 17937–17948. (b) Diccianni, J.; Lin, Q.; Diao, T. *Acc. Chem. Res.* **2020**, *53*, 906–919.

[4] For a representative example of a three-component conjunctive XEC reaction with terminal alkenes see: Shu, W.; García-Domínguez, A.; Quirós, M. T.; Mondal, R.; Cárdenas, D. J.; Nevado, C. *J. Am. Chem. Soc*. **2019**, *141*, 13812–13821.

other (Scheme 3.1b).[5] In addition, activating and directing groups are also used to achieve selectivity.[6]

Scheme 3.1. Prior Art: Conjunctive XEC Reactions.



We sought to develop a fully intramolecular reaction that would tether two electrophiles to the starting olefin and form two vicinal carbocycles in one synthetic step (Scheme 3.1c).[7]

[5] For a lead examples of a two-component conjunctive XEC reactions see: (a) Yan, C. S.; Peng, Y.; Xu, X.-B.; Wang, Y.-W. *Chem. Eur. J.* **2012**, *18*, 6039–6048. (b) Wang, K.; Ding, Z.; Zhou, Z.; Kong, W. *J. Am. Chem. Soc.* **2018**, *140*, 12364–12368. (c) Jin, Y.; Wang, C. *Angew. Chem., Int. Ed.* **2019**, *58*, 6722–6726. (d) Tian, Z.-X.; Qiao, J.-B.; Xu, G.-L.; Pang, X.; Qi, L.; Ma, W.-Y.; Zhao, Z.-Z.; Duan, J.; Du, Y.-F.; Su, P.; Liu, X.-Y.; Shu, X.-Z. *J. Am. Chem. Soc.* **2019**, *141*, 7637–7643. (e) Ma, T.; Chen, Y.; Li, Y.; Ping, Y.; Kong, W. *ACS Catal.* **2019**, *9*, 9127–9133. (f) Fan, P.; Lan, Y.; Zhang, C.; Wang, C. *J. Am. Chem. Soc.* **2020**, *142*, 2180–2186. (g) Yang, J.; Yang, L.; Gu, J; Shuai, L.; Wang, H.; Ouyang, Q.; Li, Y.-L.; Liu, H.; Gong, L. *Org. Lett.* **2022**, *24*, 2376–2380. (h) Yin, H.; Zhoa, C.; You, H.; Lin, K.; Gong, H. *Chem. Commun.* **2012**, *48*, 7034–7036. (i) Peng, Y.; Xu, X.-B.; Xiao, J.; Wang, Y.-W. *Chem. Commun.* **2014**, *50*, 472–474. (j) Kuang, Y.; Wang, X.; Anthony, D.; Diao, T. *Chem. Commun.* **2018**, *54*, 2558–2561. (k) Weires, N. A.; Slutskyy, Y.; Overman, L. E. *Angew. Chem. Int. Ed.* **2019**, *58*, 8561–8565.

[6] (a) García-Domínguez, A.; Li, Z.; Nevado, C. *J. Am. Chem. Soc.* **2017**, *139*, 6835– 6838. (b) Wang, L.; Wang, C. *Org. Lett.* **2020**, *22*, 8829–8835. (c) Zhao, Q.-W.; Yang, Z.-F.; Fu, X.-P.; Zhang, X. *Synlett* **2021**, *32*, 1565–1569. (d) Wang, X.-X.; Lu, X.; He, S.-J.; Fu, Y. *Chem. Sci.* **2020**, *11*, 7950–7956. (e) Feng, X.; Guo, L.; Zhu, S.; Chu, L. *Synlett* **2021**, *32*, 1519–1524.

[7] Examples of fully intramolecular conjunctive XEC reactions: (a) Xiao, J.; Wang, Y.-W.; Peng, Y. *Synthesis* **2017**, *49*, 3576–3581. (b) Peng, Y.; Xiao, J.; Xu, X.-B.; Duan, S.-M.; Ren, L.; Shao, Y.-L.; Wang, Y.-W. *Org. Lett.* **2016**, *18*, 5170–5173. (c) Xiao, J.; Cong, X.-W.; Yang, G.-Z.; Wang, Y.-W.; Peng, Y. *Org. Lett.* **2018**, *20*, 1651–1654. (d) Xiao, J.; Wang, Y.-W.; Qiu, Z.-P.; Peng, Y. *Synlett* **2021**, *32*, 1662–1664.

We were interested in synthesizing the vicinal cyclopentyl, cyclopropyl motifs as they are present in the bioactive molecules shown in Figure 3.1.[8]

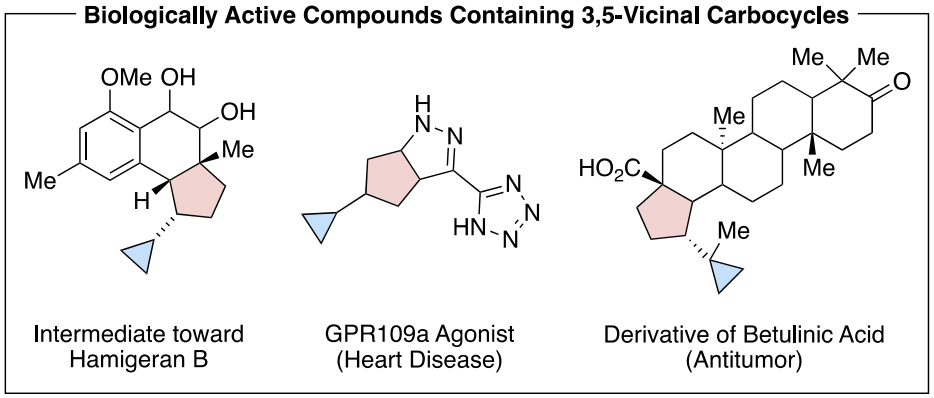


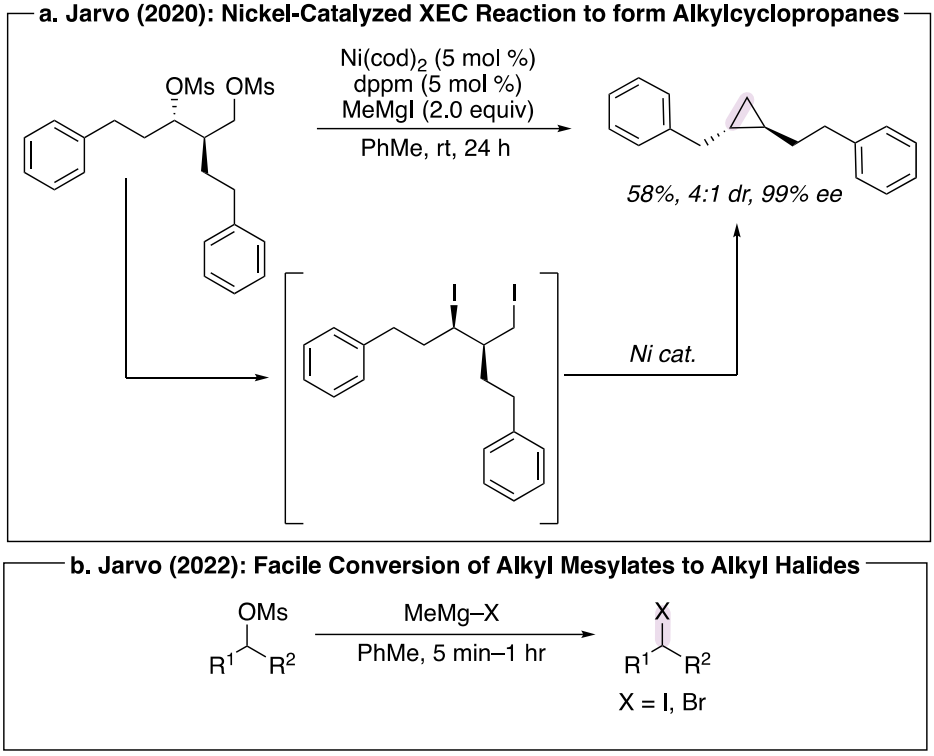
Figure 3.1. Medicinally Relevant Carbocycles.

Many of the previously developed conjunctive XEC reactions (Scheme 3.1a,b) were developed for halogenated electrophilic coupling partners. While this is advantageous for commercial access to these coupling partners, synthetic access to halide coupling partners can be challenging and thus limits the complexity of the products that could be synthesized using these methods. On the other hand, there are a variety of methods that can be used to synthesize complex alkyl alcohols which serve as precursors to pseudohalides such as alkyl sulfonates. For the development of the conjunctive XEC reaction, we envisioned a reaction of alkyl dimesylates, readily synthesized from the corresponding alcohols, that could cyclize onto the intervening alkene to form the desired ring system. Utilization of alkyl dimesylates in a nickel-catalyzed conjunctive XEC reaction was inspired by our group's previous work developing XEC reactions of 1,3-dimesylates (Scheme

[8] (a) Taber, D. F.; Tan, W. *J. Org. Chem.* **2008**, *73*, 7560–7564. (b) Wellington, K. D.; Cambie, R. C.; Rutledge, P. S.; Bergquist, P. C. *J. Nat. Prod.* **2000**, *63*, 79–85. (c) Imbriglio, J. E.; Chang, S.; Liang, R.; Raghavan, S.; Schmidt, D.; Smenton, A.; Tria, S.; Schrader, T. O.; Jung, J.-K.; Esser, C.; Taggart, A. K. P.; Cheng, K.; Carballo-Jane, E.; Waters, M. G.; Tata, J. R.; Colletti, S. L. *Bioorg. Med. Chem. Lett*. **2009**, *19*, 2121–2124. (d) Symon, A. V.; Veselova, N. N.; Kaplun, A. P.; Vlasenkova, N. K.; Fedorova, G. A.; Lyutik, A. I; Gerasimova, G. K.; Shvets, V. I. *Rus. J. Bioorg, Chem.* **2005**, *31*, 286–291.

3.2a).[9] In this work we discovered a rapid in situ conversion of alkyl mesylates to alkyl iodides which we aimed to employ in the conjunctive XEC reaction (Scheme 3.2b).[10] Here we report the first example of a nickel-catalyzed conjunctive XEC reaction of alkyl dimesylates for the synthesis of vicinal carbocycles.

Scheme 3.2. In-situ conversion of alkyl mesylates to alkyl iodides.



3.2 Results

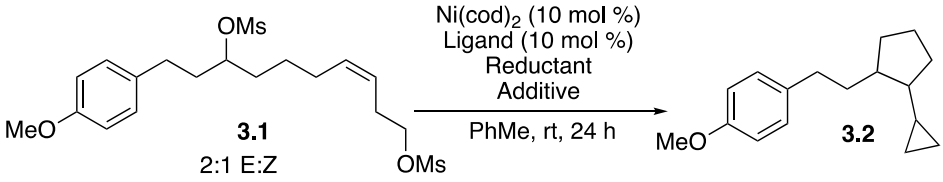
3.2.1 Optimization

We began our optimization of the conjuctive XEC reaction with unactivated dimesylate **3.1** which we hypothesized could cyclize to form product **3.2**. We began with conditions which

[9] Sanford, A. B.; Thane, T. A; McGinnis, T. M.; Chen, P.-P.; Hong, X.; Jarvo, E. R. *J. Am. Chem. Soc.* **2020**, *142*, 5017–5023.
[10] Hirbawi, N.; Lin, P. C.; Jarvo, E. R. *J. Org. Chem.* **2022**, *87*, 12352–12369.

were effective for the previously developed reaction of 1,3-dimesylates to afford cyclopropanes.[11] We were pleased to observe that these conditions afforded the desired cyclized product **3.2** in an 85% yield (Table 3.1, entry 1). We evaluated other ligands in the system (entries 2-4), including $Ni(cod)_2$ in the absence of ligand and observed that *rac*-BINAP was optimal for our system. We also evaluated several sources of reducing agents including Zn, Mn, and TDAE and found that they did not produce cyclized product **3.2**. Finally, in the absence of the nickel catalyst, we observe no conversion to product, indicating that the catalyst is necessary for reactivity (entry 9).

Table 3.1. Optimization of Conjunctive XEC Reaction.[12]



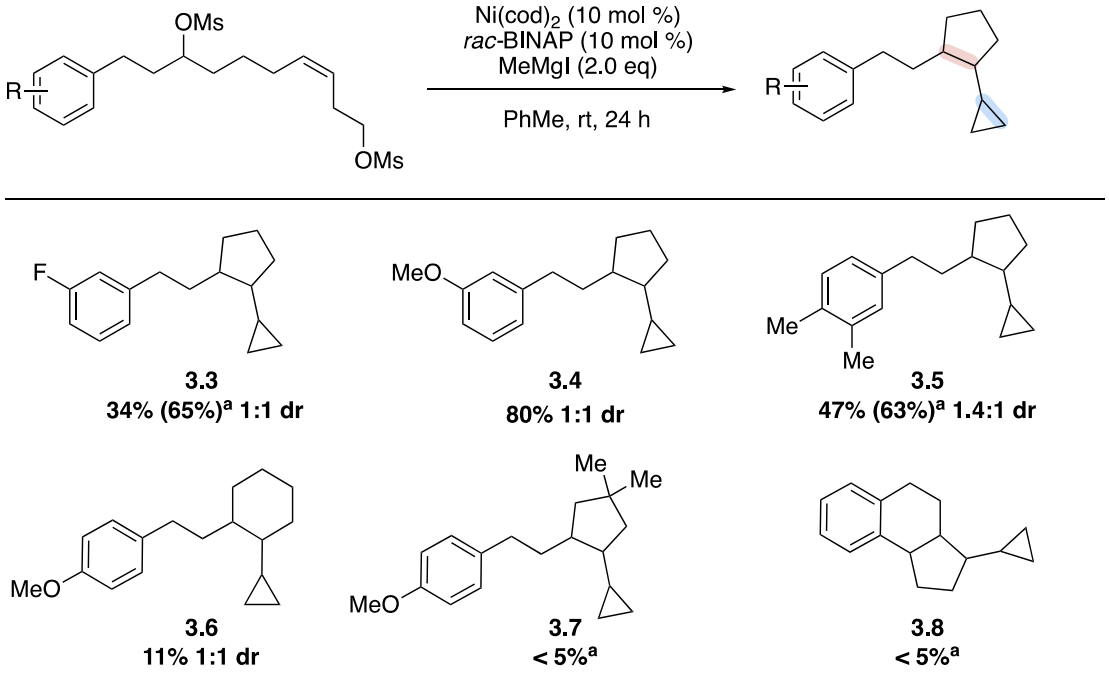
Entry	*Ligand*	*Reductant*	*Additive*	*Yield (%)[a]*
1	*rac*-BINAP	MeMgI	none	85
2	none	MeMgI	none	29
3	dppm	MeMgI	none	49
4	bipy	MeMgI	none	46
5[b]	*rac*-BINAP	Zn	NaI	<5
6[c]	*rac*-BINAP	Zn	$MgBr_2$	<5
7[d]	*rac*-BINAP	Mn	NaI and TMSCl	0
8[e]	*rac*-BINAP	TDAE	NaI	<5
9	none with no nickel	MeMgI	none	0

[a] Yield determined by ^{1}H with PhTMS as internal standard. [b] Zn (2.0 equiv), NaI (8.0 equiv). [c] Zn, $MgBr_2$ (2.0 equiv). [d] Mn and NaI (2.0 equiv), TMSCl (1.0 equiv). [e] TDAE, NaI (2.0 equiv).

[11] See reference 9.
[12] Optimization was performed by Dr. Kirsten Hewitt.

3.2.2 Evaluation of Substrate Scope

With optimized conditions in hand, we set about evaluating the scope of the reaction. We found that substitution on the pendant aryl ring has minimal influence in the reaction. Substrates **3.3, 3.4,** and **3.5** demonstrate that both electron-donating and electron-withdrawing substituents are tolerated on the pendant aryl ring (Figure 3.2). However, we observed that the reactions proceed with low diastereomeric ratios. Substrate **3.6** was synthesized to evaluate the potential to form cyclohexyl rings in the reaction however the reaction proceeded in much lower yield and 1:1 dr. In an effort to affect the diastereoslectivity in the reaction through substrate control, we attempted to synthesize **3.7** and **3.8** through the conjunctive reaction. To our surprise, however, neither of these substrates provided the desired cyclized product.

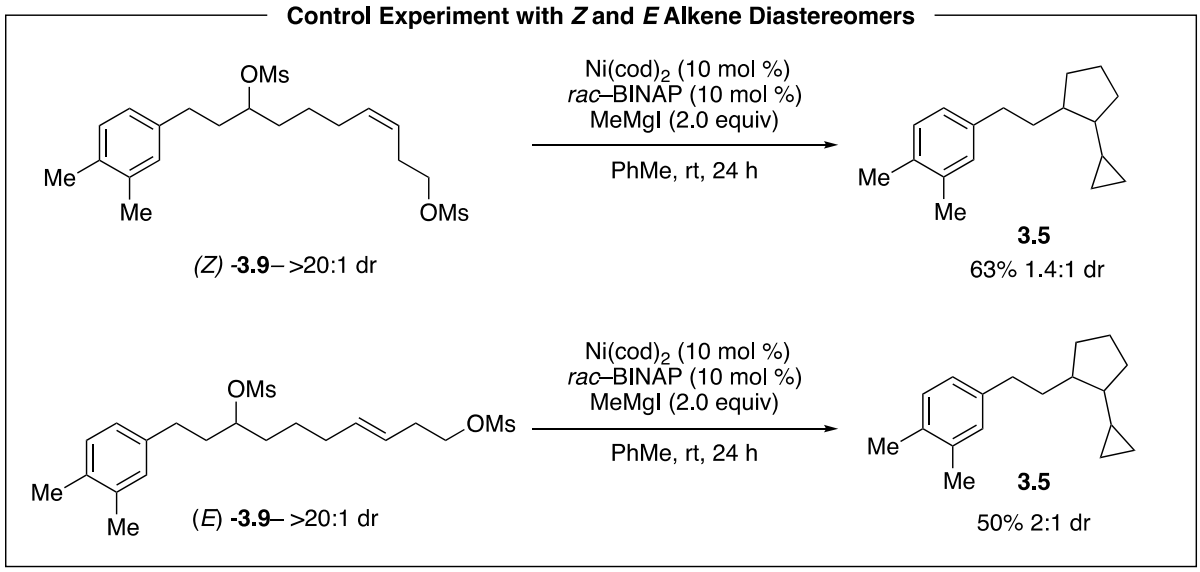


[a]Yield determined by ^{1}H NMR as compared to PhTMS as internal standard.

Figure 3.2. Scope of Nickel-Catalyzed Conjunctive XEC Reaction.

In the evaluation of the substrate scope the cyclized products were synthesized from an approximately 2:1 E:Z ratio of the starting olefin. We wanted to evaluate what affect the alkene geometry might have on the reaction, if any. We were able to separate the alkene diastereomers on silver impregnated silica gel to afford both the (*Z*)-**3.9** isomer and (E)-**3.9** isomer in >20:1 dr. We found that both diastereomers of starting material afford the cyclized product in similar yield and roughly 1:1 dr, indicating, the starting alkene geometry has little effect on the reactivity.

Scheme 3.3. Control Reaction with Single Alkene Diastereomer

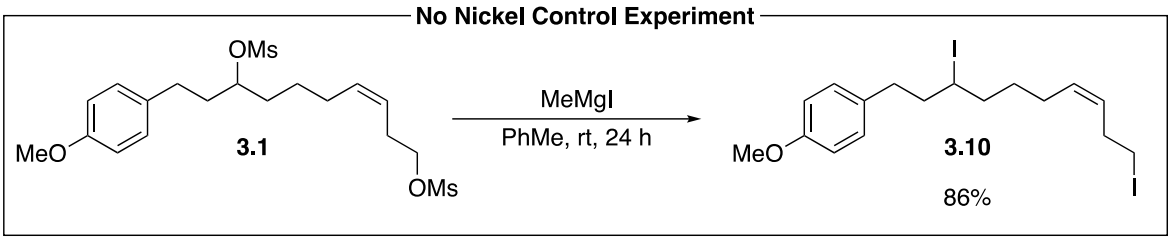


3.2.3 Mechanism

We performed several experiments to elucidate the mechanism of the conjunctive reaction.[13] When substrate **3.1** is subjected to MeMgI alone we observed high conversion to diiodide **3.10** (Scheme 3.4). Based on previous studies from our group we hypothesize that diiodide **3.10** is a key intermediate in the catalytic cycle.

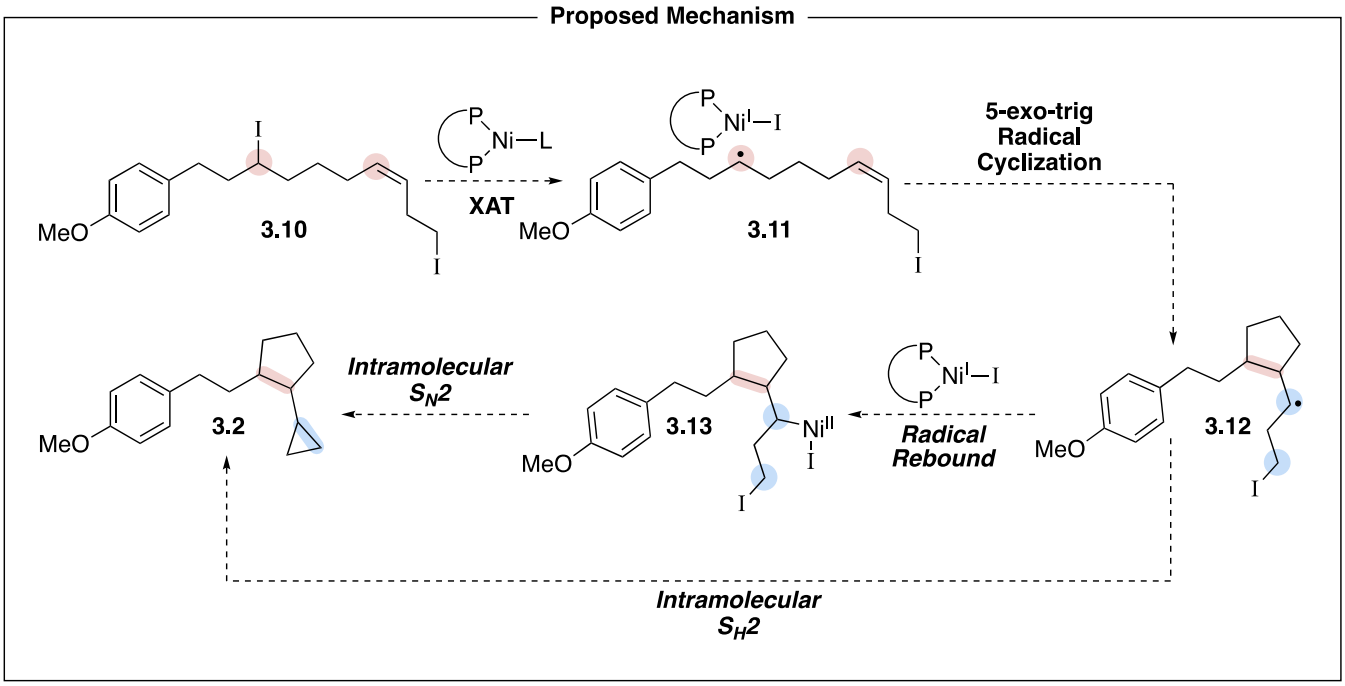
[13] Mechanistic experiments were performed by Dr. Kirsten A. Hewitt.

Scheme 3.4. Control reaction with no nickel catalyst.[14]



Diiodide **3.10** enters the catalytic cycle via halogen atom abstraction at the secondary iodide. The secondary alkyl radical **3.11** then undergoes a 5-exo-trig cyclization to afford the secondary radical **3.12**. We propose that the secondary radical **3.12** can then either re-engage the nickel catalyst to afford intermediate **3.13**, which undergoes an S_N2-like cyclization to afford the desired cyclized product or an S_H2 cyclization from **3.12** will form the cyclopropane ring.

Scheme 3.5. Proposed Mechanism.



[14] Experiment performed by Dr. Kirsten A. Hewitt.

3.3 Conclusion

We report a nickel-catalyzed intramolecular conjunctive XEC reaction of unactivated alkyl dimesylates. The reaction activates the alkyl dimesylates via MeMgI to afford alkyl diiodides which undergo nickel-mediated cyclization to afford vicinal carbocycles. The reaction is tolerant of a variety of different aryl groups and proceeds with approximately 1:1 dr of the carbocyclic products. Mechanistic experiments demonstrate that the reaction likely proceeds via radical intermediates. This reaction demonstrates the rapid construction of complex C(sp^3) ring systems from linear fragments via nickel-catalyzed conjunctive XEC.

3.4 Experimental Details

3.4.1 General Procedures

All reactions were carried out under an atmosphere of N_2 when noted. All glassware was oven- or flame-dried prior to use. Tetrahydrofuran (THF), diethyl ether (Et_2O), dichloromethane (DCM), methanol (MeOH), triethylamine (Et_3N), dimethylformamide (DMF), and toluene (PhMe) were degassed with Ar and then passed through two 4 x 36 inch columns of anhydrous neutral A-2 alumina (8 x 14 mesh; LaRoche Chemicals; activated under a flow of argon at 350 ºC for 12 h) to remove H_2O. All other solvents utilized were purchased "anhydrous" commercially, or purified as described. ^1H NMR spectra were recorded on Bruker DRX-400 (400 MHz ^1H, 100 MHz ^{13}C), GN-500 (500 MHz ^1H, 125.7 MHz ^{13}C), CRYO-500 (500 MHz ^1H, 125.7 MHz ^{13}C), or AVANCE-600 (600 MHz ^1H, 150 MHz ^{13}C) spectrometers. Proton chemical shifts are reported in ppm (δ) relative to internal tetramethylsilane (TMS, δ 0.00). Data are reported as follows: chemical shift (multiplicity [singlet (s), broad singlet (br s), doublet (d), doublet of doublets (dd), doublet of doublet of doublets (ddd), doublet of doublet of triplets (ddt), doublet of triplets (dt), triplet (t), triplet of doublets (td), triplet of triplets (tt), quartet (q), quartet of doublets (qd), quintet (quin),

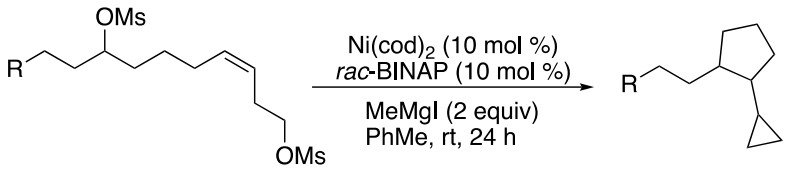
apparent singlet (as), apparent doublet (ad), apparent doublets of doublets (add), apparent doublet of triplets (adt), apparent doublet of quintets (adquin), apparent doublet of septets (adsept), apparent triplet (at), apparent triplet of doublets (atd), apparent triplet of triplets (att), apparent quartet (aq), apparent quartet of doublets (aqd), apparent quartet of triplets (aqt), apparent quintet of doublets (aquin d), apparent sextet (asext), apparent septet (asept), multiplet (m)], coupling constants [Hz], integration). Carbon chemical shifts are reported in ppm (δ) relative to TMS with the respective solvent resonance as the internal standard ($CDCl_3$, δ 77.16 ppm). Unless otherwise indicated, NMR data were collected at 25 ºC. Structural assignments were made with additional information from gCOSY, gHSQC, and gHMBC experiments. Infrared (IR) spectra were obtained on a Thermo Scientific Nicolet iS5 spectrometer with an iD5 ATR tip (neat) and are reported in terms of frequency of absorption (cm-1). Analytical thin-layer chromatography (TLC) was performed using Silica Gel 60 F254 precoated plates (0.25 mm thickness). Visualization was accomplished by irradiation with a UV lamp. Flash chromatography was performed using SiliaFlash F60 (40-63 μm, 60 Å) from SiliCycle. Automated chromatography was carried out on a Teledyne Isco CombiFlash R_f Plus. Melting points (M.p.) were obtained using a MelTemp melting point apparatus and are uncorrected. High resolution mass spectrometry was performed by the University of California, Irvine Mass Spectrometry Center.

Bis(1,5-cyclooctadiene)nickel was purchased from Strem, stored in a glove box freezer (–20 °C) under an atmosphere of N_2 and used as received. All ligands were purchased from Strem or Sigma Aldrich and were stored under N_2 atmosphere and used as received. The methylmagnesium iodide was titrated with iodine prior to use.[15] All other chemicals were purchased commercially and used as received, unless otherwise noted.

[15] Krasoviskiy, A.; Knochel, P. *Synthesis*, **2006**, *5,* 890–891.

3.4.2 Conjunctive XEC Reaction Procedures

3.4.2.1 Method A: Nickel-Catalyzed Conjunctive XEC Reaction



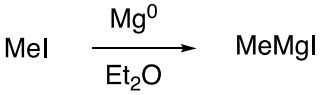
In a glovebox, an oven-dried 7 mL dram vial equipped with a stir bar was charged with dimesylate (1.0 equiv), $Ni(cod)_2$ (10. mol %), *rac*-BINAP (10. mol %) and PhMe (0.20 M in substrate). A solution of MeMgI in Et_2O (2.0 equiv) was then added dropwise via syringe. After 24 h, the reaction vial was removed from the glovebox, quenched with MeOH, filtered through a plug of silica gel eluting with Et_2O, and concentrated in vacuo. Phenyltrimethylsilane (PhTMS; 8.6 μL, 50. μmol) was added and the yield was determined by ^1H NMR based on comparison to PhTMS as internal standard before purification by column chromatography.

To remove olefin by-products resulting from β-hydride elimination, a Sharpless asymmetric dihydroxylation was performed.[16] To a flame-dried 7-mL dram vial was added AD-mix-β (1.4 g/mmol). The flask was sealed with a septum cap and placed under an atmosphere of N_2. Then *t*-BuOH (0.50 mL) and H_2O (0.50 mL) were added via syringe. The vial was cooled to 0 ºC and then unpurified reaction mixture was added dropwise as a solution in *t*-BuOH (0.50 mL) and H_2O (0.5 mL) via syringe. The mixture was allowed to stir at 0 ºC for 24 h. To quench, saturated aq. $Na_2S_2O_3$ (1.0 mL) was added and the mixture was allowed to warm to rt and stir for 1 h. Then the mixture was transferred to a separatory funnel, and the organic layer was extracted

[16] For the original report of the asymmetric dihydroxylation, see: Jacobsen, E. N.; Marko, I.; Mungall, W. S.; Schroeder, G.; Sharpless, K. B. Asymmetric Dihydroxylation via Ligand-Accelerated Catalysis. *J. Am. Chem. Soc.* **1988**, *110,* 1968–1970. For the procedure that was employed, see: Holl, K.; Schepmann, D.; Daniliuc, C. G.; Wünsch, B. Sharpless Asymmetric Dihydroxylation as the Key Step in the Enantioselective Synthesis of Spirocyclic σ1 Receptor Ligands. *Tetrahedron Asymmetry* **2014**, *25*, 268–277.

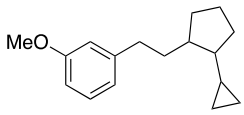
with EtOAc (x 3). The combined organic layers were washed with brine, dried over Na_2SO_4, filtered and concentrated in vacuo.

3.4.2.2 Preparation of Grignard Reagent



Under a N_2 atmosphere, a three-necked flask equipped with a stir bar, reflux condenser, and Schlenk filtration apparatus was charged with magnesium turnings (1.1 g, 45 mmol, 1.5 equiv). The flask and magnesium turnings were then flame-dried under vacuum and the flask was back-filled with N_2. Anhydrous Et_2O (7.0 mL) and a crystal of iodine (ca. 2.0 mg) were added to the flask. Freshly distilled iodomethane (1.9 mL, 31 mmol, 1.0 equiv) was slowly added over 30 min to maintain a gentle reflux. The mixture was stirred for 2 h at room temperature then filtered through the fritted Schlenk filter into a Schlenk flask under N_2 atmosphere. The magnesium turnings were washed with Et_2O (2 x 1.0 mL) then the Schlenk flask was sealed, removed, and placed under an N_2 atmosphere. The resulting methylmagnesium iodide was typically between 2.4 and 3.0 M as titrated by Knochel's method[17] and could be stored, sealed under N_2 atmosphere or in a glovebox, for up to 4 weeks.

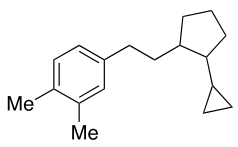
3.4.3 Characterization Data for Conjunctive XEC Reaction Products



Vicinal carbocycle (3.4) was prepared according to Method A. The following amounts of reagents were used: dimesylate **3.14** (50 mg, 0.11 mmol, 1.0 equiv), $Ni(cod)_2$ (3.0 mg, 10. μmol, 10. mol %), *rac*-BINAP (6.0 mg, 10. μmol, 10 mol %), MeMgI (70. μL, 0.22 mmol, 2.0 equiv, 2.9 M in

[17] See reference 15.

Et_2O), PhMe (0.55 mL), AD-mix-β (154 mg, 1.4 g/mmol), *t*-BuOH (1.0 mL) and H_2O (1.0 mL). Purification by column chromatography (0–1% Et_2O/pentanes) afforded the title compound as a yellow oil (22 mg, 90. μmol, 80% yield, 1:1 dr). The dr was determined by the integration of resonances attributed to the aromatic carbons in ^{13}C NMR. **TLC R_f** = 0.3 (100% hexanes); **^{1}H NMR** (500 MHz, $CDCl_3$) δ 7.19 (t, *J* = 7.8 Hz, 2H, both diastereomers), 6.80 (d, *J* = 7.50 Hz, 1H, one diastereomer), 6.79 (d, *J* = 7.50 Hz, 1H, other diastereomer), 6.76 (aq, *J* = 1.39 Hz, 2H, both diastereomers), 6.73 (dd, *J* = 7.96, 1.34 Hz, 2H, both diastereomers), 3.80 (s, 6H, both diastereomers), 2.69–2.62 (m, 2H, both diastereomers), 2.60–2.54 (m, 2H, both diastereomers), 2.23 (aq, *J* = 5.39 Hz, 1H, one diastereomers), 2.00–1.48 (m, 14H, both diastereomers), 1.44–1.11 (m, 5H, both diastereomers), 0.59–0.53 (m, 2H, both diastereomers), 0.50–0.30 (m, 4H, both diastereomers), 0.15–0.10 (m, 2H, both diastereomers), 0.01–-0.05 (m, 2H, both diastereomers); **^{13}C NMR** (125 MHz, $CDCl_3$) δ 159.7 (2C, both diastereomers), 145.2 (one diastereomer), 145.0 (other diastereomer), 129.3 (2C, both diastereomers), 121.0 (one diastereomer), 120.9 (other diastereomer), 114.4 (one diastereomer), 114.3 (other diastereomer), 110.9 (one diastereomer), 110.8 (other diastereomer), 55.3 (2C, both diastereomers), 51.0 (one diastereomer), 48.5 (other diastereomer), 46.3 (one diastereomer), 43.2 (other diastereomer), 37.3 (one diastereomer), 35.6 (other diastereomer), 35.2 (one diastereomer), 33.1 (other diastereomer), 32.6 (one diastereomer), 32.1 (other diastereomer), 31.7 (one diastereomer), 30.7 (other diastereomer), 23.6 (one diastereomer), 23.0 (other diastereomer), 15.4 (one diastereomer), 11.8 (other diastereomer), 5.5 (one diastereomer), 4.4 (other diastereomer), 3.0 (one diastereomer), 2.2 (other diastereomer); **HRMS** (TOF MS CI+) *m/z*: $[M]^+$ calcd for $C_{17}H_{24}O$, 244.1827; found 244.1821.



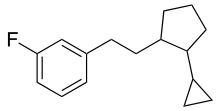
Vicinal carbocycle (3.5) was prepared according to Method A. The following amounts of reagents were used: dimesylate **3.9** (89 mg, 0.20 mmol, 1.0 equiv), $Ni(cod)_2$ (5.5 mg, 20. μmol, 10 mol %), *rac*-BINAP (12 mg, 20. μmol, 10 mol %), MeMgI (0.14 mL, 0.40 mmol, 2.0 equiv, 2.9 M in Et_2O), PhMe (1.0 mL), AD-mix-β (430 mg, 2.1 g/mmol), *t*-BuOH (1.5 mL) and H_2O (1.5 mL). Before purification, a ^1H NMR yield of 63% was obtained based on comparison to PhTMS as an internal standard. Purification by column chromatography (100% hexanes) afforded the title compound as a colorless oil (21 mg, 90. μmol, 44% yield, 1.4:1 dr). The dr was determined by the integration of resonances attributed to the aromatic carbons in ^{13}C NMR. For clarity, the ^{13}C data is tabulated individually.

TLC R_f = 0.8 (100% hexanes); **HRMS** (TOF MS CI+) *m/z*: $[M]^+$ calcd for $C_{18}H_{26}$, 242.2034; found 242.2027.

^1H NMR (500 MHz, $CDCl_3$) δ 6.97 (d, *J* = 7.6 Hz, 2H, both diastereomers), 6.91 (s, 2H, both diastereomers), 6.87 (d, *J* = 6.96 Hz, 2H, both diastereomers), 2.57–2.51 (m, 2H, both diastereomers), 2.47–2.40 (m, 2H, both diastereomers) 2.17 (s, 6H, both diastereomers), 2.15 (s, 6H, both diastereomers), 1.91–1.58 (m, 9H, both diastereomers), 1.55-1.47 (m, 3H, both diastereomers), 1.44–1.39 (m, 2H, both diastereomers), 1.34–1.22 (m, 4H, both diastereomers), 1.19–1.12 (m, 1H, one diastereomer), 1.09–1.03 (m, 1H, one diastereomer), 0.52–0.45 (m, 2H, both diastereomers), 0.42–0.22 (m, 4H, both diastereomers), 0.08–0.03 (m, 2H, both diastereomers), -0.06–-0.13 (m, 2H, both diastereomers).

Major Diastereomer: ^{13}C NMR (125 MHz, $CDCl_3$) δ 140.9, 136.3, 133.6, 129.8, 129.6, 125.7, 48.4, 43.2, 35.0, 33.4, 31.7, 30.7 (2C), 22.9, 19.4, 11.8, 5.4, 3.0.

Minor Diastereomer: ^{13}C NMR (125 MHz, $CDCl_3$) δ 140.7, 136.3, 133.6, 129.8, 129.6, 125.7, 50.9, 46.3, 37.5, 34.6, 32.5 (2C), 32.1, 22.9, 19.8, 15.4, 4.3, 2.1.

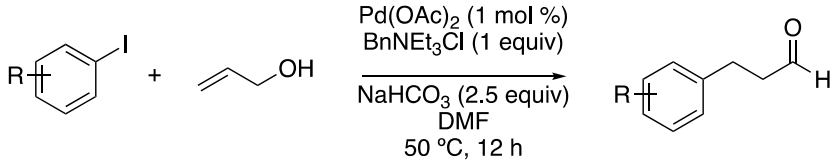


Vicinal carbocycle (3.3) was prepared according to Method A. The following amounts of reagents were used: dimesylate **3.15** (67 mg, 0.16 mmol, 1.0 equiv), $Ni(cod)_2$ (4.4 mg, 16. μmol, 10 mol %), *rac*-BINAP (10. mg, 16. μmol, 10 mol %), MeMgI (0.11 mL, 0.32 mmol, 2.0 equiv, 2.9 M in Et_2O), PhMe (1.0 mL). Before purification, a ^{1}H NMR yield of 65% was obtained based on comparison of PhTMS as an internal standard. Purification by column chromatography (100% pentanes) afforded the title compound as a colorless oil (13 mg, 50. μmol, 34% yield, 1:1 dr). The dr was determined by the integration of resonances attributed to the aromatic carbons in ^{13}C NMR. **TLC R_f** = 0.8 (100% hexanes); **^{1}H NMR** (500 MHz, $CDCl_3$) δ 7.22 (aq, *J* = 7.3 Hz, 2H, both diastereomers), 6.97 (d, *J* = 7.5 Hz, 2H, both diastereomers), 6.91–6.83 (m, 4H, both diastereomers), 2.71–2.54 (m, 4H, both diastereomers), 2.00–1.12 (m, 20H, both diastereomers), 0.59–0.29 (m, 6H, both diastereomers), 0.15–0.09 (m, 2H, both diastereomers), 0.01–-0.05 (m, 2H); **^{13}C NMR** (125 MHz, $CDCl_3$) δ 163.0 (d, *J* = 245.1 Hz, 2C, both diastereomers), 146.1 (d, *J* = 7.1 Hz, one diastereomer), 145.9 (d, *J* = 7.2 Hz, other diastereomer), 129.7 (d, *J* = 8.3 Hz, 2C, both diastereomers), 124.1 (d, *J* = 2.6 Hz, 2C, both diastereomers), 115.27 (d, *J* = 20.9 Hz, one diastereomer), 115.24 (d, *J* = 20.5 Hz, other diastereomer), 112.5 (d, *J* = 21.0 Hz, 2C, both diastereomers), 51.0 (one diastereomer), 48.4 (other diastereomer), 46.1 (one diastereomer), 43.1

(other diastereomer), 37.0 (one diastereomer), 35.24 (other diastereomer), 34.89 (one diastereomer), 33.0 (other diastereomer), 32.5 (one diastereomer), 32.1 (other diastereomer), 31.7 (one diastereomer). 30.7 (other diastereomer), 23.6 (one diastereomer), 23.0 (other diastereomer), 15.4 (one diastereomer), 11.8 (other diastereomer), 5.5 (one diastereomer), 4.4 (other diastereomer), 3.0 (one diastereomer), 2.2 (other diastereomer); **^{19}F NMR** (565 MHz, $CDCl_3$) δ -114.1 (aq, J = 8.2 Hz, 2F, both diastereomers); **HRMS** (TOF MS CI+) *m/z*: $[M]^+$ calcd for $C_{16}H_{21}F$, 232.1627; found 232.1635.

3.4.4 General Procedures for the Synthesis of Dimesylate Starting Materials

3.4.4.1 Method B: Pd-Catalyzed Heck Reaction

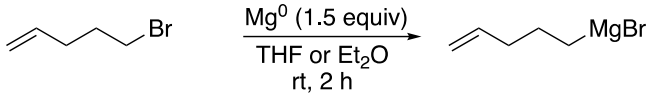


This method was adapted from a procedure reported by Su.[18] A flame dried pressure tube equipped with a stir bar was charged with aryl iodide[19] (1.0 equiv), $NaHCO_3$ (2.5 equiv), and $BnNEt_3Cl$ (1.0 equiv). The flask was sealed with a septum and pumped into a glovebox. Then the pressure tube was charged with $Pd(OAc)_2$ (1.0 mol %), sealed with septum, removed from the glovebox and placed under an atmosphere of N_2. Then DMF (0.20 M) was added via syringe followed by allyl alcohol (1.5 equiv). The pressure tube was sealed with a teflon cap, heated in an oil bath to 50 ºC and allowed to stir at that temperature for at least 5 h. After the reaction was complete, the flask was cooled to rt and allowed to stir at that temperature for 1 h. The mixture was then filtered through a pad of silica gel eluting with EtOAc. The filtrate was concentrated to

[18] Shang, Y.; Jie, X.; Jonnada, K.; Zafar, S. N.; Su, W. *Nat Commun*. **2017**, *8*, 2273.
[19] Note: if the aryl iodide starting material is a liquid, it was added via syringe after the flask was removed from the glovebox.

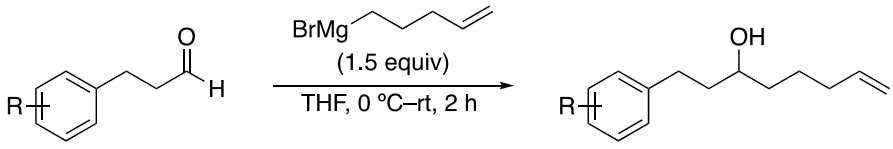
remove the excess EtOAc and then transferred to a separatory funnel. The organic layer was washed with excess H_2O (x 5) and then brine. The combined organic layers were dried over Na_2SO_4, filtered, and concentrated in vacuo. The product was purified by column chromatography.

3.4.4.2 Method C: Preparation of Grignard Reagent



To a flame dried two-neck round bottom flask equipped with a stir bar, was added magnesium turnings (1.5 equiv). The flask and magnesium turnings were then flame-dried under vacuum and the flask was back-filled with N_2. Anhydrous Et_2O or THF (2.0 M) and a crystal of iodine (ca. 2.0 mg) were added to the flask. Then 5-bromopentene (1.0 equiv) was slowly added neat over 30 min to maintain a gentle reflux. The mixture was stirred for 2 h at room temperature The resulting 4-pentenylmagnesium bromide was titrated according to Knochel's method and used immediately.[20]

3.4.4.3 Method D: Nucleophilic Grignard Addition in Aldehyde

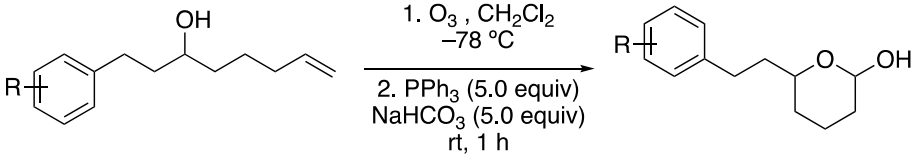


To a flame dried round bottom flask equipped with a stir bar, was added aldehyde (1.0 equiv) as a solution in THF or Et_2O (0.20 M). The flask was cooled to 0 ºC and the freshly prepared 4-pentenylmagnesium bromide (1.5 equiv) was added dropwise via syringe. The flask was warmed to rt and allowed to stir for 2 h. To quench, saturated aq. NH_4Cl was added to the reaction mixture. The biphasic solution was transferred to a separatory funnel and the organic layer was extracted

[20] See reference 15.

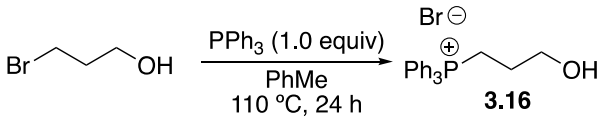
with EtOAc. The combined organic layers were washed with H_2O, brine, dried over Na_2SO_4, filtered, and concentrated in vacuo.

3.4.4.4. Method E: Ozonolysis of Terminal Alkenes



This method was adapted from a procedure reported by Taber.[21] A round-bottom flask equipped with stir bar was charged with alkene (1.0 equiv), and CH_2Cl_2 (0.10 M). The reaction was then cooled to –78 ºC, and ozone was bubbled through mixture until the solution turned blue. Ozone flow was then discontinued, and O_2 was passed through the solution for 5 min. PPh_3 (5.0 equiv) and $NaHCO_3$ (5.0 equiv) were then added to flask and the mixture was allowed to stir for at least 1 h. Then H_2O was added and the biphasic mixture was transferred to a separatory funnel. The organic layer was extracted with CH_2Cl_2 (x 3). The combined organic layers were washed with brine, dried over Na_2SO_4, filtered, and concentrated in vacuo.

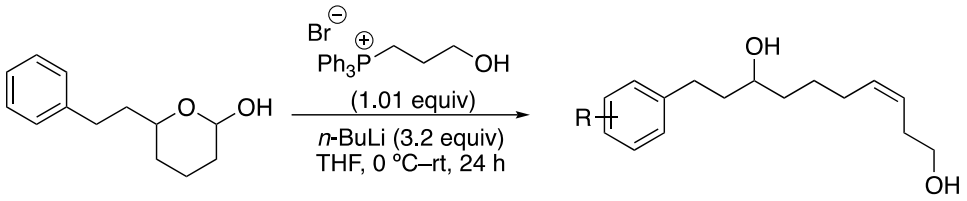
3.4.4.5 Method F: Preparation of Wittig Salt 3.16



To a flame dried round bottom flask equipped with a stir bar and reflux condenser was added 3-bromopropanol (1.0 equiv) and PhMe (1.1 M). Then PPh_3 (1.0 equiv) was added, the reaction mixture was heated in an oil bath to reflux and allowed to stir until white precipitate formed (~15–24 h). The flask was cooled to rt, the precipitate was filtered and washed with hexanes. The white solids were collected and dried under vacuum overnight.

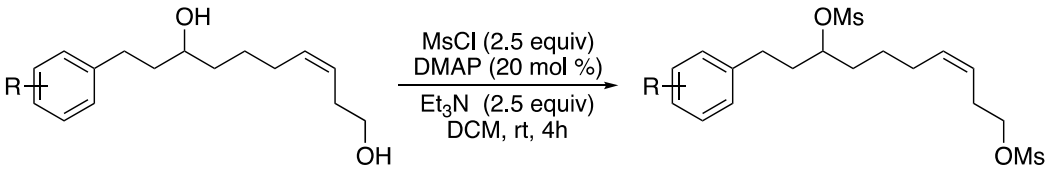
[21] Taber, D. F.; Guo, P. Convenient Access to Bicyclic and Tricyclic Diazenes. *J. Org. Chem.* **2008**, *73*, 9479–9481.

3.4.4.6 Method G: Wittig Reaction



This method was adapted from a procedure reported by Taber.[22] To a flame dried round bottom flask equipped with stir bar was added the Wittig salt **3.16** (1.01 equiv) and THF (0.2 M). The flask is cooled to 0 ºC and *n*-BuLi (3.2 equiv, 2.5 M in hexanes) was added dropwise. The dark red solution was allowed to stir at 0 ºC for 1 h. Then, a solution of lactol (1.0 equiv) in THF (1.0 M) was added and the reaction mixture was warmed to rt. The resulting orange solution was allowed to stir at rt for 24 h. To quench, saturated aq. NH_4Cl was added dropwise. The biphasic mixture was transferred to a separatory funnel. The organic layer was extracted with EtOAc (x 3). The combined organic layers were washed with brine, dried over Na_2SO_4, filtered, and concentrated in vacuo.

3.4.4.7 Method H: Mesylation Reaction

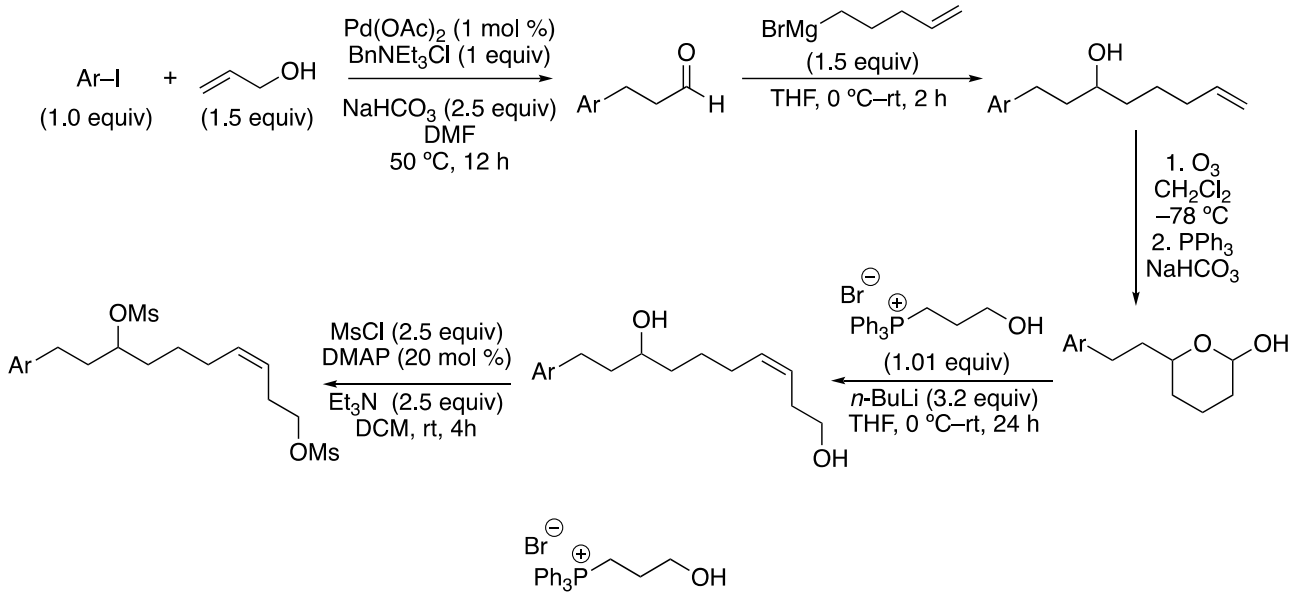


A flame dried round bottom flask equipped with a stir bar was charged with diol (1.0 equiv) and CH_2Cl_2 (0.20 M) under N_2. Then, Et_3N (1.5 equiv), DMAP (20 mol %), and MsCl (2.5 equiv) were added in that order. The reaction mixture was then stirred at rt for at least 4 h. Once complete, sat. $NaHCO_3$ was added and the reaction mixture was extracted with CH_2Cl_2 (x 3). The combined organic layers were washed with brine, dried over Na_2SO_4, and concentrated in vacuo.

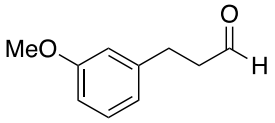
[22] See reference 21.

3.4.5 Synthesis and Characterization of Dimesylate Starting Materials

Scheme 3.6. General Synthesis of Dimesylate Starting Material



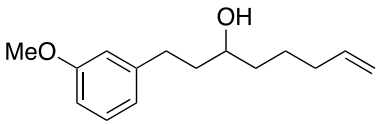
Wittig Salt (3.16) was prepared according to Method F. The following amounts of reagents were used: 4-bromoproanol (0.89 mL, 10. mmol, 1.0 equiv), PPh_3 (2.6 g, 10. mmol, 1.0 equiv), and PhMe (9.1 mL). Analytical data is consistent with literature values.[23] **^{1}H NMR** (400 MHz, $CDCl_3$) δ 7.84–7.75 (m, 9H), 7.74–7.67 (m, 6H), 4.93 (s, 1H) 3.94–3.62 (m, 4H), 1.95–1.74 (m, 2H).



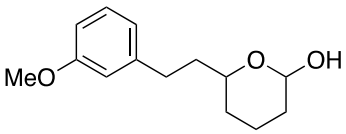
Aldehyde (3.17) was prepared according to Method B. The following amounts of reagents were used: 3-iodoanisole (0.59 mL, 5.0 mmol, 1.0 equiv), allyl alcohol (0.51 mL, 7.5 mmol, 1.5 equiv), $Pd(OAc)_2$ (22 mg, 0.10 mmol, 2.0 mol %), $BnEt_3NCl$ (1.1 g, 5.0 mmol, 1.0 equiv), $NaHCO_3$ (1.0 g, 13 mmol, 2.5 equiv), and DMF (20 mL). Purification by column chromatography (0–10% EtOAc/hexanes) afforded the title compound as a yellow oil (0.57 g, 3.4 mmol, 69% yield).

[23] Kandula, S. R. V.; Kumar, P. *Tetrahedron Asymmetry* **2005**, *16*, 3268–3274.

Analytical data is consistent with literature values.[24] **^{1}H NMR** (500 MHz, $CDCl_3$) δ 9.83 (t, *J* = 1.4 Hz, 1H), 7.22 (td, *J* = 7.5, 1.0 Hz, 1H), 6.80–6.75 (m, 3H), 3.81 (s, 3H), 2.95 (t, *J* = 7.5 Hz, 2H), 2.79 (t, *J* = 8.1Hz, 2H).

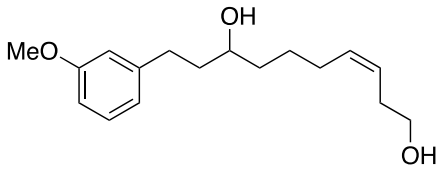


Alcohol (3.18) was prepared according to Method D. The following amounts of reagents were used: aldehyde **3.17** (0.57 g, 3.4 mmol, 1.0 equiv), 4-pentenylmagnesium bromide (5.1 mL, 5.1 mmol, 1.5 equiv, 1.0 M in THF), and THF (17 mL). Purification by column chromatography (0–10% EtOAc/hexanes) afforded the title compound as a brown oil (0.49 g, 2.1 mmol, 61% yield). **^{1}H NMR** (500 MHz, $CDCl_3$) δ 7.20 (t, *J* = 8.0 Hz, 1H), 6.79 (d, *J* = 7.5 Hz, 1H), 6.75–6.72 (m, 2H), 5.80 (ddt, *J* = 17.8, 10.1, 6.4 Hz, 1H), 4.98 (ddt, *J* = 17.1, 2.0, 1.6 Hz, 1H), 4.95 (ddt, *J* = 10.2, 2.0, 1.0 Hz, 1H), 3.80 (s, 3H), 3.63 (br s, 1H), 2.77 (ddd, *J* = 13.8, 9.7, 5.7 Hz, 1H), 2.65 (ddd, *J* = 14.0, 9.1, 7.0 Hz, 1H), 2.07 (aq, *J* = 6.1 Hz, 2H), 1.84–1.70 (m, 2H), 1.57–1.40 (m, 4H), 1.33 (br s, 1H).

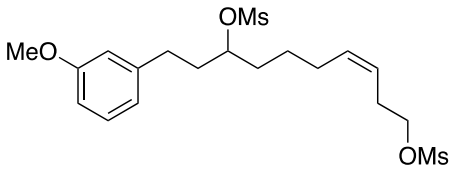


Lactol (3.19) was prepared according to Method E. The following amounts of reagents were used: alkene **3.18** (0.46 g, 2.0 mmol, 1.0 equiv), ozone (excess), $NaHCO_3$ (0.28 g, 3.4 mmol, 1.7 equiv), PPh_3 (0.89 g. 3.4 mmol, 1.7 equiv), and CH_2Cl_2 (2.0 mL). The crude residue was taken on with minimal purification.

[24] Huang, H.; Yu, C.; Zhang, Y.; Zhang, Y.; Mariano, P. S.; Wang, W. *J. Am. Chem. Soc.* **2017**, *139*, 9799–9802.



Diol (3.20) was prepared according to method G. The following amounts of reagents were used: lactol **3.19** (0.32 g, 1.3 mmol, 1.0 equiv), Wittig salt **3.16** (0.53 g, 0.37 mmol, 1.01 equiv), *n*-BuLi (1.7 mL, 4.2 mmol, 3.2 equiv, 2.5 M in hexane), and THF (6.5 mL). The crude residue was taken on with minimal purification.

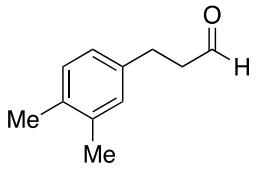


Dimesylate (3.14) was prepared according to Method H. The following amounts of reagents were used: diol **3.20** (190 mg, 0.67 mmol, 1.0 equiv), MsCl (0.15 mL, 2.0 mmol, 3.0 equiv), DMAP (16 mg, 0.13 mmol, 0.20 equiv), Et_3N (0.28 mL, 2.0 mmol, 3.0 equiv), and CH_2Cl_2 (3.4 mL). Purification by column chromatography (0–50% EtOAc/hexanes) afforded the title compound as a yellow oil (170 mg, 0.39 mmol, 19% yield over 3 steps, 1.5:1 dr). For clarity, the ^1H and ^{13}C data are tabulated individually.

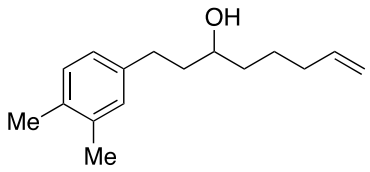
TLC $\mathbf{R_f}$ = 0.2 (50% EtOAc/hexanes); **HRMS** (TOF MS ES+) *m/z*: $[M+Na]^+$ calcd for $C_{19}H_{30}O_7S_2Na$, 457.1331; found 457.1336.

Major Diastereomer ^{1}H NMR (600 MHz, $CDCl_3$) δ 7.21 (d, *J* = 8.2 Hz, 1H), 6.79 (d, *J* = 7.4 Hz, 1H), 6.75–6.74 (m, 2H), 5.56–5.52 (m, 1H), 5.41–5.36 (m, 1H), 4.76 (quin, *J* = 6.0 Hz, 1H), 4.20 (t, *J* = 6.7 Hz, 2H), 3.80 (s, 3H), 3.01 (s, 3H), 3.00 (s, 3H), 2.76–2.71(m, 1H), 2.70–2.65 (m,1H), 2.49 (dt, *J* = 7.1, 6.3 Hz, 2H), 2.15–1.95 (m, 4H), 1.80–1.70 (m, 2H), 1.54–1.43 (m, 2H); **^{13}C NMR** (125 MHz, $CDCl_3$) δ 159.9, 142.6, 133.1, 129.7, 123.9, 120.8, 114.3, 111.6, 82.9, 69.3, 55.3, 37.6, 36.1, 34.2, 32.5, 21.5, 27.5, 27.0, 24.8.

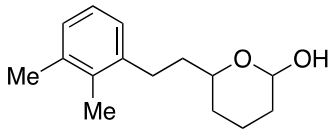
Minor Diastereomer ^{1}H NMR (600 MHz, $CDCl_3$) δ 7.21 (d, *J* = 8.2 Hz, 1H), 6.79 (d, *J* = 7.4 Hz, 1H), 6.75–6.74 (m, 2H), 5.56–5.52 (m, 1H), 5.41–5.36 (m, 1H), 4.76 (quint, *J* = 6.0 Hz, 1H), 4.22 (t, *J* = 6.5 Hz, 2H), 3.80 (s, 3H), 3.005 (s, 3H), 2.997 (s, 3H), 2.76–2.71(m, 1H), 2.70–2.65 (m,1H), 2.44 (dt, *J* = 6.7, 6.2 Hz, 2H), 2.15–1.95 (m, 4H), 1.80–1.70 (m, 2H), 1.54–1.43 (m, 2H); **^{13}C NMR** (125 MHz, $CDCl_3$) δ 159.9, 142.6, 133.8, 129.7, 124.8, 120.8, 114.3, 111.6, 83.1, 69.5, 55.3, 37.6, 36.1, 34.0, 32.5, 31.5, 27.5, 27.0, 24.5.



Aldehyde (3.21) was prepared according to Method B. The following amounts of reagents were used: 4-iodo-*o*-xylene (0.85 mL, 6.0 mmol, 1.0 equiv), allyl alcohol (0.61 mL, 9.0 mmol, 1.5 equiv), $Pd(OAc)_2$ (27 mg, 0.12 mmol, 2.0 mol %), $BnEt_3NCl$ (1.4 g, 6.0 mmol, 1.0 equiv), $NaHCO_3$ (1.3 g, 15 mmol, 2.5 equiv), and DMF (24 mL). Purification by column chromatography (0–5% EtOAc/hexanes) afforded the title compound as a yellow oil (0.56 g, 3.4 mmol, 57% yield). For clarity, the ^{1}H and ^{13}C data are tabulated individually. **TLC R_f** = 0.7 (50% EtOAc/hexanes); **^{1}H NMR** (500 MHz, $CDCl_3$) δ 9.81 (t, *J* = 1.5 Hz, 1H), 7.05 (d, *J* = 7.6 Hz, 1H), 6.96 (s, 1H), 6.92 (d, *J* = 7.6 Hz, 1H), 2.89 (t, *J* = 7.5 Hz, 2H), 2.75 (t, *J* = 8.0 Hz, 2H), 2.23 (s, 3H), 2.22 (s, 3H); **^{13}C NMR** (126 MHz, $CDCl_3$) δ 201.9, 137.7, 136.8, 134.5, 129.9, 129.7, 125.6, 45.5, 27.7, 19.8, 19.3; **HRMS** (TOF MS CI+) *m/z*: $[M]^+$ calcd for $C_{11}H_{14}O$, 162.1045; found 162.1044.



Alcohol (3.22) was prepared according to Method D**.** The following amounts of reagents were used: aldehyde **3.21** (0.56 g, 3.4 mmol, 1.0 equiv), 4-pentenylmagnesium bromide (3.9 mL, 5.1 mmol, 1.5 equiv, 1.3 M in Et_2O), Et_2O (17 mL). Purification by column chromatography (0–20% EtOAc/hexanes) afforded the title compound as a yellow oil (0.43 g, 1.8 mmol, 54% yield). **TLC R_f** = 0.7 (20% EtOAc/hexanes); **^{1}H NMR** (500 MHz, $CDCl_3$) δ 7.04 (d, *J* = 7.6 Hz, 1H), 6.97 (s, 1H), 6.93 (d, *J* = 7.6 Hz, 1H), 5.80 (ddt, *J* = 17.0, 10.3, 6.6 Hz, 1H), 4.98 (ddt, *J* = 17.1, 2.0, 1.5 Hz, 1H), 4.95 (ddt, *J* = 10.2, 2.1, 1.1 Hz, 1H), 3.63 (br s, 1H), 2.72 (ddd, *J* = 13.8, 9.3, 6.0 Hz, 1H), 2.60 (ddd, *J* = 13.7, 8.9, 6.1 Hz, 1H), 2.23 (s, 3H), 2.22 (s, 3H), 2.07 (aq, *J* = 5.6 Hz, 2H), 1.81–1.68 (m, 2H), 1.56–1.40 (m, 4H), 1.32 (d, *J* = 4.3 Hz, 1H); **^{13}C NMR** (126 MHz, $CDCl_3$) δ 139.6, 138.7, 136.5, 134.0, 129.8, 129.7, 125.8, 114.7, 71.4, 39.3, 37.0, 33.7, 31.6, 24.9, 19.8, 19.3; **HRMS** (TOF MS CI+) *m/z*: $[M+Na]^+$ calcd for $C_{16}H_{24}ONa$, 255.1725; found 255.1723.

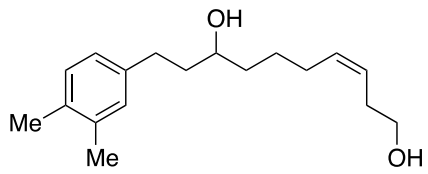


Lactol (3.23) was prepared according to Method E. The following amounts of reagents were used: alkene **3.22** (0.42 g, 1.3 mmol, 1.0 equiv), ozone (excess), $NaHCO_3$ (190 mg, 2.2 mmol, 1.7 equiv), PPh_3 (0.58 g. 2.2 mmol, 1.7 mmol), CH_2Cl_2 (1.3 mL). Purification by column chromatography (0–20% EtOAc/hexanes) afforded the title compound as a colorless oil (240 mg, 1.0 mmol, 80% yield, 1.5:1 dr). For clarity, the ^{1}H and ^{13}C data are tabulated individually.

TLC R_f = 0.6 (30% EtOAc/hexanes); **HRMS** (TOF MS CI+) *m/z*: $[M+Na]^+$ calcd for $C_{15}H_{22}O_2Na$, 257.1518; found 257.1523.

Major Diastereomer ^{1}H NMR (500 MHz, $CDCl_3$) δ 7.04 (d, *J* = 7.6 Hz, 1H), 6.97 (s, 1H), 6.93 (d, *J* = 7.5 Hz, 1H), 4.70 (t, *J* = 7.7 Hz, 1H), 3.44–3.39 (m, 1H), 2.84 (d, *J* = 6.1 Hz, 1H), 2.76–2.52 (m, 2H), 2.23 (s, 3H), 1.92–1.80 (m, 3H), 1.78–1.61 (m, 3H), 1.54–1.48 (m, 2H), 1.36–1.20 (m, 3H); **^{13}C NMR** (126 MHz, $CDCl_3$) δ 139.6, 136.5, 133.9, 129.9, 129.6, 125.8, 96.5, 75.5, 37.8, 33.0, 31.3, 30.5, 29.8, 22.1, 19.3.

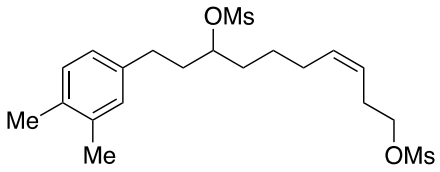
Minor Diastereomer ^{1}H NMR (500 MHz, $CDCl_3$) δ 7.04 (d, *J* = 7.6 Hz, 1H), 6.97 (s, 1H), 6.93 (d, *J* = 7.5 Hz, 1H), 5.33 (s, 1H), 3.96–3.91 (m, 1H), 2.76–2.52 (m, 2H), 2.33 (brs, 1H), 2.22 (s, 3H), 1.92–1.80 (m, 3H), 1.78–1.61 (m, 3H), 1.54–1.48 (m, 2H), 1.36–1.20 (m, 3H); **^{13}C NMR** (126 MHz, $CDCl_3$) δ 139.8, 136.5, 133.9, 129.8, 129.6, 125.8, 92.0, 68.1, 38.1, 33.0, 31.3, 31.2, 29.8, 22.1, 19.3.



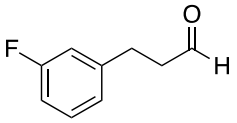
Diol (3.24) was prepared according to Method G**.** The following amounts of reagents were used: lactol **3.23** (240 mg, 1.0 mmol. 1.0 equiv), Wittig salt **3.16** (0.41 g, 1.01 mmol, 1.01 equiv), *n*-BuLi (1.3 mL, 3.2 mmol, 3.2 equiv, 2.5 M in hexanes) and THF (5.0 mL). Purification by column chromatography (0–50% EtOAc/hexanes) afforded the title compound as a yellow oil (0.16 g, 0.59 mmol, 59% yield, 1.5:1 dr). Diastereomers were separated on Ag impregnated silica[25] by column chromatography to afford the title compound as a brown oil (95 mg, 0.34 mmol, >20:1 dr *Z:E*). **TLC R_f** = 0.4 (50% EtOAc/hexanes); **^{1}H NMR** (500 MHz, $CDCl_3$) δ 7.04 (d, *J* = 7.6 Hz, 1H), 6.98 (s, 1H), 6.93 (d, *J* = 7.5 Hz, 1H), 5.55 (dt, *J* = 10.8, 8.0 Hz, 1H), 5.38 (dt, *J* = 10.0, 8.3 Hz,

[25] Lawrence, B. M. *J. Chromatog.* **1968**, *38*, 535–537.

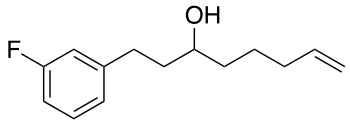
1H), 3.64 (t, J = 6.4 Hz, 3H), 2.75–2.69 (m, 1H), 2.63–2.57 (m, 1H), 2.30 (dt, J = 6.7, 6.2 Hz, 2H), 2.24 (s, 3H), 2.22 (s, 3H), 2.09 (quint, 6.6 Hz, 2H), 1.80–1.67 (m, 2H), 1.54–1.37 (m, 6H); **^{13}C NMR** (125 MHz, $CDCl_3$) δ 139.5, 136.6, 134.0, 133.0, 129.8, 129.7, 125.8, 125.6, 71.3, 62.3, 39.3, 37.0, 31.6, 30.8, 27.3, 25.7, 19.8, 19.3. **HRMS** (TOF MS CI+) *m/z*: $[M+Na]^+$ calcd for $C_{18}H_{28}O_2Na$, 299.1987; found 299.1995.



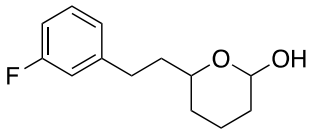
Dimesylate (3.9) was prepared according to Method H. The following amounts of reagents were used: diol **3.24** (89 mg, 0.32 mmol, 1.0 equiv), MsCl (70. µL, 0.96 mmol, 3.0 equiv), DMAP (8.0 mg, 60. µmol, 0.20 equiv), Et_3N (0.13 mL, 0.96 mmol, 3.0 equiv), and CH_2Cl_2 (1.6 mL). Purification by column chromatography (0–50% EtOAc/hexanes) afforded the title compound as a yellow oil (95 mg, 0.22 mmol, 69% yield, >20:1 dr). **TLC R_f** = 0.7 (50% EtOAc/hexanes); **^{1}H NMR** (400 MHz, $CDCl_3$) δ 7.05 (d, J = 7.7 Hz, 1H), 6.96 (s, 1H), 6.92 (d, J = 7.6 Hz, 1H), 5.53 (dtt, J = 10.8, 7.3, 1.4 Hz, 1H), 5.38 (dtt, J = 10.8, 7.3, 1.5 Hz, 1H), 4.76 (quin, J = 6.1 Hz, 1H), 4.20 (t, J = 6.8 Hz, 2H), 3.000 (s, 3H), 2.996 (s, 3H), 2.73–2.58 (m, 2H), 2.49 (dt, J = 7.3, 7.0 Hz, 2H), 2.24 (s, 3H), 2.23 (s, 3H), 2.09 (quin, J = 6.3 Hz, 2H), 2.04–1.95 (m, 2H), 1.79–1.72 (m, 2H), 1.54–1.46 (m, 2H); **^{13}C NMR** (125 MHz, $CDCl_3$) δ 138.3, 136.8, 134.4, 133.2, 129.9, 129.8, 125.7, 123.9, 83.2, 69.3, 38.9, 37.6, 36.4, 34.2, 30.9, 27.5, 27.1, 24.8, 19.9, 19.4; **HRMS** (TOF MS CI+) *m/z*: $[M+Na]^+$ calcd for $C_{20}H_{32}O_6S_2Na$, 455.1538; found 455.1523.



Aldehyde (3.25) was prepared according to Method B. The following amounts of reagents were used: 3-fluoroiodobenzene (0.70 mL, 6.0 mmol, 1.0 equiv), allyl alcohol (0.61 mL, 9.0 mmol, 1.5 equiv), $Pd(OAc)_2$ (27 mg, 0.12 mmol, 2.0 mol %), $BnEt_3NCl$ (1.4 g, 6.0 mmol, 1.0 equiv), $NaHCO_3$ (1.3 g, 15 mmol, 2.5 equiv), and DMF (24 mL). Purification by column chromatography (0–10% EtOAc/hexanes) afforded the title compound as a yellow oil (470 mg, 3.1 mmol, 51% yield). Analytical data is consistent with literature values.[26] **^{1}H NMR** (500 MHz, $CDCl_3$) δ 9.82 (d, *J* = 1.1 Hz, 1H), 7.25 (dd, *J* = 14.6, 7.4 Hz, 1H), 6.97 (d, *J* = 7.6 Hz, 1H), 6.91–6.88 (m, 2H), 2.96 (t, *J* = 7.5 Hz, 2H), 2.78 (t, *J* = 7.5 Hz, 2H).



Alcohol (3.26) was prepared according to Method D. The following amounts of reagents were used: aldehyde **3.25** (0.47 g, 3.1 mmol, 1.0 equiv), 4-pentenylmagnesium bromide (4.5 mL, 5.8 mmol, 0.97 equiv, 1.3 M in THF), and THF (16 mL). The crude residue was taken on without further purification.



Lactol (3.27) was prepared according to Method E. The following amounts of reagents were used: alkene **3.26** (0.69 g, 3.1 mmol, 1.0 equiv), $NaHCO_3$ (0.44 g, 5.3 mmol, 1.7 equiv), PPh_3 (1.4 g, 5.3 mmol, 1.7 equiv), $NaHCO_3$ (0.44 g, 5.3 mmol, 1.7 equiv), and CH_2Cl_2 (3.1 mL). Purification by column chromatography (0–30% EtOAc/hexanes) afforded the title compound as a white solid

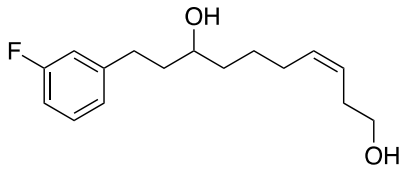
[26] Fujihara, T.; Cong, C.; Iwai, T.; Terao, T.; Tsuji, Y. *Synlett* **2012**, *23*, 2389–2392.

(0.35 g, 1.6 mmol, 50% yield over two steps, 1.6:1 dr) containing CH_2Cl_2 (12 mg, 0.15 mmol, 5%). For clarity, the ^1H and ^{13}C data are tabulated individually.

TLC R_f = 0.7 (50% EtOAc/hexanes); **HRMS** (TOF MS CI+) *m/z*: $[M+Na]^+$ calcd for $C_{13}H_{17}FO_2Na$, 247.1110; found 247.1098.

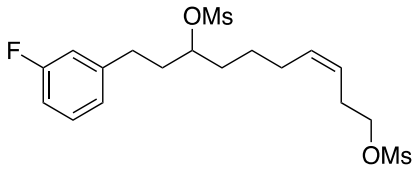
Major Diastereomer ^1H NMR (400 MHz, $CDCl_3$) δ 7.23 (dd, *J* = 14.3, 7.8 Hz, 1H), 6.96 (d, *J* = 7.7 Hz, 1H), 6.90–6.85 (m, 2H), 4.70 (ddd, *J* = 9.5, 6.3, 1.5 Hz, 1H), 3.43–3.37 (m, 1H), 2.85 (d, *J* = 6.4 Hz, 1H), 2.82–2.62 (m, 1H), 1.94–1.83 (m, 2H), 1.80–1.56 (m, 5H**)**, 1.37–1.20 (m, 2H); **^{13}C NMR** (151 MHz, $CDCl_3$) δ 163.1 (d, *J* = 244.1 Hz), 144.9 (d, *J* = 7.2 Hz), 129.8 (d, *J* = 8.3 Hz), 124.2 (d, *J* = 2.7 Hz), 115.4 (d, *J* = 20.7 Hz), 112.8 (d, *J* = 21.0 Hz), 96.6, 75.4, 37.4, 33.0, 31.6, 30.6, 22.2; **^{19}F NMR** (565 MHz, $CDCl_3$) δ -113.8–-113.9 (m, 1F).

Minor Diastereomer ^1H NMR (400 MHz, $CDCl_3$) δ 7.23 (dd, *J* = 14.3, 7.8 Hz, 1H), 6.96 (d, *J* = 7.7 Hz, 1H), 6.90–6.85 (m, 2H), (5.33 (br s, 1H), 3.96–3.90 (m, 1H), 2.85 (d, *J* = 6.4 Hz, 1H), 2.82–2.62 (m, 1H), 1.94–1.83 (m, 2H), 1.80–1.56 (m, 5H**)**, 1.37–1.20 (m, 2H); **^{13}C NMR** (151 MHz, $CDCl_3$) δ 163.1 (d, *J* = 244.1 Hz), 145.1 (d, *J* = 7.2 Hz), 129.8 (d, *J* = 8.5 Hz), 124.2 (d, *J* = 2.6 Hz), 115.4 (d, *J* = 20.7 Hz), 112.8 (d, *J* = 21.0 Hz), 92.1, 68.0, 37.7, 31.6, 31.4, 29.9, 17.5; **^{19}F NMR** (565 MHz, $CDCl_3$) δ -113.8–-113.9 (m, 1F).



Diol (3.28) was prepared according to Method G. The following amounts of reagents were used: lactol **3.27** (0.35 g, 1.6 mmol, 1.0 equiv), Wittig salt **3.16** (0.63 g, 1.6 mmol, 1.0 equiv), *n*-BuLi

(2.0 mL, 5.0 mmol, 3.2 equiv), and THF (8.0 mL). Purification by column chromatography (0–50% EtOAc/hexanes) afforded the title compound as a yellow oil (200 mg, 0.75 mmol, 48% yield, 1:1 dr). **TLC R_f** = 0.4 (50% EtOAc/hexanes); **^{1}H NMR** (500 MHz, $CDCl_3$) δ 7.23 (aq, *J* = 7.3 Hz, 2H, both diastereomers), 6.97 (d, *J* = 7.5 Hz, 2H, both diastereomers), 6.91–6.85 (m, 4H, both diastereomers), 5.57–5.52 (m, 2H, both diastereomers), 5.42–5.37 (m, 2H, both diastereomers), 3.65–3.62 (m, 6H, both diastereomers), 2.82–2.77 (m, 2H, both diastereomers), 2.69–2.64 (m, 2H, both diastereomers), 2.31 (dt (*J* = 7.2, 6.2 Hz, 2H, one diastereomer), 2.26 (dt, *J* = 6.5, 6.1 Hz, 2H, other diastereomer), 2.12–2.02 (m, 4H, both diastereomers), 1.80–1.68 (m, 4H, both diastereomers), 1.61 (brs, 2H, both diastereomers), 1.53–1.38 (m, 10H, both diastereomers); **^{13}C NMR** (125 MHz, $CDCl_3$) δ 163.0 (d, *J* = 245.3 Hz, 2C, both diastereomers), 144.82 (d, *J* = 7.0 Hz, one diastereomer), 144.79 (d, *J* = 7.1 Hz, other diastereomer), 133.7 (one diastereomer), 132.9 (other diastereomer), 129.8 (d, *J* = 8.4 Hz, 2C, both diastereomers), 126.4 (one diastereomer), 125.7 (other diastereomer), 124.1 (d, *J* = 2.6 Hz, 2C, both diastereomers), 115.3 (d, *J* = 20.8 Hz, one diastereomer), 112.7 (d, *J* = 21.0 Hz, other diastereomer), 71.03 (one diastereomer), 71.02 (other diastereomer), 63.3 (one diastereomer), 62.1 (other diastereomer), 38.81 (one diastereomer), 38.79 (other diastereomer), 37.11 (one diastereomer), 37.09 (other diastereomer), 36.0 (2C, both diastereomers), 32.6 (one diastereomer), 31.83 (one diastereomer), 31.82 (other diastereomer), 30.82 (other diastereomer), 27.2 (2C, both diastereomers), 25.7 (one diastereomers), 25.4 (other diastereomers); **^{19}F NMR** (565 MHz, $CDCl_3$) δ -113.7 (apparq, *J* = 8.2 Hz, 2F, both diastereomers); **HRMS** (TOF MS CI+) *m/z*: $[M+Na]^+$ calcd for $C_{16}H_{23}FO_2Na$, 289.1580; found 289.1569.



Dimesylate (3.15) was prepared according to Method H. The following amounts of reagents were used: diol **3.28** (197 mg, 0.74 mmol, 1.0 equiv), MsCl (0.17 mL, 2.2 mmol, 3.0 equiv), DMAP (18 mg, 0.15 mmol, 0.20 equiv), Et_3N (0.31 mL, 2.0 mmol, 3.0 equiv), and CH_2Cl_2 (3.7 mL). Purification by column chromatography (0–30% EtOAc/hexanes) afforded the title compound as a yellow oil (0.24 g, 0.56 mmol, 75% yield, 1:1 dr). **TLC R_f** = 0.3 (50% EtOAc/hexanes); **^{1}H NMR** (600 MHz, $CDCl_3$) δ 7.27–7.23 (m, 2H, both diastereomers), 6.98 (d, *J* = 7.2 Hz, 2H, both diastereomers), 6.91–6.88 (m, 4H, both diastereomers), 5.56–5.52 (m, 2H), 5.42–5.38 (m, 2H), 4.78–4.75 (m, 2H, both diastereomers), 4.21 (aq, *J* = 6.2 Hz, 4H, both diastereomers), 3.02 (s, 3H, one diastereomer), 3.01 (s, 3H, other diastereomer), 3.001 (s, 3H, one diastereomer), 2.999 (s, 3H, other diastereomer), 2.79–2.68 (m, 4H, both diastereomers), 2.50 (dt *J* = 7.2, 6.2 Hz, 2H, one diastereomer), 2.44 (dt *J* = 6.9, 6.2 Hz, 2H, other diastereomer), 2.13–1.95 (m, 8H, both diastereomers), 1.79–1.70 (m, 4H, both diastereomers), 1.53–1.44 (m, 4H, both diastereomers); **^{13}C NMR** (125 MHz, $CDCl_3$) δ 163.0 (d, *J* = 242.4 Hz, 2C, both diastereomers), 143.6 (d, *J* = 2.1 Hz, one diastereomer), 143.5 (d, *J* = 2.0 Hz, other diastereomer), 133.8 (one diastereomer) 133.1 (other diastereomer), 130.1 (d, *J* = 8.4 Hz, 2C, both diastereomers), 124.8 (one diastereomer), 124.2 (d, *J* = 2.4 Hz, 2C, both diastereomers), 124.0 (other diastereomer), 115.34 (d, *J* = 21.3 Hz, one diastereomer), 115.33 (d, *J* = 21.2 Hz, other diastereomer), 113.24 (d, *J* = 21.2 Hz, one diastereomer), 113.23 (d, *J* = 21.2 Hz, other diastereomer), 82.7 (one diastereomer), 82.6 (other diastereomer), 69.5 (one diastereomer), 69.3 (other diastereomer), 38.9 (2C, both diastereomers), 37.63 (one diastereomer), 37.64 (other diastereomer), 36.0 (2C, both diastereomers), 34.2 (2C, both diastereomers), 34.0 (2C, both diastereomers), 32.5 (one diastereomer), 32.2 (other diastereomer), 31.1 (2C, both diastereomers), 27.6 (one diastereomer), 27.0 (other diastereomer);

^{19}F NMR (565 MHz, $CDCl_3$) δ -113.3 to -113.4 (m, 2F, both diastereomers); **HRMS** (TOF MS ES+) *m/z*: $[M+Na]^+$ calcd for $C_{18}H_{27}FO_6S_2Na$, 445.1131; found 445.1118.

Chapter 4

Structure Reactivity-Relationships of Nickel-Catalyzed Cross-Coupling Reactions

4.1 Introduction

Over the course of the last several decades, new methodology for catalytic cross-coupling (XC) and cross-electrophile coupling (XEC), especially methods utilizing nickel catalysts, have rapidly expanded.[1] Recent work has targeted the development of methods to couple C(sp^3) electrophiles. The types of C(sp^3) bonds that can be activated include C–O, C–N, C–S, C–Br, C–I, C–Cl, and even C-F and C–H bond; however, the mechanistic pathways by which these electrophiles are activated with nickel catalysts can differ meaningfully from one another. These mechanistic differences originate from one important property of nickel catalysts, the range of available oxidation states. Nickel can readily access the 0, I, II, and III oxidation states which allow it to enter both one- and two-electron mechanistic pathways in a catalytic reaction.

The one- and two- electron mechanisms can be further defined by the specific intermediates the mechanism proceeds through. The colloquial "one-electron" mechanisms typically proceed through open-shell nickel intermediates (Figure 4.1, intermediate **4.1**) whereas the "two-electron" mechanisms proceed through closed-shell nickel intermediates (Figure 4.1, intermediate, **4.2**). Open-shell pathways are typically observed with electrophiles prone to homolytic cleavage such as alkyl halides. Activation of these electrophiles is described as halogen atom abstraction or halogen atom transfer (XAT). Closed-shell pathways are typically observed with electrophiles more prone to heterolytic cleavage and activation is described as polar oxidative addition. It is important to note that the stereochemical outcomes of cross-coupled product are often dictated by

[1] (a) Tamao, K.; Miyaura, N. Introduction to Cross-Coupling Reactions. In *Cross-Coupling Reactions a Practical Guide*; Miyaura, N., Ed.; Topics in Current Chemistry, Vol. 219; Springer, 2022; pp 1-9. (b) Tasker, S. Z.; Standley, E. A.; Jamison, T. F. *Nature* **2014**, *509*, 299–309. (c) Diccianni, J. B.; Diao, T. *Trends Chem.* **2019**, *1*, 830–844.

which pathway (open or closed) the reaction proceeds through. Because the open-shell pathway goes through radical intermediates, the stereochemical information of the starting material is ablated. This feature allows for control of absolute configuration with the use of a chiral ligand. On the other hand, a closed-shell oxidative addition is typically stereospecific and thus the absolute configuration of the product is dictated by that of the starting material. Therefore, studying the factors that influence predilection for open or closed-shell intermediates is especially important for the development of new reactions and advancing our knowledge of product outcomes for existing manifolds.

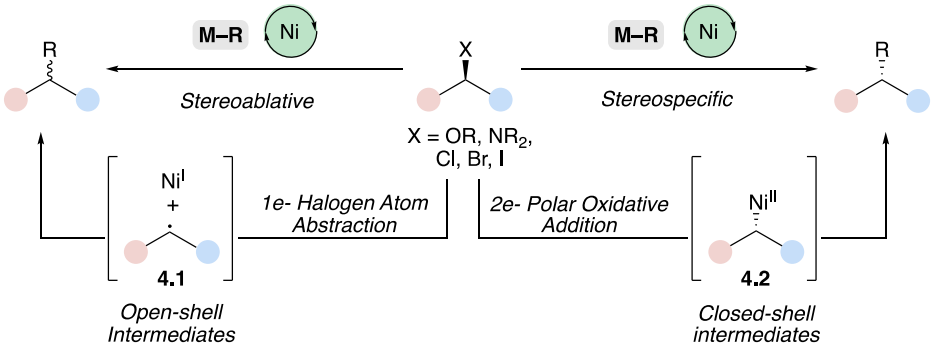


Figure 4.1. Mechanisms of nickel-catalyzed oxidative addition.

While the distinction between the open- and closed-shell pathways has influence on both the optimal substrate type for a XC reaction and the stereochemical outcomes, little is known about

the influence of ligands on these two pathways.[2,3] Despite this, analysis of cross-coupling literature demonstrates a categorical difference between reactions that proceed via an open- or closed-shell pathway and the ligands employed. Specifically, reactions that proceed via the open-shell pathways typically employ nitrogen-based ligands and reactions that proceed via the closed-shell pathway typically employ phosphine ligands. Figure 4.2 demonstrates examples of this trend as it appears in both open- and closed-shell Suzuki, Negishi, and Kumada reactions.[4]

While this reactivity is certainly intriguing, there is insufficient data to make direct comparisons between reaction outcomes and ligand identity. The reported ligand evaluation for these reactions is often limited to one class of ligand either phosphine or nitrogen and so the XC reactivity across a broad range of ligands is relatively unknown. Despite this, recent work has shown that ligand parameterization and correlation with reactivity has augmented our mechanistic

[2] For representative studies of the influence of nitrogen ligands on nickel redox states see: (a) Lin, Q.; Dawson, G.; Diao, T. *Synlett.* **2021**, *32*, 1606-1620. (b) McNicholas, B. J.; Tong, Z. J.; Bím, D.; Turro, R. F.; Kazmierczak, N. P.; Chalupský, J.; Reisman, S. E.; Hadt, R. G. *Inorg. Chem*. **2023**, *62*, 14010-14027. (c) Zackasee, J. L. S.; Al Zubaydi, S.; Truesdell, B. L.; Sevov, C. S. *ACS Catal.* **2022**, *12*, 1161-1166. (d) Wagner, C. L.; Herrera, G.; Lin, Q.; Hu, C. T.; Diao, T. *J. Am. Chem. Soc.* **2021**, *143*, 5295-5300. (e) Lin, Q.; Fu, Y.; Liu, P.; Diao, T. *J. Am. Chem. Soc.* **2021**, *143*, 14196-14206. (f) Ju, L.; Ling, Q.; LiBretto, N. J.; Wagner, C. L.; Hu, C. T.; Miller, J. T.; Diao, T. *J. Am. Chem. Soc.* **2021**, *143*, 14458-14463. (g) Ju. L.; Hu, C. T.; Diao, T. *Organometallics* **2022**, *41*, 1748-1753. (h) Lin, Q.; Spielvogel, E. H.; Diao, T. *Chem* **2023**, *9*, 1-14. (i) Budnikova, Y. H.; Perichon, J.; Yakhvarov, D. G.; Kargin, Y. M.; Sinyashin, O. G. *J. Org. Chem.* **2001**, *630*, 185-192. (j) Tang, T.; Jones, E.; Wild, T.; Hazra, A.; Minteer, S. D.; Sigman, M. S. *J. Am. Chem. Soc.* **2022**, *144*, 20056-2006. (k) Tang, T.; Friede, N. C.; Minteer, S. D.; Sigman, M. S. *Eur. J. Org. Chem.* **2022**, e202200064. (l) Ting, S. I.; Williams, W. L.; Doyle, A. G. *J. Am. Chem. Soc.* **2022**, *144*, 5575-5582. (m) Tang, T.; Hazra, A.; Min, D. S.; Williams, W. L.; Jones, E.; Doyle, A. G.; Sigman, M. S. *J. Am. Chem. Soc.* **2023**, *145*, 8689-8699. (n) Dawson, G.; Lin, Q.; Neary, M. C.; Diao, T. *J. Am. Chem. Soc.* **2023**, *145*, 20551-20561.

[3] For representative studies of the influence of P-ligands on nickel redox states see: (a) Yang, J.; Neary, M. C.; Diao, T. *J. Am. Chem. Soc.* **2024**, *146*, 6360–6368. (b) Guard, L. M.; Beromi, M. M.; Brudvig, G. W.; Hazari, N.; Vinyard, D. J. *Angew. Chem. Int. Ed.* **2015**, *54*, 13352-13356. (c) Diccianni, J. B.; Katigbak, J.; Hu, C.; Diao, T. *J. Am. Chem. Soc.* **2019**, *141*, 1788-1796. (d) Lin, Q.; Dawson, G.; Diao, T. *Synlett.* **2021**, *32*, 1606-1620.

[4] (a) Zhou, J.; Fu, G. C. *J. Am. Chem. Soc.* **2004**, *126*, 1340–1341. (b) González-Bobes, F.; Fu, G. C. *J. Am. Chem. Soc.* **2006**, *128*, 5360–5361. (c) Giovannini, R.; Knochel, P. *J. Am. Chem. Soc.* **1998**, *120*, 11186–11187. (d) Smith, S. W.; Fu, G. C. *J. Am. Chem. Soc.* **2008**, *130*, 126–12647. (e) Vechorkin, O.; Proust, V.; Hu, X. *J. Am. Chem. Soc.* **2009**, *131*, 9756–9766. (f) Breitenfeld, J.; Wodrich, M. D.; Hu, X. *Organometallics*, **2014**, *33*, 5708–5715. (g) Lou, S.; Fu, G. C. *J. Am. Chem. Soc.* **2010**, *132,* 1264–1266. (h) Harris, M. R.; Hanna, L. E.; Greene, M. A.; Moore, C. E.; Jarvo, E. R. *J. Am. Chem. Soc.* **2013**, *135*, 3303–3306. (i) Wisniewska, H. M.; Swift, E. C.; Jarvo, E. R. *J. Am. Chem. Soc.* **2013**, *135*, 9083–9090. (j) Tollefson, E. J.; Dawson, D. D.; Osborne, C. A.; Jarvo, E. R. *J. Am. Chem. Soc.* **2014**, *136*, 14951–14958. (k) Taylor, B. H. L.; Harris, M. R.; Jarvo, E. R. *Angew. Chem. Int. Ed.* **2012**, *51*, 7790–7793.

understanding of nickel-catalyzed reactions.[5] Therefore, we are interested further examining the trend in a systematic and targeted way to investigate the relationship between open- and closed-shell mechanistic pathways and ligand identity.

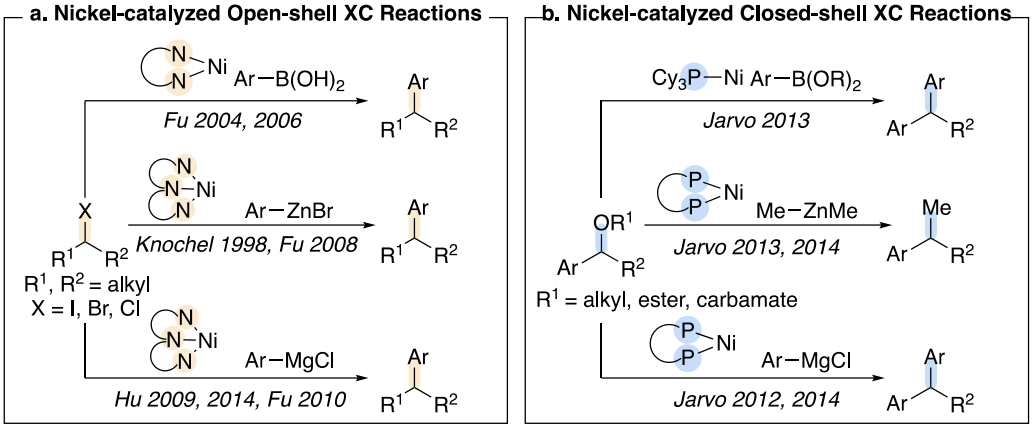


Figure 4.2. Nickel-catalyzed XC Reactions (a) Open-shell reactions that utilize nitrogen-based ligands. (b) Closed-shell reactions that utilize phosphorous-based ligands.

There have been limited but notable studies that have examined the relationship of phosphine vs nitrogen-based ligands in nickel-catalyzed XC or XEC reactions. In 2017, Schoenebeck demonstrated two divergent pathways for the nickel-catalyzed trifluoromethylthiolation of aryl halides. In reactions of aryl bromides and iodides, the Ni(dppf) catalyst activates the aryl halide via a Ni^0/Ni^{II} pathway while bipyridine ligands can selectively activate aryl chlorides via a Ni^I/Ni^{III} cycle (Figure 4.3a).[6] In 2022 the Sevov group reported a

[5] (a) Tcyrulnikov, S.; Hubbell, A. K.; Pedra, D.; Reyes, G. P.; Monfette, S.; Weix, D. J.; Hansen, E. C. *J. Am. Chem. Soc.* **2024**, *146*, 6947-6954. (b) Gensch, T.; Smith, S. R.; Colacot, T. J.; Timsina, Y. N.; Xu, G.; Glasspoole, B. W.; Sigman, M. S. *ACS Catal.* **2022**, *12*, 7773-7780. (c) Duran-Camacho, G.; Bland, D. C.; Li, F.; Neufeldt, S. R.; Sandford, M. S. *ACS Catal.* **2024**, *14*, 6404-6412. (d) Wu, K.; Doyle, A. G. *Nat. Chem.* **2017**, *9*, 779-784. (e) Newman-Stonebraker, S. H.; Smith, S. R.; Borowski, J. E.; Peters, E.; Gensch, T.; Johnson, H. C.; Sigman, M. S.; Doyle, A. G. *Science* **2021**, *374*, 301-308. (f) Kramer, P. C. J.; Van Leeuwen, P. W. N. M.; Reek, J. N. H. *Acc. Chem. Res.* **2001**, *34*, 895-904. (g) See reference 2(c) (h) Newman-Stonebraker, S. H.; Wang, J. Y.; Jeffrey, P. D.; Doyle, A. G. *J. Am. Chem. Soc.* **2022**, *144*, 19635-19648. (i) Akana, M. E.; Tcyrulnikov, S.; Akana-Schneider, B. D.; Reyes, G. P. Monfette, S.; Sigman, M. S.; Hansen, E. C.; Weix, D. J. *J. Am. Chem. Soc.* **2024**, *146*, 3043-3051.

[6] (a) Kalvet, I.; Guo, Q.; Tizzard, G. J.; Schoenebeck, F. *ACS Catal.* **2017**, *7*, 2126-2132. (b) Zhang, C. -P.; Vicic, D. A. *J. Am. Chem. Soc.* **2011**, *134*, 183–185.

nickel-catalyzed electroreductive XEC reaction of aryl chlorides, bromides, and triflates with tertiary alkyl bromides in which the oxidation states of the nickel catalyst were selectively controlled with the complementary use of a bispyrazoylpyridine (bpp) and a quinazolinap (iPrQ) ligand.[7] This study identified a dual catalytic cycle facilitated by ligand exchange in which an open-shell mechanism with the bpp ligand activated the tertiary alkyl bromide via halogen abstraction with Ni^{I} **4.3** and a closed shell mechanism with the iPrQ ligand activates the aryl bromide via oxidative addition with Ni^{0} **4.4** (Figure 4.3b). Finally, in work from Rousseaux in 2020, the leaving group dependence of polar versus radical reactivity of nickel-catalyzed cyclopropane arylation reactions also appeared to be influenced by the phosphine or nitrogen-based ligand identity.[8,9]

[7] Hamby, T. B.; LaLama, M. J.; Sevov, C. S. *Science* **2022**, *376*, 410–416.
[8] Mills, L. R.; Monteith, J. J.; Dos Passos Gomes, G.; Aspuru-Guzik, A.; Rousseaux, S. A. L. *J. Am. Chem. Soc.* **2020**, *142*, 13246–13254.
[9] The Weix group has also developed reactions that proceed via dual catalytics cycles with conjunctive use of Ni(N-based ligands) and Pd(P-based ligands) catalysts. See: (a) Kang, K.; Huang, L.; Weix, D. J. *J. Am. Chem. Soc.* **2020**, *142*, 10634–10640. (b) Kang, K.; Loud, N. L.; DiBenedetto, T. A.; Weix, D. J. *J. Am. Chem. Soc.* **2021**, *143*, 21484–21491. (c) Olivares, A. M.; Weix, D. J. *J. Am. Chem. Soc*. **2018**, *140*, 2446–2449. (d) Huang, L.; Ackerman, L. K. G.; Kang, K.; Parsons, A. M.; Weix, D. J. *J. Am. Chem. Soc.* **2019**, *141*, 10978–10983.

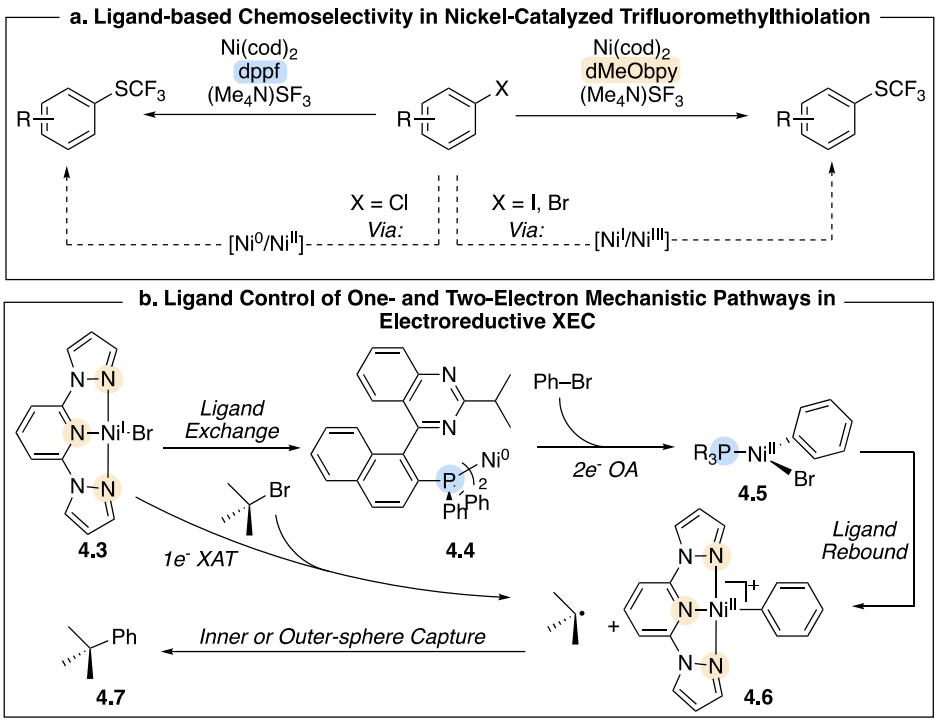


Figure 4.3. Reactions employing P vs. N Ligand-Based Control. (a) Activation of aryl halides via Ni^0/Ni^{II} or Ni^I/Ni^{III} in trifluoromethylthiolation reactions. (b) Electroreductive XEC reaction facilitated by phosphine/nitrogen ligand exchange.

Both of these studies provided necessary insight into phosphine versus nitrogen selectivity for different reaction pathways. However, they both focused on two specific phosphine and nitrogen-based ligands. In 2022 our group was the first to demonstrate a broad phosphine versus nitrogen-based ligand study which evaluated over 40 ligands in a nickel-catalyzed XEC reaction of 4-halotetrahydropyrans (Figure 4.4).[10] In this work, a chemoselective trend was observed where the reactions that occurred at the alkyl chloride and proceeded through an open-shell pathway exclusively provided reduction product **4.8** with nitrogen-based ligands. In contrast, reactions that afforded cyclopropane **4.9** were exclusively formed in the presence of phosphine ligands. Importantly, the mechanisms for formation of the XEC product have been previously studied and

[10] Thane, T. A.; Jarvo, E. R. *Org. Lett.* **2022**, *24*, 5003–5008.

are known to proceed through a closed-shell oxidative addition and experimental evidence demonstrated that reduction is formed through an open-shell hydrodehalogenation mechanism.

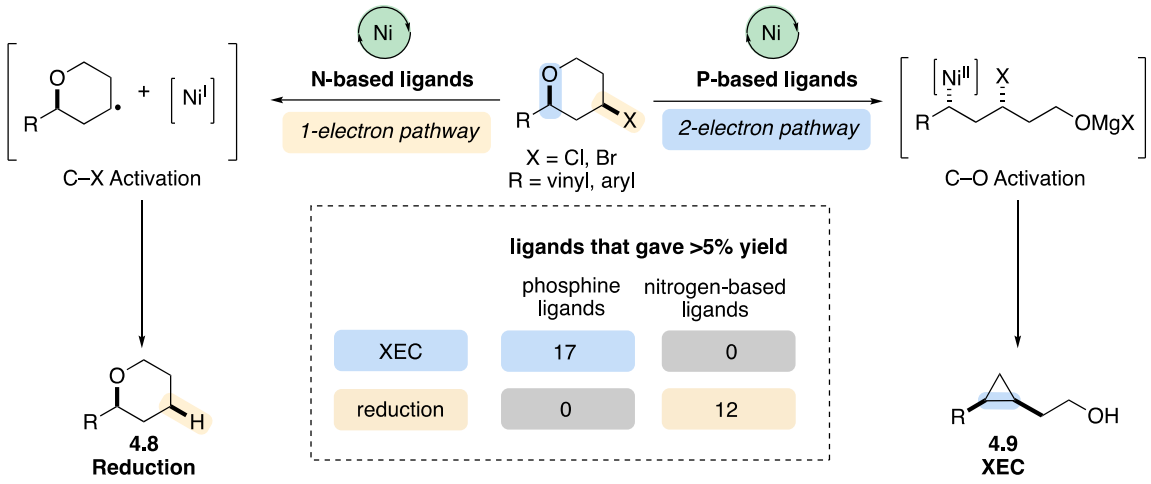


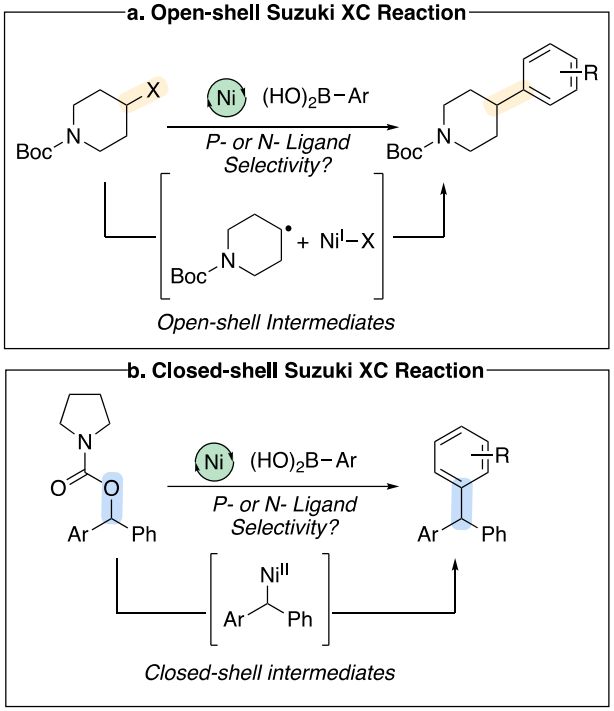
Figure 4.4 Control of open- and closed-shell pathways with phosphine and nitrogen-based ligands.

This work was the first example of comprehensive phosphine versus nitrogen-based ligand evaluation of a chemoselective reaction involving C–Cl/Br and C–O electrophiles. We were interested in further evaluating a broad scope of open- and closed-shell ligand-based selectivity in other synthetically useful XC reactions. Specifically, we sought to evaluate how this trend applies to Suzuki-type XC reactions.

Suzuki couplings of C(sp^2) electrophiles with C(sp^2) coupling partners are widely used in medicinal chemistry because it is a relatively safe and scalable method to form new C(sp^2)-C(sp^2) bonds.[11] Furthermore, the functional group compatibility of boronic acids allows for both early and late-stage derivatization. While the adoption of C(sp^2)-C(sp^2) XC methods has led to an explosion of biaryl, "flat" fragments in medicinal compound libraries, recent studies have shown

[11] Lovering, F.; Bikker, J.; Humblet, C. *J. Med. Chem.* **2009**, *52*, 6752–6756.

that higher fraction of C(sp^3) character is correlated with more successful candidates in the clinic.[12] Because of this, we were interested in studying XC methods that afford new C(sp^3) centers such as C(sp^2)-C(sp^3) Suzuki coupling reactions. In the last two decades, numerous methods have been developed for both the stereospecific and stereoablative Suzuki coupling of C(sp^2)-C(sp^3) centers.[13] We hypothesized that nickel-catalyzed C(sp^2)-C(sp^3) Suzuki coupling reactions could provide a synthetically useful case study to evaluate phosphine versus nitrogen-based ligand selectivity in open- and closed-shell pathways (Scheme 4.1).



Scheme 4.1. Evaluation of P vs. N-Based Ligand Control in Nickel-Catalyzed Suzuki Reactions

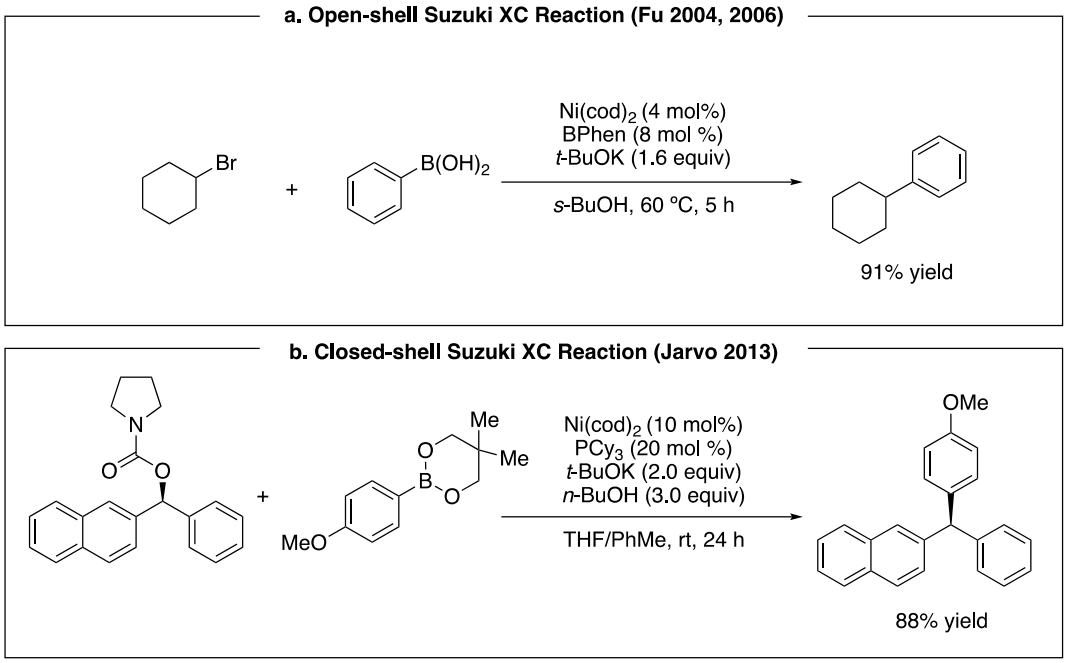
[12] (a) Lovering, F. *Med. Comm. Commun.* **2013**, *4*, 515–519. (b) Brown, D. G.; Boström, J. *J. Med. Chem.* **2016**, *59,* 4443–4458.

[13] For representative reactions see: (a) See reference 4(a), 4(b), and 4(h) (b) Huang, K.; Li, G.; Huang, W. –P.; Yu, D. -G.; Shi, Z. -J. *Chem. Commun.* **2011**, *47*, 7224–7226. (c) Maity, P.; Shacklady-McAtee, D. M.; Yap, G. P. A.; Sirianni, E. R.; Watson, M. P. *J. Am. Chem. Soc.* **2013**, *135*, 280–285. (d) Shacklady-McAtee, D. M.; Roberts, K. M.; Basch, C. H.; Song, Y. -G.; Watson, M. P. *Tetrahedron* **2014**, *70*, 4257–4263. (e) Zultanski, S. L.; Fu, G. C. *J. Am. Chem. Soc.* **2013**, *135*, 624–627.

4.2 Results

To study the role of phosphine and nitrogen-based ligands in nickel catalyzed Suzuki reactions, we started with previously developed open and closed-shell Suzuki XC reactions from the literature (Scheme 4.2). In 2004, the Fu group was the first to report a Suzuki reaction of secondary alkyl bromides and iodides with aryl and vinyl boronic acids.[14] They later extended this work to include secondary alkyl chlorides.[15] Experimental evidence from these studies indicated the presence of radical intermediates from the alkyl halide implying that the reaction proceeds through an open-shell pathway.[16] In 2013, the Jarvo group reported a nickel-catalyzed Suzuki XC reaction of alkyl pivalates and carbamates with aryl boronic esters.[17] Mechanistic studies indicate that the reaction proceeds through a stereospecific closed-shell oxidative addition.[18] We chose to proceed with these two Suzuki reactions to evaluate ligand role in the open- vs. closed-shell pathways.

[14] See reference 4(a)
[15] See reference 4(b)
[16] (a) See reference 4(a). (b) Powel, D. A.; Toshihide, M.; Fu, G. C. *J. Am. Chem. Soc.* **2005**, *127*, 510–511. (b) For a detailed mechanistic investigation with phenoxyimine ligand see: Mills, R. L.; Simmons, E. M.; Lee, H.; Nester, E. Kim, J. Wisniewski, S. R.; Pecoraro, M. V.; Chirik, P. J. *J. Am. Chem. Soc.* **2024**, *146*, 10124–10141.
[17] See reference 4(h).
[18] Zhang, S. -Q.; Taylor, B. H. L.; Ji, C. -L.; Gao, Y.; Harris, M. R.; Hanna, L. E.; Jarvo, E. R.; Houk, K. N.; Hong, X. *J Am. Chem. Soc.* **2017**, *139*, 12994–13005.



Scheme 4.2. Previously developed open- and closed-shell Suzuki reactions.

In an effort to amplify the breadth of this study, we selected 27 different phosphine and nitrogen-based ligands which spanned a broad range of structural diversity, electronic properties, and reported efficacy in both XC and XEC reactions (Figure 4.5). We hypothesized that a broad scope in ligand evaluation would be critical to demonstrate differences in reactivity between the open and closed-shell reactions and provide insight into the underlying catalyst properties at play.

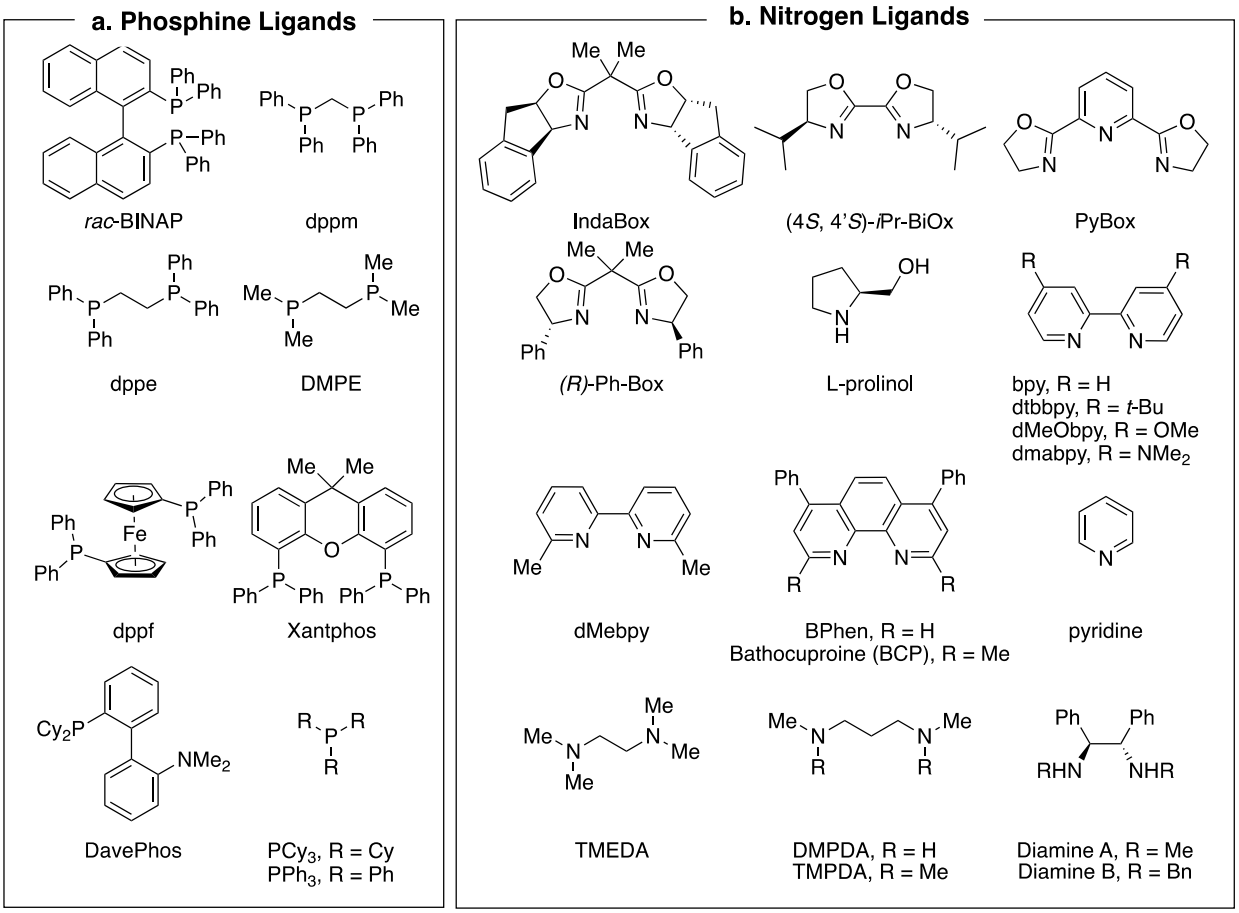
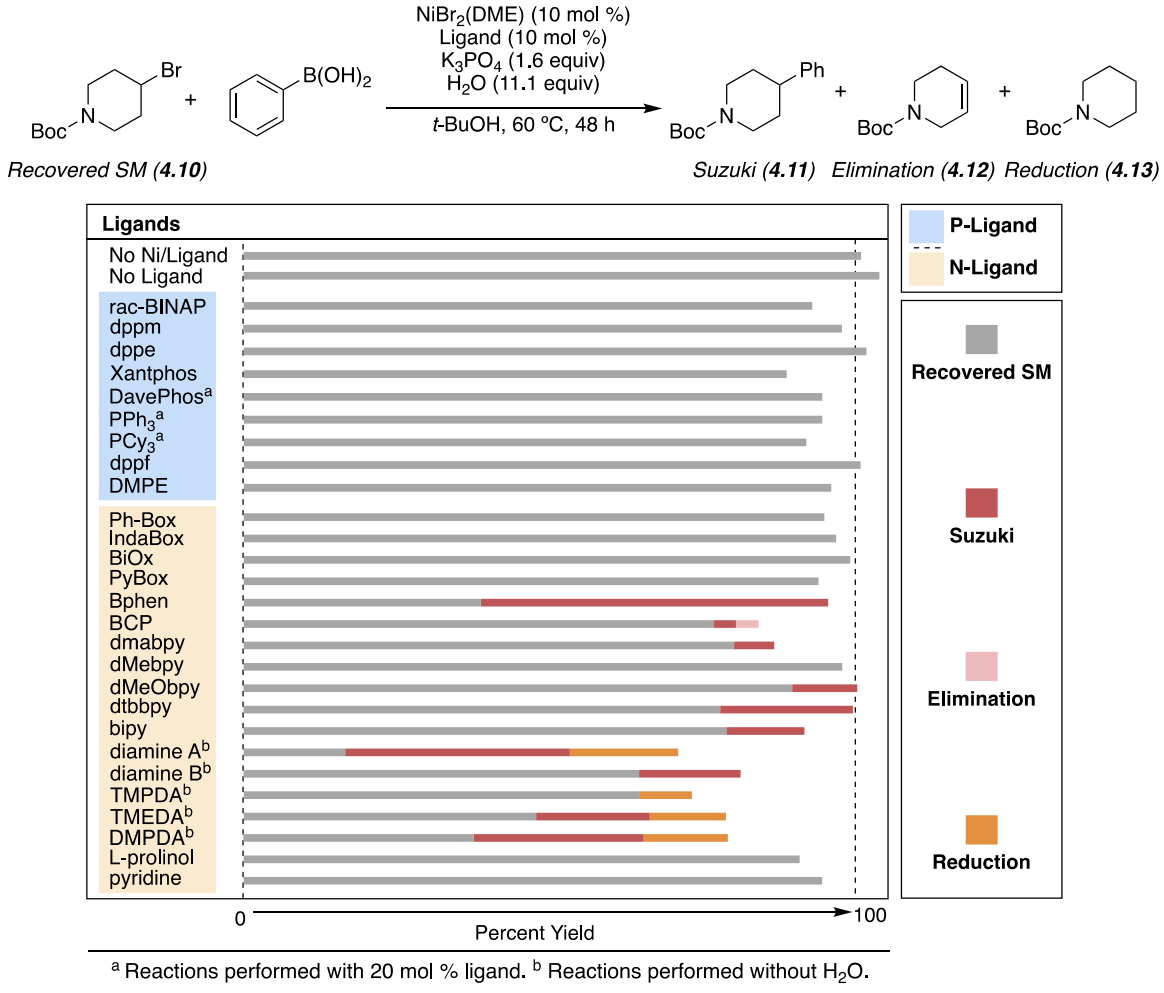


Figure 4.5. Phosphine and Nitrogen-based ligands selected for their reported efficacy in nickel-catalyzed XC reactions.

The first reaction we tested was the open-shell Suzuki cross-coupling of secondary alkyl halides. Table 4.1 demonstrates evaluation of the Suzuki reaction with alkyl bromide **4.10** and phenyl boronic acid. To fully evaluate the observed reactivity, all products in the reaction that were produced from the starting alkyl halide were identified by ^{1}H NMR spectroscopy. In addition to quantifying remaining bromide **4.10**, and cross-coupled product **4.11**, we also identified olefin by-product **4.12** which could be produced from base-mediated elimination or nickel-mediated β-hydride elimination and reduction product **4.13** which comes from the hydrodehalogenation pathway. Under the evaluation of the 9 phosphine ligands in our data set, we only observe

recovered starting material in the reaction, indicating that phosphine ligands are not activating the alkyl halide in this reaction. In reactions where the nitrogen-based ligands were employed, we begin to see formation of Suzuki-coupled product **4.11**, consistent with our original hypothesis that nitrogen-based ligands are required for open-shell reactivity. We also note that in the absence of a phosphine or nitrogen ligand, or nickel catalyst, we also do not observe reactivity.

Table 4.1.[19] Reactivity of Secondary Alkyl Bromide in Open-Shell Suzuki Reactions with Phosphine and Nitrogen-Based Ligands.

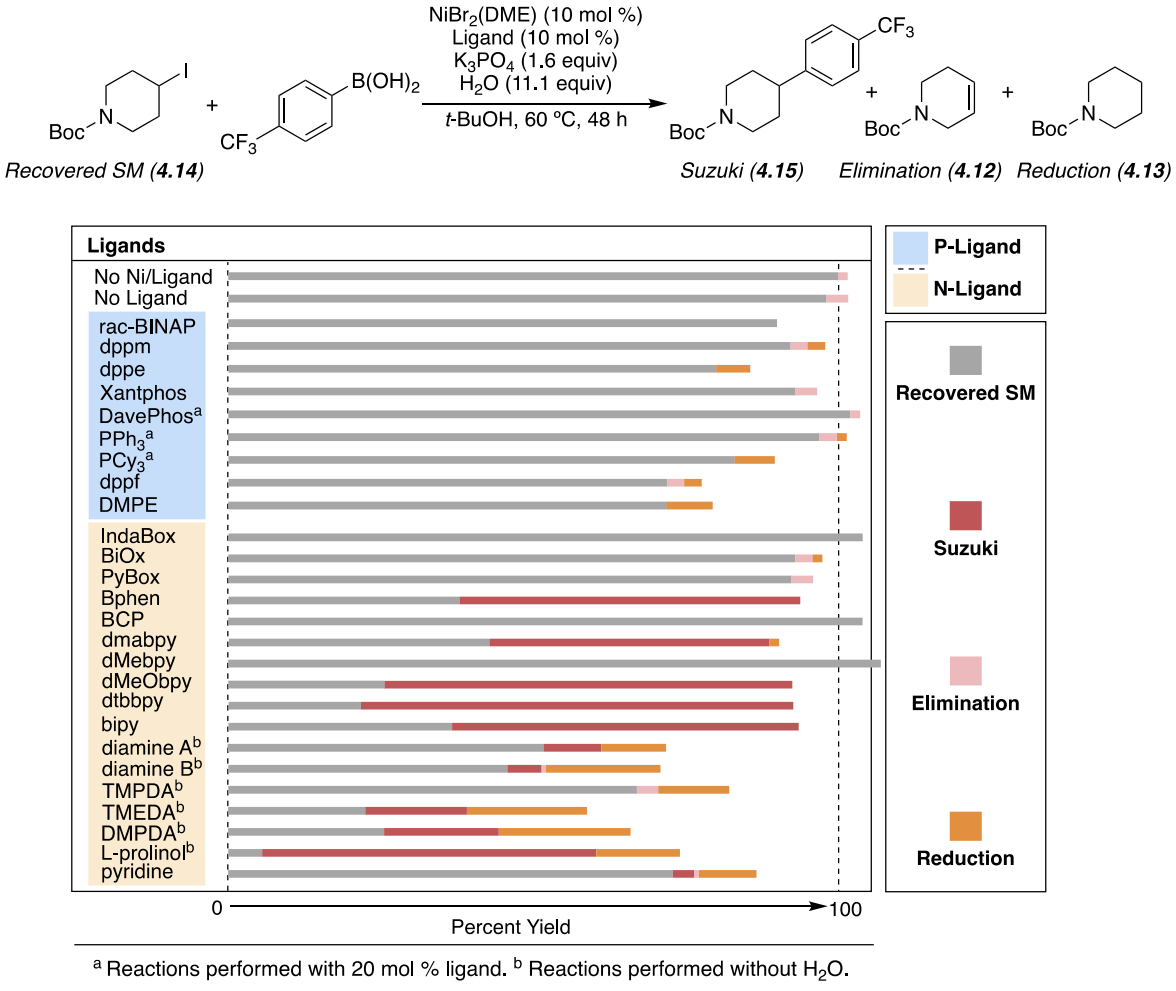


[a] Reactions performed with 20 mol % ligand. [b] Reactions performed without H_2O.

[19] Yields obtained by ^1H NMR by comparison with PhTMS as internal standard.

We continued to evaluate this trend over a series of alkyl halides and boronic acids. Tables 4.2 and 4.3 demonstrate that the trend still holds with both more active electrophiles such as secondary alkyl iodides (Table 4.2) and less active electrophiles such as secondary alkyl chlorides (Table 4.3). While we observed differences in the respective yields with each ligand evaluated, the general trend of reactivity correlating with the nitrogen-based ligands continues to hold.

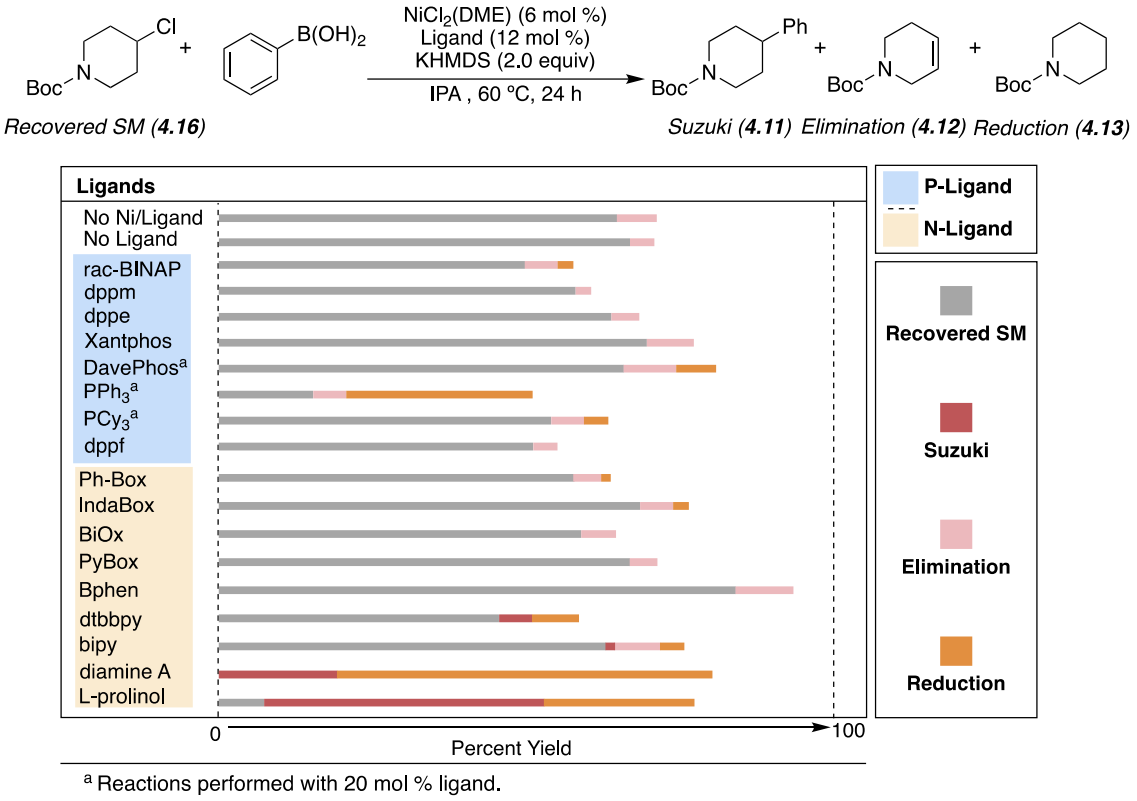
Table 4.2.[20] Reactivity of Secondary Alkyl Iodide in Open-Shell Suzuki Reactions with Phosphine and Nitrogen-Based Ligands.



[a] Reactions performed with 20 mol % ligand. [b] Reactions performed without H_2O.

[20] Yields obtained by ^1H NMR by comparison with PhTMS as internal standard.

Table 4.3.[21] Reactivity of Secondary Alkyl Chloride in Open-Shell Suzuki Reactions with Phosphine and Nitrogen-Based Ligands.



[a] Reactions performed with 20 mol % ligand.

The data from the open-shell Suzuki reactions we evaluated demonstrate a distinct trend in which the desired Suzuki coupled product is only formed in the presence of nitrogen-based ligands, consistent which our original hypothesis that reactions proceeding through open-shell intermediates require a nitrogen-based ligand. The data also show that the trend is consistent for various alkyl halides and boronic acid coupling partners and reaction conditions.

To evaluate the hypothesis in a closed-shell reaction, we turned our attention to the Suzuki reaction of alkyl carbamates previously developed by our group (vida supra). In the evaluation of the closed-shell Suzuki reaction, we observe that Suzuki product is formed nearly exclusively in

[21] Yields obtained by ^{1}H NMR by comparison with PhTMS as internal standard.

the reactions run with phosphines (Figure 4.6).[22] These data are also consistent with our original hypothesis that reactions that proceed through closed shell intermediates require phosphine ligands.

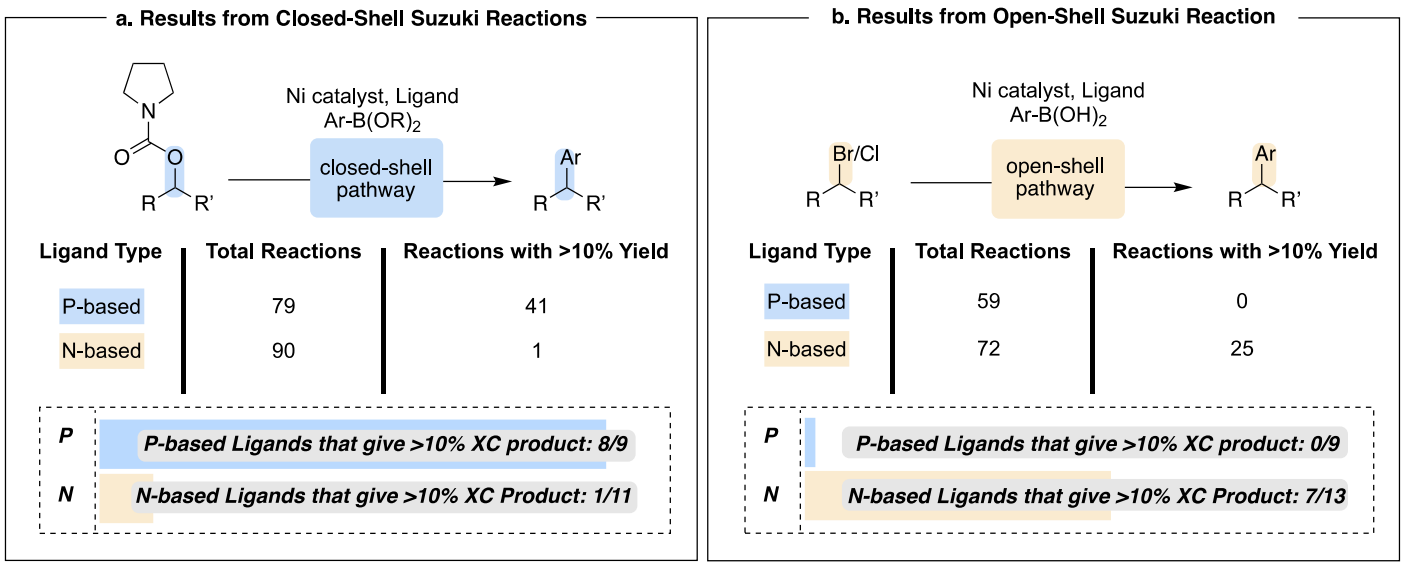


Figure 4.6. Phosphine vs. Nitrogen Ligand-based Reactivity Trends in Open- and Closed-Shell Suzuki Reactions.

4.3 Conclusion

In this chapter we report a systematic ligand-reactivity evaluation for nickel-catalyzed Suzuki XC reactions. We have demonstrated that nickel-catalyzed Suzuki XC reactions that proceed through open-shell intermediates require nitrogen-based ligands. On the other hand, we have also shown through this evaluation that the closed-shell Suzuki pathway requires phosphine ligands. The relationship between the electrophile and the type of ligand employed in each of these reactions appears to be a key facet in reactivity. Evaluation of the nickel catalysts involved in these reactions is underway.

4.4 Experimental Details

[22] Evaluation of the closed-shell Suzuki reactions was performed by Anjali S. Bardhan.

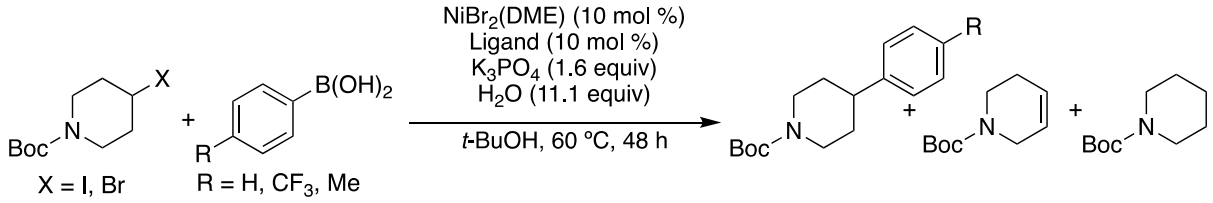
4.4.1 General Procedures

All reactions were carried out under a N_2 atmosphere, unless otherwise stated. 2-propanol and *t*-BuOH were purchased "anhydrous" commercially or were purified as described. ^{1}H NMR were recorded on Bruker DRX-400 (400 MHz 1H, 100 MHz 13C), CRYO-500 (500 MHz 1H, 125.7 MHz 13C), GN-500 (500 MHz 1H, 125.7 MHz 13C), or AVANCE-600 (150 MHz 13C) spectrometers. NMR data were collected at 25 °C. Flash chromatography was performed using either SiliaFlash F60 (40–63 μm, 60 Å) from SiliCycle, or Teledyne Isco Combiflash® Rf+ automated flash chromatography system.

$NiBr_2$(DME) and $NiCl_2$(DME) were purchased from Strem, stored in a glove box under an atmosphere of N_2 and used as received. All ligands were purchased from Strem, Sigma Aldrich, or AmBeed, stored under N_2 atmosphere in a glovebox, and used as received. K_3PO_4 was flame-dried under vacuum prior to use and stored under N_2 atmosphere in a glovebox. All other chemicals were purchased commercially and used as received, unless otherwise noted.

4.4.2 General Procedures for Nickel-Catalyzed Open-Shell Suzuki XC Reactions

4.4.2.1 Method A: Nickel-Catalyzed Open-Shell Suzuki XC Reaction of Alkyl Bromides and Iodides

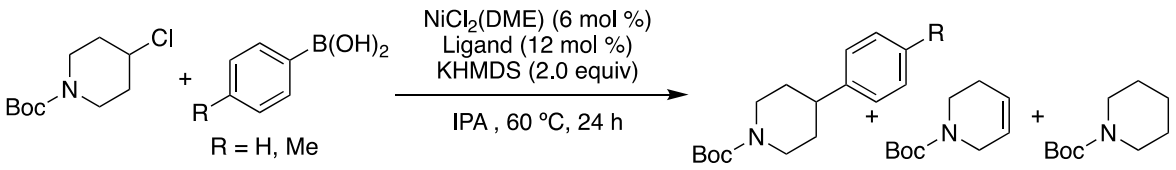


The following procedure was adapted from a report by Fu.[23][24] To a flame-dried 7 mL vial was added alkyl halide (1.0 equiv) and boronic acid (1.8 equiv). The vial was transferred to a

[23] See reference 4(a).
[24] Conditions were adapted from Chloe D. Wong.

glovebox and charged with $NiBr_2(DME)$ (0.10 equiv), ligand (0.10–0.20 equiv), and K_3PO_4 (1.6 equiv). Note: TMPDA, TMEDA, DMPDA, L-prolinol, and pyridine ligands were added as a 1.0 M solution in *t*-BuOH outside of the glovebox. The vial was sealed with a septa cap and removed from the glovebox. Under N_2, the vial was charged with *t*-BuOH (0.1 M) and H_2O (11.1 equiv). The N_2 inlet was then removed, and septa was resealed with Dowsil 732 Multi-Purpose Sealent. The reaction was transferred to an oil bath, heated to 60 ºC, and allowed to stir for 48 h. The reaction was then cooled to room temperature, diluted with E_2O, and filtered through a plug of silica washing with ~10 mL Et_2O. The filtrate was then concentrated under vacuum and phenyltrimethylsilane (PhTMS; 8.6 μL, 50 μmol) was added as internal standard for analysis by ^1H NMR.

4.4.2.2 Method B: Nickel-Catalyzed Open-Shell Suzuki XC Reaction of Alkyl Chlorides



The following procedure was adapted from a report by Fu.[25] To a flame-dried 7 mL vial was added alkyl chloride (1.0 equiv). In separate vial was added boronic acid (1.6 equiv). The vials were transferred to a glovebox where $NiCl_2(DME)$ (0.10 equiv), ligand (0.10 equiv), and KHMDS (2.0 equiv), 2-propanol (0.20 M in substrate), and a stir bar were added to the vial with boronic acid. Note: L-prolinol ligand was added as a 1.0 M solution in 2-propanol. The reaction was allowed to stir for 5 minutes at room temperature. Alkyl chloride was then dissolved in 2-propanol (0.20M in substrate) and charged to the reaction. The reaction was sealed, removed from the glovebox, heated to 60 °C, and allowed to stir for 24 h. The reaction was then cooled to room

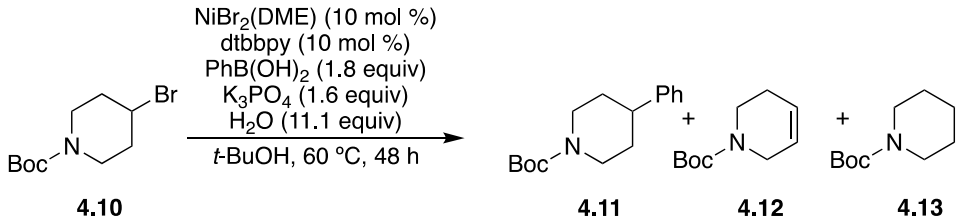
[25] See reference 4(b).

temperature, filtered through a plug of silica and washed with Et_2O. The filtrate was concentrated under vacuum and phenyltrimethylsilane (PhTMS; 8.6 μL, 50 μmol) was added as internal standard for analysis by ^1H NMR.

4.4.3 Representative Reactions

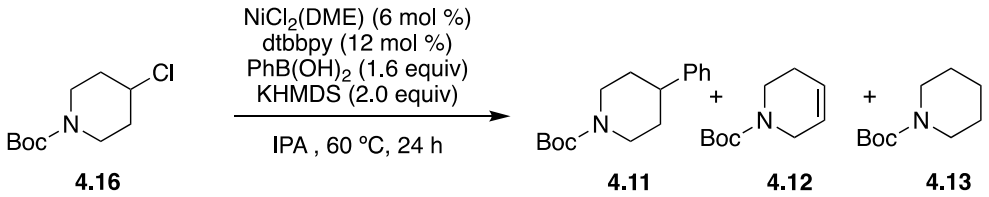
The following experiments are representative examples of the methods used to quantify the products of the open-shell Suzuki XC reactions.

4.4.3.1 Representative Reaction of 4-Bromopiperidine with Phenyl Boronic Acid



The following experiment was performed according to Method A. The following amounts of reagents were used: N-boc-4-bromopiperidine (26 mg, 0.10 mmol, 1.0 equiv), phenyl boronic acid (22 mg, 0.18 mmol, 1.8 equiv), $NiBr_2$(DME) (3.1 mg, 10. μmol, 0.010 equiv), dtbbpy (2.7 mg, 10. μmol, 0.010 equiv), K_3PO_4 (34 mg, 0.16 mmol, 1.6 equiv), H_2O (20 μL, 1.1 mmol, 11 equiv), *t*-BuOH (1.0 mL, 0.10 M). ^1H NMR yields were obtained by comparison of the proton alpha to the bromide in SM, the benzylic proton in **4.11**, alkene protons in **4.12**, and the protons alpha to the nitrogen in **4.13** as compared to PhTMS (8.6 μL) as internal standard. Analysis of the ^1H NMR spectrum identified 78% **4.10**, 22% yield of **4.11**, 0% yield of **4.12**, and 0% yield of **4.13**.

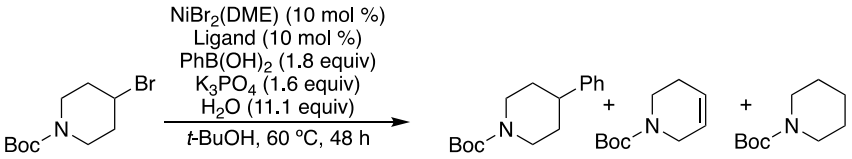
4.4.3.2 Representative Reaction of 4-chloropiperidine with Phenyl Boronic Acid



The following experiment was performed according to Method B. The following amounts of reagents were used: N-boc-4-chloropiperidine (22 mg, 0.10 mmol, 1.0 equiv), phenyl boronic acid (20. mg, 0.16 mmol, 1.6 equiv), $NiCl_2$(DME) (1.3 mg, 6.0 μmol, 0.06 equiv), dtbbpy (3.2 mg, 12 μmol, 0.12 equiv), KHMDS (40. mg, 0.20 mmol, 2.0 equiv), and 2-propanol (1.0 mL, 0.10 M). ^{1}H NMR yields were obtained by comparison of the proton alpha to the chloride in SM, the benzylic proton in **4.11**, alkene protons in **4.12**, and the protons alpha to the nitrogen in **4.13** as compared to PhTMS (8.6 μL) as internal standard. Analysis of the ^{1}H NMR spectrum identified 46% **4.16**, 6% yield of **4.11**, 0% yield of **4.12**, and 8% yield of **4.13**.

4.4.4 Tables with Nickel-Catalyzed Open-Shell Suzuki XC Reaction Data

Table 4.4. Open-Shell Suzuki XC Reaction with 4-Bromopiperidine and Phenyl Boronic Acid

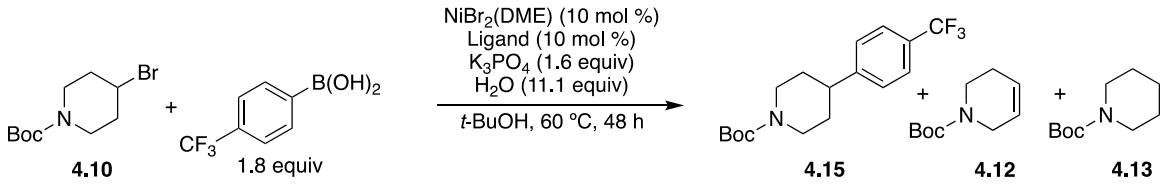


4.10 **4.11** **4.12** **4.13**

Ligand	4.10 (%)[a,b]	4.11 (%)[a,b]	4.12 (%)[a,b]	4.13 (%)[a,b]
No Ni/Ligand	101	0	0	0
No ligand	104	0	0	0
rac-BINAP	93	0	0	0
dppm	98	0	0	0
dppe	102	0	0	0
Xantphos	89	0	0	0
DavePhos[c]	94	0	0	0
PPh_3[c]	94	0	0	0
PCy_3[c]	92	0	0	0
dppf	101	0	0	0
DMPE	96	0	0	0
Ph-Box	95	0	0	0
IndaBox	97	0	0	0
BiOx	99	0	0	0
PyBox	94	0	0	0
Bphen	39	57	0	0
BCP	77	4	4	0
dMebpy	98	0	0	0
dMeObpy	90	11	0	0
dmabpy	80	7	0	0
dtbbpy	78	22	0	0
bipy	79	13	0	0
diamine A[d]	17	37	0	18
diamine B[d]	65	17	0	0
TMPDA[d]	65	0	0	9
TMEDA[d]	48	19	0	13
DMPDA[d]	38	28	0	14
L-prolinol	91	0	0	0
pyridine[c]	94	0	0	0

[a]Reactions were performed on a 0.10 mmol scale. [b]Yield determined by ^1H NMR by comparison to PhTMS as internal standard. [c]Reactions performed with 0.20 equiv ligand. [d]No H_2O added to the reaction.

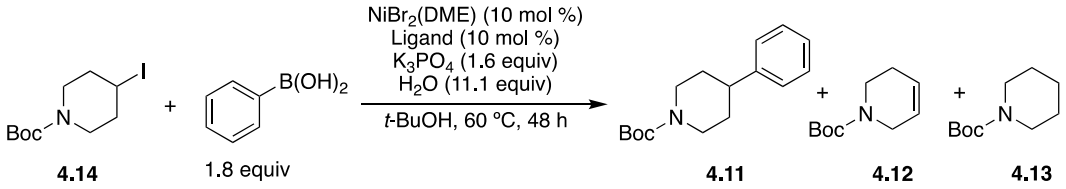
Table 4.5. Open-Shell Suzuki XC Reaction with 4-Bromopiperidine and Trifluoromethylphenyl Boronic Acid



Ligand	4.10 (%)[a,b]	4.15 (%)[a,b]	4.12 (%)[a,b]	4.13 (%)[a,b]
No Ni/Ligand	67	0	0	0
No ligand	96	0	0	0
rac-BINAP	82	0	0	0
dppm	93	0	0	0
dppe	88	0	0	0
Xantphos	99	0	0	0
DavePhos[c]	99	0	0	0
PPh_3[c]	92	0	3	6
PCy_3[c]	64	0	0	13
dppf	99	0	0	0
DMPE	47	0	0	24
IndaBox	90	0	0	0
BiOx	101	0	0	0
PyBox	98	0	0	0
Bphen	63	18	0	0
BCP	100	0	0	0
dMeObpy	92	6	2	0
dmabpy	81	14	0	0
dtbbpy	64	30	2	0
bipy	99	7	0	0
diamine A[d]	47	9	0	0
diamine B[d]	47	6	0	19
TMPDA[d]	60	0	0	13
TMEDA[d]	30	11	0	21
DMPDA[d]	42	11	0	5
L-prolinol[d]	12	26	0	15
pyridine[c]	68	0	0	0

[a]Reactions were performed on a 0.10 mmol scale. [b]Yield determined by ^1H NMR by comparison to PhTMS as internal standard. [c]Reactions performed with 0.20 equiv ligand. [d]No H_2O added to the reaction.

Table 4.6. Open-Shell Suzuki XC Reaction with 4-Iodopiperidine and Phenyl Boronic Acid

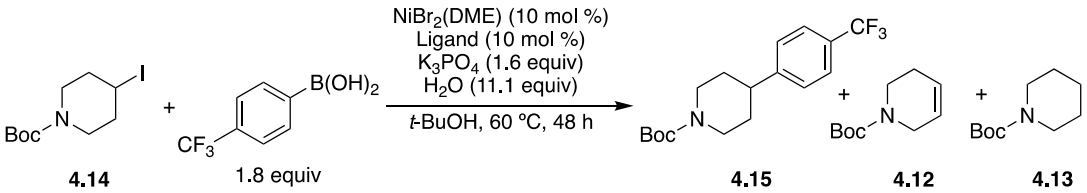


4.14 1.8 equiv **4.11** **4.12** **4.13**

Ligand	4.14 (%)[a,b]	4.11 (%)[a,b]	4.12 (%)[a,b]	4.13 (%)[a,b]
No Ni/Ligand	104	0	0	0
No ligand	86	0	2	0
rac-BINAP	99	0	0	0
dppm	95	0	0	0
dppe	70	0	1	10
Xantphos	100	0	0	0
DavePhos[c]	96	0	0	0
PPh_3[c]	101	0	0	0
PCy_3[c]	87	0	0	0
dppf	81	0	7	0
DMPE	63	6	4	13
IndaBox	101	0	0	0
BiOx	94	0	0	0
PyBox	95	0	2	0
Bphen	49	49	0	0
BCP	101	0	0	0
dMebpy	84	0	9	0
dMeObpy	85	11	3	0
dmabpy	94	0	6	0
dtbbpy	85	12	0	0
bipy	56	37	0	0
diamine A[d]	6	39	0	21
diamine B[d]	70	9	2	8
TMPDA[d]	53	6	4	7
TMEDA[d]	30	33	0	9
DMPDA[d]	15	38	1	11
L-prolinol[d]	49	15	2	12
pyridine[c]	60	9	3	10

[a]Reactions were performed on a 0.10 mmol scale. [b]Yield determined by ^1H NMR by comparison to PhTMS as internal standard. [c]Reactions performed with 0.20 equiv ligand. [d]No H_2O added to the reaction.

Table 4.7. Open-Shell Suzuki XC Reaction with 4-Iodopiperidine and Trifluoromethylphenyl Boronic Acid

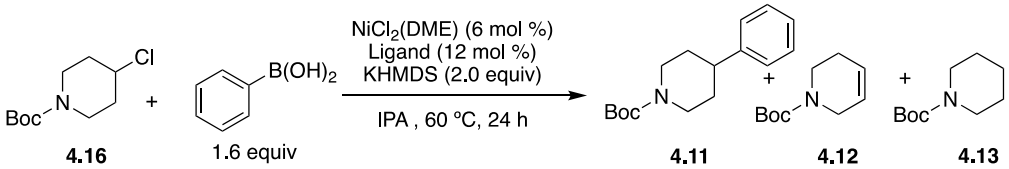


4.14 1.8 equiv **4.15** **4.12** **4.13**

Ligand	4.14 (%)[a,b]	4.15 (%)[a,b]	4.12 (%)[a,b]	4.13 (%)[a,b]
No Ni/Ligand	100	0	2	0
No ligand	98	0	4	0
rac-BINAP	90	0	0	0
dppm	92	0	3	3
dppe	80	0	0	6
Xantphos	93	0	4	0
DavePhos[c]	102	0	2	0
PPh_3[c]	97	0	3	2
PCy_3[c]	83	0	0	7
dppf	72	0	3	3
DMPE	72	0	0	8
IndaBox	104	0	0	0
BiOx	93	0	3	2
PyBox	92	0	4	0
Bphen	38	56	0	0
BCP	104	0	0	0
dMebpy	107	0	0	0
dMeObpy	26	67	0	0
dmabpy	43	46	0	2
dtbbpy	22	71	0	0
bipy	37	57	0	0
diamine A[d]	52	10	0	11
diamine B[d]	46	6	1	19
TMPDA[d]	67	0	4	12
TMEDA[d]	23	17	0	20
DMPDA[d]	26	19	0	22
L-prolinol[d]	6	55	0	14
pyridine[c]	73	4	1	10

[a]Reactions were performed on a 0.10 mmol scale. [b]Yield determined by ^{1}H NMR by comparison to PhTMS as internal standard. [c]Reactions performed with 0.20 equiv ligand. [d]No H_2O added to the reaction.

Table 4.8. Open-Shell Suzuki XC Reaction with 4-Chloropiperidine Phenyl Boronic Acid

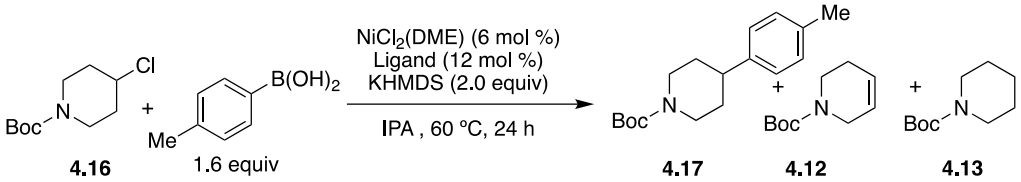


4.16 1.6 equiv **4.11** **4.12** **4.13**

Ligand	4.16 (%)[a,b]	4.11 (%)[a,b]	4.12 (%)[a,b]	4.13 (%)[a,b]
No Ni/Ligand	66	0	7	0
No ligand	68	0	4	0
rac-BINAP	51	0	6	3
dppm	59	0	3	0
dppe	65	0	5	0
Xantphos	71	0	8	0
DavePhos[c]	67	0	9	7
PPh_3[c]	16	0	6	31
PCy_3[c]	55	0	6	4
dppf	52	0	4	0
Ph-Box	59	0	5	2
IndaBox	70	0	6	3
BiOx	60	0	6	0
PyBox	68	0	5	0
Bphen	85	0	10	0
dtbbpy	46	6	0	8
bipy	64	2	9	4
diamine A[d]	0	20	0	62
L-prolinol	8	46	0	25

[a]Reactions were performed on a 0.10 mmol scale. [b]Yield determined by ^1H NMR by comparison to PhTMS as internal standard. [c]Reactions performed with 0.20 equiv ligand.

Table 4.9. Open-Shell Suzuki XC Reaction with 4-Chloropiperidine and *p*-Tolyl Boronic Acid

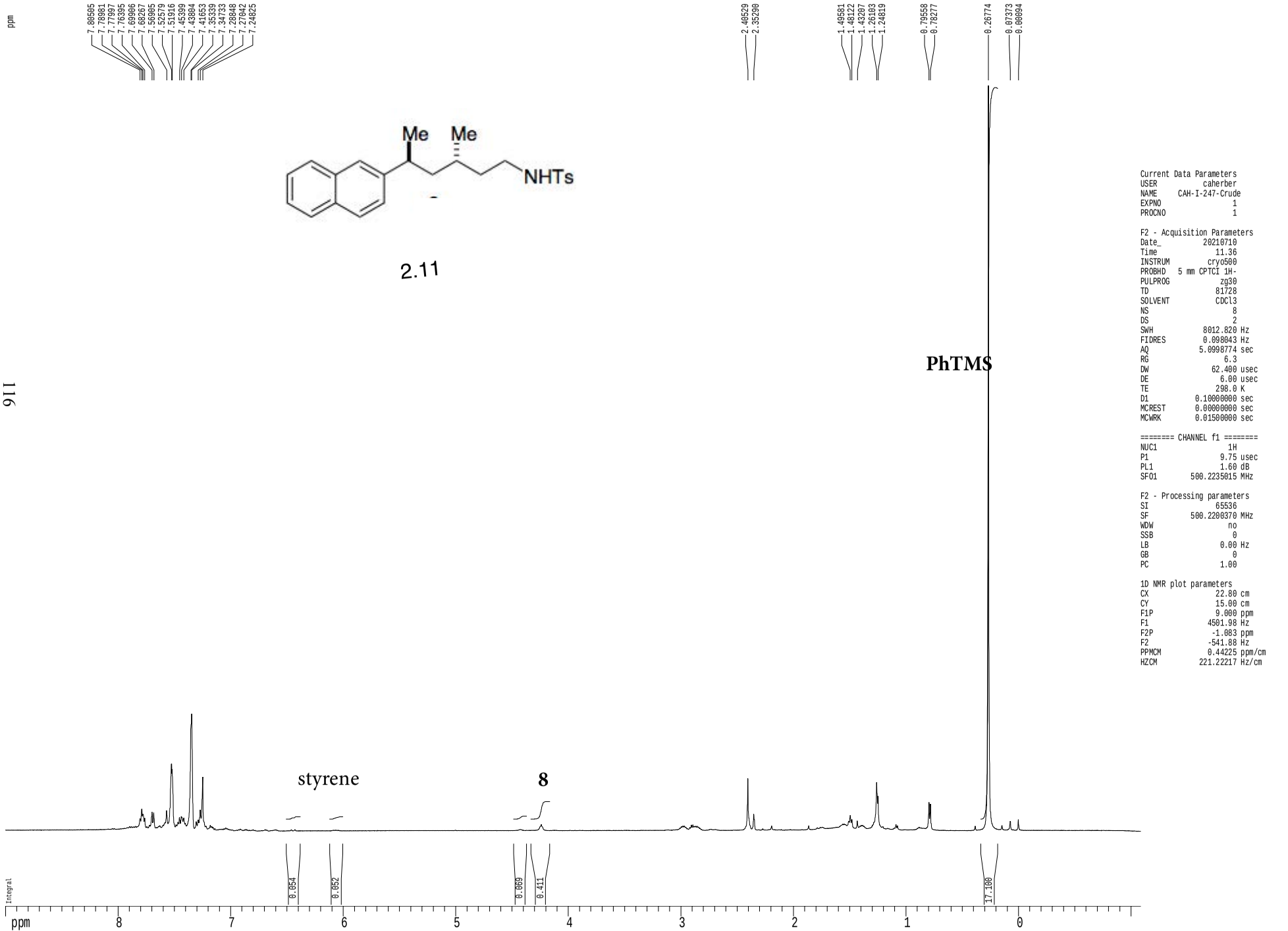


4.16 1.6 equiv **4.17** **4.12** **4.13**

Ligand	4.16 (%)[a,b]	4.17 (%)[a,b]	4.12 (%)[a,b]	4.13 (%)[a,b]
No Ni/Ligand	61	0	4	0
No ligand	67	0	5	0
rac-BINAP	63	0	4	0
dppm	65	0	5	2
dppe	68	0	4	0
Xantphos	66	0	4	0
DavePhos[c]	65	0	4	4
PPh_3[c]	20	0	10	34
PCy_3[c]	69	0	5	6
dppf	58	0	5	0
Ph-Box	60	0	6	2
IndaBox	72	0	5	0
BiOx	72	0	4	0
PyBox	63	0	4	0
Bphen	61	5	10	2
dtbbpy	63	5	8	6
bipy	74	3	6	4
diamine A[d]	0	9	0	50
L-prolinol	0	39	0	36

[a]Reactions were performed on a 0.10 mmol scale. [b]Yield determined by ^{1}H NMR by comparison to PhTMS as internal standard. [c]Reactions performed with 0.20 equiv ligand.

1H spectrum



116

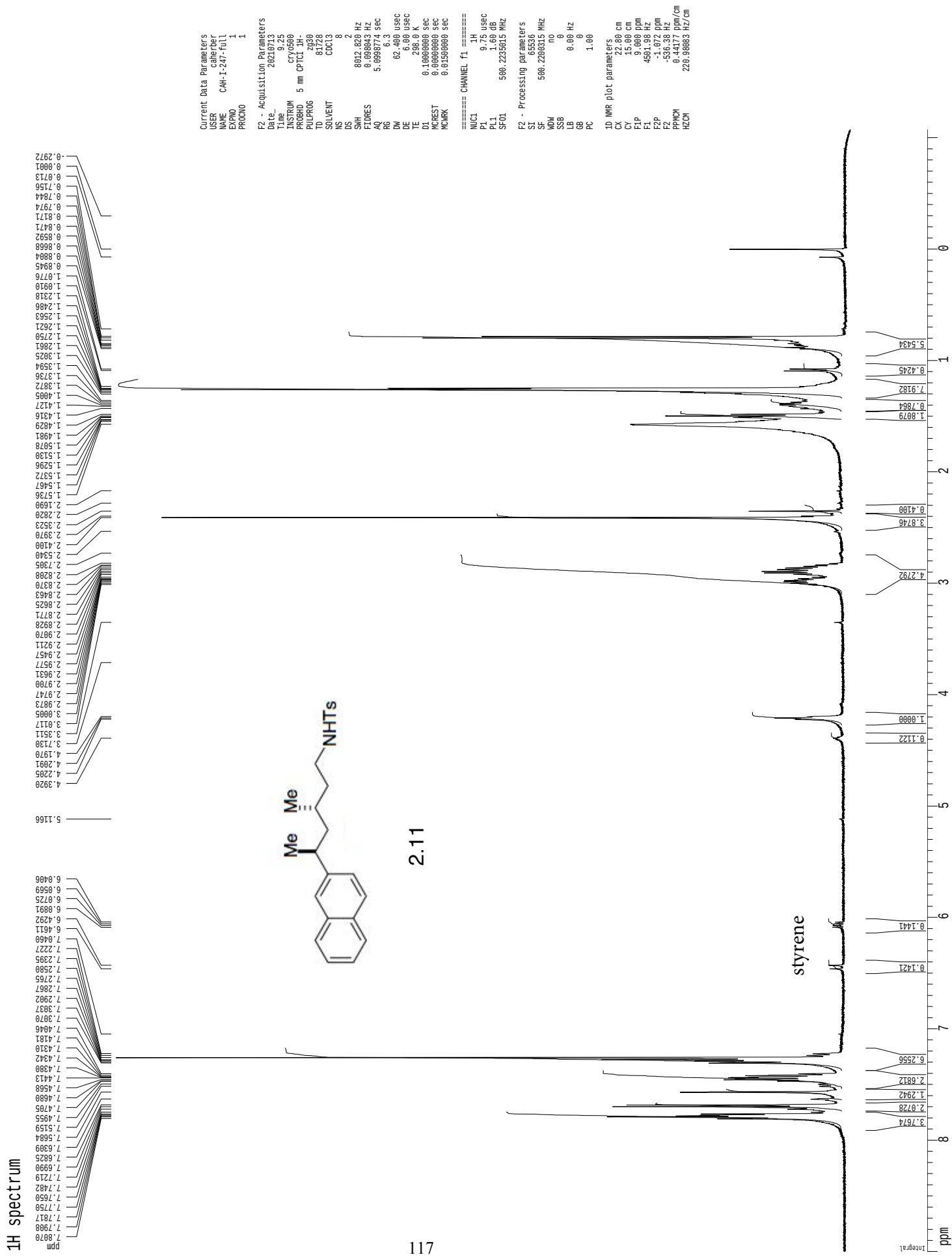
```
Current Data Parameters
USER            caherber
NAME      CAH-I-247-Crude
EXPNO                   1
PROCNO                  1

F2 - Acquisition Parameters
Date_          20210710
Time              11.36
INSTRUM         cryo500
PROBHD   5 mm CPTCI 1H-
PULPROG            zg30
TD                81728
SOLVENT           CDCl3
NS                    8
DS                    2
SWH            8012.820 Hz
FIDRES         0.098043 Hz
AQ             5.0998774 sec
RG                  6.3
DW                62.400 usec
DE                 6.00 usec
TE                298.0 K
D1           0.10000000 sec
MCREST       0.00000000 sec
MCWRK        0.01500000 sec

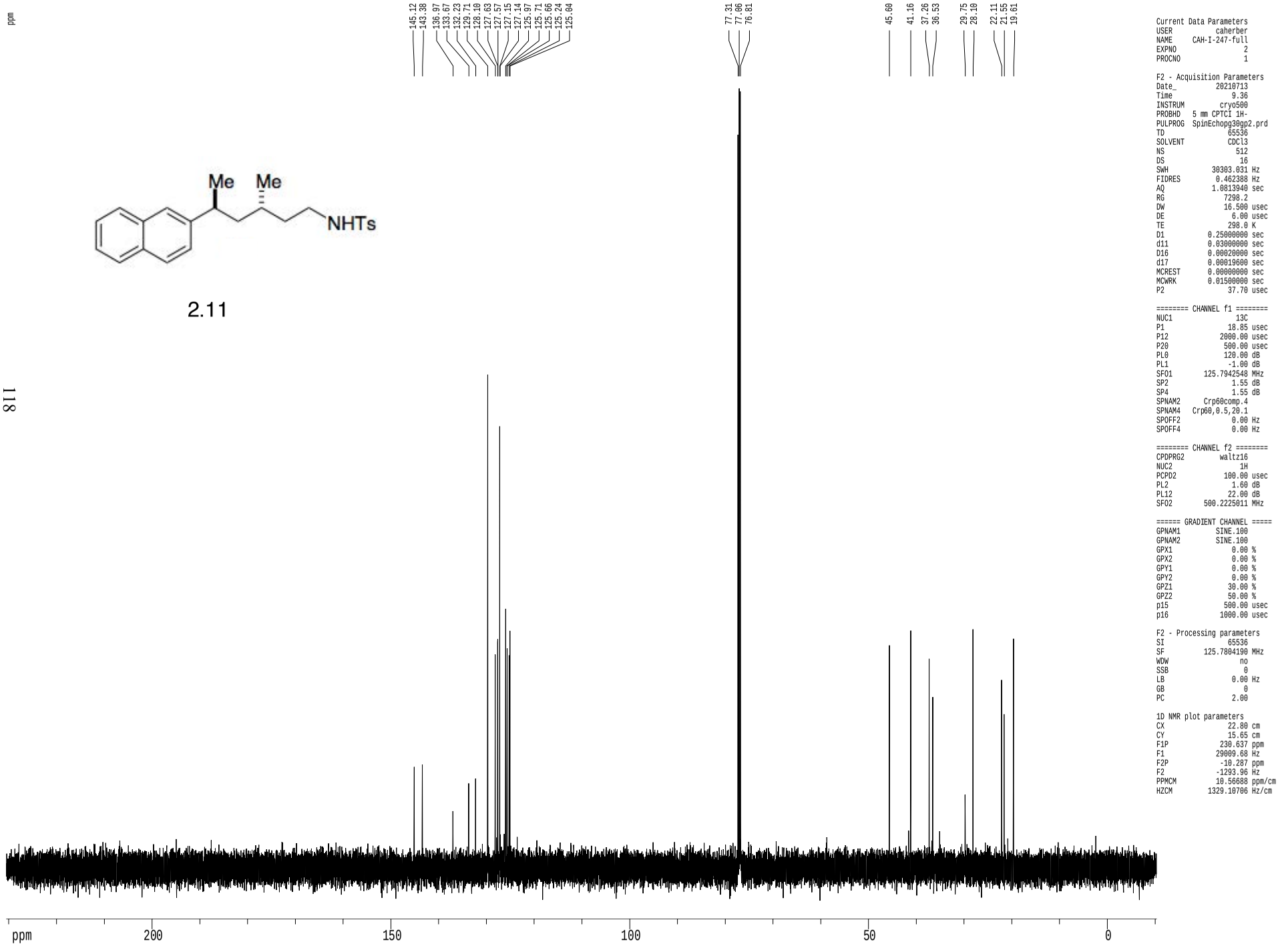
======= CHANNEL f1 =======
NUC1                  1H
P1                 9.75 usec
PL1                1.60 dB
SFO1         500.2235015 MHz

F2 - Processing parameters
SI                 65536
SF           500.2200370 MHz
WDW                   no
SSB                    0
LB                 0.00 Hz
GB                     0
PC                 1.00

1D NMR plot parameters
CX                22.80 cm
CY                15.00 cm
F1P               9.000 ppm
F1              4501.98 Hz
F2P              -1.083 ppm
F2              -541.88 Hz
PPMCM           0.44225 ppm/cm
HZCM          221.22217 Hz/cm
```


1H spectrum
Current Data Parameters
USER caherher
NAME CAH-I-247-full
EXPNO 1
PROCNO 1
F2 - Acquisition Parameters
Date_ 20210713
Time_ 9.25
INSTRUM cryo500
PROBHD 5 mm CPTCI 1H-
PULPROG zg30
TD 81728
SOLVENT CDCl3
NS 8
DS 2
SWH 8012.820 Hz
FIDRES 0.098043 Hz
AQ 5.0998774 sec
RG 6.3
DW 62.400 usec
DE 6.00 usec
TE 298.0 K
D1 0.10000000 sec
MCREST 0.00000000 sec
MCWRK 0.01500000 sec
======== CHANNEL f1 ========
NUC1 1H
P1 9.75 usec
PL1 1.60 dB
SFO1 500.2235015 MHz
F2 - Processing parameters
SI 65536
SF 500.2200315 MHz
WDW no
SSB 0
LB 0.00 Hz
GB 0
PC 1.00
1D NMR plot parameters
CX 22.80 cm
CY 15.00 cm
F1P 9.000 ppm
F1 4501.98 Hz
F2P -1.072 ppm
F2 -536.38 Hz
PPMCM 0.44177 ppm/cm
HZCM 220.98083 Hz/cm
NHTs
Me
Me
Me
2.11
styrene
ppm
Integral

Z-restored spin-echo 13C spectrum with 1H decoupling



Current Data Parameters
USER caherber
NAME CAH-I-247-full
EXPNO 2
PROCNO 1

F2 - Acquisition Parameters
Date_ 20210713
Time 9.36
INSTRUM cryo500
PROBHD 5 mm CPTCI 1H-
PULPROG SpinEchopg30gp2.prd
TD 65536
SOLVENT CDCl3
NS 512
DS 16
SWH 30303.031 Hz
FIDRES 0.462388 Hz
AQ 1.0813940 sec
RG 7298.2
DW 16.500 usec
DE 6.00 usec
TE 298.0 K
D1 0.25000000 sec
d11 0.03000000 sec
D16 0.00020000 sec
d17 0.00019600 sec
MCREST 0.00000000 sec
MCWRK 0.01500000 sec
P2 37.70 usec

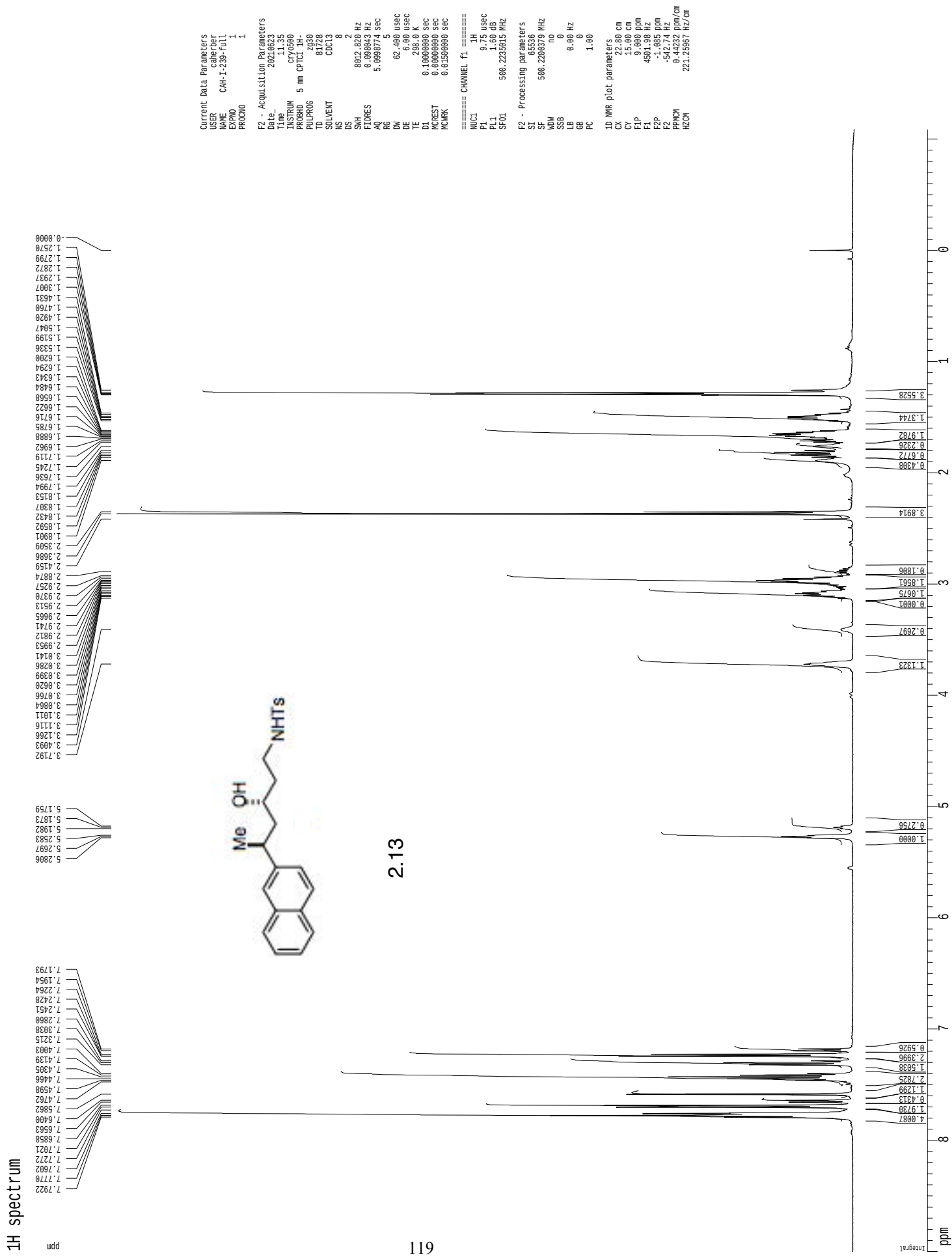
======== CHANNEL f1 ========
NUC1 13C
P1 18.85 usec
P12 2000.00 usec
P20 500.00 usec
PL0 120.00 dB
PL1 -1.00 dB
SFO1 125.7942548 MHz
SP2 1.55 dB
SP4 1.55 dB
SPNAM2 Crp60comp.4
SPNAM4 Crp60,0.5,20.1
SPOFF2 0.00 Hz
SPOFF4 0.00 Hz

======== CHANNEL f2 ========
CPDPRG2 waltz16
NUC2 1H
PCPD2 100.00 usec
PL2 1.60 dB
PL12 22.00 dB
SFO2 500.2225011 MHz

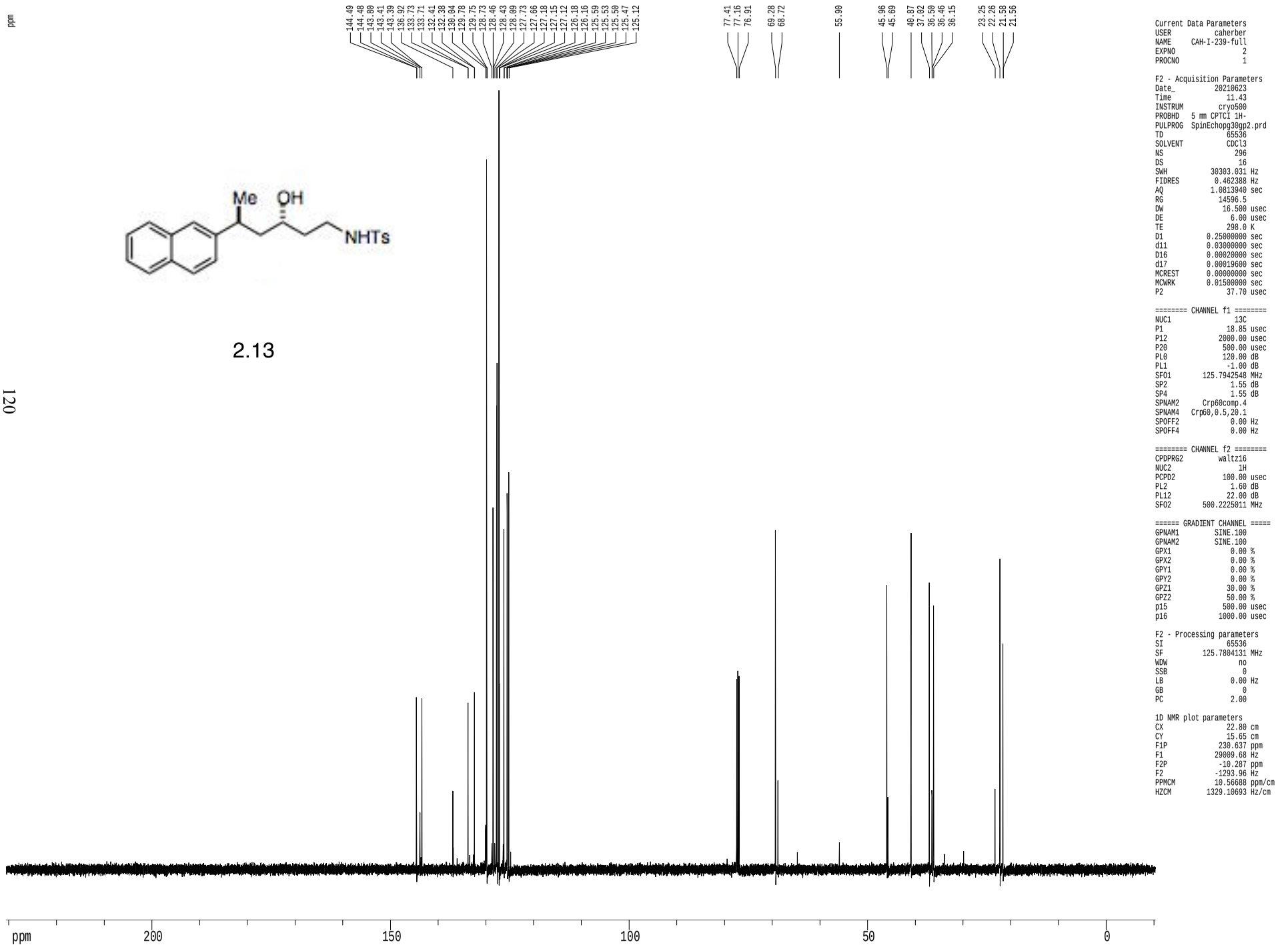
====== GRADIENT CHANNEL =====
GPNAM1 SINE.100
GPNAM2 SINE.100
GPX1 0.00 %
GPX2 0.00 %
GPY1 0.00 %
GPY2 0.00 %
GPZ1 30.00 %
GPZ2 50.00 %
p15 500.00 usec
p16 1000.00 usec

F2 - Processing parameters
SI 65536
SF 125.7804190 MHz
WDW no
SSB 0
LB 0.00 Hz
GB 0
PC 2.00

1D NMR plot parameters
CX 22.80 cm
CY 15.65 cm
F1P 230.637 ppm
F1 29009.68 Hz
F2P -10.287 ppm
F2 -1293.96 Hz
PPMCM 10.56688 ppm/cm
HZCM 1329.10706 Hz/cm


1H spectrum
Current Data Parameters
USER caherher
NAME CAH-I-239-full
EXPNO 1
PROCNO 1
F2 - Acquisition Parameters
Date_ 20210623
Time 11.35
INSTRUM cryo500
PROBHD 5 mm CPTCI 1H-
PULPROG zg30
TD 81728
SOLVENT CDCl3
NS 8
DS 2
SWH 8012.820 Hz
FIDRES 0.098043 Hz
AQ 5.0998774 sec
RG 5
DW 62.400 usec
DE 6.00 usec
TE 298.0 K
D1 0.10000000 sec
MCREST 0.00000000 sec
MCWRK 0.01500000 sec
======= CHANNEL f1 =======
NUC1 1H
P1 9.75 usec
PL1 1.60 dB
SFO1 500.2235015 MHz
F2 - Processing parameters
SI 65536
SF 500.2200379 MHz
WDW no
SSB 0
LB 0.00 Hz
GB 0
PC 1.00
1D NMR plot parameters
CX 22.80 cm
CY 15.00 cm
F1P 9.000 ppm
F1 4501.98 Hz
F2P -1.005 ppm
F2 -542.74 Hz
PPMCM 0.44232 ppm/cm
HZCM 221.25967 Hz/cm
NHTs
OH
Me
2.13
ppm
Integral

Z-restored spin-echo 13C spectrum with 1H decoupling




```
Current Data Parameters
USER            caherber
NAME      CAH-I-239-full
EXPNO                   2
PROCNO                  1

F2 - Acquisition Parameters
Date_          20210623
Time              11.43
INSTRUM         cryo500
PROBHD   5 mm CPTCI 1H-
PULPROG  SpinEchopg30gp2.prd
TD                65536
SOLVENT           CDCl3
NS                  296
DS                   16
SWH           30303.031 Hz
FIDRES         0.462388 Hz
AQ             1.0813940 sec
RG               14596.5
DW                16.500 usec
DE                 6.00 usec
TE                298.0 K
D1             0.25000000 sec
d11            0.03000000 sec
D16            0.00020000 sec
d17            0.00019600 sec
MCREST         0.00000000 sec
MCWRK          0.01500000 sec
P2                37.70 usec

======== CHANNEL f1 ========
NUC1                13C
P1                18.85 usec
P12             2000.00 usec
P20              500.00 usec
PL0              120.00 dB
PL1               -1.00 dB
SFO1         125.7942548 MHz
SP2                1.55 dB
SP4                1.55 dB
SPNAM2      Crp60comp.4
SPNAM4   Crp60,0.5,20.1
SPOFF2               0.00 Hz
SPOFF4               0.00 Hz

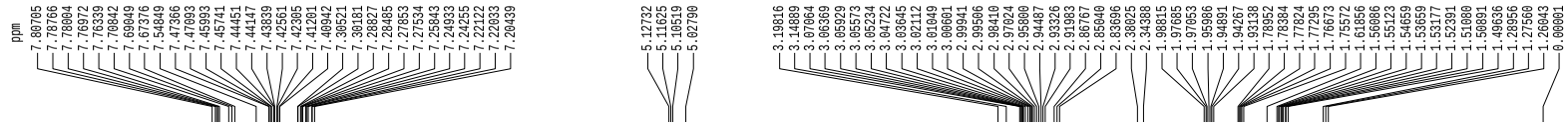
======== CHANNEL f2 ========
CPDPRG2          waltz16
NUC2                1H
PCPD2            100.00 usec
PL2                1.60 dB
PL12              22.00 dB
SFO2         500.2225011 MHz

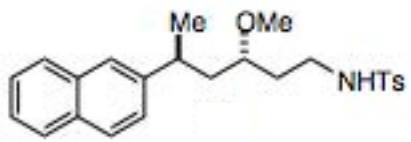
====== GRADIENT CHANNEL =====
GPNAM1         SINE.100
GPNAM2         SINE.100
GPX1                0.00 %
GPX2                0.00 %
GPY1                0.00 %
GPY2                0.00 %
GPZ1               30.00 %
GPZ2               50.00 %
p15              500.00 usec
p16             1000.00 usec

F2 - Processing parameters
SI                  65536
SF           125.7804131 MHz
WDW                    no
SSB                     0
LB                   0.00 Hz
GB                      0
PC                   2.00

1D NMR plot parameters
CX                  22.80 cm
CY                  15.65 cm
F1P               230.637 ppm
F1              29009.68 Hz
F2P               -10.287 ppm
F2              -1293.96 Hz
PPMCM            10.56688 ppm/cm
HZCM          1329.10693 Hz/cm
```

1H spectrum





2.10

121


```
Current Data Parameters
USER            caherber
NAME            CAH-I-212
EXPNO                   2
PROCNO                  1

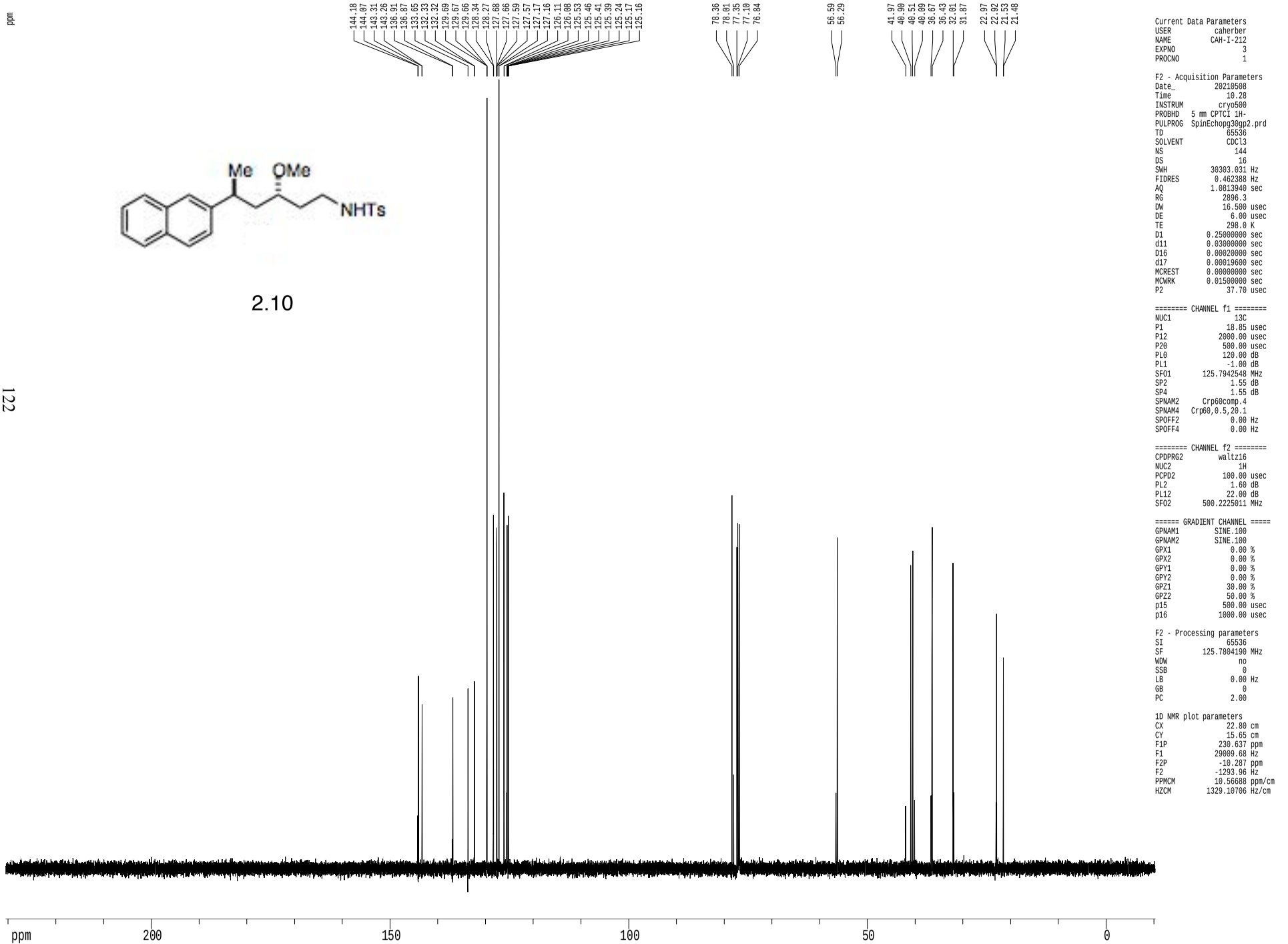
F2 - Acquisition Parameters
Date_          20210508
Time                10.24
INSTRUM          cryo500
PROBHD   5 mm CPTCI 1H-
PULPROG             zg30
TD                 81728
SOLVENT            CDCl3
NS                     8
DS                     2
SWH             8012.820 Hz
FIDRES          0.098043 Hz
AQ              5.0998774 sec
RG                     4
DW                62.400 usec
DE                 6.00 usec
TE                298.0 K
D1           0.10000000 sec
MCREST       0.00000000 sec
MCWRK        0.01500000 sec

======= CHANNEL f1 =======
NUC1                   1H
P1                  9.75 usec
PL1                 1.60 dB
SFO1         500.2235015 MHz

F2 - Processing parameters
SI                 65536
SF           500.2200364 MHz
WDW                   no
SSB                    0
LB                  0.00 Hz
GB                     0
PC                  1.00

1D NMR plot parameters
CX                 22.80 cm
CY                 15.00 cm
F1P                9.000 ppm
F1               4501.98 Hz
F2P               -1.082 ppm
F2               -541.27 Hz
PPMCM            0.44220 ppm/cm
HZCM           221.19518 Hz/cm
```

Z-restored spin-echo 13C spectrum with 1H decoupling




```
Current Data Parameters
USER            caherber
NAME            CAH-I-212
EXPNO                   3
PROCNO                  1

F2 - Acquisition Parameters
Date_            20210508
Time                10.28
INSTRUM           cryo500
PROBHD   5 mm CPTCI 1H-
PULPROG  SpinEchopg30gp2.prd
TD                  65536
SOLVENT             CDCl3
NS                    144
DS                     16
SWH            30303.031 Hz
FIDRES          0.462388 Hz
AQ              1.0813940 sec
RG                 2896.3
DW                16.500 usec
DE                 6.00 usec
TE                298.0 K
D1            0.25000000 sec
d11           0.03000000 sec
D16           0.00020000 sec
d17           0.00019600 sec
MCREST        0.00000000 sec
MCWRK         0.01500000 sec
P2                37.70 usec

======== CHANNEL f1 ========
NUC1                13C
P1                18.85 usec
P12             2000.00 usec
P20              500.00 usec
PL0              120.00 dB
PL1               -1.00 dB
SFO1         125.7942548 MHz
SP2                1.55 dB
SP4                1.55 dB
SPNAM2      Crp60comp.4
SPNAM4   Crp60,0.5,20.1
SPOFF2               0.00 Hz
SPOFF4               0.00 Hz

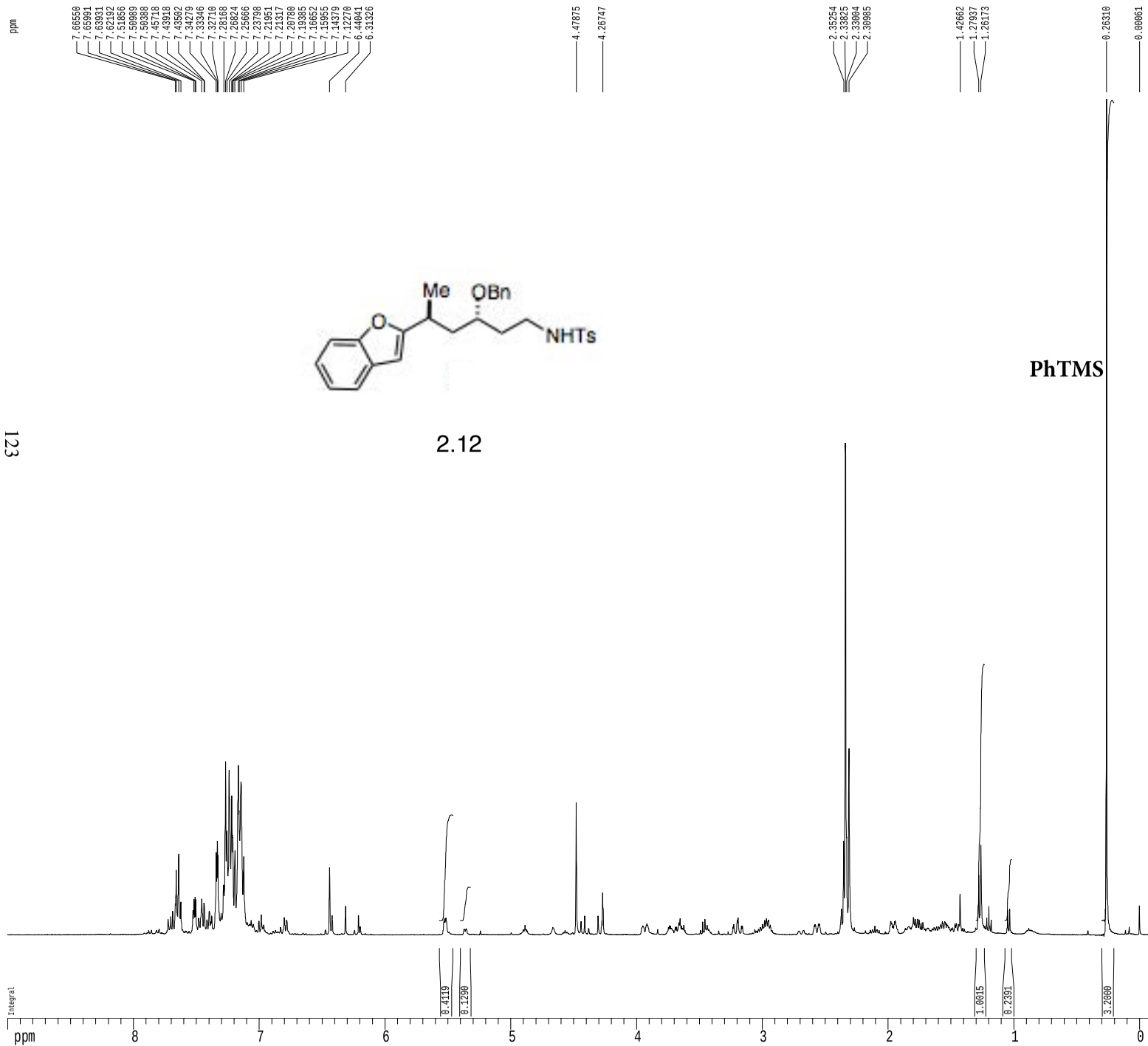
======== CHANNEL f2 ========
CPDPRG2          waltz16
NUC2                1H
PCPD2             100.00 usec
PL2                1.60 dB
PL12              22.00 dB
SFO2         500.2225011 MHz

====== GRADIENT CHANNEL =====
GPNAM1          SINE.100
GPNAM2          SINE.100
GPX1                0.00 %
GPX2                0.00 %
GPY1                0.00 %
GPY2                0.00 %
GPZ1               30.00 %
GPZ2               50.00 %
p15               500.00 usec
p16              1000.00 usec

F2 - Processing parameters
SI                  65536
SF           125.7804190 MHz
WDW                    no
SSB                     0
LB                   0.00 Hz
GB                      0
PC                   2.00

1D NMR plot parameters
CX                  22.80 cm
CY                  15.65 cm
F1P               230.637 ppm
F1              29009.68 Hz
F2P               -10.287 ppm
F2              -1293.96 Hz
PPMCM            10.56688 ppm/cm
HZCM          1329.10706 Hz/cm
```

1H spectrum



Current Data Parameters
USER caherber
NAME CAH-I-233-Crude
EXPNO 1
PROCNO 1

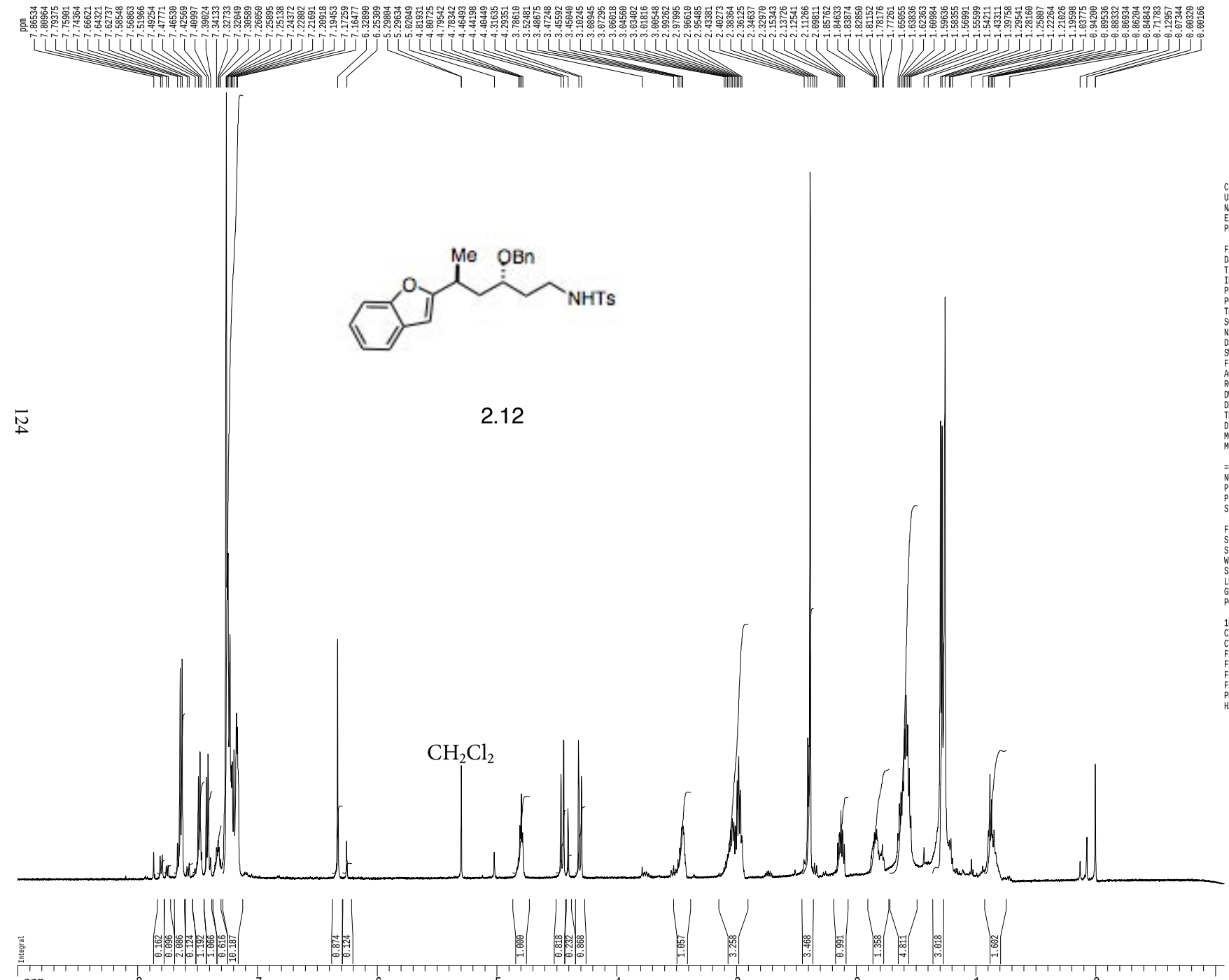
F2 - Acquisition Parameters
Date_ 20210604
Time 16.44
INSTRUM drx400
PROBHD 5 mm QNP H/F/P
PULPROG zg30
TD 65536
SOLVENT CDCl3
NS 8
DS 2
SWH 6410.256 Hz
FIDRES 0.097813 Hz
AQ 5.1118579 sec
RG 71.8
DW 78.000 usec
DE 4.50 usec
TE 298.0 K
D1 0.10000000 sec
MCREST 0.00000000 sec
MCWRK 0.01500000 sec

======= CHANNEL f1 =======
NUC1 1H
P1 12.00 usec
PL1 -1.60 dB
SFO1 400.1328009 MHz

F2 - Processing parameters
SI 65536
SF 400.1300427 MHz
WDW no
SSB 0
LB 0.00 Hz
GB 0
PC 2.00

1D NMR plot parameters
CX 22.80 cm
CY 15.00 cm
F1P 9.000 ppm
F1 3601.17 Hz
F2P -1.117 ppm
F2 -446.91 Hz
PPMCM 0.44372 ppm/cm
HZCM 177.54726 Hz/cm

1H spectrum




```
Current Data Parameters
USER            caherber
NAME      CAH-I-246-full
EXPNO                  1
PROCNO                 1

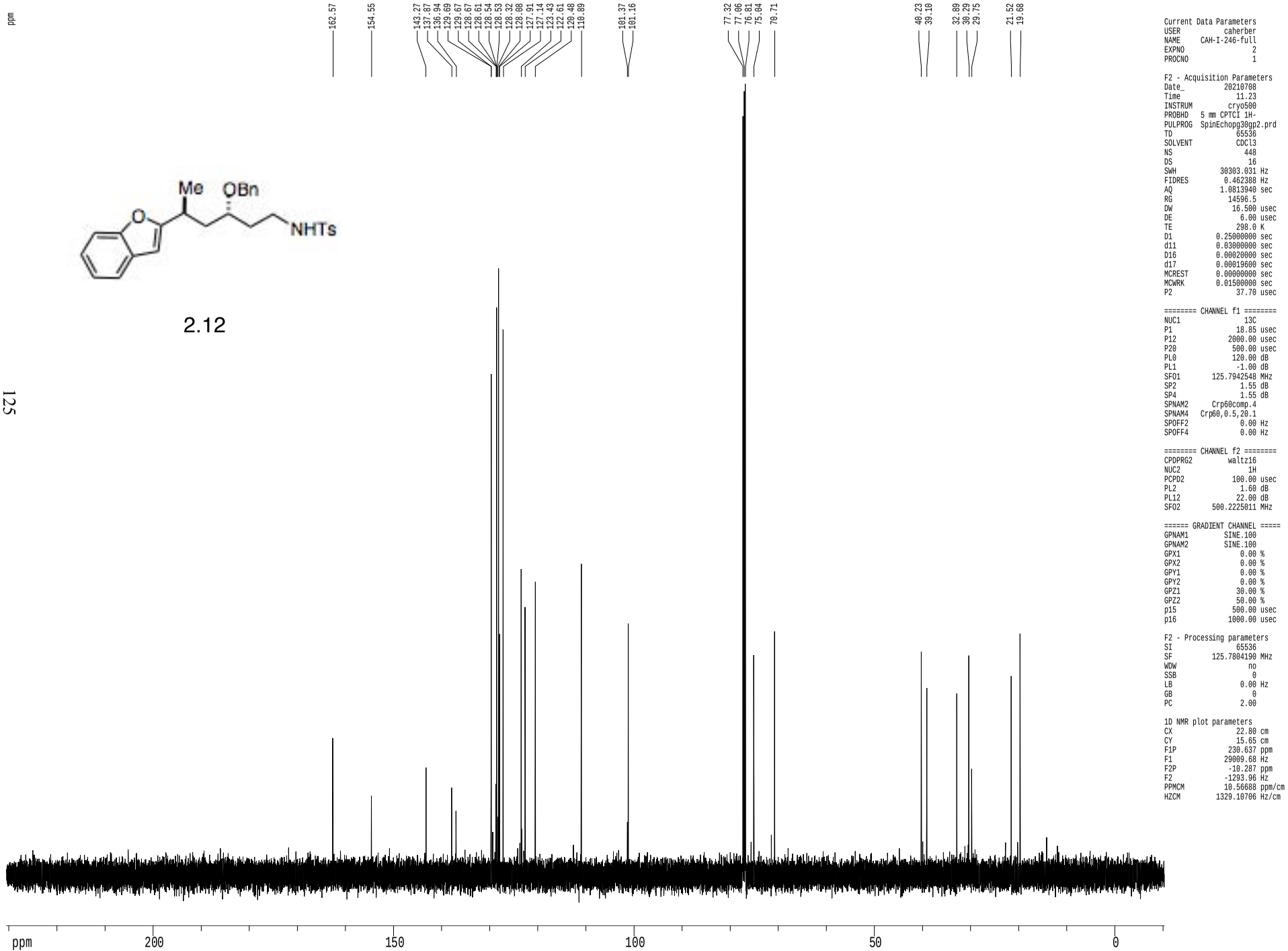
F2 - Acquisition Parameters
Date_           20210708
Time               11.14
INSTRUM          cryo500
PROBHD   5 mm CPTCI 1H-
PULPROG             zg30
TD                 81728
SOLVENT            CDCl3
NS                     8
DS                     2
SWH             8012.820 Hz
FIDRES             0.098043 Hz
AQ              5.0998774 sec
RG                   6.3
DW                62.400 usec
DE                 6.00 usec
TE                298.0 K
D1             0.10000000 sec
MCREST         0.00000000 sec
MCWRK          0.01500000 sec

======= CHANNEL f1 =======
NUC1                   1H
P1                  9.75 usec
PL1                 1.60 dB
SFO1          500.2235015 MHz

F2 - Processing parameters
SI                 65536
SF            500.2200313 MHz
WDW                   no
SSB                    0
LB                  0.00 Hz
GB                     0
PC                  1.00

1D NMR plot parameters
CX                 22.80 cm
CY                 15.00 cm
F1P                9.000 ppm
F1               4501.98 Hz
F2P               -1.072 ppm
F2               -536.14 Hz
PPMCM            0.44175 ppm/cm
HZCM           220.97008 Hz/cm
```

Z-restored spin-echo 13C spectrum with 1H decoupling




```
Current Data Parameters
USER            caherber
NAME      CAH-I-246-full
EXPNO                   2
PROCNO                  1

F2 - Acquisition Parameters
Date_           20210708
Time               11.23
INSTRUM          cryo500
PROBHD   5 mm CPTCI 1H-
PULPROG  SpinEchopg30gp2.prd
TD                 65536
SOLVENT            CDCl3
NS                   448
DS                    16
SWH           30303.031 Hz
FIDRES         0.462388 Hz
AQ            1.0813940 sec
RG              14596.5
DW               16.500 usec
DE                6.00 usec
TE               298.0 K
D1            0.25000000 sec
d11           0.03000000 sec
D16           0.00020000 sec
d17           0.00019600 sec
MCREST        0.00000000 sec
MCWRK         0.01500000 sec
P2                37.70 usec

======== CHANNEL f1 ========
NUC1                13C
P1                18.85 usec
P12             2000.00 usec
P20              500.00 usec
PL0              120.00 dB
PL1               -1.00 dB
SFO1        125.7942548 MHz
SP2               1.55 dB
SP4               1.55 dB
SPNAM2      Crp60comp.4
SPNAM4    Crp60,0.5,20.1
SPOFF2             0.00 Hz
SPOFF4             0.00 Hz

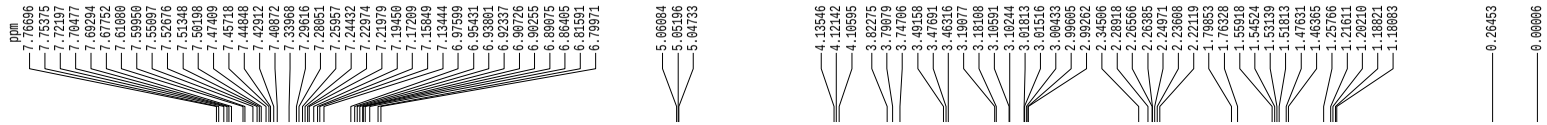
======== CHANNEL f2 ========
CPDPRG2          waltz16
NUC2                1H
PCPD2            100.00 usec
PL2                1.60 dB
PL12              22.00 dB
SFO2        500.2225011 MHz

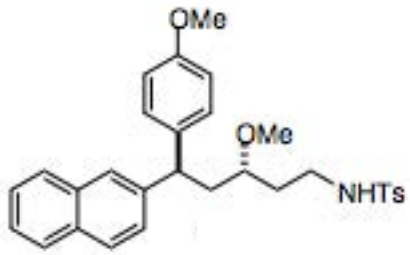
====== GRADIENT CHANNEL =====
GPNAM1          SINE.100
GPNAM2          SINE.100
GPX1               0.00 %
GPX2               0.00 %
GPY1               0.00 %
GPY2               0.00 %
GPZ1              30.00 %
GPZ2              50.00 %
p15              500.00 usec
p16             1000.00 usec

F2 - Processing parameters
SI                 65536
SF          125.7804190 MHz
WDW                   no
SSB                    0
LB                0.00 Hz
GB                     0
PC                2.00

1D NMR plot parameters
CX                22.80 cm
CY                15.65 cm
F1P              230.637 ppm
F1             29009.68 Hz
F2P              -10.287 ppm
F2             -1293.96 Hz
PPMCM           10.56688 ppm/cm
HZCM          1329.10706 Hz/cm
```

1H spectrum

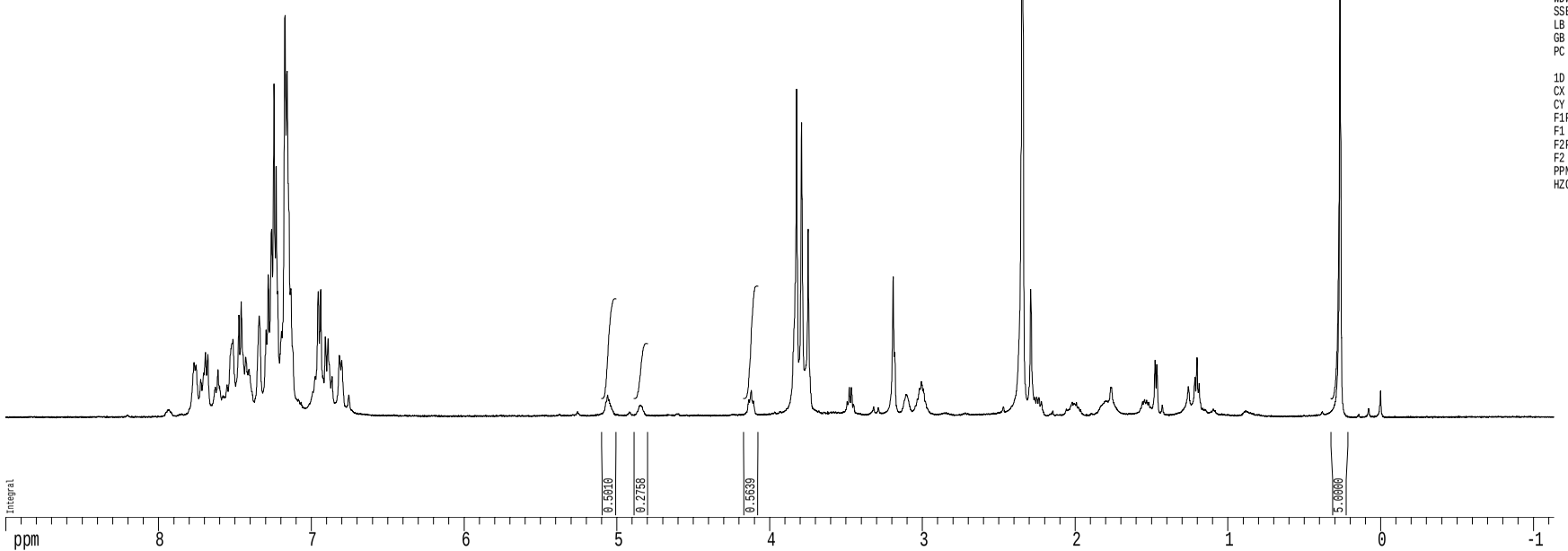




2.15

PhTMS

126




```
Current Data Parameters
USER            caherber
NAME      CAH-I-284-Crude
EXPNO                  1
PROCNO                 1

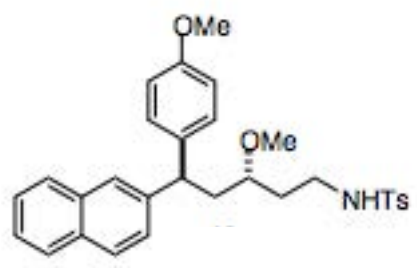
F2 - Acquisition Parameters
Date_          20210917
Time              10.29
INSTRUM           gn500
PROBHD   5 mm broadband
PULPROG            zg30
TD                81728
SOLVENT           CDCl3
NS                    8
DS                    2
SWH            8012.820 Hz
FIDRES         0.098043 Hz
AQ             5.0998774 sec
RG                 90.5
DW                62.400 usec
DE                 6.00 usec
TE                298.0 K
D1           0.10000000 sec
MCREST       0.00000000 sec
MCWRK        0.01500000 sec

======= CHANNEL f1 =======
NUC1                  1H
P1                12.00 usec
PL1               -6.00 dB
SFO1         498.6534906 MHz

F2 - Processing parameters
SI                 65536
SF           498.6500485 MHz
WDW                   no
SSB                    0
LB                0.00 Hz
GB                     0
PC                1.00

1D NMR plot parameters
CX                22.80 cm
CY                15.00 cm
F1P               9.000 ppm
F1              4487.85 Hz
F2P              -1.132 ppm
F2              -564.38 Hz
PPMCM           0.44438 ppm/cm
HZCM          221.58908 Hz/cm
```

1H



2.15

127

Current Data Parameters
USER caherber
NAME CAH-I-285-fll-600
EXPNO 4
PROCNO 1

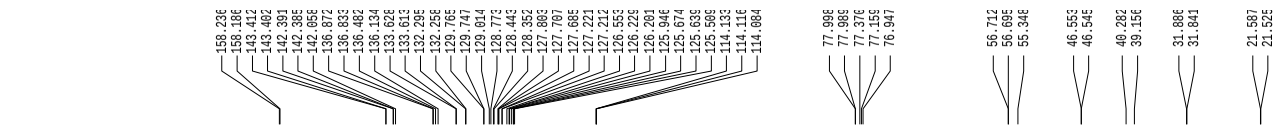
F2 - Acquisition Parameters
Date_ 20210920
Time 10.59
INSTRUM av600
PROBHD 5 mm CPBBO BB-
PULPROG zg30
TD 98074
SOLVENT CDCl3
NS 8
DS 2
SWH 9615.385 Hz
FIDRES 0.098042 Hz
AQ 5.0998979 sec
RG 10
DW 52.000 usec
DE 14.23 usec
TE 298.0 K
D1 0.10000000 sec
TD0 1

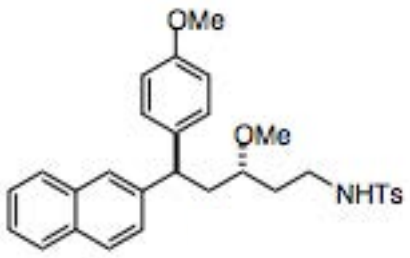
======== CHANNEL f1 ========
SFO1 600.1342009 MHz
NUC1 1H
P1 9.50 usec

F2 - Processing parameters
SI 65536
SF 600.1300407 MHz
WDW no
SSB 0
LB 0.00 Hz
GB 0
PC 1.00

1D NMR plot parameters
CX 22.80 cm
CY 15.00 cm
F1P 9.000 ppm
F1 5401.17 Hz
F2P -1.079 ppm
F2 -647.47 Hz
PPMCM 0.44206 ppm/cm
HZCM 265.29141 Hz/cm

13C





2.15

128


```
Current Data Parameters
USER            caherber
NAME      CAH-I-285-fll-600
EXPNO                  5
PROCNO                 1

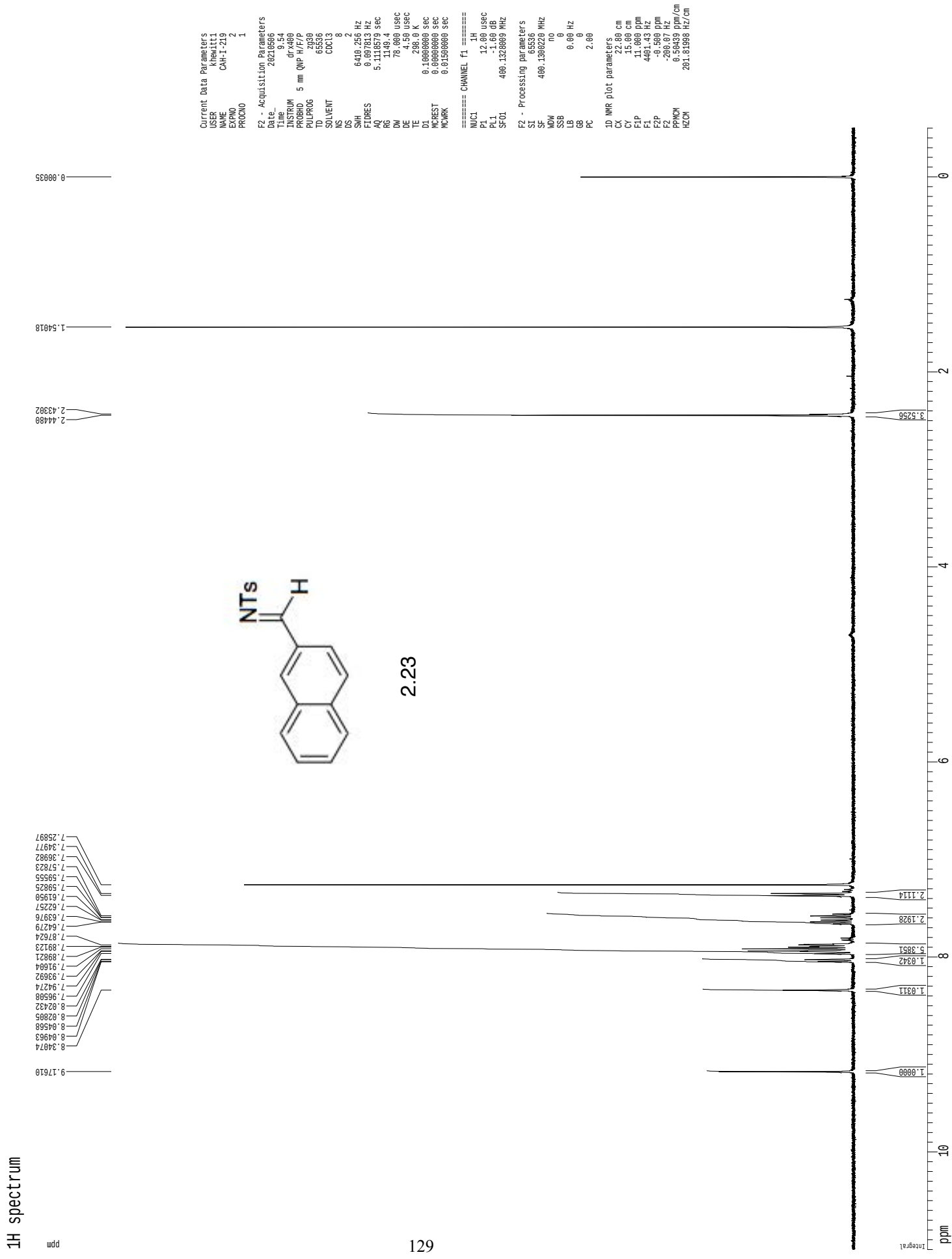
F2 - Acquisition Parameters
Date_           20210920
Time               11.09
INSTRUM            av600
PROBHD   5 mm CPBBO BB-
PULPROG          zgdc30
TD                65536
SOLVENT           CDCl3
NS                  307
DS                    4
SWH           36231.883 Hz
FIDRES         0.552855 Hz
AQ             0.9044468 sec
RG                 2050
DW               13.800 usec
DE               19.63 usec
TE                298.1 K
D1            0.40000001 sec
D11           0.03000000 sec
TD0                    1

======== CHANNEL f1 ========
SFO1         150.9194080 MHz
NUC1                 13C
P1                10.10 usec

F2 - Processing parameters
SI                 65536
SF           150.9027986 MHz
WDW                   no
SSB                    0
LB                0.00 Hz
GB                     0
PC                1.00

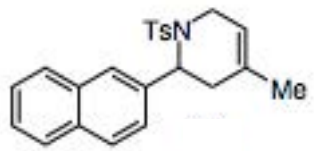
1D NMR plot parameters
CX                22.80 cm
CY                15.00 cm
F1P              230.117 ppm
F1             34725.34 Hz
F2P               -9.984 ppm
F2             -1506.54 Hz
PPMCM           10.53074 ppm/cm
HZCM          1589.11780 Hz/cm
```

ppm 200 150 100 50 0


1H spectrum
Current Data Parameters
USER khewitt1
NAME CAH-I-219
EXPNO 2
PROCNO 1
F2 - Acquisition Parameters
Date_ 20210506
Time 9.54
INSTRUM drx400
PROBHD 5 mm QNP H/F/P
PULPROG zg30
TD 65536
SOLVENT CDCl3
NS 8
DS 2
SWH 6410.256 Hz
FIDRES 0.097813 Hz
AQ 5.1118579 sec
RG 1149.4
DW 78.000 usec
DE 4.50 usec
TE 298.0 K
D1 0.10000000 sec
MCREST 0.00000000 sec
MCWRK 0.01500000 sec
======= CHANNEL f1 =======
NUC1 1H
P1 12.00 usec
PL1 -1.60 dB
SFO1 400.1328009 MHz
F2 - Processing parameters
SI 65536
SF 400.1300220 MHz
WDW no
SSB 0
LB 0.00 Hz
GB 0
PC 2.00
1D NMR plot parameters
CX 22.80 cm
CY 15.00 cm
F1P 11.000 ppm
F1 4401.43 Hz
F2P -0.500 ppm
F2 -200.07 Hz
PPMCM 0.50439 ppm/cm
HZCM 201.81998 Hz/cm
NTs
H
2.23
0.00035
1.54018
2.44180
2.43302
3.5256
2.1114
2.1928
5.3851
1.0342
1.0311
1.0000
9.17610
8.34074
8.04963
8.04568
8.02805
8.02432
7.96508
7.94274
7.93692
7.91604
7.89821
7.89123
7.87624
7.64279
7.63976
7.62257
7.61950
7.59825
7.59555
7.57823
7.36982
7.34977
7.25897
ppm
Integral

1H spectrum





2.24

130

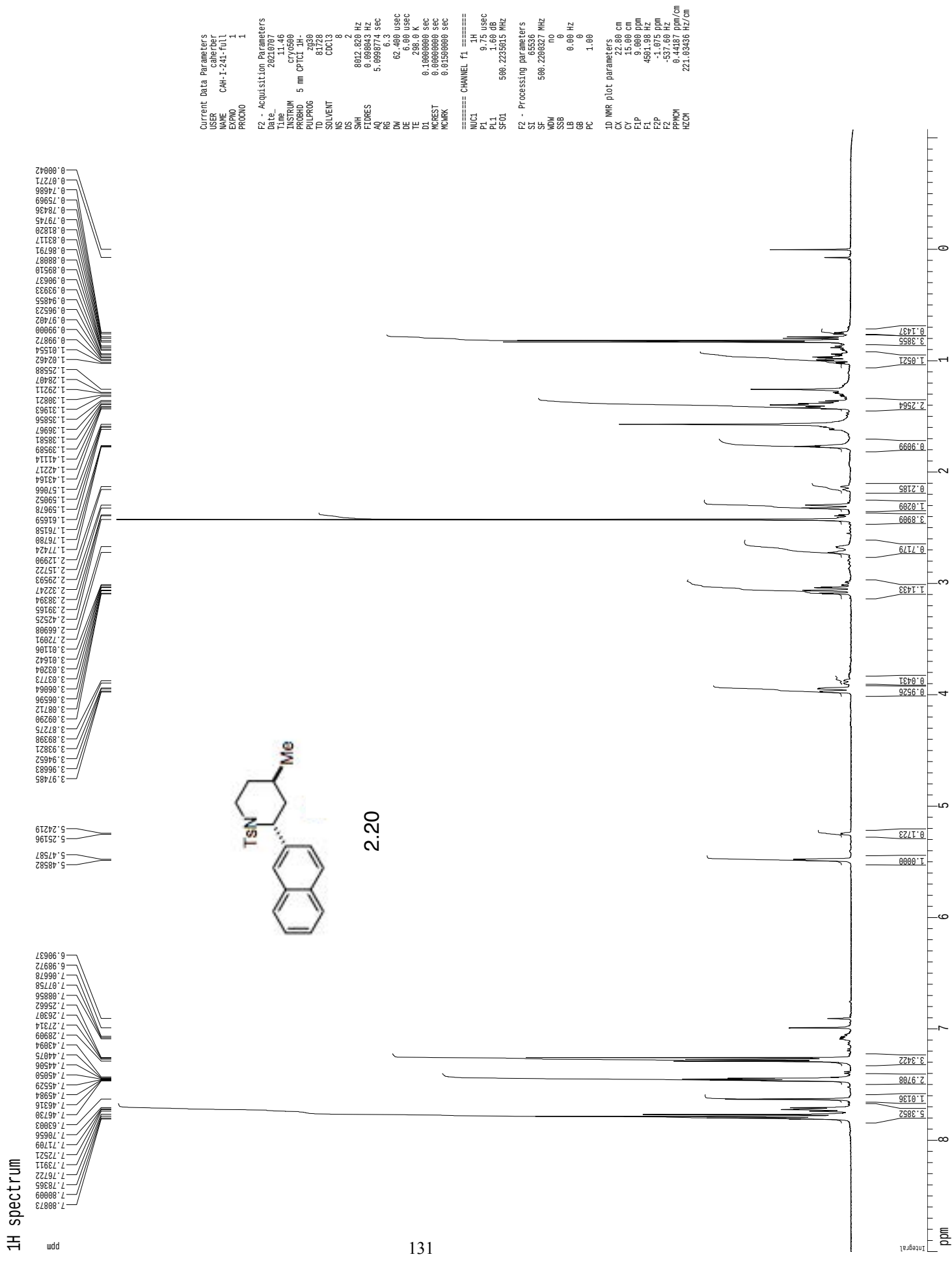
Current Data Parameters
USER caherber
NAME CAH-I-221
EXPNO 1
PROCNO 1

F2 - Acquisition Parameters
Date_ 20210525
Time 11.17
INSTRUM drx400
PROBHD 5 mm QNP H/F/P
PULPROG zg30
TD 65536
SOLVENT CDCl3
NS 8
DS 2
SWH 6410.256 Hz
FIDRES 0.097813 Hz
AQ 5.1118579 sec
RG 50.8
DW 78.000 usec
DE 4.50 usec
TE 298.0 K
D1 0.10000000 sec
MCREST 0.00000000 sec
MCWRK 0.01500000 sec

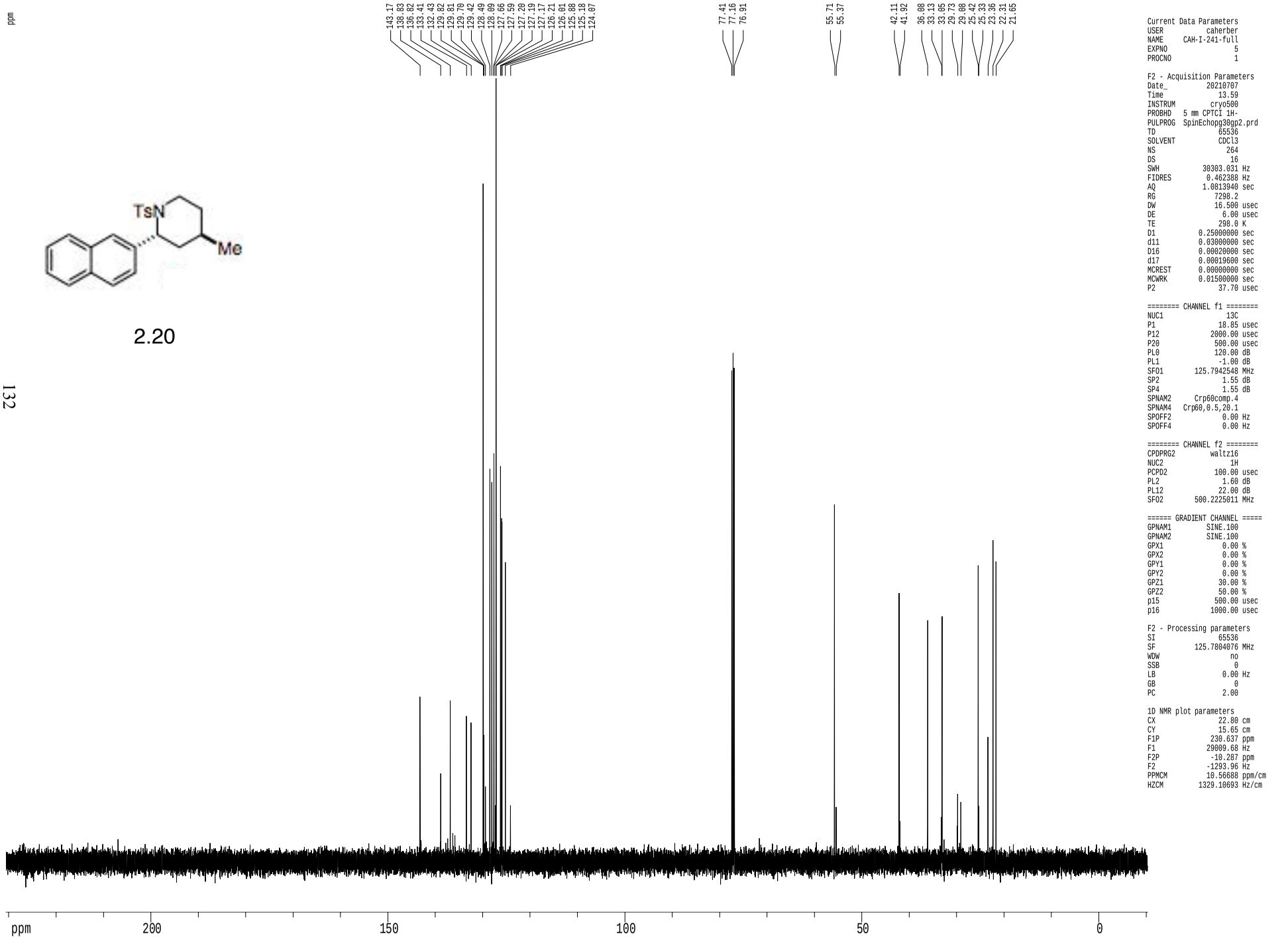
======= CHANNEL f1 =======
NUC1 1H
P1 12.00 usec
PL1 -1.60 dB
SFO1 400.1328009 MHz

F2 - Processing parameters
SI 65536
SF 400.1300333 MHz
WDW no
SSB 0
LB 0.00 Hz
GB 0
PC 2.00

1D NMR plot parameters
CX 22.80 cm
CY 15.00 cm
F1P 9.000 ppm
F1 3601.17 Hz
F2P -1.093 ppm
F2 -437.51 Hz
PPMCM 0.44269 ppm/cm
HZCM 177.13533 Hz/cm


1H spectrum
Current Data Parameters
USER caherher
NAME CAH-I-241-full
EXPNO 1
PROCNO 1
F2 - Acquisition Parameters
Date_ 20210707
Time 11.46
INSTRUM CryoQ500
PROBHD 5 mm CPTCI 1H-
PULPROG zg30
TD 81728
SOLVENT CDCl3
NS 8
DS 2
SWH 8012.820 Hz
FIDRES 0.098043 Hz
AQ 5.0998774 sec
RG 6.3
DW 62.400 usec
DE 6.00 usec
TE 298.0 K
D1 0.10000000 sec
MCREST 0.00000000 sec
MCWRK 0.01500000 sec
======= CHANNEL f1 =======
NUC1 1H
P1 9.75 usec
PL1 1.60 dB
SFO1 500.2235015 MHz
F2 - Processing parameters
SI 65536
SF 500.2200327 MHz
WDW no
SSB 0
LB 0.00 Hz
GB 0
PC 1.00
1D NMR plot parameters
CX 22.80 cm
CY 15.00 cm
F1P 9.000 ppm
F1 4501.98 Hz
F2P -1.075 ppm
F2 -537.68 Hz
PPMCM 0.44187 ppm/cm
HZCM 221.03436 Hz/cm
Me
TsN
2.20
ppm
Integral

Z-restored spin-echo 13C spectrum with 1H decoupling



Current Data Parameters
USER caherber
NAME CAH-I-241-full
EXPNO 5
PROCNO 1

F2 - Acquisition Parameters
Date_ 20210707
Time 13.59
INSTRUM cryo500
PROBHD 5 mm CPTCI 1H-
PULPROG SpinEchopg30gp2.prd
TD 65536
SOLVENT CDCl3
NS 264
DS 16
SWH 30303.031 Hz
FIDRES 0.462388 Hz
AQ 1.0813940 sec
RG 7298.2
DW 16.500 usec
DE 6.00 usec
TE 298.0 K
D1 0.25000000 sec
d11 0.03000000 sec
D16 0.00020000 sec
d17 0.00019600 sec
MCREST 0.00000000 sec
MCWRK 0.01500000 sec
P2 37.70 usec

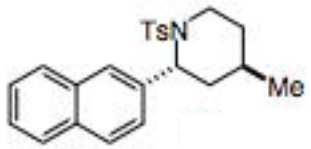
======== CHANNEL f1 ========
NUC1 13C
P1 18.85 usec
P12 2000.00 usec
P20 500.00 usec
PL0 120.00 dB
PL1 -1.00 dB
SFO1 125.7942548 MHz
SP2 1.55 dB
SP4 1.55 dB
SPNAM2 Crp60comp.4
SPNAM4 Crp60,0.5,20.1
SPOFF2 0.00 Hz
SPOFF4 0.00 Hz

======== CHANNEL f2 ========
CPDPRG2 waltz16
NUC2 1H
PCPD2 100.00 usec
PL2 1.60 dB
PL12 22.00 dB
SFO2 500.2225011 MHz

====== GRADIENT CHANNEL =====
GPNAM1 SINE.100
GPNAM2 SINE.100
GPX1 0.00 %
GPX2 0.00 %
GPY1 0.00 %
GPY2 0.00 %
GPZ1 30.00 %
GPZ2 50.00 %
p15 500.00 usec
p16 1000.00 usec

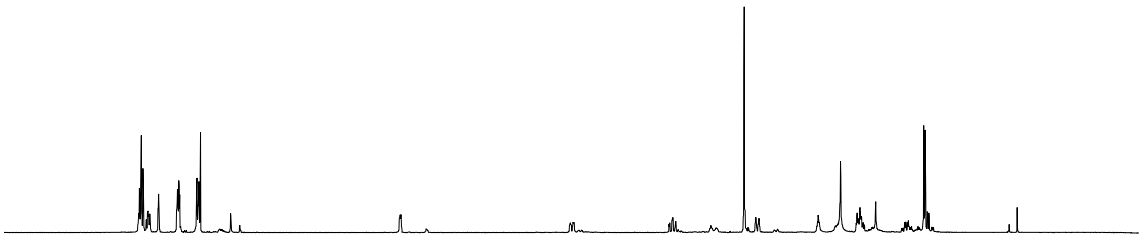
F2 - Processing parameters
SI 65536
SF 125.7804076 MHz
WDW no
SSB 0
LB 0.00 Hz
GB 0
PC 2.00

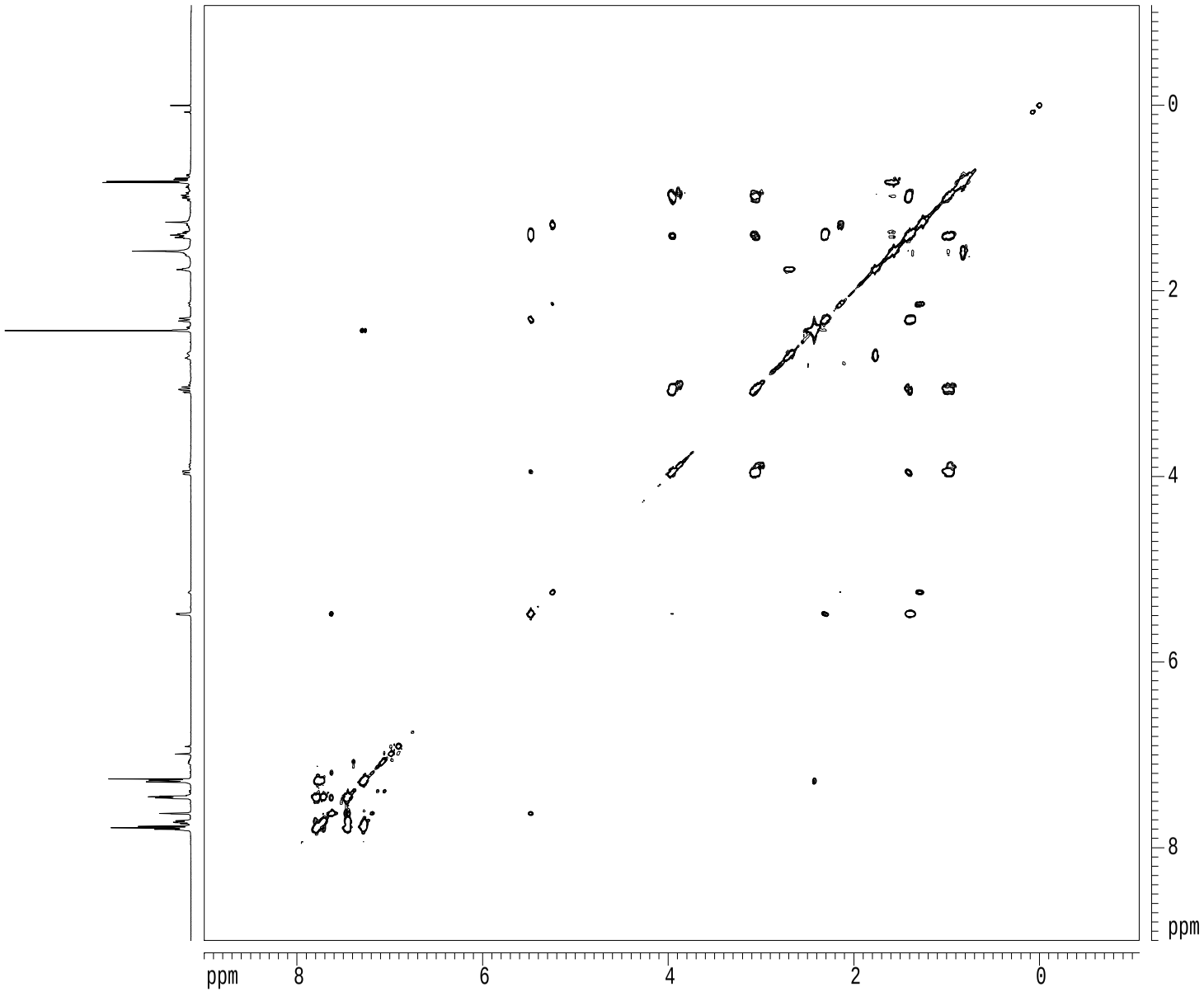
1D NMR plot parameters
CX 22.80 cm
CY 15.65 cm
F1P 230.637 ppm
F1 29009.68 Hz
F2P -10.287 ppm
F2 -1293.96 Hz
PPMCM 10.56688 ppm/cm
HZCM 1329.10693 Hz/cm



2.20

gcosy60





133

```
        Current Data Parameters
USER            caherber
NAME      CAH-I-241-full
EXPNO                  2
PROCNO                 1

      F2 - Acquisition Parameters
Date_           20210707
Time               11.49
INSTRUM          cryo500
PROBHD   5 mm CPTCI 1H-
PULPROG    cosygp60.prd
TD                  2048
SOLVENT            CDCl3
NS                     1
DS                    16
SWH             8012.820 Hz
FIDRES             3.912510 Hz
AQ              0.1278452 sec
RG                 143.7
DW                62.400 usec
DE                 6.00 usec
TE                298.0 K
d0             0.00000300 sec
D1             1.00000000 sec
d13            0.00000300 sec
D16            0.00020000 sec
IN0            0.00012480 sec

     ======== CHANNEL f1 ========
NUC1                  1H
P1                 9.75 usec
PL1                1.60 dB
SF01         500.2235015 MHz

     ====== GRADIENT CHANNEL =====
GPNAM1        SMSQ10.100
GPNAM2        SMSQ10.100
GPX1               0.00 %
GPX2               0.00 %
GPY1               0.00 %
GPY2               0.00 %
GPZ1              17.00 %
GPZ2              17.00 %
P16             1000.00 usec

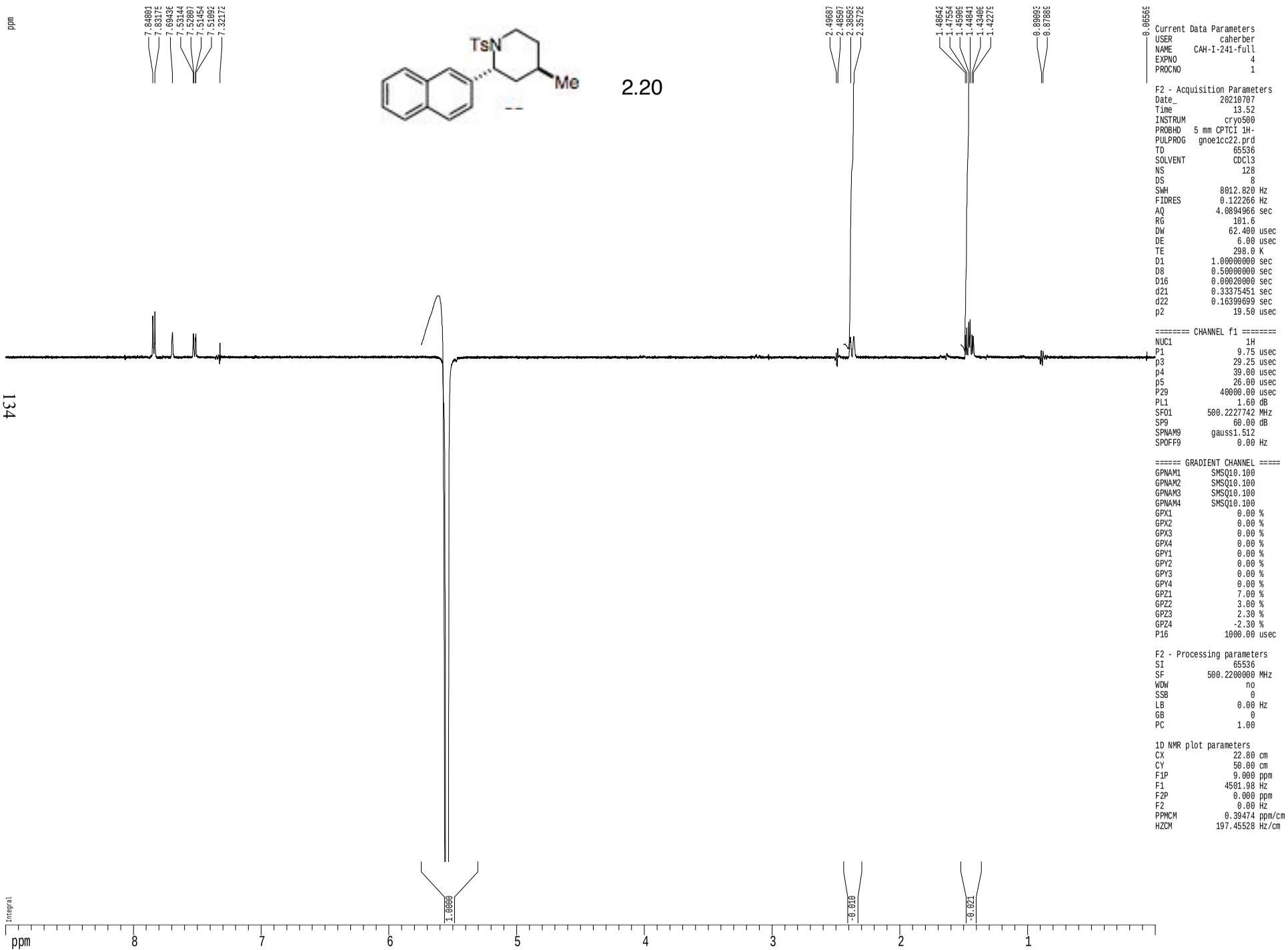
      F1 - Acquisition parameters
ND0                    1
TD                   512
SF01           500.2235 MHz
FIDRES         15.650040 Hz
SW               16.018 ppm
FnMODE                QF

      F2 - Processing parameters
SI                  1024
SF           500.2200327 MHz
WDW                 SINE
SSB                    0
LB                 0.00 Hz
GB                     0
PC                  1.00

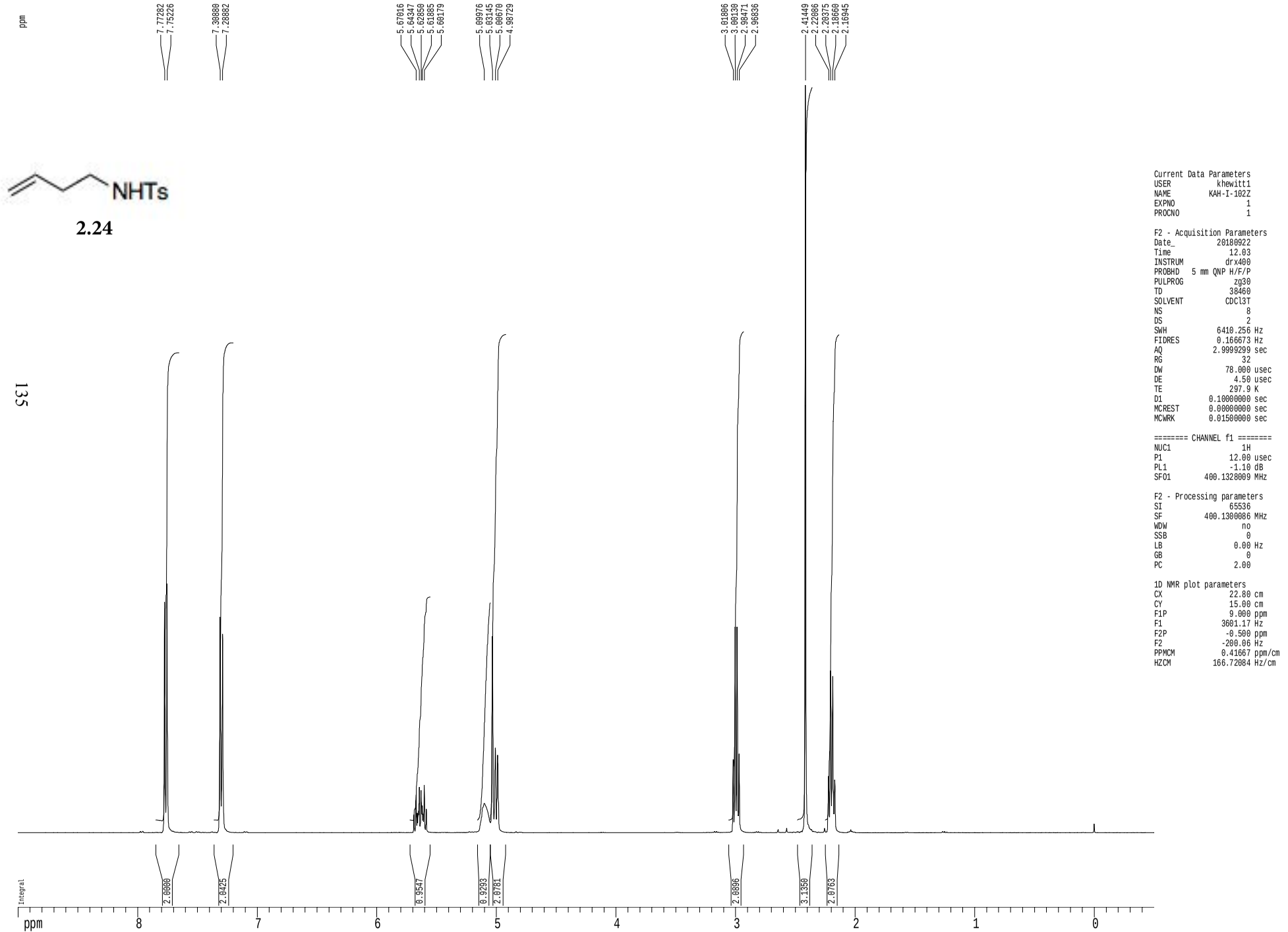
      F1 - Processing parameters
SI                  1024
MC2                   QF
SF           500.2200327 MHz
WDW                 SINE
SSB                    0
LB                 0.00 Hz
GB                     0

        2D NMR plot parameters
CX2               15.00 cm
CX1               15.00 cm
F2PLO             9.000 ppm
F2LO            4501.98 Hz
F2PHI            -1.075 ppm
F2HI             -537.60 Hz
F1PLO             9.000 ppm
F1LO            4501.98 Hz
F1PHI            -1.075 ppm
F1HI             -537.60 Hz
F2PPMCM          0.67165 ppm/cm
F2HZCM         335.97217 Hz/cm
F1PPMCM          0.67165 ppm/cm
F1HZCM         335.97217 Hz/cm
```

gnoe


ppm
7.84881
7.83175
7.69436
7.53144
7.52807
7.51454
7.51092
7.32172
TsN
Me
2.20
2.49687
2.48567
2.38583
2.35728
1.48642
1.47554
1.45985
1.44841
1.43406
1.42279
0.89093
0.87886
0.06568
Current Data Parameters
USER caherber
NAME CAH-I-241-full
EXPNO 4
PROCNO 1
F2 - Acquisition Parameters
Date_ 20210707
Time 13.52
INSTRUM cryo500
PROBHD 5 mm CPTCI 1H-
PULPROG gnoe1cc22.prd
TD 65536
SOLVENT CDCl3
NS 128
DS 8
SWH 8012.820 Hz
FIDRES 0.122266 Hz
AQ 4.0894966 sec
RG 101.6
DW 62.400 usec
DE 6.00 usec
TE 298.0 K
D1 1.00000000 sec
D8 0.50000000 sec
D16 0.00020000 sec
d21 0.33375451 sec
d22 0.16399699 sec
p2 19.50 usec
======= CHANNEL f1 =======
NUC1 1H
P1 9.75 usec
p3 29.25 usec
p4 39.00 usec
p5 26.00 usec
P29 40000.00 usec
PL1 1.60 dB
SFO1 500.2227742 MHz
SP9 60.00 dB
SPNAM9 gauss1.512
SPOFF9 0.00 Hz
===== GRADIENT CHANNEL ====
GPNAM1 SMSQ10.100
GPNAM2 SMSQ10.100
GPNAM3 SMSQ10.100
GPNAM4 SMSQ10.100
GPX1 0.00 %
GPX2 0.00 %
GPX3 0.00 %
GPX4 0.00 %
GPY1 0.00 %
GPY2 0.00 %
GPY3 0.00 %
GPY4 0.00 %
GPZ1 7.00 %
GPZ2 3.00 %
GPZ3 2.30 %
GPZ4 -2.30 %
P16 1000.00 usec
F2 - Processing parameters
SI 65536
SF 500.2200000 MHz
WDW no
SSB 0
LB 0.00 Hz
GB 0
PC 1.00
1D NMR plot parameters
CX 22.80 cm
CY 50.00 cm
F1P 9.000 ppm
F1 4501.98 Hz
F2P 0.000 ppm
F2 0.00 Hz
PPMCM 0.39474 ppm/cm
HZCM 197.45528 Hz/cm
Integral
1.0000
0.810
0.821
ppm
8
7
6
5
4
3
2
1

1H spectrum



2.24

135

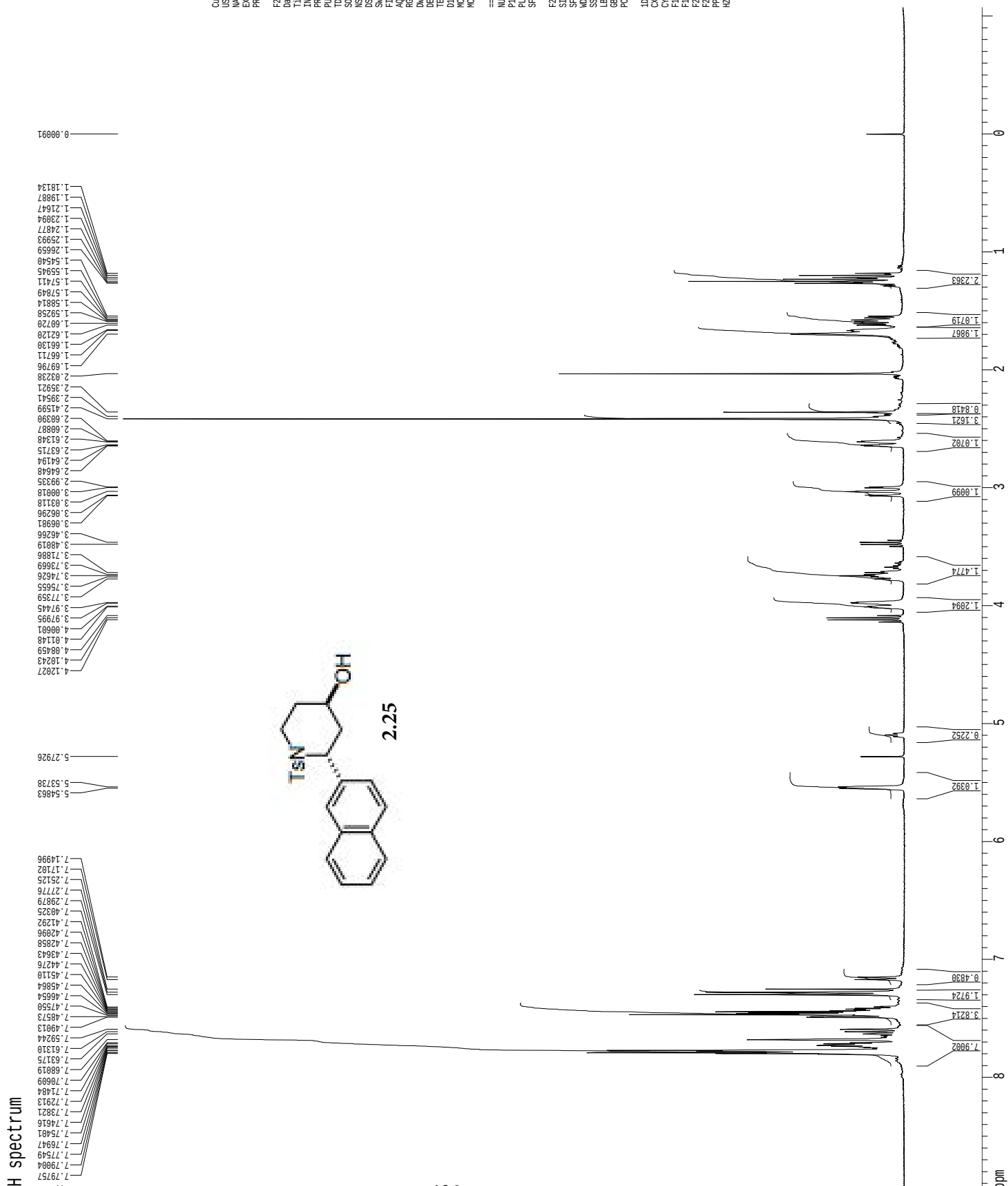
```
Current Data Parameters
USER            khewitt1
NAME          KAH-I-102Z
EXPNO                  1
PROCNO                 1

F2 - Acquisition Parameters
Date_           20180922
Time               12.03
INSTRUM          drx400
PROBHD   5 mm QNP H/F/P
PULPROG            zg30
TD                38460
SOLVENT           CDCl3T
NS                     8
DS                     2
SWH            6410.256 Hz
FIDRES        0.166673 Hz
AQ            2.9999299 sec
RG                    32
DW               78.000 usec
DE                4.50 usec
TE                297.9 K
D1           0.10000000 sec
MCREST       0.00000000 sec
MCWRK        0.01500000 sec

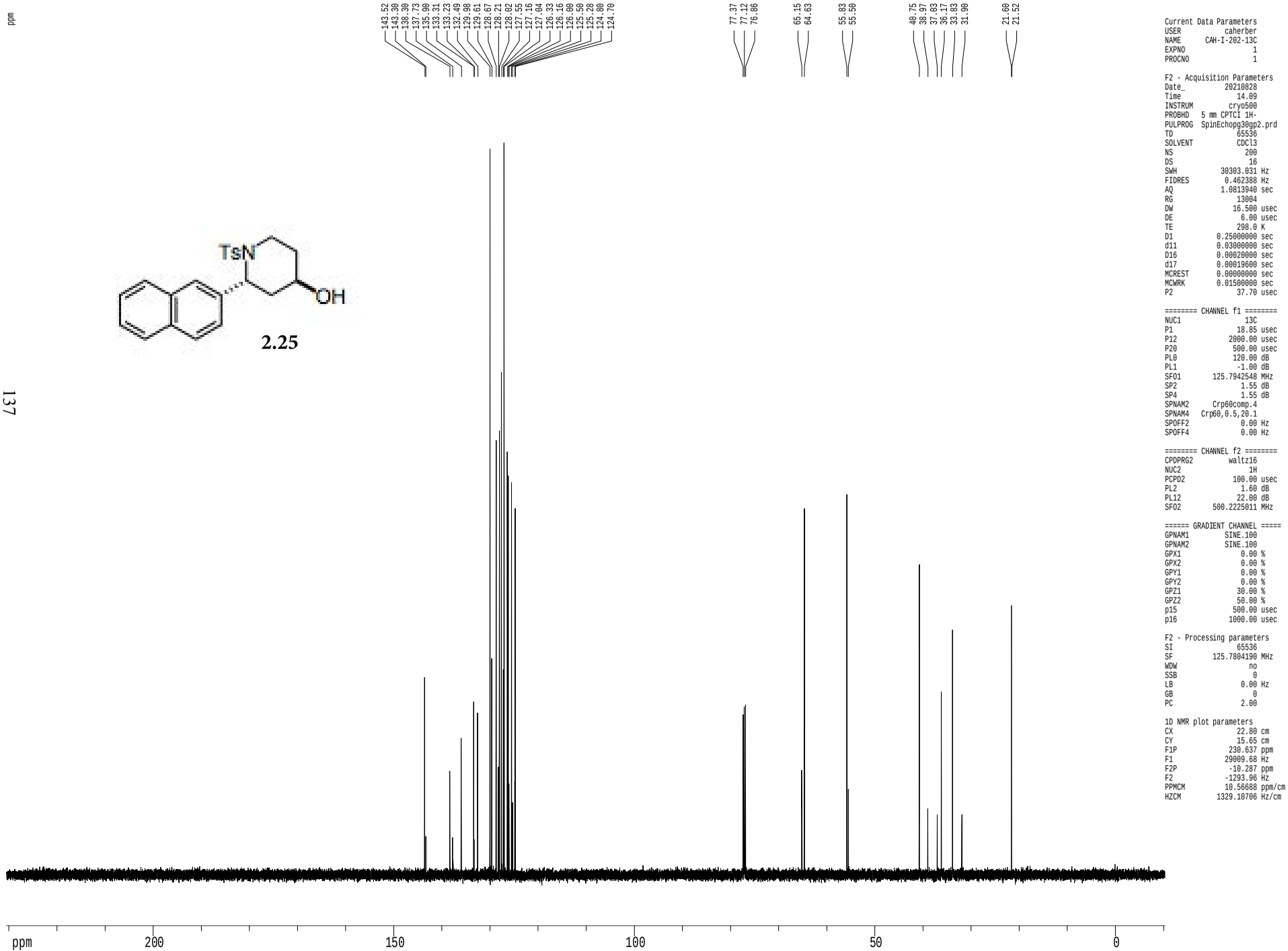
======= CHANNEL f1 =======
NUC1                  1H
P1               12.00 usec
PL1              -1.10 dB
SFO1        400.1328009 MHz

F2 - Processing parameters
SI                 65536
SF          400.1300086 MHz
WDW                   no
SSB                    0
LB                0.00 Hz
GB                     0
PC                2.00

1D NMR plot parameters
CX                22.80 cm
CY                15.00 cm
F1P               9.000 ppm
F1              3601.17 Hz
F2P              -0.500 ppm
F2              -200.06 Hz
PPMCM           0.41667 ppm/cm
HZCM          166.72084 Hz/cm
```


1H spectrum
Current Data Parameters
USER caherher
NAME CAH-I-201
EXPNO 1
PROCNO 1
F2 - Acquisition Parameters
Date_ 20210330
Time 18.04
INSTRUM dr'400
PROBHD 5 mm QNP H/F/P
PULPROG zg30
TD 65536
SOLVENT CDCl3
NS 8
DS 2
SWH 6410.256 Hz
FIDRES 0.097813 Hz
AQ 5.1118579 sec
RG 128
DW 78.000 usec
DE 4.50 usec
TE 298.0 K
D1 0.10000000 sec
MCREST 0.00000000 sec
MCWRK 0.01500000 sec
======= CHANNEL f1 =======
NUC1 1H
P1 12.00 usec
PL1 -1.60 dB
SFO1 400.1328009 MHz
F2 - Processing parameters
SI 65536
SF 400.1300245 MHz
WDW no
SSB 0
LB 0.00 Hz
GB 0
PC 2.00
1D NMR plot parameters
CX 22.80 cm
CY 15.00 cm
F1P 9.000 ppm
F1 3601.17 Hz
F2P -1.071 ppm
F2 -428.71 Hz
PPMCM 0.44173 ppm/cm
HZCM 176.74925 Hz/cm
TsN
OH
2.25
ppm
Integral

Z-restored spin-echo 13C spectrum with 1H decoupling



Current Data Parameters
USER caherber
NAME CAH-I-202-13C
EXPNO 1
PROCNO 1

F2 - Acquisition Parameters
Date_ 20210828
Time 14.09
INSTRUM cryo500
PROBHD 5 mm CPTCI 1H-
PULPROG SpinEchopg30gp2.prd
TD 65536
SOLVENT CDCl3
NS 200
DS 16
SWH 30303.031 Hz
FIDRES 0.462388 Hz
AQ 1.0813940 sec
RG 13004
DW 16.500 usec
DE 6.00 usec
TE 298.0 K
D1 0.25000000 sec
d11 0.03000000 sec
D16 0.00020000 sec
d17 0.00019600 sec
MCREST 0.00000000 sec
MCWRK 0.01500000 sec
P2 37.70 usec

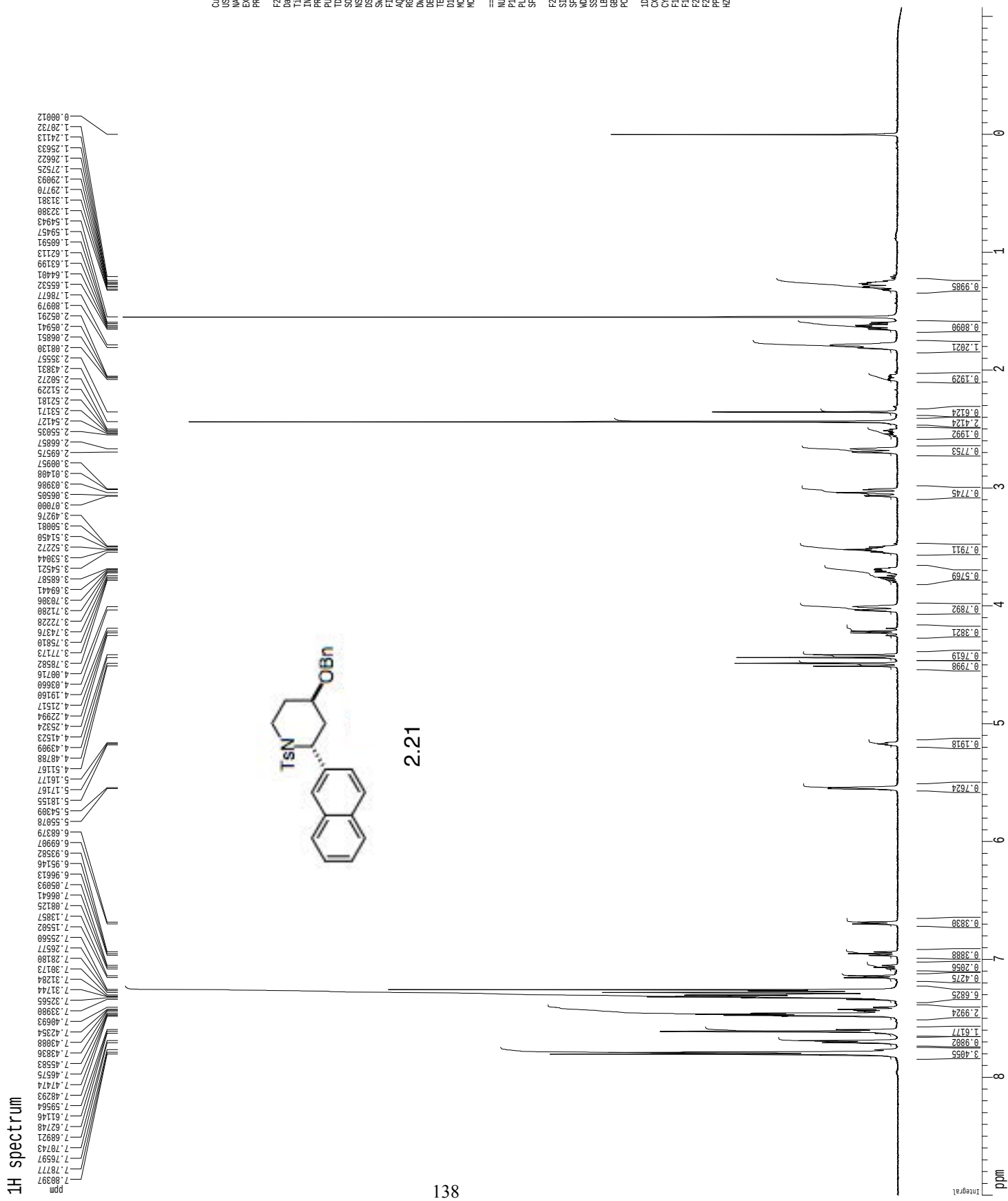
======== CHANNEL f1 ========
NUC1 13C
P1 18.85 usec
P12 2000.00 usec
P20 500.00 usec
PL0 120.00 dB
PL1 -1.00 dB
SFO1 125.7942548 MHz
SP2 1.55 dB
SP4 1.55 dB
SPNAM2 Crp60comp.4
SPNAM4 Crp60,0.5,20.1
SPOFF2 0.00 Hz
SPOFF4 0.00 Hz

======== CHANNEL f2 ========
CPDPRG2 waltz16
NUC2 1H
PCPD2 100.00 usec
PL2 1.60 dB
PL12 22.00 dB
SFO2 500.2225011 MHz

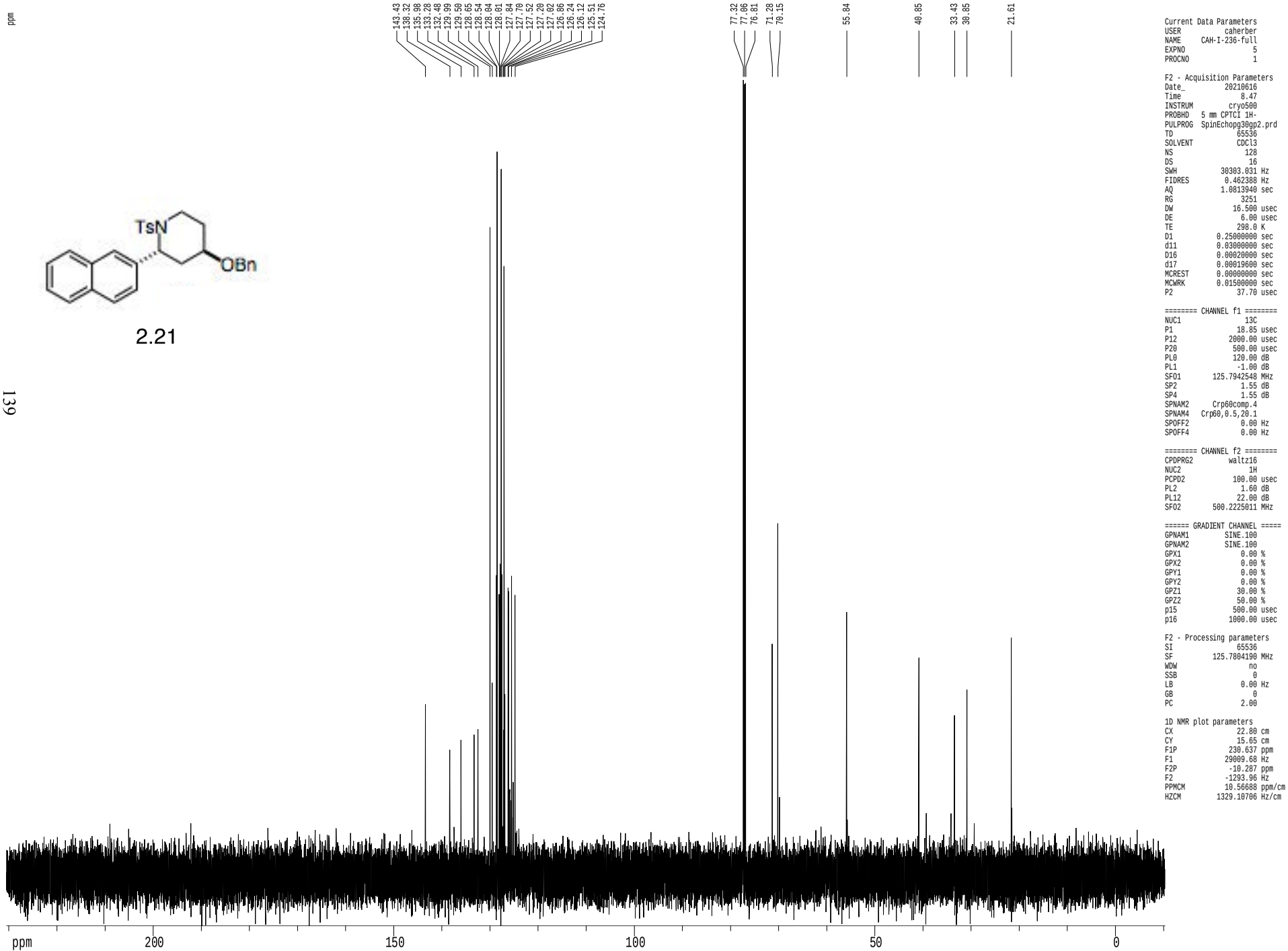
====== GRADIENT CHANNEL =====
GPNAM1 SINE.100
GPNAM2 SINE.100
GPX1 0.00 %
GPX2 0.00 %
GPY1 0.00 %
GPY2 0.00 %
GPZ1 30.00 %
GPZ2 50.00 %
p15 500.00 usec
p16 1000.00 usec

F2 - Processing parameters
SI 65536
SF 125.7804190 MHz
WDW no
SSB 0
LB 0.00 Hz
GB 0
PC 2.00

1D NMR plot parameters
CX 22.80 cm
CY 15.65 cm
F1P 230.637 ppm
F1 29009.68 Hz
F2P -10.287 ppm
F2 -1293.96 Hz
PPMCM 10.56688 ppm/cm
HZCM 1329.10706 Hz/cm


1H spectrum
Current Data Parameters
USER caherher
NAME CAH-I-236-full
EXPNO 1
PROCNO 1
F2 - Acquisition Parameters
Date_ 20210616
Time 7.56
INSTRUM cryo500
PROBHD 5 mm CPTCI 1H-
PULPROG zg30
TD 48074
SOLVENT CDCl3
NS 8
DS 2
SWH 8012.820 Hz
FIDRES 0.166677 Hz
AQ 2.9998677 sec
RG 5.7
DW 62.400 usec
DE 6.00 usec
TE 298.0 K
D1 0.10000000 sec
MCREST 0.00000000 sec
MCWRK 0.01500000 sec
======== CHANNEL f1 ========
NUC1 1H
P1 9.75 usec
PL1 1.60 dB
SFO1 500.2235015 MHz
F2 - Processing parameters
SI 65536
SF 500.2200329 MHz
WDW no
SSB 0
LB 0.00 Hz
GB 0
PC 1.00
1D NMR plot parameters
CX 22.80 cm
CY 15.00 cm
F1P 9.000 ppm
F1 4501.98 Hz
F2P -1.075 ppm
F2 -537.73 Hz
PPMCM 0.44189 ppm/cm
HZCM 221.03986 Hz/cm
TsN
OBn
2.21
ppm
Integral

Z-restored spin-echo 13C spectrum with 1H decoupling



Current Data Parameters
USER caherber
NAME CAH-I-236-full
EXPNO 5
PROCNO 1

F2 - Acquisition Parameters
Date_ 20210616
Time 8.47
INSTRUM cryo500
PROBHD 5 mm CPTCI 1H-
PULPROG SpinEchopg30gp2.prd
TD 65536
SOLVENT CDCl3
NS 128
DS 16
SWH 30303.031 Hz
FIDRES 0.462388 Hz
AQ 1.0813940 sec
RG 3251
DW 16.500 usec
DE 6.00 usec
TE 298.0 K
D1 0.25000000 sec
d11 0.03000000 sec
D16 0.00020000 sec
d17 0.00019600 sec
MCREST 0.00000000 sec
MCWRK 0.01500000 sec
P2 37.70 usec

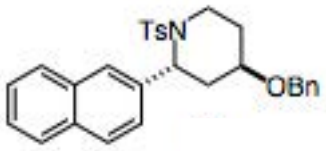
======== CHANNEL f1 ========
NUC1 13C
P1 18.85 usec
P12 2000.00 usec
P20 500.00 usec
PL0 120.00 dB
PL1 -1.00 dB
SFO1 125.7942548 MHz
SP2 1.55 dB
SP4 1.55 dB
SPNAM2 Crp60comp.4
SPNAM4 Crp60,0.5,20.1
SPOFF2 0.00 Hz
SPOFF4 0.00 Hz

======== CHANNEL f2 ========
CPDPRG2 waltz16
NUC2 1H
PCPD2 100.00 usec
PL2 1.60 dB
PL12 22.00 dB
SFO2 500.2225011 MHz

====== GRADIENT CHANNEL =====
GPNAM1 SINE.100
GPNAM2 SINE.100
GPX1 0.00 %
GPX2 0.00 %
GPY1 0.00 %
GPY2 0.00 %
GPZ1 30.00 %
GPZ2 50.00 %
p15 500.00 usec
p16 1000.00 usec

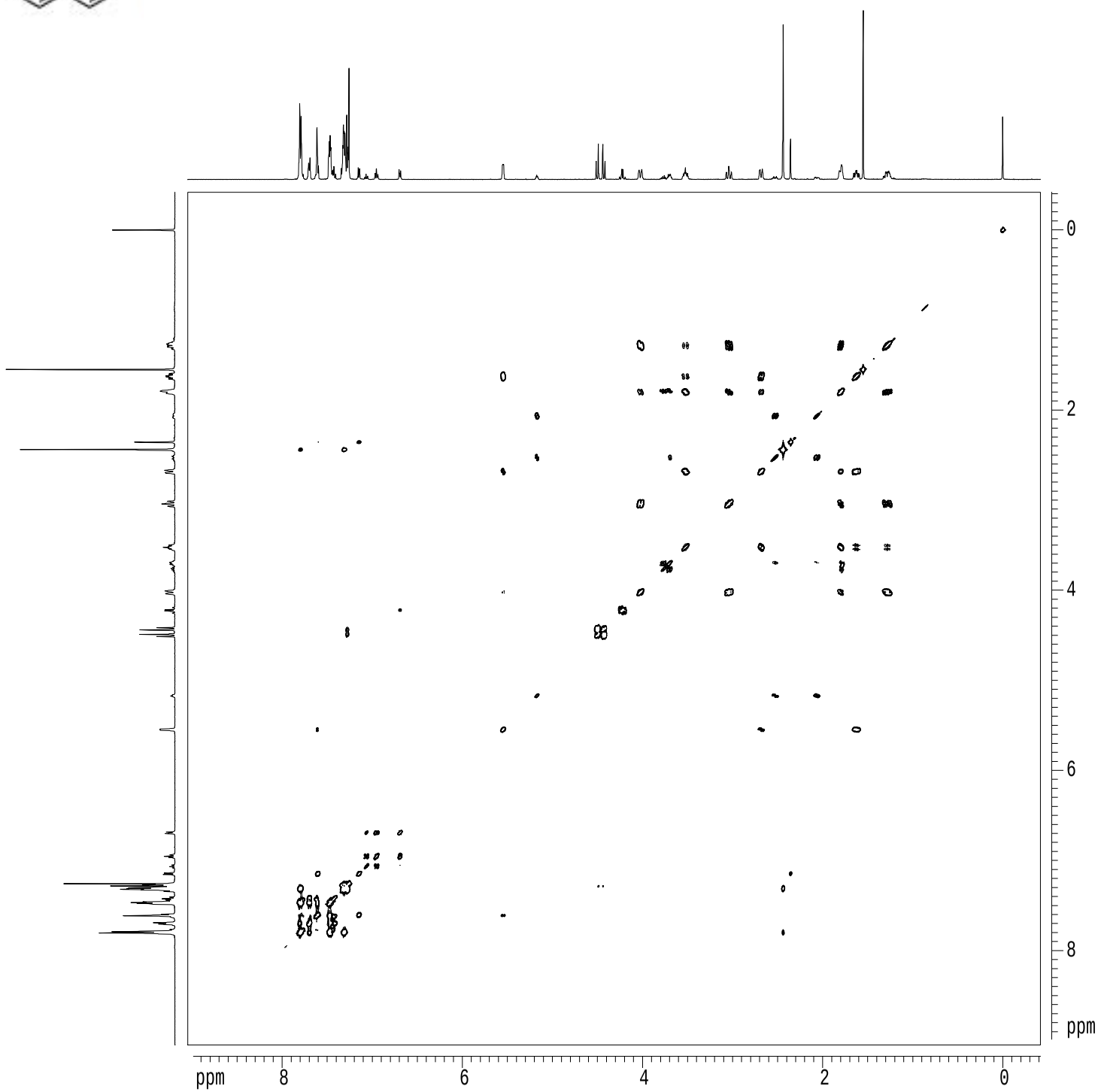
F2 - Processing parameters
SI 65536
SF 125.7804190 MHz
WDW no
SSB 0
LB 0.00 Hz
GB 0
PC 2.00

1D NMR plot parameters
CX 22.80 cm
CY 15.65 cm
F1P 230.637 ppm
F1 29009.68 Hz
F2P -10.287 ppm
F2 -1293.96 Hz
PPMCM 10.56688 ppm/cm
HZCM 1329.10706 Hz/cm



2.21

gcosy60



Current Data Parameters

USER	caherber
NAME	CAH-I-236-full
EXPNO	2
PROCNO	1

F2 - Acquisition Parameters

Date_	20210616
Time	8.03
INSTRUM	cryo500
PROBHD	5 mm CPTCI 1H-
PULPROG	cosygp60.prd
TD	2048
SOLVENT	CDCl3
NS	1
DS	16
SWH	4734.849 Hz
FIDRES	2.311938 Hz
AQ	0.2163188 sec
RG	322.5
DW	105.600 usec
DE	6.00 usec
TE	298.0 K
d0	0.00000300 sec
D1	1.00000000 sec
d13	0.00000300 sec
D16	0.00020000 sec
IN0	0.00021120 sec

======== CHANNEL f1 ========

NUC1	1H
P1	9.75 usec
PL1	1.60 dB
SFO1	500.2221588 MHz

====== GRADIENT CHANNEL =====

GPNAM1	SMSQ10.100
GPNAM2	SMSQ10.100
GPX1	0.00 %
GPX2	0.00 %
GPY1	0.00 %
GPY2	0.00 %
GPZ1	17.00 %
GPZ2	17.00 %
P16	1000.00 usec

F1 - Acquisition parameters

ND0	1
TD	512
SFO1	500.2222 MHz
FIDRES	9.247751 Hz
SW	9.465 ppm
FnMODE	QF

F2 - Processing parameters

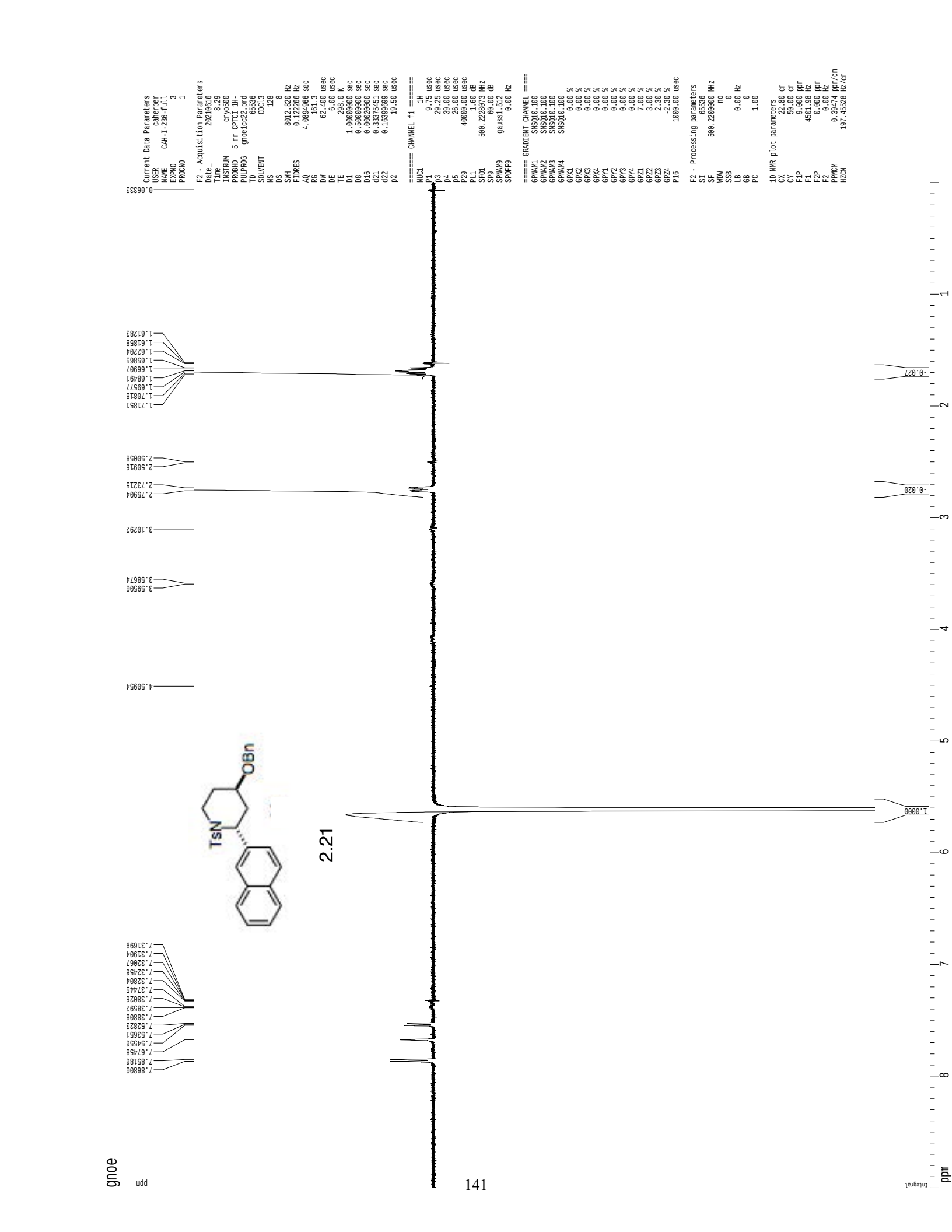
SI	1024
SF	500.2200329 MHz
WDW	SINE
SSB	0
LB	0.00 Hz
GB	0
PC	1.00

F1 - Processing parameters

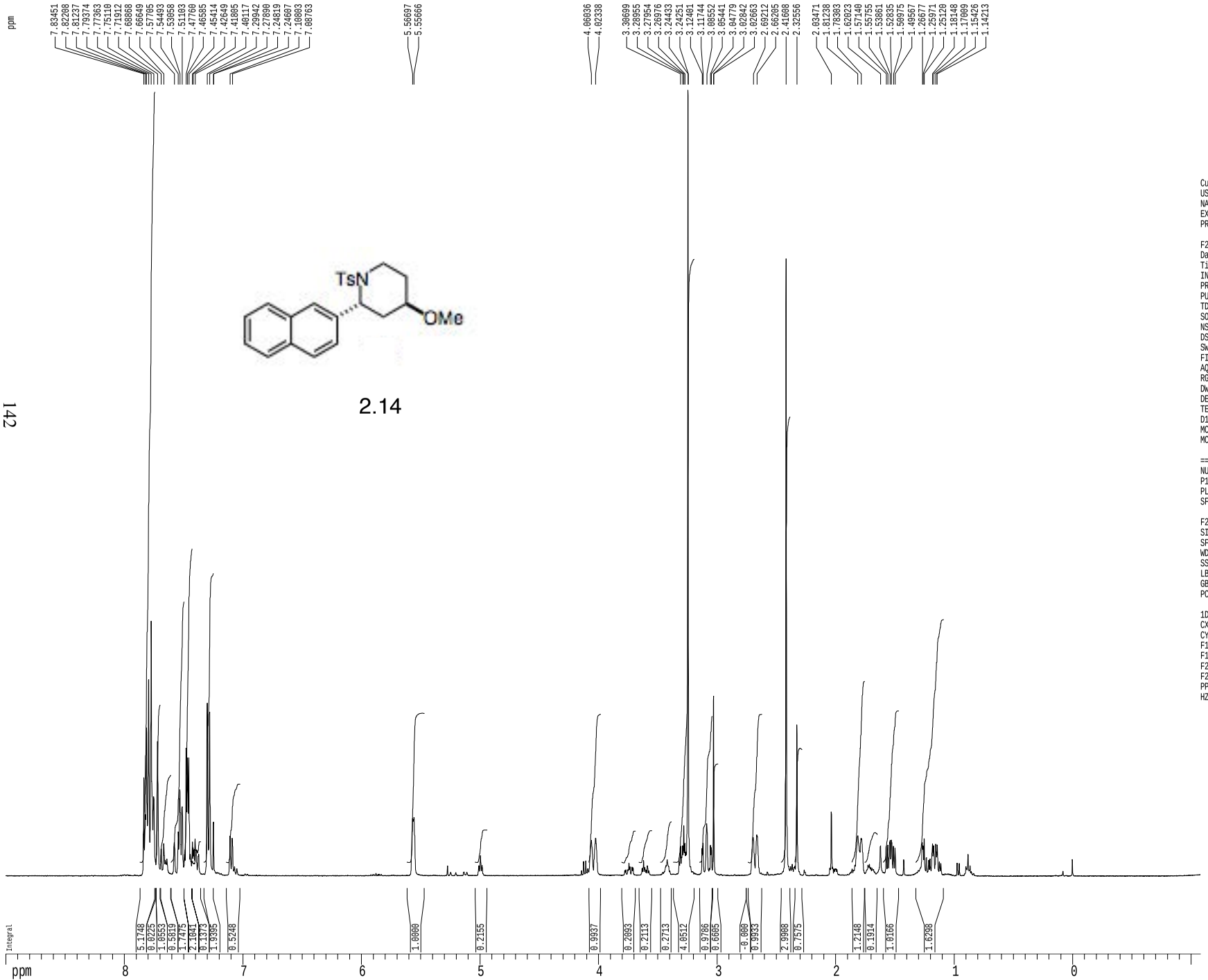
SI	1024
MC2	QF
SF	500.2200329 MHz
WDW	SINE
SSB	0
LB	0.00 Hz
GB	0

2D NMR plot parameters

CX2	15.00 cm
CX1	15.00 cm
F2PLO	9.048 ppm
F2LO	4526.21 Hz
F2PHI	-0.417 ppm
F2HI	-208.63 Hz
F1PLO	9.048 ppm
F1LO	4526.21 Hz
F1PHI	-0.417 ppm
F1HI	-208.63 Hz
F2PPMCM	0.63104 ppm/cm
F2HZCM	315.65659 Hz/cm
F1PPMCM	0.63104 ppm/cm
F1HZCM	315.65659 Hz/cm


gnoe
ppm
2.21
OBn
TsN
Integral

1H spectrum




```
Current Data Parameters
USER            caherber
NAME            CAH-I-209
EXPNO                   1
PROCNO                  1

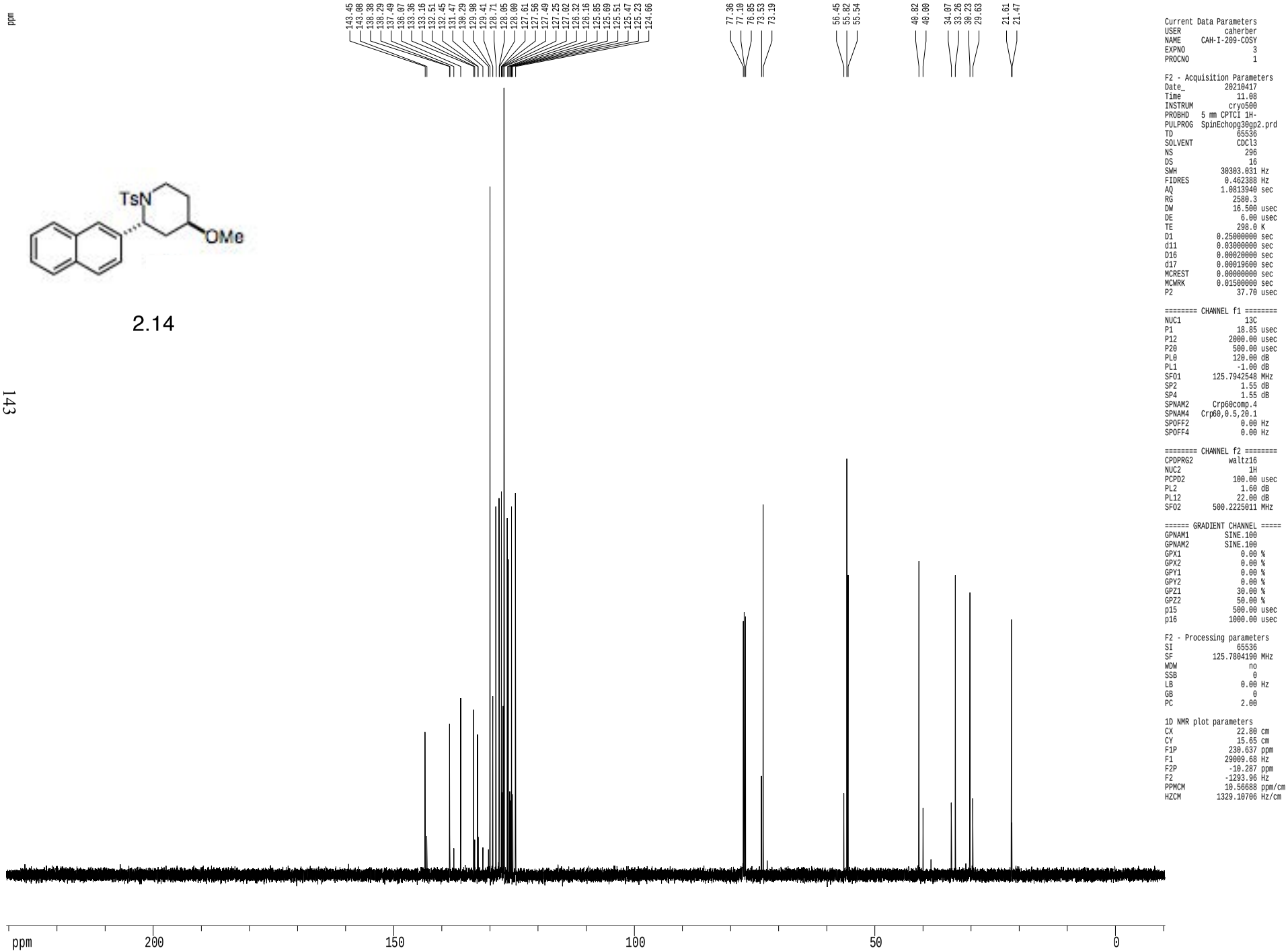
F2 - Acquisition Parameters
Date_            20210415
Time                17.05
INSTRUM           drx400
PROBHD   5 mm QNP H/F/P
PULPROG              zg30
TD                  65536
SOLVENT             CDCl3
NS                      8
DS                      2
SWH              6410.256 Hz
FIDRES           0.097813 Hz
AQ               5.1118579 sec
RG                    114
DW                 78.000 usec
DE                  4.50 usec
TE                 298.0 K
D1              0.10000000 sec
MCREST          0.00000000 sec
MCWRK           0.01500000 sec

======= CHANNEL f1 =======
NUC1                   1H
P1                 12.00 usec
PL1                -1.60 dB
SFO1         400.1328009 MHz

F2 - Processing parameters
SI                  65536
SF           400.1300267 MHz
WDW                    no
SSB                     0
LB                 0.00 Hz
GB                      0
PC                 2.00

1D NMR plot parameters
CX                 22.80 cm
CY                 15.00 cm
F1P                9.000 ppm
F1               3601.17 Hz
F2P               -1.077 ppm
F2               -430.96 Hz
PPMCM            0.44198 ppm/cm
HZCM           176.84787 Hz/cm
```

Z-restored spin-echo 13C spectrum with 1H decoupling




```
Current Data Parameters
USER            caherber
NAME      CAH-I-209-COSY
EXPNO                  3
PROCNO                 1

F2 - Acquisition Parameters
Date_           20210417
Time              11.08
INSTRUM          cryo500
PROBHD   5 mm CPTCI 1H-
PULPROG  SpinEchopg30gp2.prd
TD                65536
SOLVENT           CDCl3
NS                  296
DS                   16
SWH           30303.031 Hz
FIDRES         0.462388 Hz
AQ             1.0813940 sec
RG                2580.3
DW                16.500 usec
DE                 6.00 usec
TE                298.0 K
D1           0.25000000 sec
d11          0.03000000 sec
D16          0.00020000 sec
d17          0.00019600 sec
MCREST       0.00000000 sec
MCWRK        0.01500000 sec
P2                37.70 usec

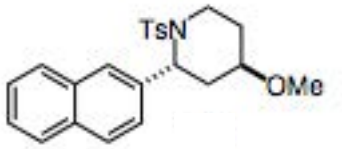
======== CHANNEL f1 ========
NUC1                13C
P1                18.85 usec
P12             2000.00 usec
P20              500.00 usec
PL0              120.00 dB
PL1               -1.00 dB
SFO1        125.7942548 MHz
SP2               1.55 dB
SP4               1.55 dB
SPNAM2      Crp60comp.4
SPNAM4   Crp60,0.5,20.1
SPOFF2               0.00 Hz
SPOFF4               0.00 Hz

======== CHANNEL f2 ========
CPDPRG2          waltz16
NUC2                1H
PCPD2            100.00 usec
PL2                1.60 dB
PL12              22.00 dB
SFO2        500.2225011 MHz

====== GRADIENT CHANNEL =====
GPNAM1         SINE.100
GPNAM2         SINE.100
GPX1               0.00 %
GPX2               0.00 %
GPY1               0.00 %
GPY2               0.00 %
GPZ1              30.00 %
GPZ2              50.00 %
p15              500.00 usec
p16             1000.00 usec

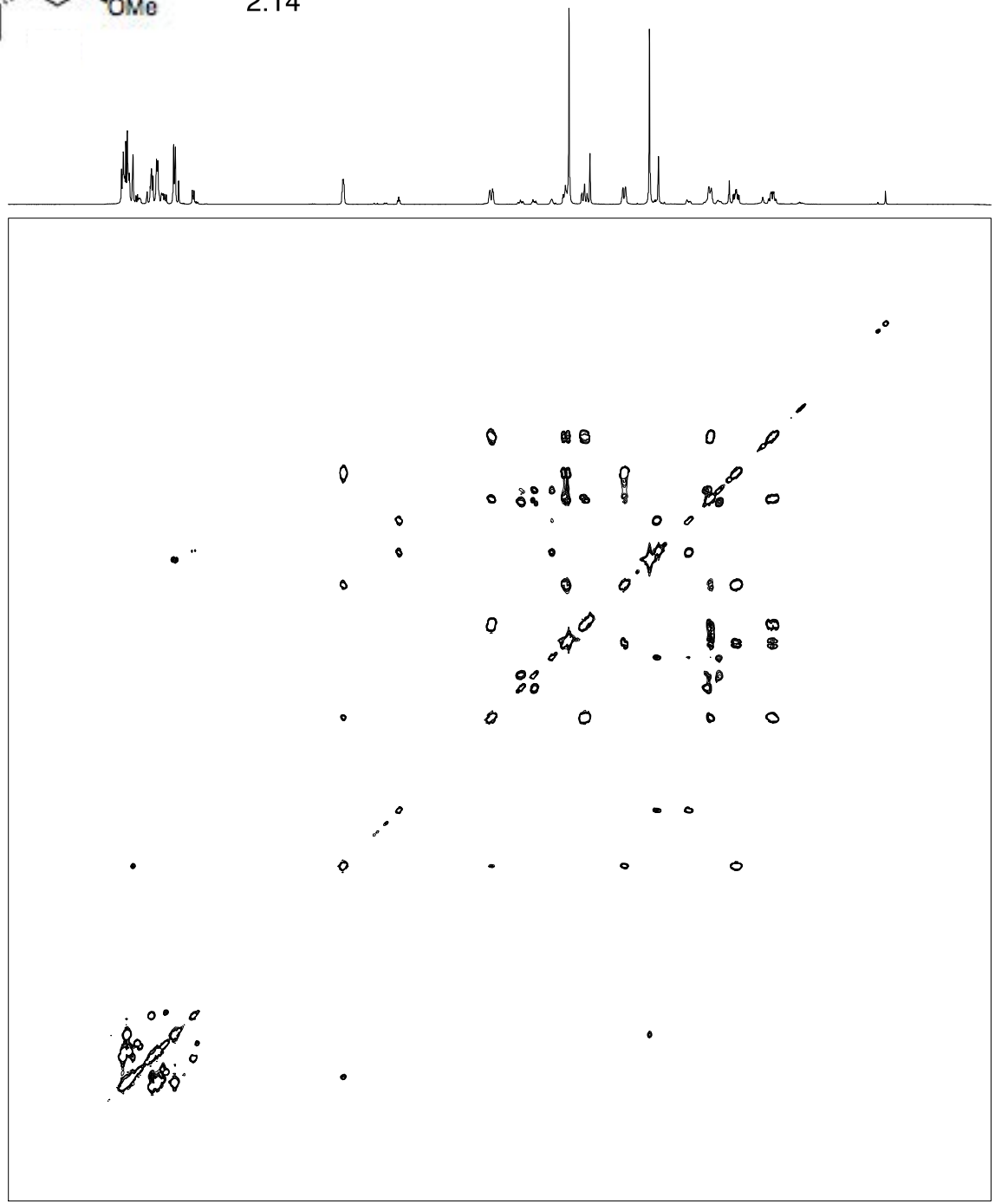
F2 - Processing parameters
SI                 65536
SF          125.7804190 MHz
WDW                   no
SSB                    0
LB                 0.00 Hz
GB                     0
PC                 2.00

1D NMR plot parameters
CX                22.80 cm
CY                15.65 cm
F1P             230.637 ppm
F1             29009.68 Hz
F2P             -10.287 ppm
F2             -1293.96 Hz
PPMCM          10.56688 ppm/cm
HZCM         1329.10706 Hz/cm
```



2.14

gcosy60



144

```
        Current Data Parameters
USER            caherber
NAME      CAH-I-209-COSY
EXPNO                  2
PROCNO                 1

      F2 - Acquisition Parameters
Date_           20210417
Time              10.51
INSTRUM         cryo500
PROBHD   5 mm CPTCI 1H-
PULPROG    cosygp60.prd
TD                 2048
SOLVENT           CDCl3
NS                    1
DS                   16
SWH            8012.820 Hz
FIDRES         3.912510 Hz
AQ             0.1278452 sec
RG                 35.9
DW               62.400 usec
DE                6.00 usec
TE               298.0 K
d0            0.00000300 sec
D1            1.00000000 sec
d13           0.00000300 sec
D16           0.00020000 sec
IN0           0.00012480 sec

     ======== CHANNEL f1 ========
NUC1                 1H
P1                 9.75 usec
PL1                1.60 dB
SF01        500.2235015 MHz

     ====== GRADIENT CHANNEL =====
GPNAM1       SMSQ10.100
GPNAM2       SMSQ10.100
GPX1               0.00 %
GPX2               0.00 %
GPY1               0.00 %
GPY2               0.00 %
GPZ1              17.00 %
GPZ2              17.00 %
P16             1000.00 usec

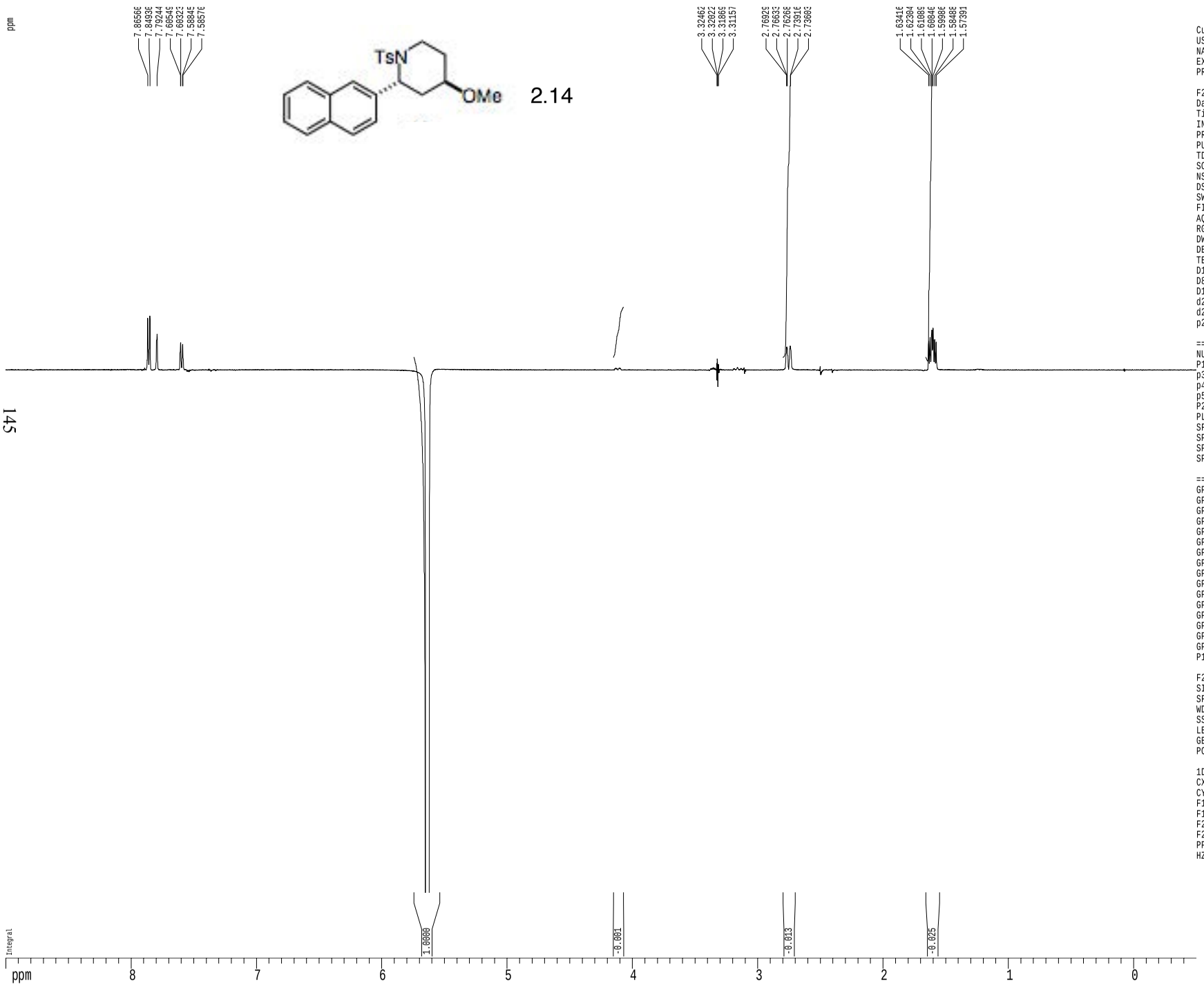
      F1 - Acquisition parameters
ND0                  1
TD                 512
SFO1          500.2235 MHz
FIDRES        15.650040 Hz
SW              16.018 ppm
FnMODE               QF

      F2 - Processing parameters
SI                1024
SF          500.2200362 MHz
WDW               SINE
SSB                  0
LB                0.00 Hz
GB                   0
PC                1.00

      F1 - Processing parameters
SI                1024
MC2                 QF
SF          500.2200362 MHz
WDW               SINE
SSB                  0
LB                0.00 Hz
GB                   0

        2D NMR plot parameters
CX2              15.00 cm
CX1              15.00 cm
F2PLO             9.000 ppm
F2LO           4501.98 Hz
F2PHI            -1.082 ppm
F2HI           -541.03 Hz
F1PLO             9.000 ppm
F1LO           4501.98 Hz
F1PHI            -1.082 ppm
F1HI           -541.03 Hz
F2PPMCM         0.67211 ppm/cm
F2HZCM        336.20062 Hz/cm
F1PPMCM         0.67211 ppm/cm
F1HZCM        336.20062 Hz/cm
```

gnoe



145

Current Data Parameters
USER caherber
NAME CAH-I-209-noe
EXPNO 2
PROCNO 1

F2 - Acquisition Parameters
Date_ 20210417
Time 14.16
INSTRUM cryo500
PROBHD 5 mm CPTCI 1H-
PULPROG gnoe1cc22.prd
TD 65536
SOLVENT CDCl3
NS 128
DS 8
SWH 8012.820 Hz
FIDRES 0.122266 Hz
AQ 4.0894966 sec
RG 80.6
DW 62.400 usec
DE 6.00 usec
TE 298.0 K
D1 1.00000000 sec
D8 0.50000000 sec
D16 0.00020000 sec
d21 0.33375451 sec
d22 0.16399699 sec
p2 19.50 usec

======= CHANNEL f1 =======
NUC1 1H
P1 9.75 usec
p3 29.25 usec
p4 39.00 usec
p5 26.00 usec
P29 40000.00 usec
PL1 1.60 dB
SFO1 500.2228198 MHz
SP9 60.00 dB
SPNAM9 gauss1.512
SPOFF9 0.00 Hz

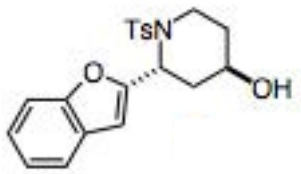
===== GRADIENT CHANNEL =====
GPNAM1 SMSQ10.100
GPNAM2 SMSQ10.100
GPNAM3 SMSQ10.100
GPNAM4 SMSQ10.100
GPX1 0.00 %
GPX2 0.00 %
GPX3 0.00 %
GPX4 0.00 %
GPY1 0.00 %
GPY2 0.00 %
GPY3 0.00 %
GPY4 0.00 %
GPZ1 7.00 %
GPZ2 3.00 %
GPZ3 2.30 %
GPZ4 -2.30 %
P16 1000.00 usec

F2 - Processing parameters
SI 65536
SF 500.2200000 MHz
WDW no
SSB 0
LB 0.00 Hz
GB 0
PC 1.00

1D NMR plot parameters
CX 22.80 cm
CY 50.00 cm
F1P 9.000 ppm
F1 4501.98 Hz
F2P -0.500 ppm
F2 -250.11 Hz
PPMCM 0.41667 ppm/cm
HZCM 208.42500 Hz/cm

1H spectrum





2.26

146

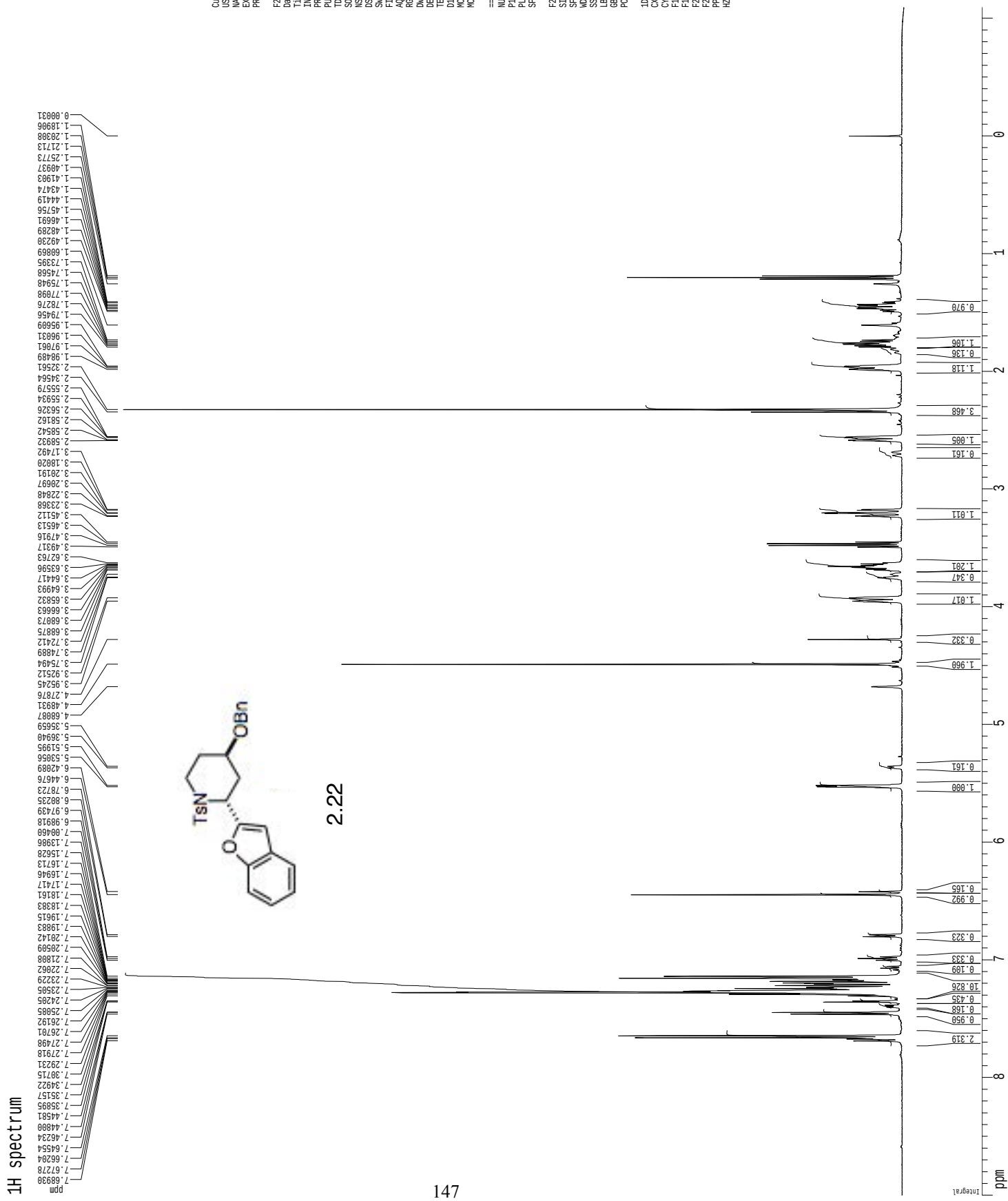
Current Data Parameters
USER caherber
NAME CAH-I-215
EXPNO 2
PROCNO 1

F2 - Acquisition Parameters
Date_ 20210503
Time 13.54
INSTRUM drx400
PROBHD 5 mm QNP H/F/P
PULPROG zg30
TD 65536
SOLVENT CDCl3
NS 8
DS 2
SWH 6410.256 Hz
FIDRES 0.097813 Hz
AQ 5.1118579 sec
RG 512
DW 78.000 usec
DE 4.50 usec
TE 298.0 K
D1 0.10000000 sec
MCREST 0.00000000 sec
MCWRK 0.01500000 sec

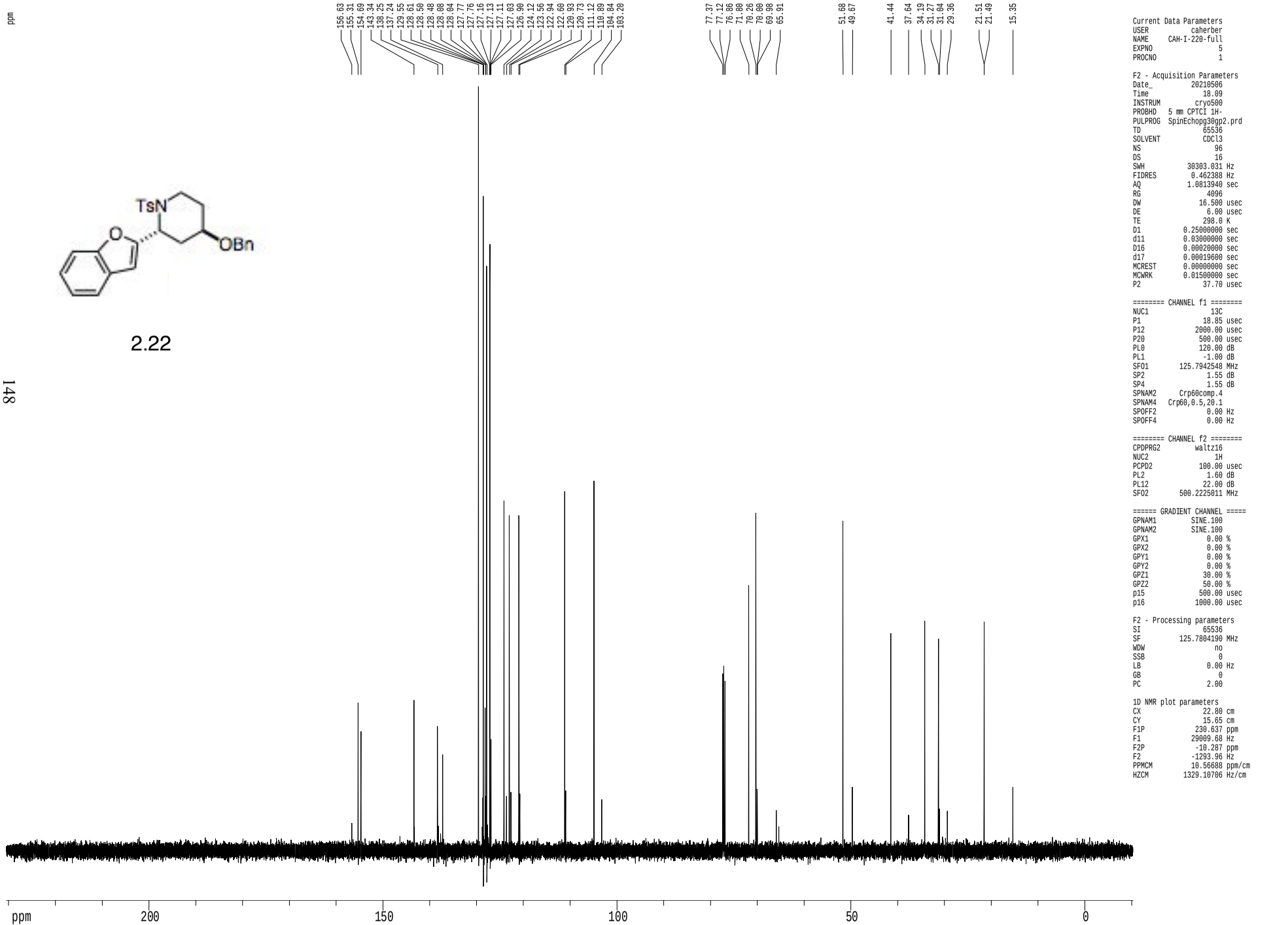
======= CHANNEL f1 =======
NUC1 1H
P1 12.00 usec
PL1 -1.60 dB
SFO1 400.1328009 MHz

F2 - Processing parameters
SI 65536
SF 400.1300223 MHz
WDW no
SSB 0
LB 0.00 Hz
GB 0
PC 2.00

1D NMR plot parameters
CX 22.80 cm
CY 15.00 cm
F1P 9.000 ppm
F1 3601.17 Hz
F2P -1.066 ppm
F2 -426.56 Hz
PPMCM 0.44149 ppm/cm
HZCM 176.65485 Hz/cm


1H spectrum
Current Data Parameters
USER caherher
NAME CAH-I-220-full
EXPNO 1
PROCNO 1
F2 - Acquisition Parameters
Date_ 20210506
Time_ 17.24
INSTRUM CryoQ60
PROBHD 5 mm CPTCI 1H-
PULPROG zg30
TD 48074
SOLVENT CDCl3
NS 8
DS 2
SWH 8012.820 Hz
FIDRES 0.166677 Hz
AQ 2.9998677 sec
RG 4
DW 62.400 usec
DE 6.00 usec
TE 298.0 K
D1 0.10000000 sec
MCREST 0.00000000 sec
MCWRK 0.01500000 sec
======= CHANNEL f1 =======
NUC1 1H
P1 9.75 usec
PL1 1.60 dB
SFO1 500.2235015 MHz
F2 - Processing parameters
SI 65536
SF 500.2200401 MHz
WDW no
SSB 0
LB 0.00 Hz
GB 0
PC 1.00
1D NMR plot parameters
CX 22.80 cm
CY 15.00 cm
F1P 9.000 ppm
F1 4501.98 Hz
F2P -1.089 ppm
F2 -544.94 Hz
PPMCM 0.44252 ppm/cm
HZCM 221.35622 Hz/cm
OBn
TsN
O
2.22
ppm
Integral

Z-restored spin-echo 13C spectrum with 1H decoupling




```
Current Data Parameters
USER            caherber
NAME      CAH-I-220-full
EXPNO                   5
PROCNO                  1

F2 - Acquisition Parameters
Date_            20210506
Time                18.09
INSTRUM           cryo500
PROBHD   5 mm CPTCI 1H-
PULPROG  SpinEchopg30gp2.prd
TD                  65536
SOLVENT             CDCl3
NS                     96
DS                     16
SWH           30303.031 Hz
FIDRES         0.462388 Hz
AQ             1.0813940 sec
RG                  4096
DW                16.500 usec
DE                 6.00 usec
TE                298.0 K
D1           0.25000000 sec
d11          0.03000000 sec
D16          0.00020000 sec
d17          0.00019600 sec
MCREST       0.00000000 sec
MCWRK        0.01500000 sec
P2                37.70 usec

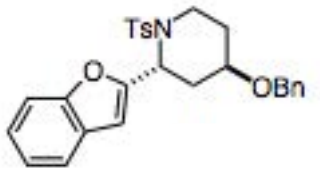
======== CHANNEL f1 ========
NUC1                13C
P1                 18.85 usec
P12              2000.00 usec
P20               500.00 usec
PL0               120.00 dB
PL1                -1.00 dB
SFO1         125.7942548 MHz
SP2                1.55 dB
SP4                1.55 dB
SPNAM2      Crp60comp.4
SPNAM4   Crp60,0.5,20.1
SPOFF2               0.00 Hz
SPOFF4               0.00 Hz

======== CHANNEL f2 ========
CPDPRG2          waltz16
NUC2                1H
PCPD2             100.00 usec
PL2                1.60 dB
PL12              22.00 dB
SFO2         500.2225011 MHz

====== GRADIENT CHANNEL =====
GPNAM1          SINE.100
GPNAM2          SINE.100
GPX1                0.00 %
GPX2                0.00 %
GPY1                0.00 %
GPY2                0.00 %
GPZ1               30.00 %
GPZ2               50.00 %
p15               500.00 usec
p16              1000.00 usec

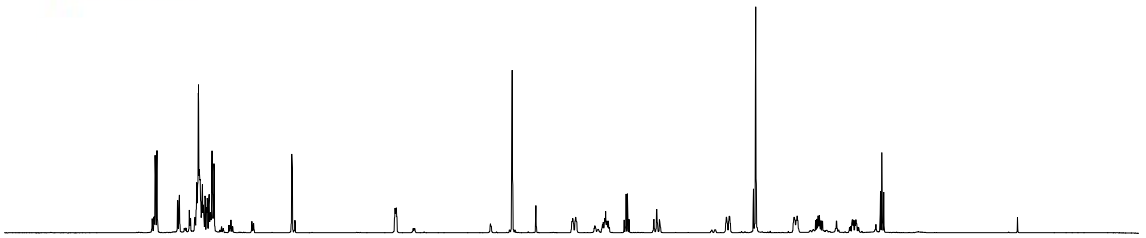
F2 - Processing parameters
SI                  65536
SF           125.7804190 MHz
WDW                    no
SSB                     0
LB                 0.00 Hz
GB                      0
PC                 2.00

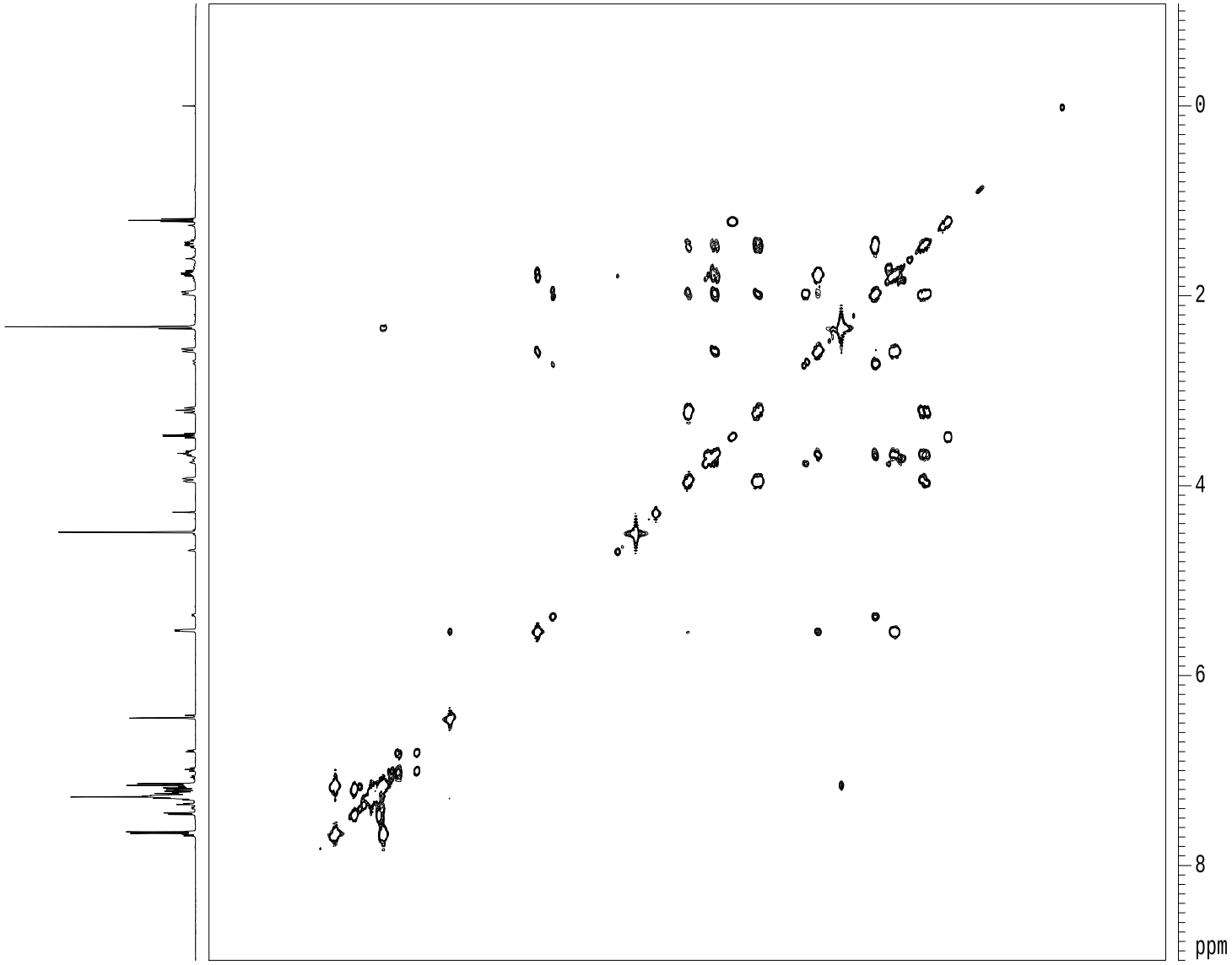
1D NMR plot parameters
CX                 22.80 cm
CY                 15.65 cm
F1P              230.637 ppm
F1             29009.68 Hz
F2P              -10.287 ppm
F2             -1293.96 Hz
PPMCM           10.56688 ppm/cm
HZCM          1329.10706 Hz/cm
```



2.22

gcosy60






```
Current Data Parameters
USER            caherber
NAME      CAH-I-220-full
EXPNO                   2
PROCNO                  1

F2 - Acquisition Parameters
Date_           20210506
Time               17.27
INSTRUM          cryo500
PROBHD   5 mm CPTCI 1H-
PULPROG    cosygp60.prd
TD                 2048
SOLVENT           CDCl3
NS                    2
DS                   16
SWH            8012.820 Hz
FIDRES         3.912510 Hz
AQ             0.1278452 sec
RG                 35.9
DW               62.400 usec
DE                6.00 usec
TE               298.0 K
d0            0.00000300 sec
D1            1.00000000 sec
d13           0.00000300 sec
D16           0.00020000 sec
IN0           0.00012480 sec

======== CHANNEL f1 ========
NUC1                 1H
P1                 9.75 usec
PL1                1.60 dB
SF01        500.2235015 MHz

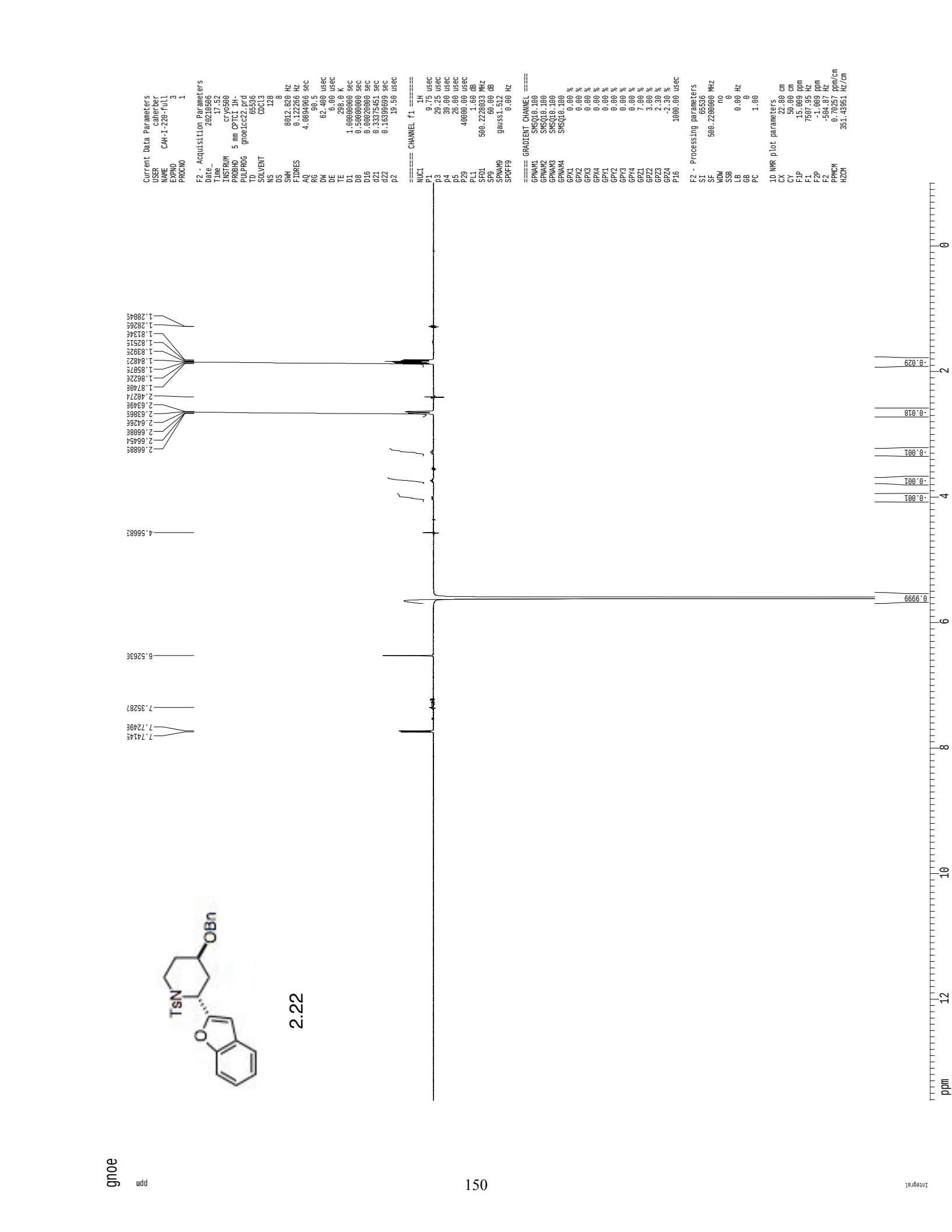
====== GRADIENT CHANNEL =====
GPNAM1       SMSQ10.100
GPNAM2       SMSQ10.100
GPX1               0.00 %
GPX2               0.00 %
GPY1               0.00 %
GPY2               0.00 %
GPZ1              17.00 %
GPZ2              17.00 %
P16             1000.00 usec

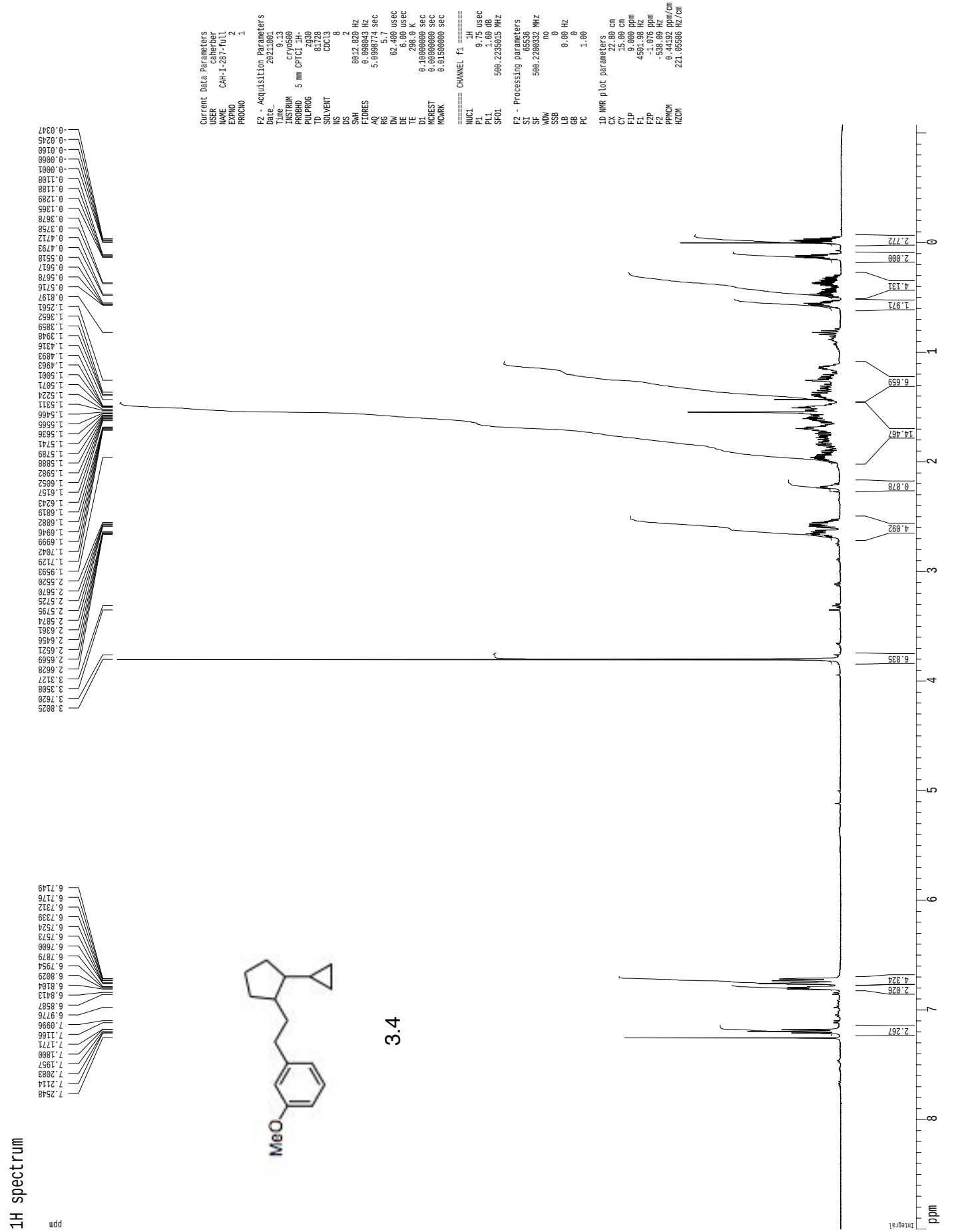
F1 - Acquisition parameters
ND0                   1
TD                  269
SFO1          500.2235 MHz
FIDRES        29.787437 Hz
SW               16.018 ppm
FnMODE               QF

F2 - Processing parameters
SI                 1024
SF          500.2200329 MHz
WDW                SINE
SSB                   0
LB                 0.00 Hz
GB                    0
PC                 1.00

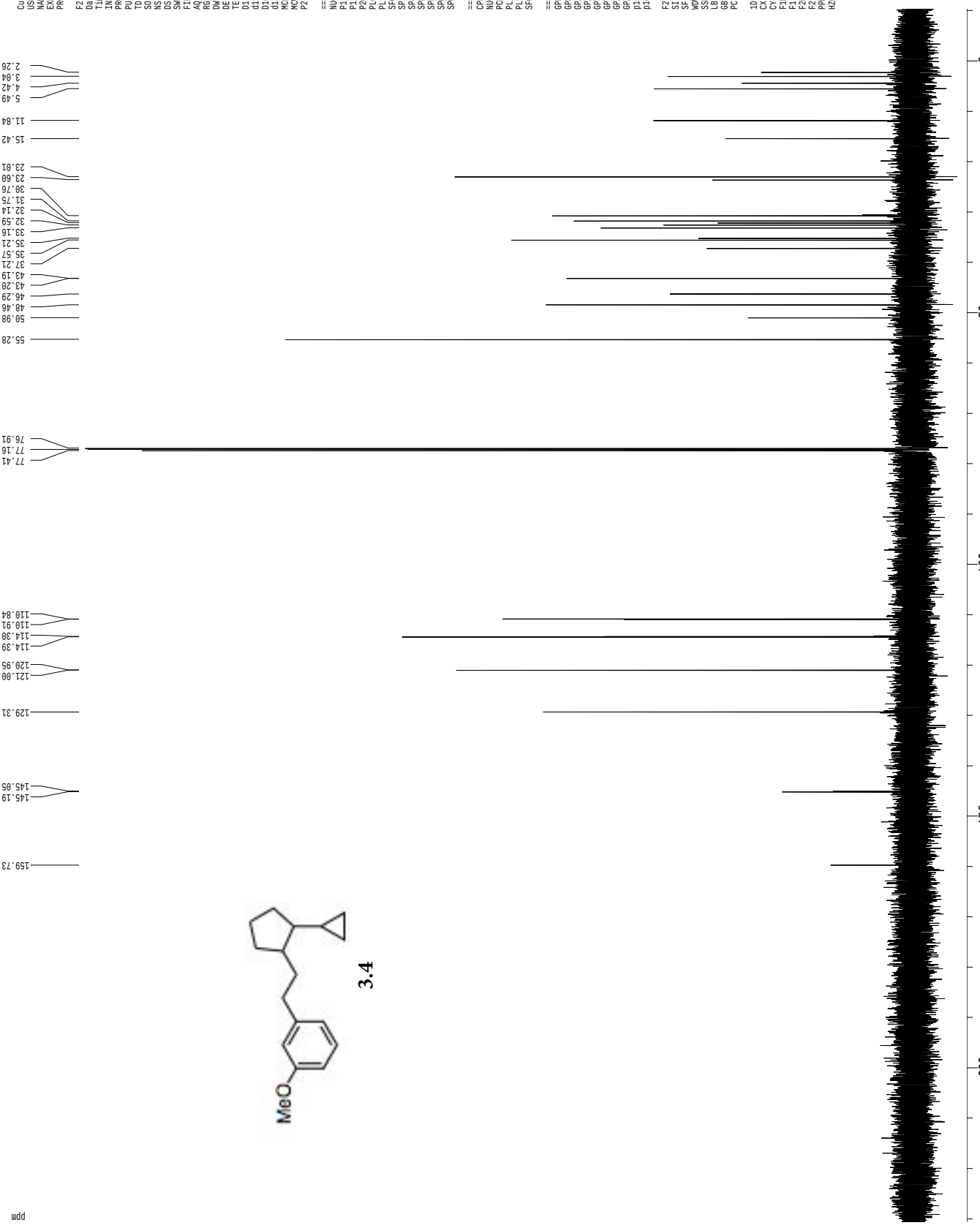
F1 - Processing parameters
SI                 1024
MC2                  QF
SF          500.2200329 MHz
WDW                SINE
SSB                   0
LB                 0.00 Hz
GB                    0

2D NMR plot parameters
CX2               15.00 cm
CX1               15.00 cm
F2PLO              9.000 ppm
F2LO            4501.98 Hz
F2PHI             -1.075 ppm
F2HI            -537.73 Hz
F1PLO              9.000 ppm
F1LO            4501.98 Hz
F1PHI             -1.075 ppm
F1HI            -537.73 Hz
F2PPMCM          0.67167 ppm/cm
F2HZCM         335.98087 Hz/cm
F1PPMCM          0.67167 ppm/cm
F1HZCM         335.98087 Hz/cm
```

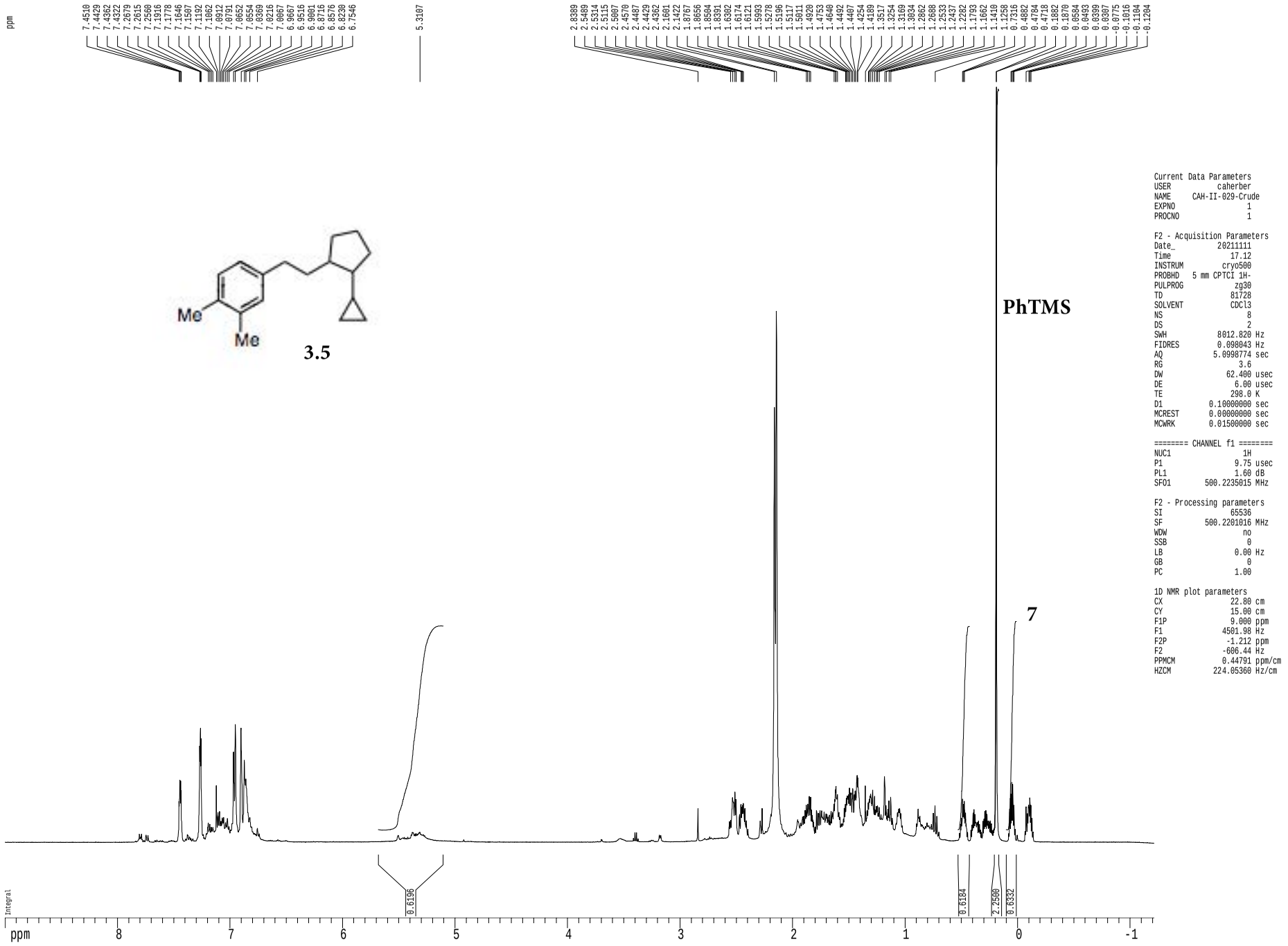

gnoe
ppm
Integral
2.22
OBn
TsN
O
Current Data Parameters
USER caherber
NAME CAH-I-228-full
EXPNO 3
PROCNO 1
F2 - Acquisition Parameters
Date_ 20210506
Time 17.52
INSTRUM cryo500
PROBHD 5 mm CPTCI 1H-
PULPROG gnoe1cc22.prd
TD 65536
SOLVENT CDCl3
NS 128
DS 8
SWH 8012.820 Hz
FIDRES 0.122266 Hz
AQ 4.0894966 sec
RG 90.5
DW 62.400 usec
DE 6.00 usec
TE 298.0 K
D1 1.00000000 sec
D8 0.15000000 sec
D16 0.00020000 sec
d21 0.33375451 sec
d22 0.16399699 sec
p2 19.50 usec
======= CHANNEL f1 =======
NUC1 1H
P1 9.75 usec
p3 29.25 usec
p4 39.00 usec
p5 26.00 usec
P29 40000.00 usec
PL1 1.60 dB
SFO1 500.2228033 MHz
SP9 60.00 dB
SPNAM9 gauss1.512
SPOFF9 0.00 Hz
===== GRADIENT CHANNEL ====
GPNAM1 SMSQ10.100
GPNAM2 SMSQ10.100
GPNAM3 SMSQ10.100
GPNAM4 SMSQ10.100
GPX1 0.00 %
GPX2 0.00 %
GPX3 0.00 %
GPX4 0.00 %
GPY1 0.00 %
GPY2 0.00 %
GPY3 0.00 %
GPY4 0.00 %
GPZ1 7.00 %
GPZ2 3.00 %
GPZ3 2.30 %
GPZ4 -2.30 %
P16 1000.00 usec
F2 - Processing parameters
SI 65536
SF 500.2200000 MHz
WDW no
SSB 0
LB 0.00 Hz
GB 0
PC 1.00
1D NMR plot parameters
CX 22.80 cm
CY 50.00 cm
F1P 15.009 ppm
F1 7507.95 Hz
F2P -1.009 ppm
F2 -504.87 Hz
PPMCM 0.70257 ppm/cm
HZCM 351.43951 Hz/cm
1.28045
1.28269
1.81346
1.82516
1.83925
1.84823
1.85075
1.86226
1.87406
2.40274
2.63496
2.63869
2.64266
2.66008
2.66454
2.66886
4.56683
6.52636
7.35287
7.72498
7.74146
-0.029
-0.018
-0.001
-0.001
-0.001
0.9999
0
2
4
6
8
10
12
ppm

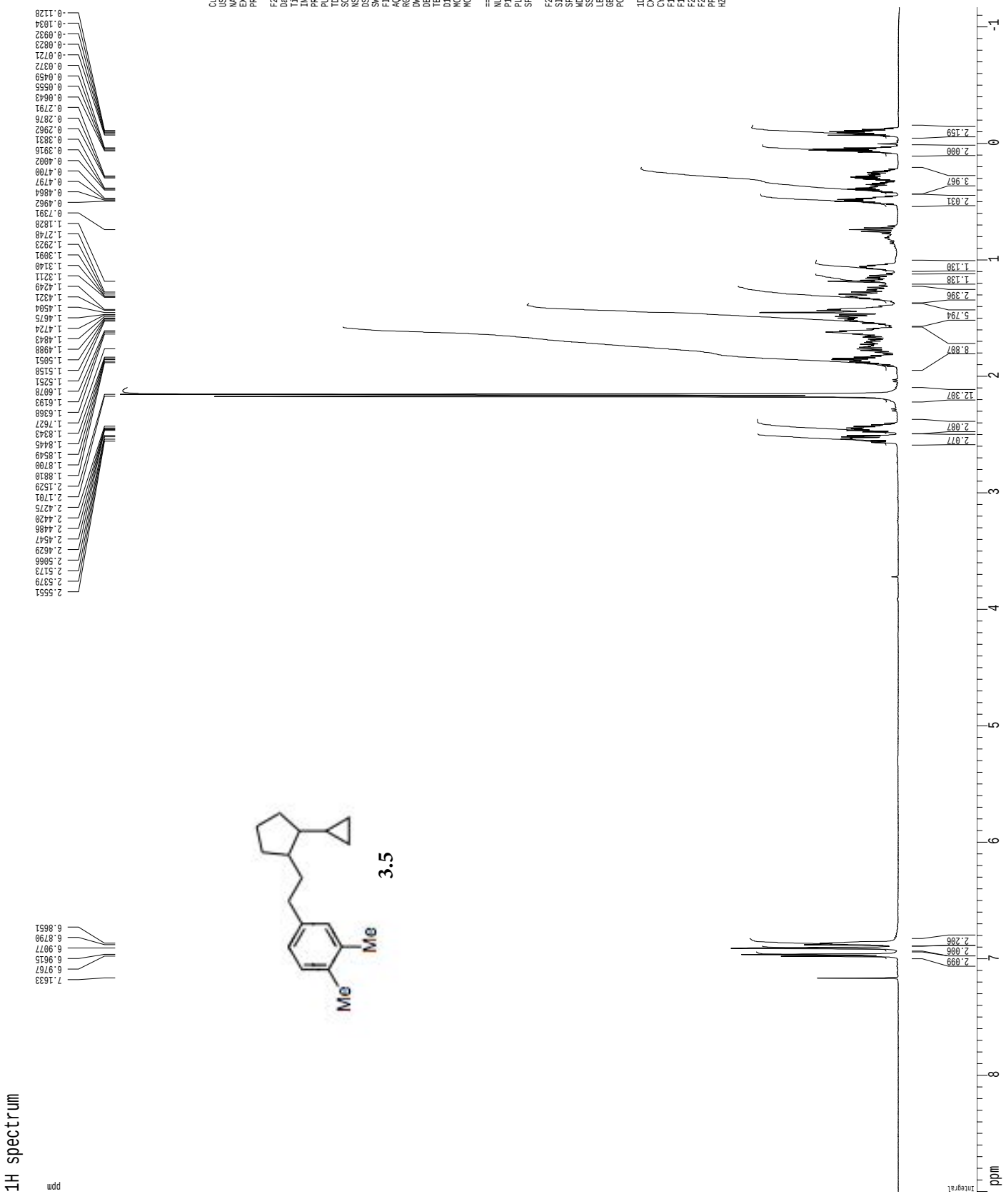

1H spectrum
3.4
MeO
Current Data Parameters
F2 - Acquisition Parameters
F2 - Processing parameters
1D NMR plot parameters
ppm
integral

Z-restored spin-echo 13C spectrum with 1H decoupling

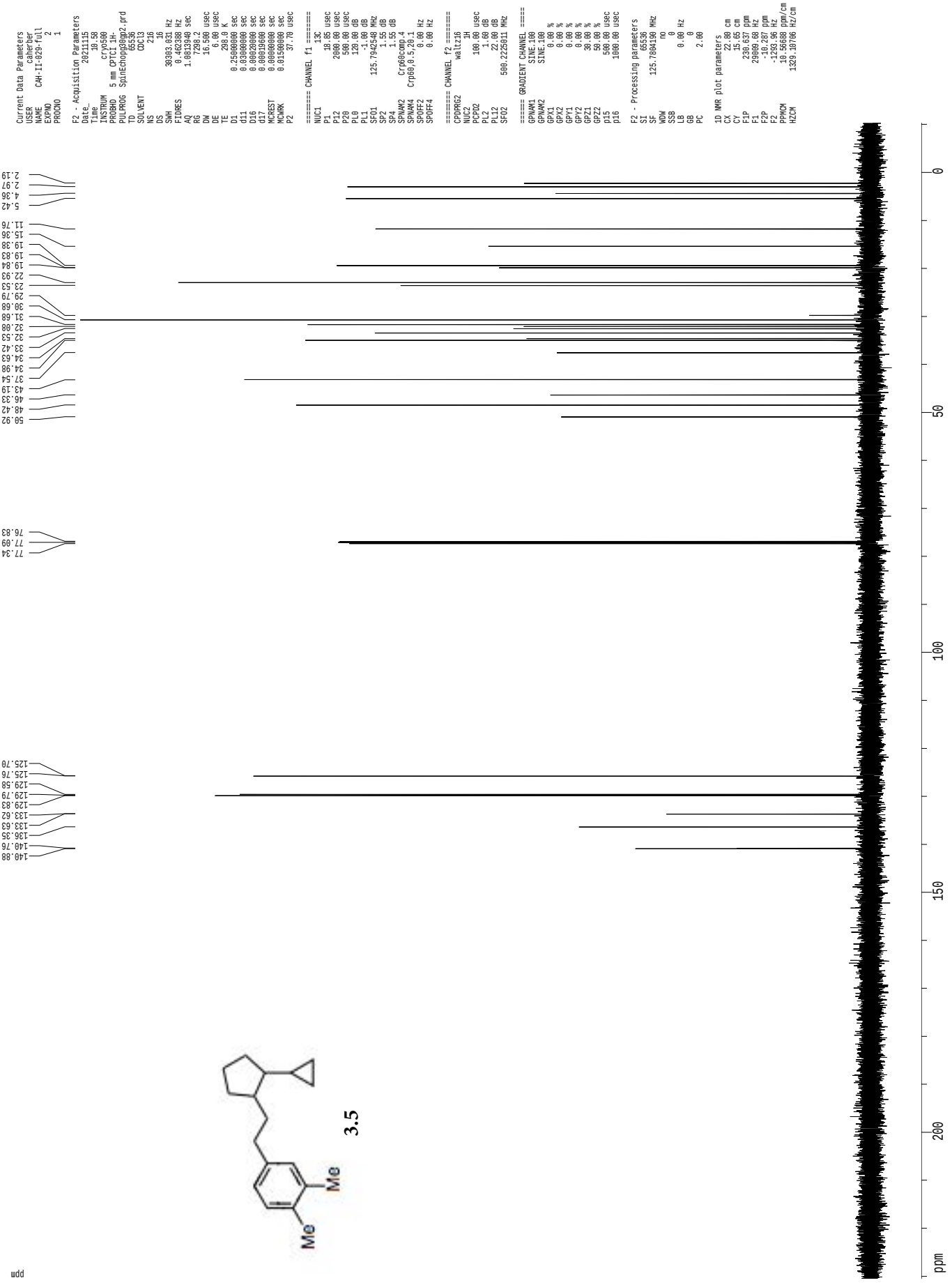


1H spectrum

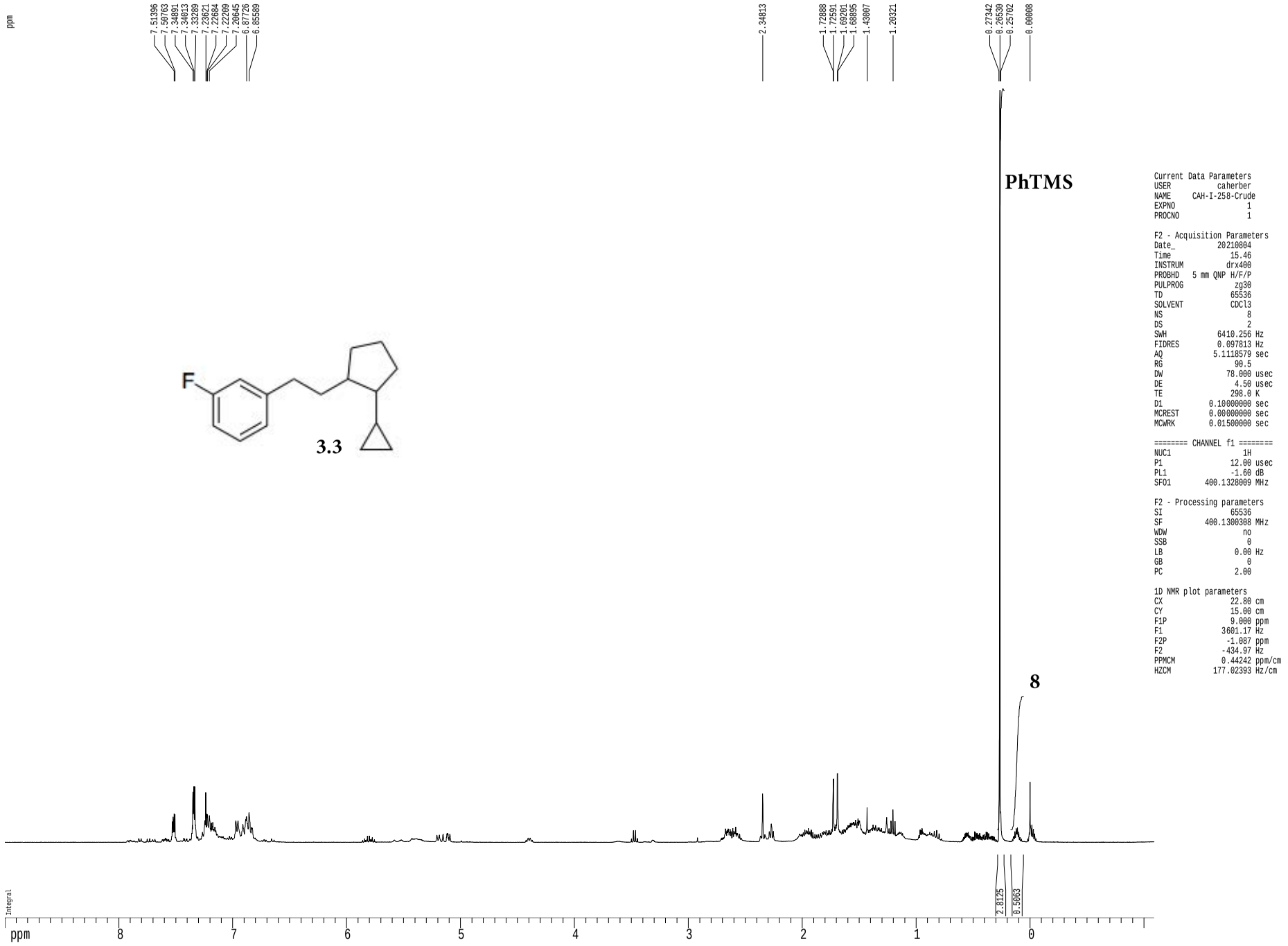

ppm
7.4510
7.4429
7.4362
7.4322
7.2679
7.2615
7.2560
7.1916
7.1778
7.1646
7.1507
7.1192
7.1062
7.0912
7.0791
7.0652
7.0554
7.0369
7.0216
7.0067
6.9667
6.9516
6.9001
6.8716
6.8576
6.8230
6.7546
5.3107
2.8389
2.5489
2.5314
2.5115
2.5007
2.4570
2.4487
2.4429
2.4362
2.1601
2.1422
1.8767
1.8656
1.8504
1.8391
1.6302
1.6174
1.6121
1.5993
1.5278
1.5196
1.5117
1.5011
1.4920
1.4753
1.4640
1.4492
1.4407
1.4254
1.4189
1.3517
1.3254
1.3169
1.3034
1.2862
1.2688
1.2533
1.2437
1.2282
1.1793
1.1662
1.1410
1.1258
0.7316
0.4882
0.4704
0.4718
0.1882
0.1870
0.0584
0.0493
0.0399
0.0397
-0.0775
-0.1016
-0.1104
-0.1204
Me
Me
3.5
PhTMS
7
Current Data Parameters
USER caherber
NAME CAH-II-029-Crude
EXPNO 1
PROCNO 1
F2 - Acquisition Parameters
Date_ 20211111
Time 17.12
INSTRUM cryo500
PROBHD 5 mm CPTCI 1H-
PULPROG zg30
TD 81728
SOLVENT CDCl3
NS 8
DS 2
SWH 8012.820 Hz
FIDRES 0.098043 Hz
AQ 5.0998774 sec
RG 3.6
DW 62.400 usec
DE 6.00 usec
TE 298.0 K
D1 0.10000000 sec
MCREST 0.00000000 sec
MCWRK 0.01500000 sec
======== CHANNEL f1 ========
NUC1 1H
P1 9.75 usec
PL1 1.60 dB
SFO1 500.2235015 MHz
F2 - Processing parameters
SI 65536
SF 500.2201016 MHz
WDW no
SSB 0
LB 0.00 Hz
GB 0
PC 1.00
1D NMR plot parameters
CX 22.80 cm
CY 15.00 cm
F1P 9.000 ppm
F1 4501.98 Hz
F2P -1.212 ppm
F2 -606.44 Hz
PPMCM 0.44791 ppm/cm
HZCM 224.05360 Hz/cm
Integral
0.6196
0.6184
2.2500
0.6332
ppm
8
7
6
5
4
3
2
1
0
-1


1H spectrum
Current Data Parameters
USER calherber
NAME CAH-II-029-full
EXPNO 1
PROCNO 1
F2 - Acquisition Parameters
Date_ 20211113
Time 12:39
INSTRUM cryo500
PROBHD 5 mm CPTCI 1H-
PULPROG zg30
TD 81728
SOLVENT CDCl3
NS 8
DS 2
SWH 8012.820 Hz
FIDRES 0.098043 Hz
AQ 5.0998774 sec
RG 6.3
DW 62.400 usec
DE 6.00 usec
TE 298.0 K
D1 0.10000000 sec
MCREST 0.00000000 sec
MCWRK 0.01500000 sec
======== CHANNEL f1 ========
NUC1 1H
P1 9.75 usec
PL1 1.00 dB
SFO1 500.2235015 MHz
F2 - Processing parameters
SI 65536
SF 500.2200792 MHz
WDW no
SSB 0
LB 0.00 Hz
GB 0
PC 1.00
1D NMR plot parameters
CX 22.80 cm
CY 15.00 cm
F1P 9.000 ppm
F1 4501.98 Hz
F2P -1.168 ppm
F2 -584.06 Hz
PPMCM 0.44595 ppm/cm
HZCM 223.07208 Hz/cm
Me
Me
3.5
ppm
Integral

Z-restored spin-echo 13C spectrum with 1H decoupling



1H spectrum



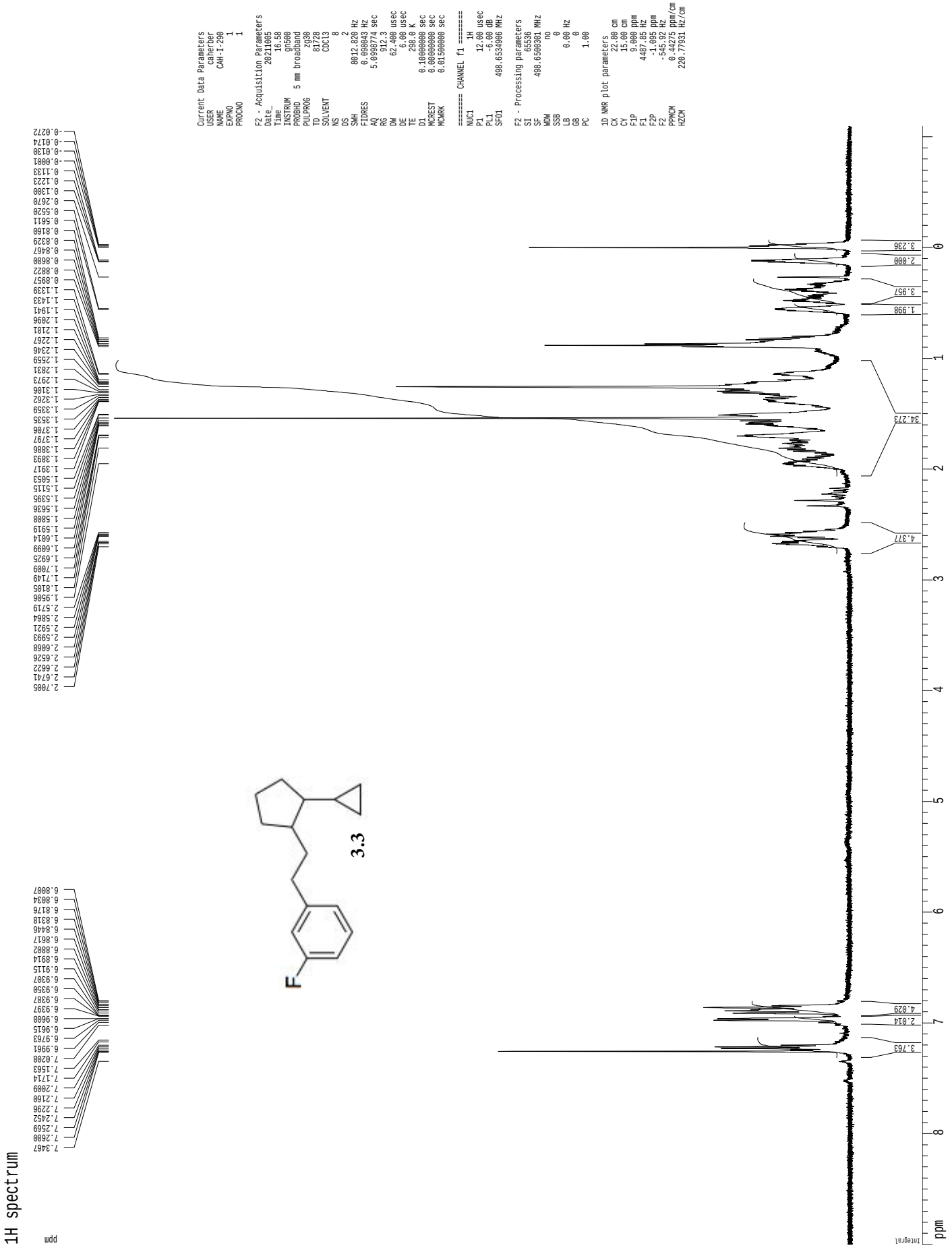
Current Data Parameters
USER caherber
NAME CAH-I-258-Crude
EXPNO 1
PROCNO 1

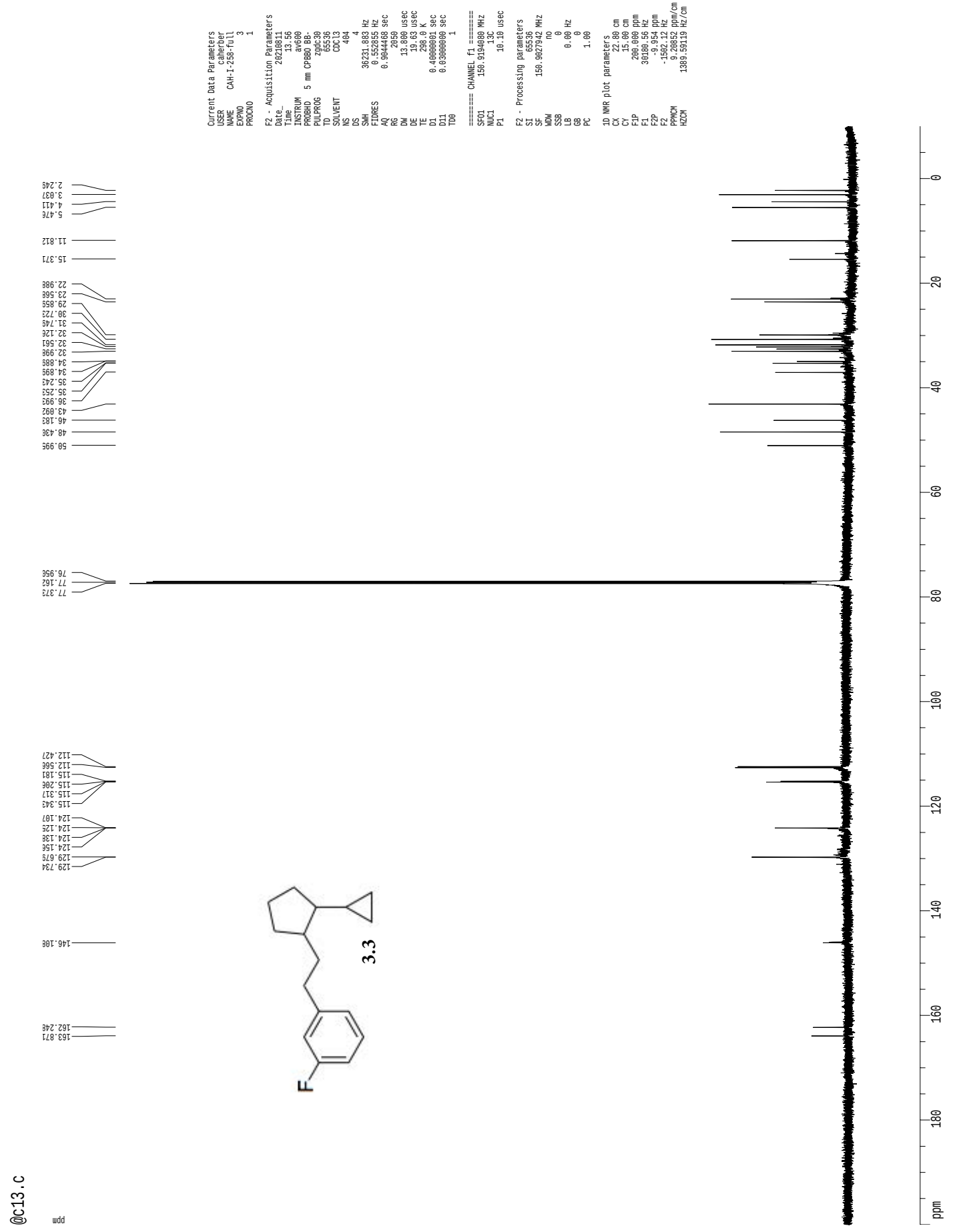
F2 - Acquisition Parameters
Date_ 20210804
Time 15.46
INSTRUM drx400
PROBHD 5 mm QNP H/F/P
PULPROG zg30
TD 65536
SOLVENT CDCl3
NS 8
DS 2
SWH 6410.256 Hz
FIDRES 0.097813 Hz
AQ 5.1118579 sec
RG 90.5
DW 78.000 usec
DE 4.50 usec
TE 298.0 K
D1 0.10000000 sec
MCREST 0.00000000 sec
MCWRK 0.01500000 sec

======== CHANNEL f1 ========
NUC1 1H
P1 12.00 usec
PL1 -1.60 dB
SFO1 400.1328009 MHz

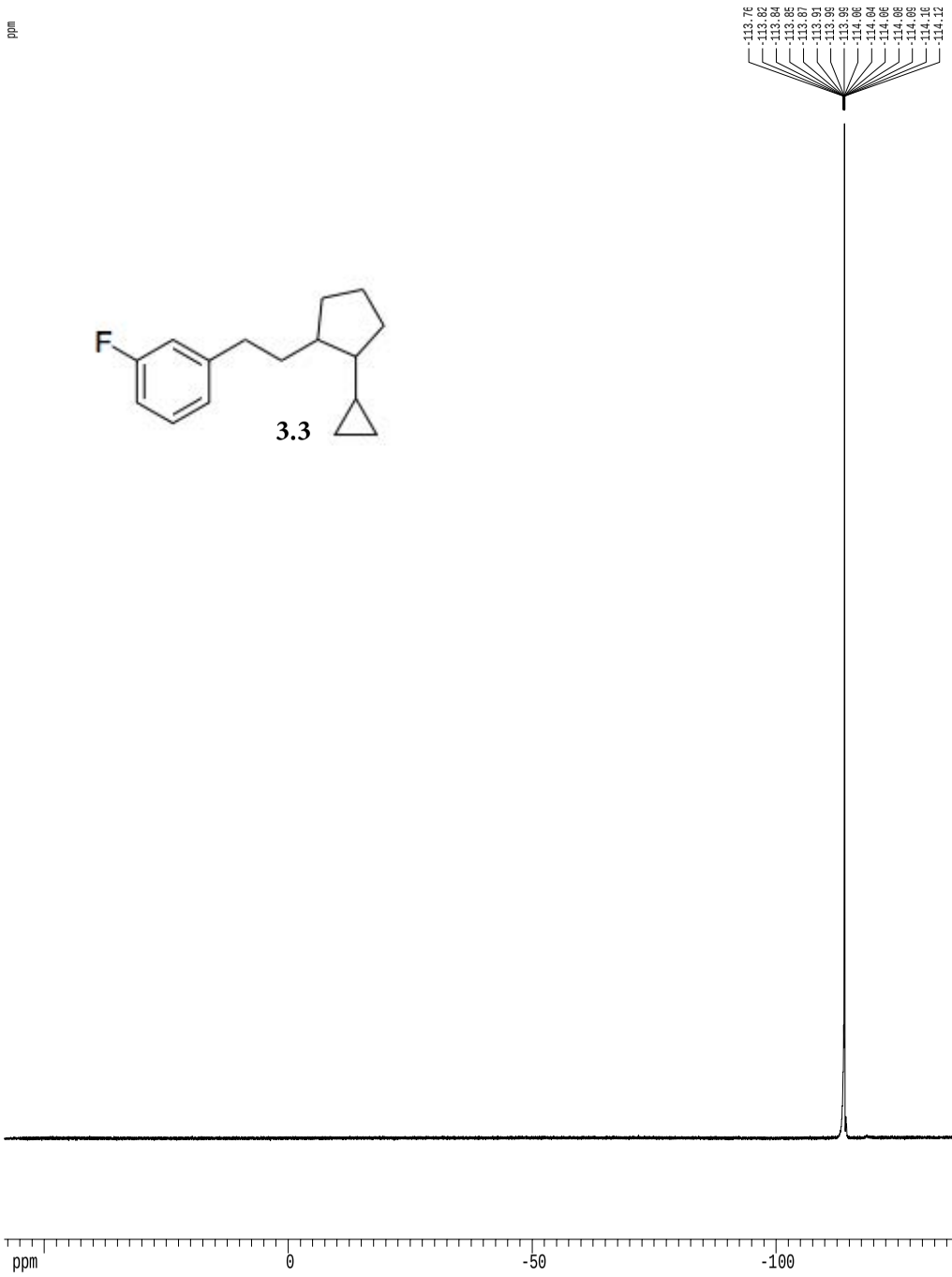
F2 - Processing parameters
SI 65536
SF 400.1300308 MHz
WDW no
SSB 0
LB 0.00 Hz
GB 0
PC 2.00

1D NMR plot parameters
CX 22.80 cm
CY 15.00 cm
F1P 9.000 ppm
F1 3601.17 Hz
F2P -1.087 ppm
F2 -434.97 Hz
PPMCM 0.44242 ppm/cm
HZCM 177.02393 Hz/cm


1H spectrum
ppm
integral
3.3
F
Current Data Parameters
USER calherber
NAME CAH-I-280
EXPNO 1
PROCNO 1
F2 - Acquisition Parameters
Date_ 20211005
Time 16.58
INSTRUM gn500
PROBHD 5 mm broadband
PULPROG zg30
TD 81728
SOLVENT CDCl3
NS 8
DS 2
SWH 8012.820 Hz
FIDRES 0.098043 Hz
AQ 5.0998774 sec
RG 912.3
DW 62.400 usec
DE 6.00 usec
TE 298.0 K
D1 0.10000000 sec
MCREST 0.00000000 sec
MCWRK 0.01500000 sec
======== CHANNEL f1 ========
NUC1 1H
P1 12.00 usec
PL1 -6.00 dB
SFO1 498.6534906 MHz
F2 - Processing parameters
SI 65536
SF 498.6500301 MHz
WDW no
SSB 0
LB 0.00 Hz
GB 0
PC 1.00
1D NMR plot parameters
CX 22.80 cm
CY 15.00 cm
F1P 9.000 ppm
F1 4487.85 Hz
F2P -1.005 ppm
F2 -545.92 Hz
PPMCM 0.44275 ppm/cm
HZCM 220.77931 Hz/cm
3.236
2.000
3.957
1.998
34.273
4.377
4.029
2.014
3.763


@c13.c
wdd
Current Data Parameters
USER caherber
NAME CAH-I-258-full
EXPNO 3
PROCNO 1
F2 - Acquisition Parameters
Date_ 20210811
Time 13.56
INSTRUM av600
PROBHD 5 mm CPBBO BB-
PULPROG zgdc30
TD 65536
SOLVENT CDCl3
NS 404
DS 4
SWH 36231.883 Hz
FIDRES 0.552855 Hz
AQ 0.9044468 sec
RG 2050
DW 13.800 usec
DE 19.63 usec
TE 298.0 K
D1 0.40000001 sec
D11 0.03000000 sec
TD0 1
======== CHANNEL f1 =======
SFO1 150.9194080 MHz
NUC1 13C
P1 10.10 usec
F2 - Processing parameters
SI 65536
SF 150.9027942 MHz
WDW no
SSB 0
LB 0.00 Hz
GB 0
PC 1.00
1D NMR plot parameters
CX 22.80 cm
CY 15.00 cm
F1P 200.000 ppm
F1 30180.56 Hz
F2P -0.954 ppm
F2 -1582.12 Hz
PPMCM 9.20852 ppm/cm
HZCM 1389.59119 Hz/cm
5.476
4.411
3.037
2.249
11.812
15.373
22.988
23.568
29.859
30.723
31.749
32.126
32.561
32.998
34.889
34.899
35.243
35.253
36.993
43.092
46.183
48.438
50.995
76.956
77.162
77.373
112.427
112.566
115.181
115.206
115.317
115.343
124.107
124.125
124.138
124.156
129.679
129.734
146.108
162.248
163.873
3.3
F
ppm
0
20
40
60
80
100
120
140
160
180

@f19.c



Current Data Parameters
USER caherber
NAME CAH-I-258-full
EXPNO 2
PROCNO 1

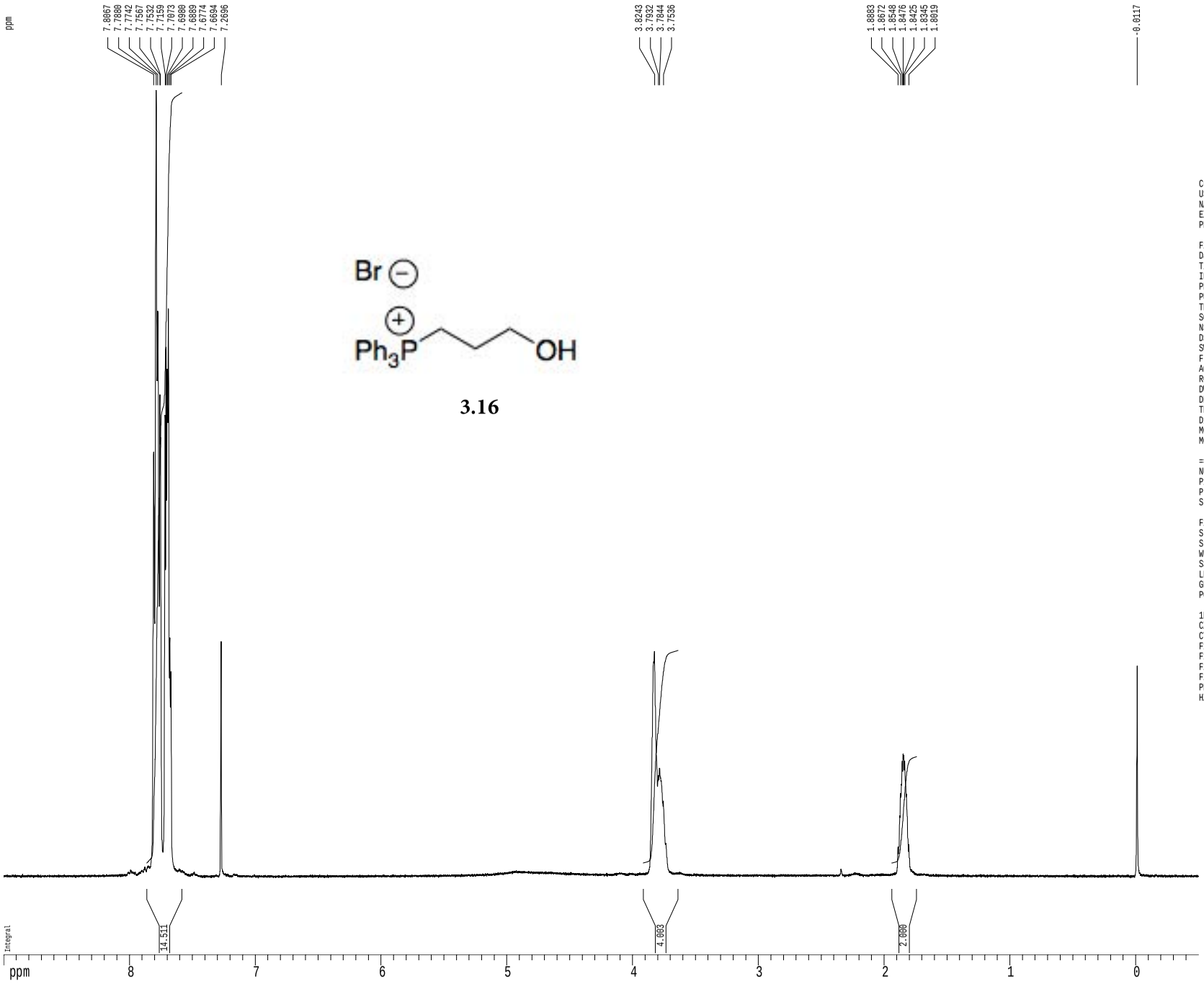
F2 - Acquisition Parameters
Date_ 20210811
Time 13.43
INSTRUM av600
PROBHD 5 mm CPBBO BB-
PULPROG zgflqn30
TD 131072
SOLVENT CDCl3
NS 16
DS 2
SWH 178571.422 Hz
FIDRES 1.362392 Hz
AQ 0.3670516 sec
RG 575
DW 2.800 usec
DE 18.00 usec
TE 298.0 K
D1 3.00000000 sec
TD0 1

======== CHANNEL f1 ========
SFO1 564.6299196 MHz
NUC1 19F
P1 18.25 usec

F2 - Processing parameters
SI 131072
SF 564.6863882 MHz
WDW no
SSB 0
LB 0.00 Hz
GB 0
PC 1.00

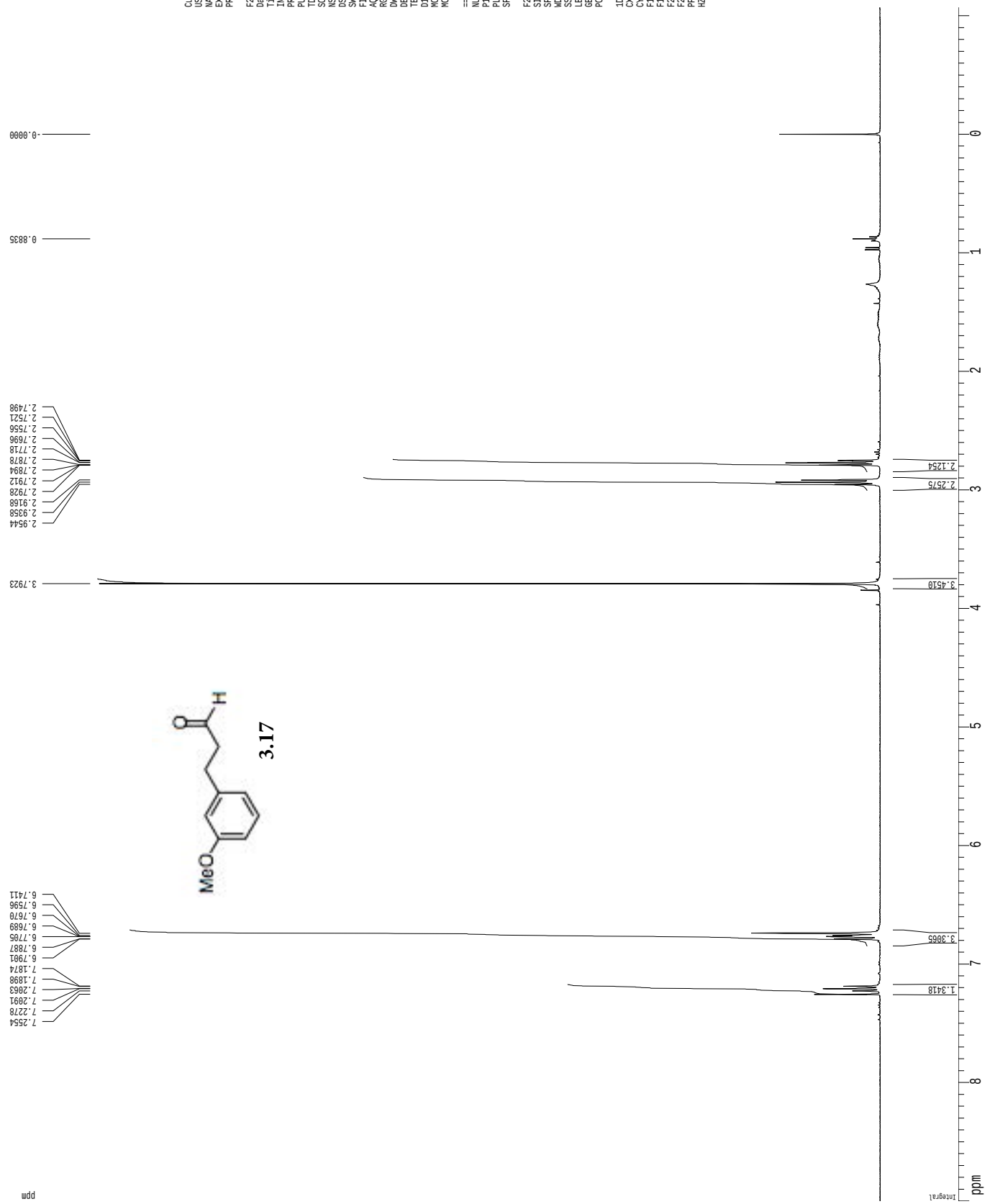
1D NMR plot parameters
CX 22.80 cm
CY 15.00 cm
F1P 58.116 ppm
F1 32817.10 Hz
F2P -258.116 ppm
F2 -145754.33 Hz
PPMCM 13.86979 ppm/cm
HZCM 7832.08057 Hz/cm

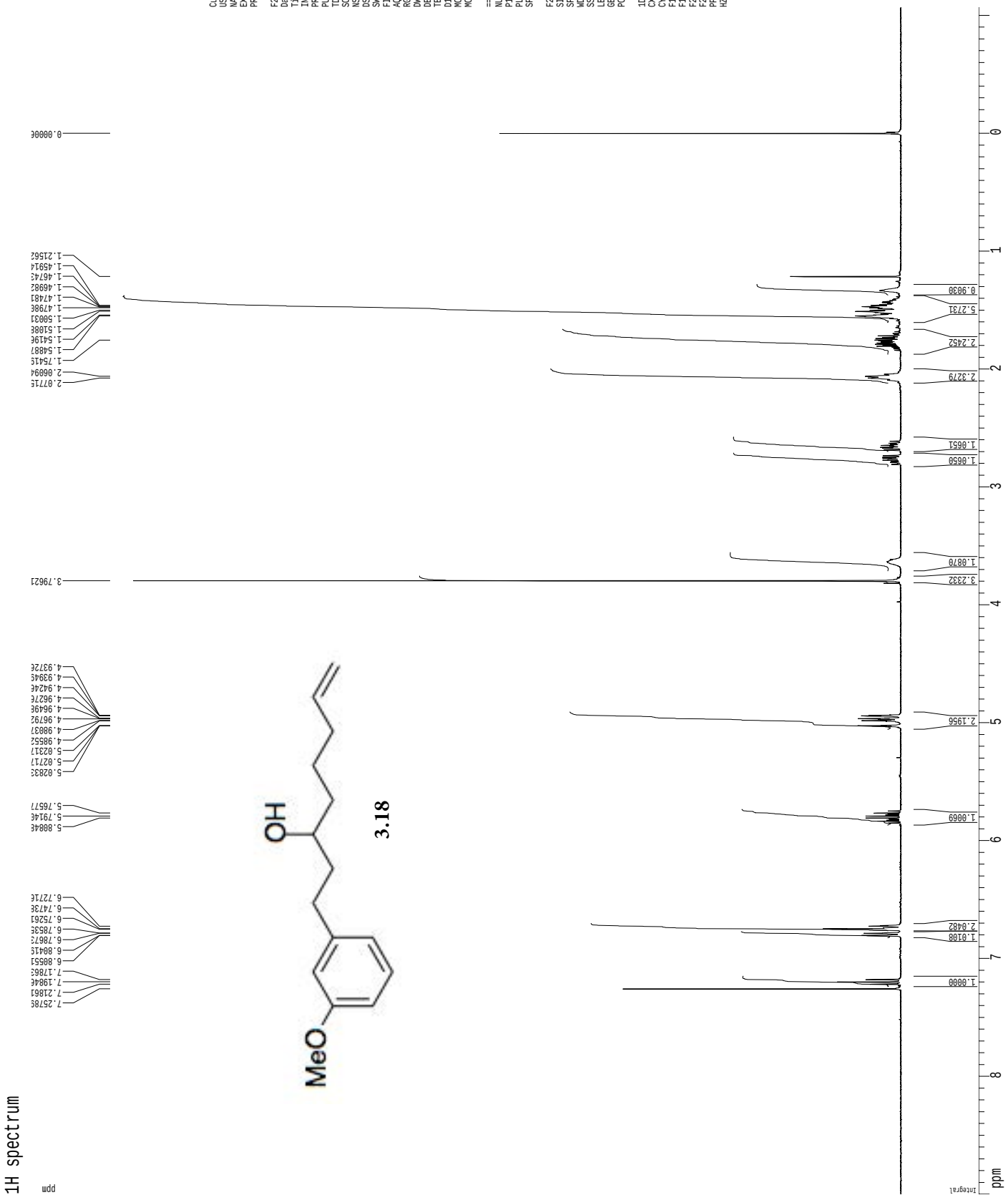
1H spectrum



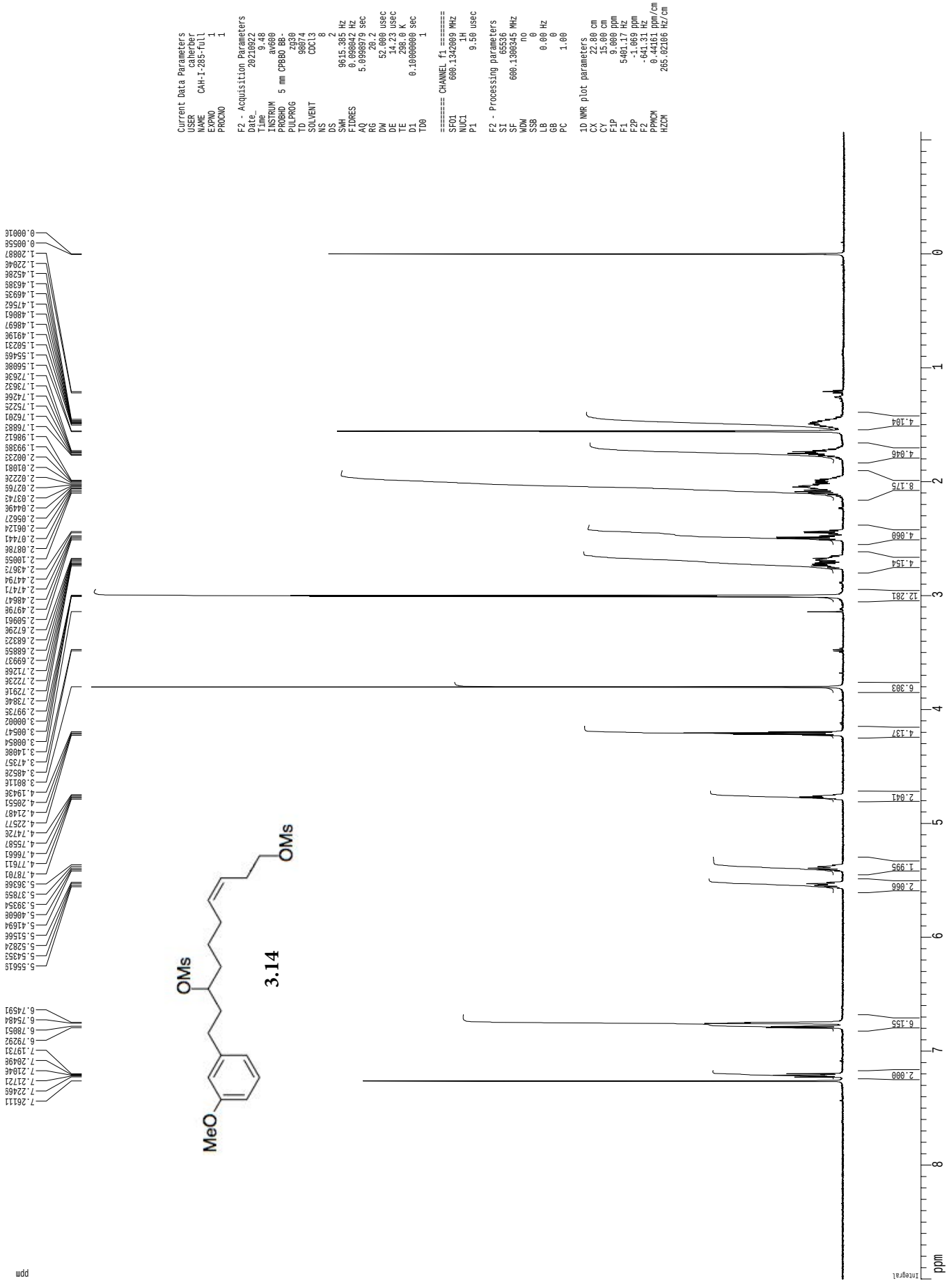
3.16

1H spectrum

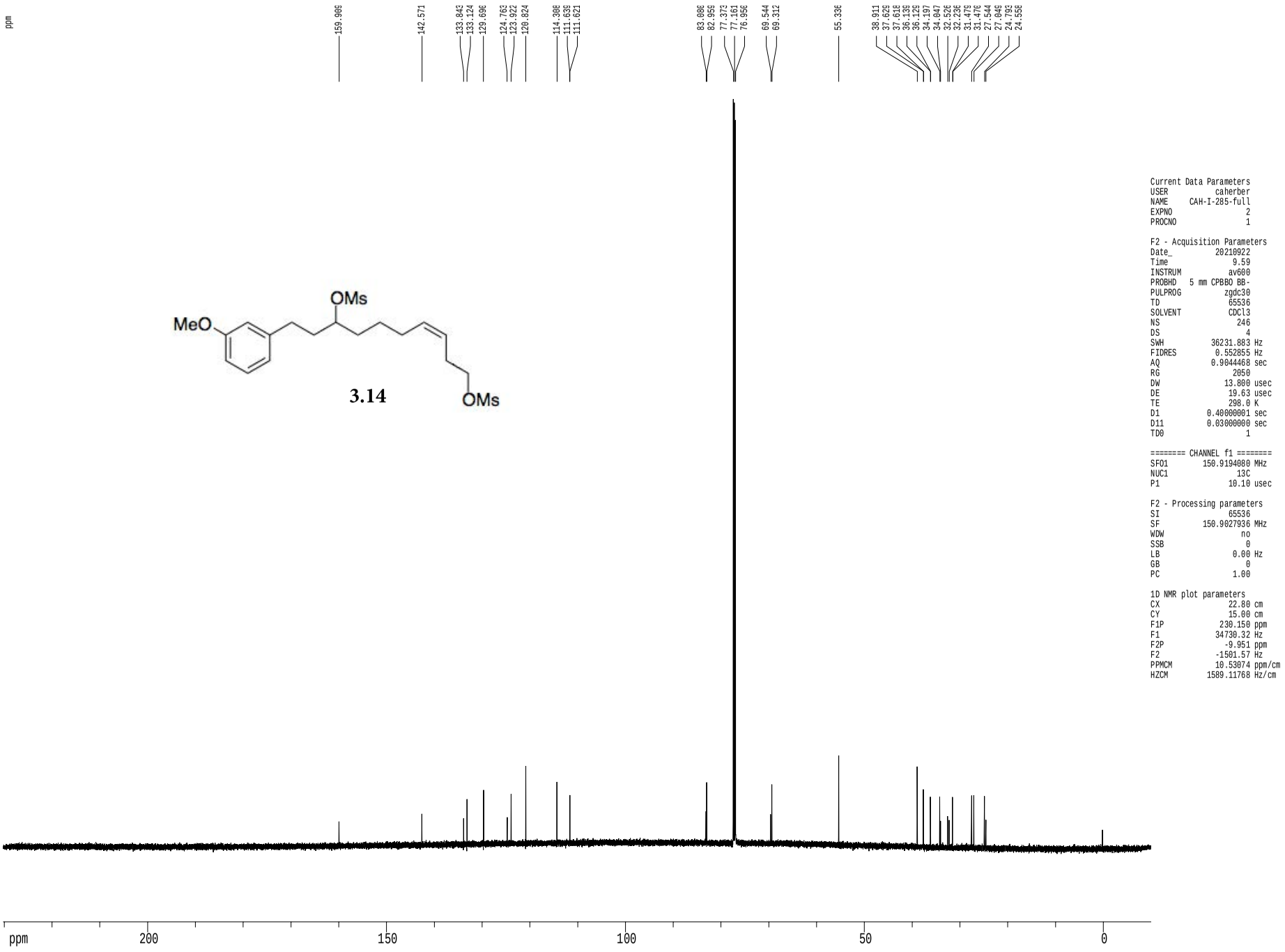

Current Data Parameters
USER calherber
NAME CAH-I-263
EXPNO 1
PROCNO 1
F2 - Acquisition Parameters
Date_ 20210619
Time 9.20
INSTRUM drx400
PROBHD 5 mm QNP H/F/P
PULPROG zg30
TD 65536
SOLVENT CDCl3
NS 8
DS 2
SWH 6410.256 Hz
FIDRES 0.097813 Hz
AQ 5.1118579 sec
RG 322.5
DW 78.000 usec
DE 4.50 usec
TE 298.0 K
D1 0.10000000 sec
MCREST 0.00000000 sec
MCWRK 0.01500000 sec
======== CHANNEL f1 ========
NUC1 1H
P1 12.00 usec
PL1 -1.00 dB
SFO1 400.1328009 MHz
F2 - Processing parameters
SI 65536
SF 400.1300232 MHz
WDW no
SSB 0
LB 0.00 Hz
GB 0
PC 2.00
1D NMR plot parameters
CX 22.80 cm
CY 15.00 cm
F1P 9.000 ppm
F1 3601.17 Hz
F2P -1.060 ppm
F2 -427.44 Hz
PPMCM 0.44159 ppm/cm
HZCM 176.69353 Hz/cm
0.0000
0.8835
2.7498
2.7521
2.7556
2.7696
2.7718
2.7878
2.7894
2.7912
2.7928
2.9168
2.9358
2.9544
3.7923
6.7411
6.7596
6.7670
6.7689
6.7705
6.7887
6.7901
7.1874
7.1898
7.2063
7.2091
7.2278
7.2554
2.1254
2.2575
3.4510
3.3065
1.3418
MeO
3.17
integral
ppm


1H spectrum
Current Data Parameters
USER calherber
NAME CAH-I-267
EXPNO 1
PROCNO 1
F2 - Acquisition Parameters
Date_ 20210825
Time 10.12
INSTRUM drx400
PROBHD 5 mm Multinucl
PULPROG zg30
TD 65536
SOLVENT CDCl3
NS 8
DS 2
SWH 6410.256 Hz
FIDRES 0.097813 Hz
AQ 5.1118579 sec
RG 645.1
DW 78.000 usec
DE 4.50 usec
TE 297.9 K
D1 0.10000000 sec
MCREST 0.00000000 sec
MCWRK 0.01500000 sec
======== CHANNEL f1 ========
NUC1 1H
P1 12.00 usec
PL1 -1.10 dB
SFO1 400.1328000 MHz
F2 - Processing parameters
SI 65536
SF 400.1300224 MHz
WDW no
SSB 0
LB 0.00 Hz
GB 0
PC 2.00
1D NMR plot parameters
CX 22.80 cm
CY 15.00 cm
F1P 9.000 ppm
F1 3601.17 Hz
F2P -1.066 ppm
F2 -426.66 Hz
PPMCM 0.44150 ppm/cm
HZCM 176.65921 Hz/cm
OH
MeO
3.18
ppm
Integral

1H spectrum


Current Data Parameters
USER caherber
NAME CAH-I-285-full
EXPNO 1
PROCNO 1
F2 - Acquisition Parameters
Date_ 20210922
Time 9.48
INSTRUM av600
PROBHD 5 mm CPBBO BB-
PULPROG 2d30
TD 98874
SOLVENT CDCl3
NS 2
DS 2
SWH 9615.385 Hz
FIDRES 0.098042 Hz
AQ 5.0999979 sec
RG 28.2
DW 52.000 usec
DE 14.23 usec
TE 298.0 K
D1 0.10000000 sec
TD0 1
======== CHANNEL f1 ========
SFO1 600.1342009 MHz
NUC1 1H
P1 9.50 usec
F2 - Processing parameters
SI 65536
SF 600.1300345 MHz
WDW no
SSB 0
LB 0.00 Hz
GB 0
PC 1.00
1D NMR plot parameters
CX 22.80 cm
CY 15.00 cm
F1P 9.000 ppm
F1 5401.17 Hz
F2P -1.059 ppm
F2 -641.31 Hz
PPMCM 0.44161 ppm/cm
HZCM 265.02106 Hz/cm
OMs
OMs
MeO
3.14
4.184
4.046
8.175
4.060
4.154
12.281
6.303
4.137
2.041
1.995
2.066
6.155
2.000
ppm
Integral

13C Spectrum



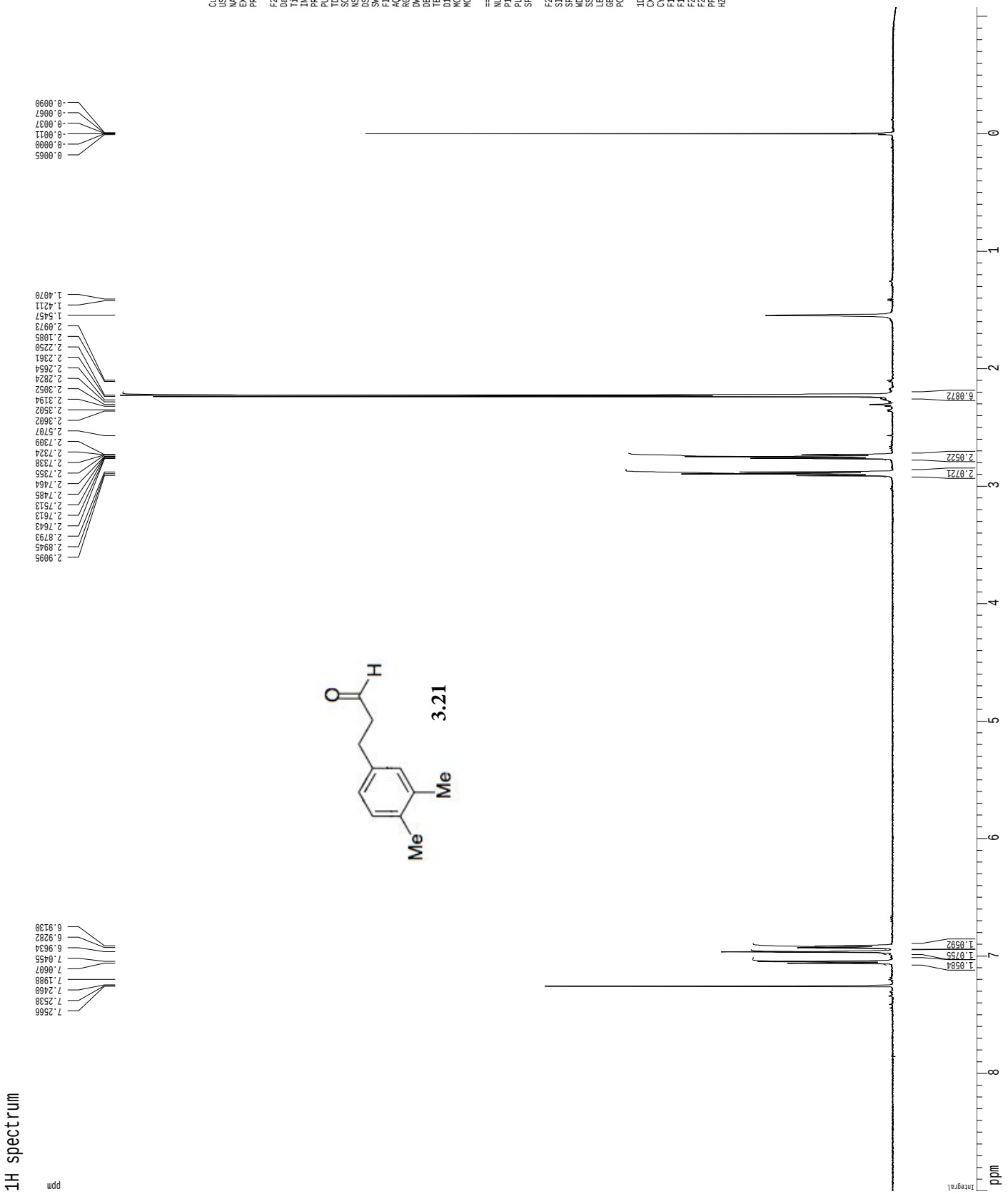
Current Data Parameters
USER caherber
NAME CAH-I-285-full
EXPNO 2
PROCNO 1

F2 - Acquisition Parameters
Date_ 20210922
Time 9.59
INSTRUM av600
PROBHD 5 mm CPBBO BB-
PULPROG zgdc30
TD 65536
SOLVENT CDCl3
NS 246
DS 4
SWH 36231.883 Hz
FIDRES 0.552855 Hz
AQ 0.9044468 sec
RG 2050
DW 13.800 usec
DE 19.63 usec
TE 298.0 K
D1 0.40000001 sec
D11 0.03000000 sec
TD0 1

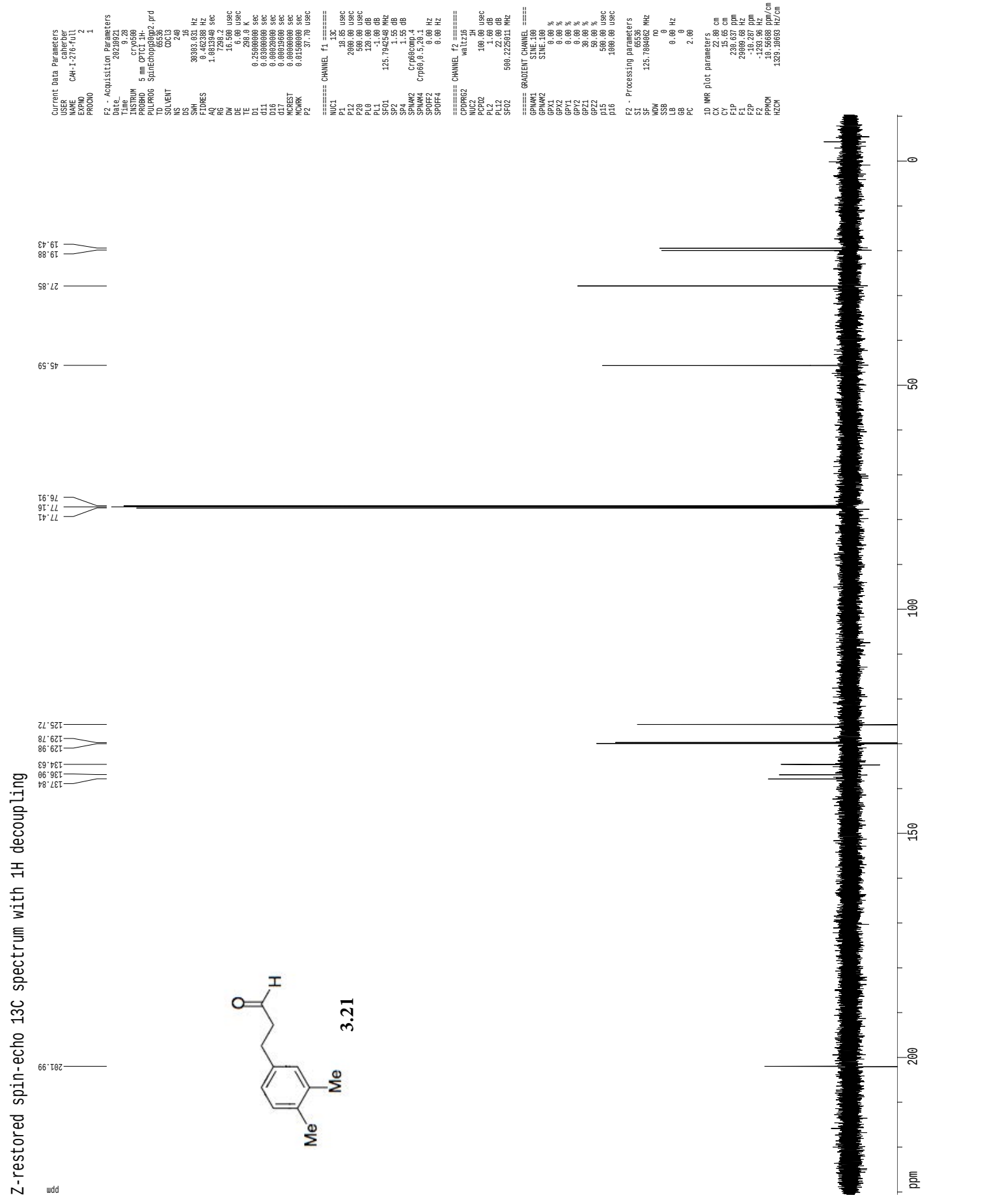
======== CHANNEL f1 ========
SFO1 150.9194080 MHz
NUC1 13C
P1 10.10 usec

F2 - Processing parameters
SI 65536
SF 150.9027936 MHz
WDW no
SSB 0
LB 0.00 Hz
GB 0
PC 1.00

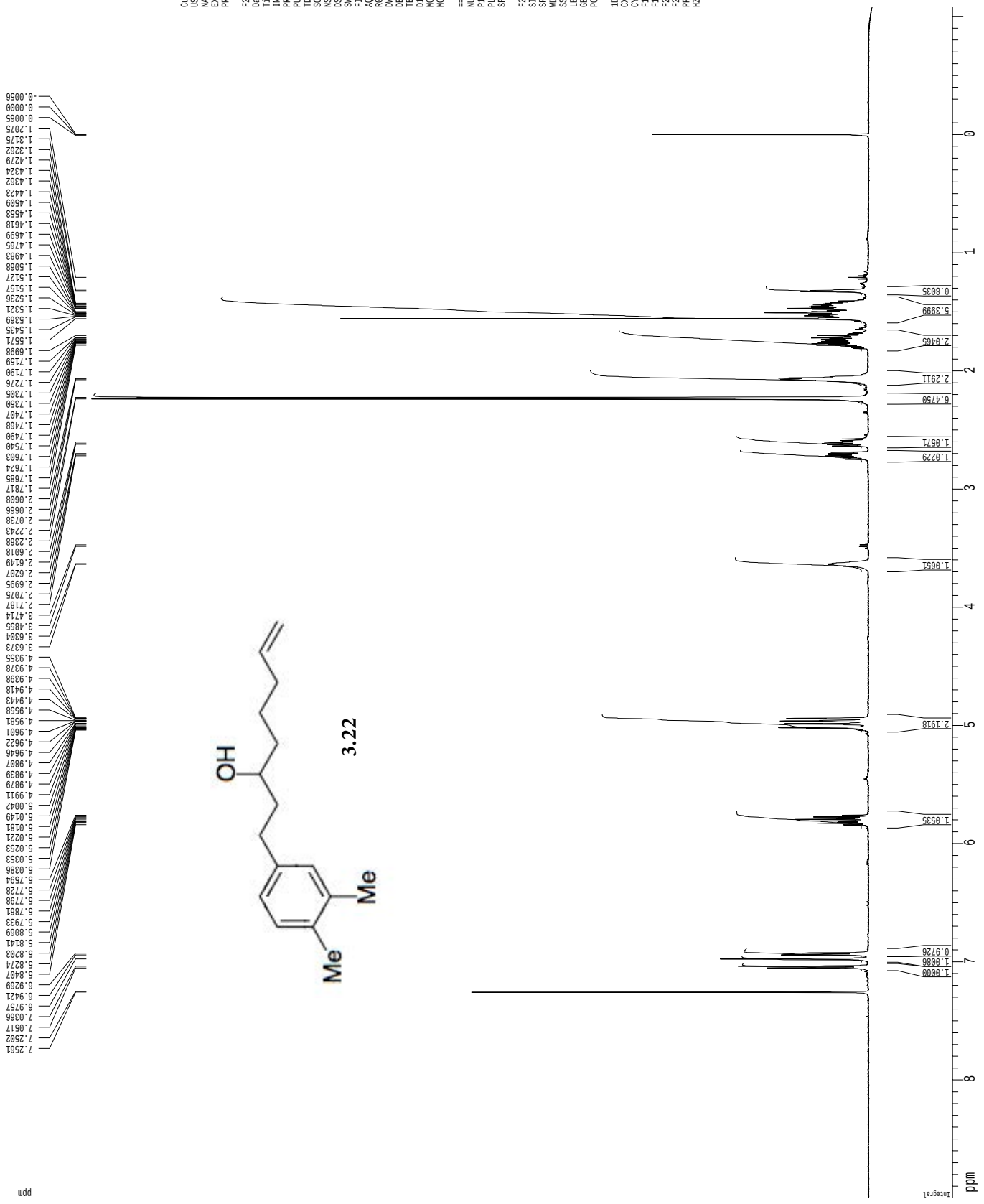
1D NMR plot parameters
CX 22.80 cm
CY 15.00 cm
F1P 230.150 ppm
F1 34730.32 Hz
F2P -9.951 ppm
F2 -1501.57 Hz
PPMCM 10.53074 ppm/cm
HZCM 1589.11768 Hz/cm


1H spectrum
Current Data Parameters
USER caherber
NAME CAH-I-276-full
EXPNO 1
PROCNO 1
F2 - Acquisition Parameters
Date_ 20210921
Time 9:21
INSTRUM cryo500
PROBHD 5 mm CPTCI 1H-
PULPROG zg30
TD 81728
SOLVENT CDCl3
NS 8
DS 2
SWH 8012.820 Hz
FIDRES 0.098043 Hz
AQ 5.0998774 sec
RG 5.7
DW 62.400 usec
DE 6.00 usec
TE 298.0 K
D1 0.10000000 sec
MCREST 0.00000000 sec
MCWRK 0.01500000 sec
======== CHANNEL f1 ========
NUC1 1H
P1 9.75 usec
PL1 1.00 dB
SFO1 500.2235015 MHz
F2 - Processing parameters
SI 65536
SF 500.2200335 MHz
WDW no
SSB 0
LB 0.00 Hz
GB 0
PC 1.00
1D NMR plot parameters
CX 22.80 cm
CY 15.00 cm
F1P 9.000 ppm
F1 4501.98 Hz
F2P -1.076 ppm
F2 -538.34 Hz
PPMCM 0.44194 ppm/cm
HZCM 221.06656 Hz/cm
0.0065
0.0000
0.0011
0.0037
0.0067
0.0090
1.4070
1.4211
1.5457
2.0973
2.1085
2.2250
2.2361
2.2654
2.2824
2.3052
2.3194
2.3502
2.3602
2.5707
2.7309
2.7324
2.7338
2.7355
2.7464
2.7485
2.7513
2.7613
2.7643
2.8793
2.8945
2.9095
6.9130
6.9282
6.9634
7.0455
7.0607
7.1988
7.2460
7.2538
7.2566
O
H
Me
Me
3.21
6.0872
2.0522
2.0721
1.0592
1.0755
1.0584
integral
ppm
0
1
2
3
4
5
6
7
8

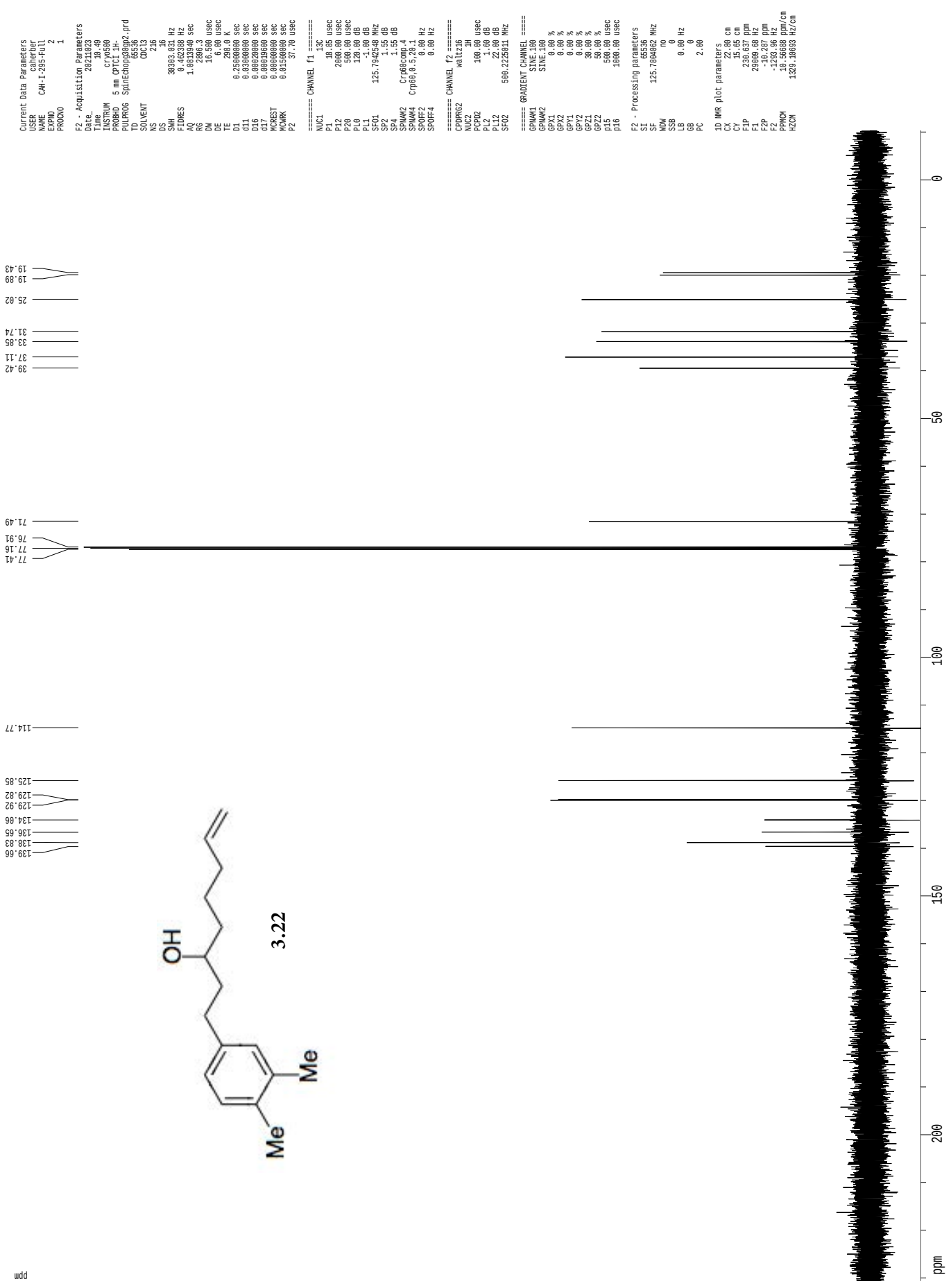
Z-restored spin-echo 13C spectrum with 1H decoupling



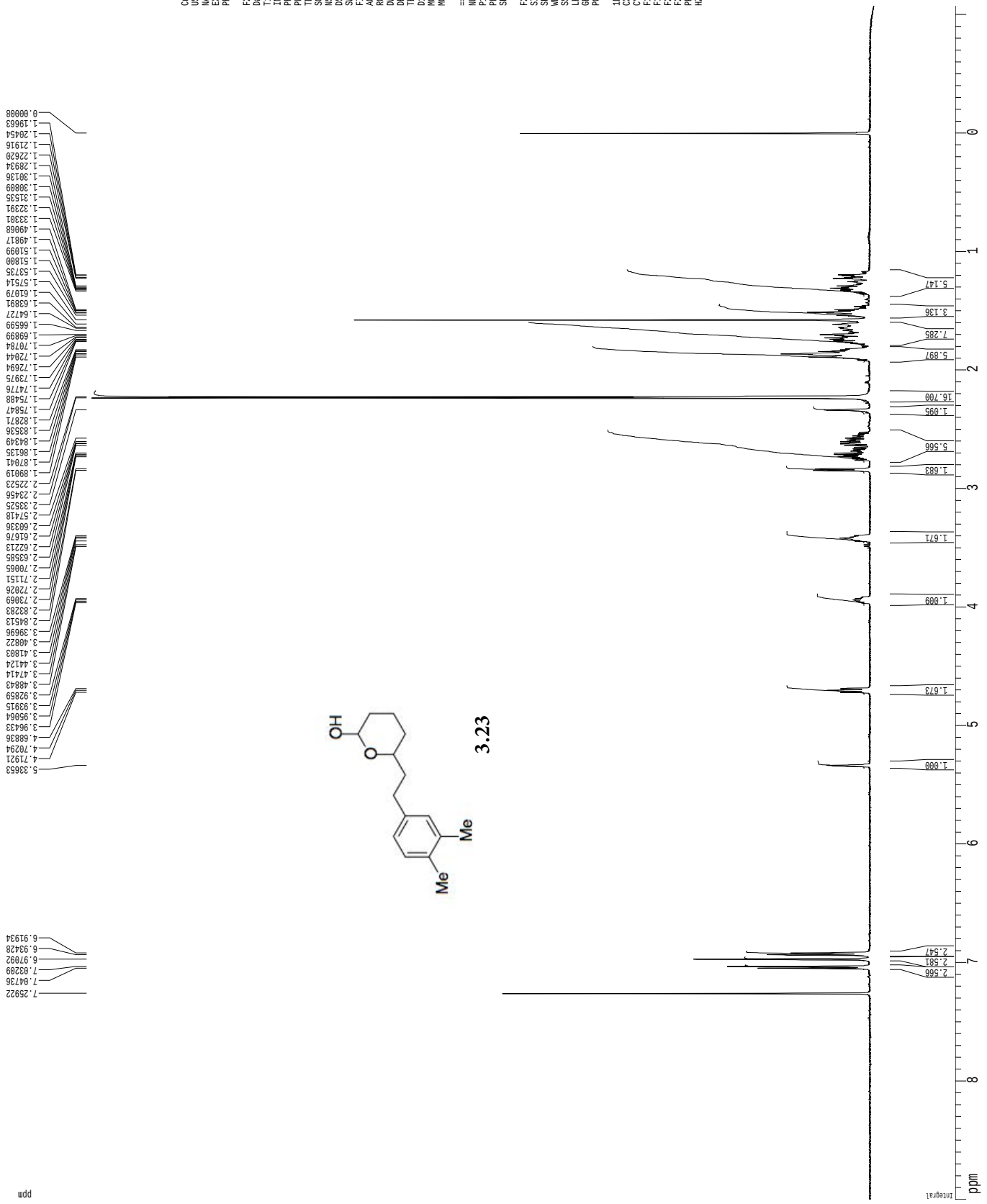
1H spectrum

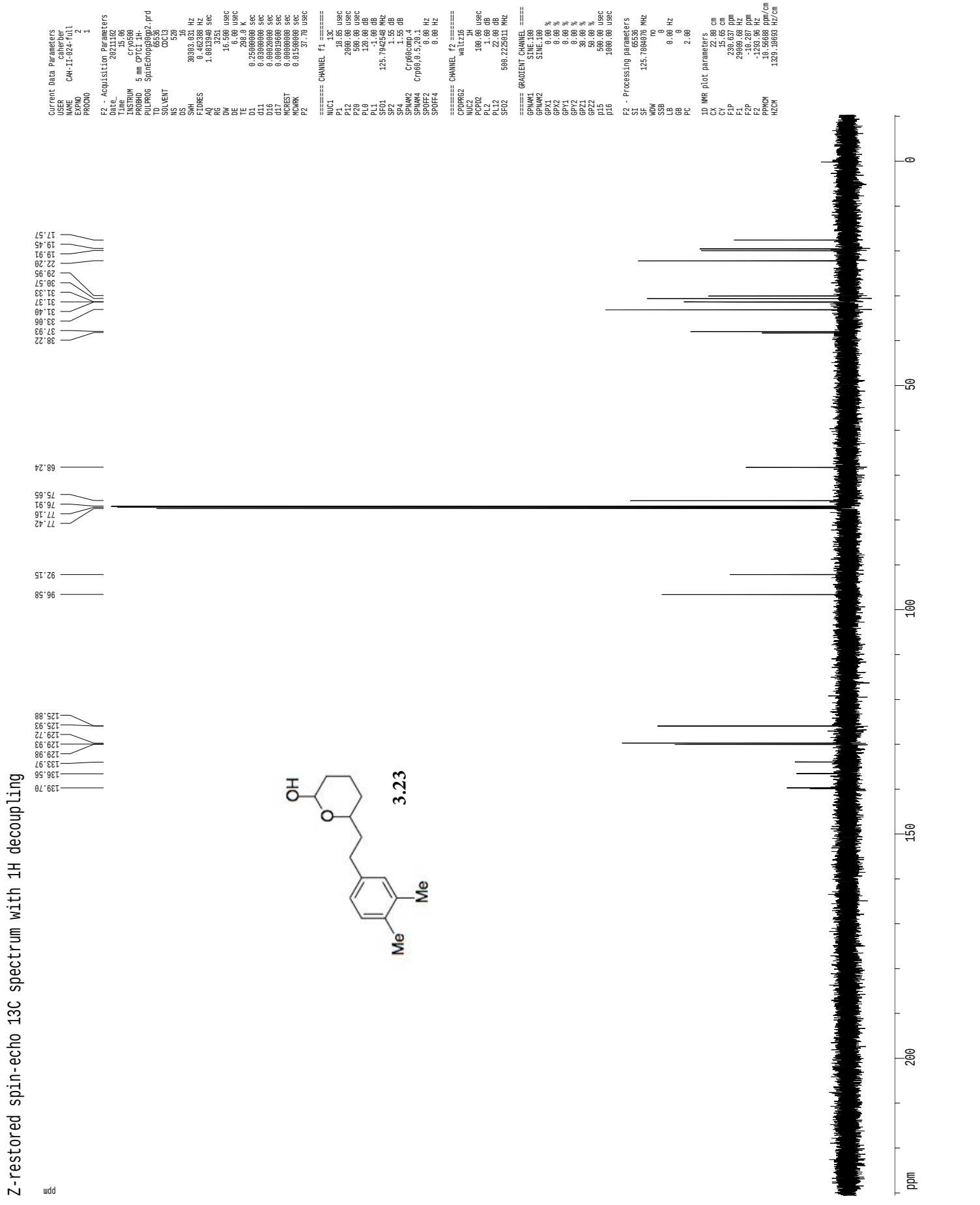

Current Data Parameters
USER caherber
NAME CAH-I-295-Full
EXPNO 1
PROCNO 1
F2 - Acquisition Parameters
Date_ 20211023
Time 10.44
INSTRUM cryo500
PROBHD 5 mm CPTCI 1H-
PULPROG zg30
TD 81728
SOLVENT CDCl3
NS 8
DS 2
SWH 8012.820 Hz
FIDRES 0.098043 Hz
AQ 5.0998774 sec
RG 6.3
DW 62.400 usec
DE 6.00 usec
TE 298.0 K
D1 0.10000000 sec
MCREST 0.00000000 sec
MCWRK 0.01500000 sec
======== CHANNEL f1 ========
NUC1 1H
P1 9.75 usec
PL1 1.00 dB
SFO1 500.2235015 MHz
F2 - Processing parameters
SI 65536
SF 500.2200331 MHz
WDW no
SSB 0
LB 0.00 Hz
GB 0
PC 1.00
1D NMR plot parameters
CX 22.80 cm
CY 15.00 cm
F1P 9.000 ppm
F1 4501.98 Hz
F2P -1.075 ppm
F2 -537.97 Hz
PPMCM 0.44191 ppm/cm
HZCM 221.05046 Hz/cm
OH
Me
Me
3.22
0.8035
5.3999
2.0465
2.2911
6.4750
1.0571
1.0229
1.0651
2.1918
1.0535
0.9726
1.0086
1.0000
integral
ppm

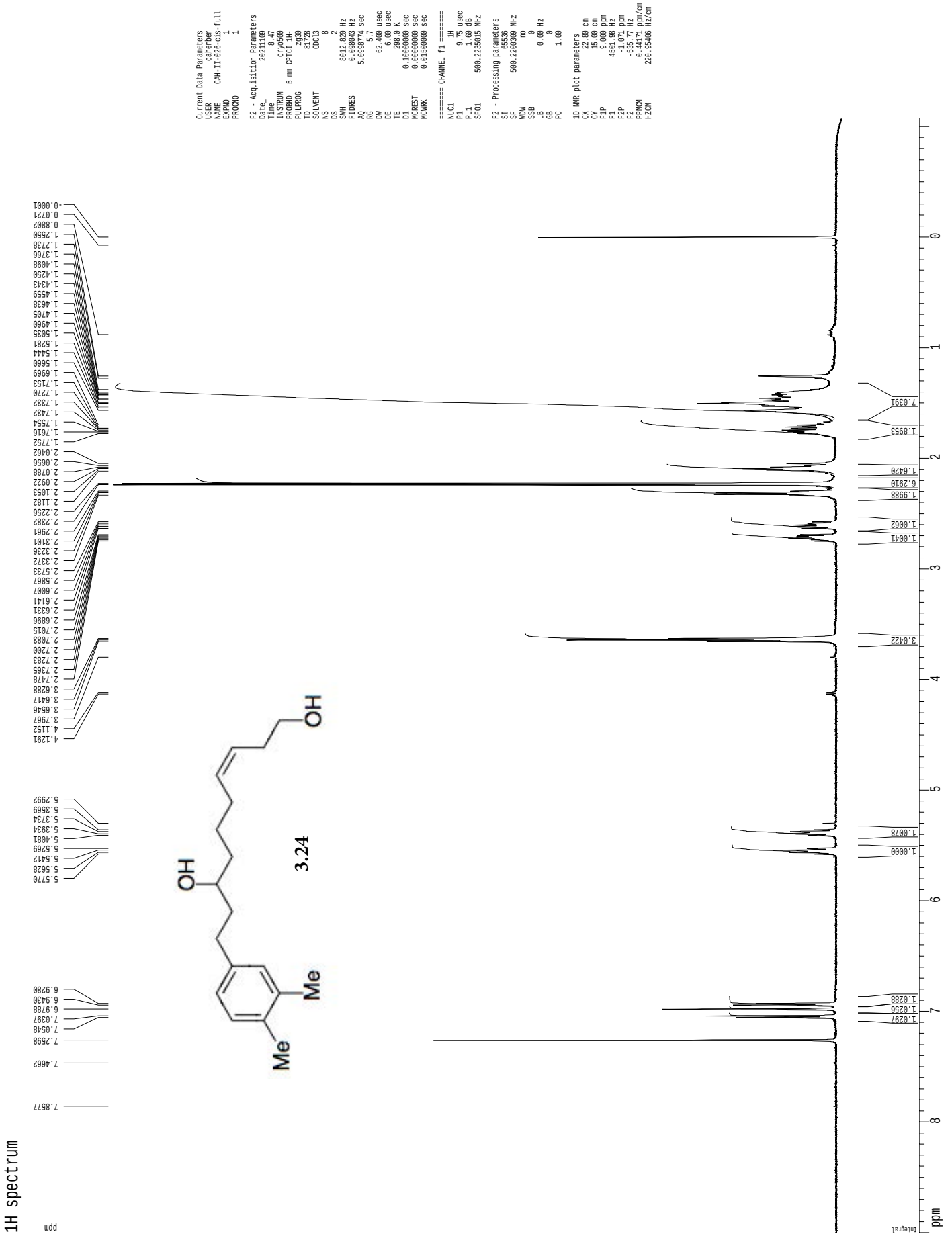
Z-restored spin-echo 13C spectrum with 1H decoupling



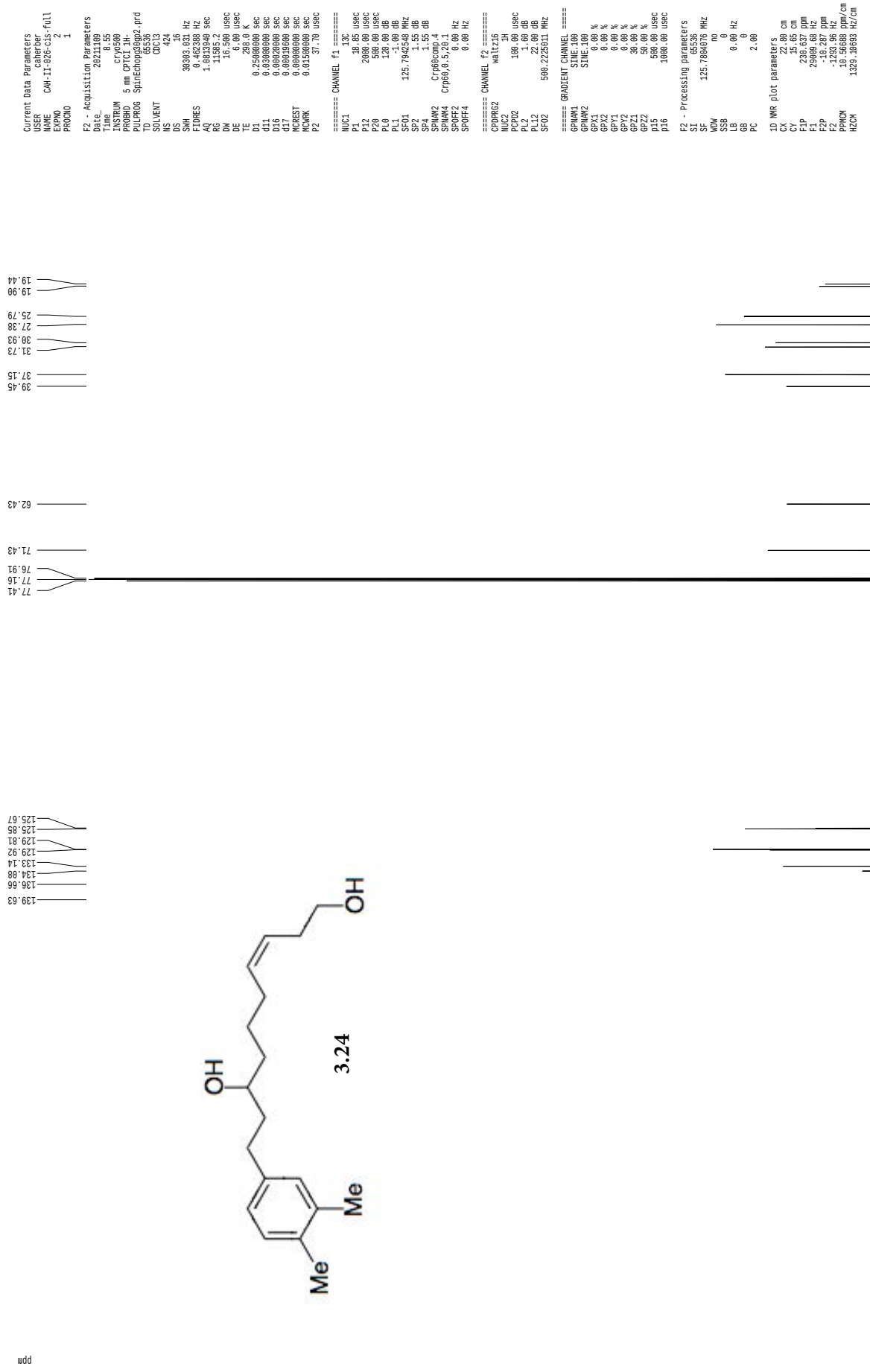
1H spectrum


Current Data Parameters
USER caherber
NAME CAH-II-024-full
EXPNO 1
PROCNO 1
F2 - Acquisition Parameters
Date_ 20211102
Time 14:54
INSTRUM cryo500
PROBHD 5 mm CPTCI 1H-
PULPROG zg30
TD 81728
SOLVENT CDCl3
NS 8
DS 2
SWH 8012.820 Hz
FIDRES 0.098043 Hz
AQ 5.0998774 sec
RG 5
DW 62.400 usec
DE 6.00 usec
TE 298.0 K
D1 0.10000000 sec
MCREST 0.00000000 sec
MCWRK 0.01500000 sec
======== CHANNEL f1 ========
NUC1 1H
P1 9.75 usec
PL1 1.00 dB
SFO1 500.2235015 MHz
F2 - Processing parameters
SI 65536
SF 500.2200313 MHz
WDW no
SSB 0
LB 0.00 Hz
GB 0
PC 1.00
1D NMR plot parameters
CX 22.80 cm
CY 15.00 cm
F1P 9.000 ppm
F1 4501.98 Hz
F2P -1.072 ppm
F2 -536.14 Hz
PPMCM 0.44175 ppm/cm
HZCM 220.97003 Hz/cm
OH
O
Me
Me
3.23
integral
ppm

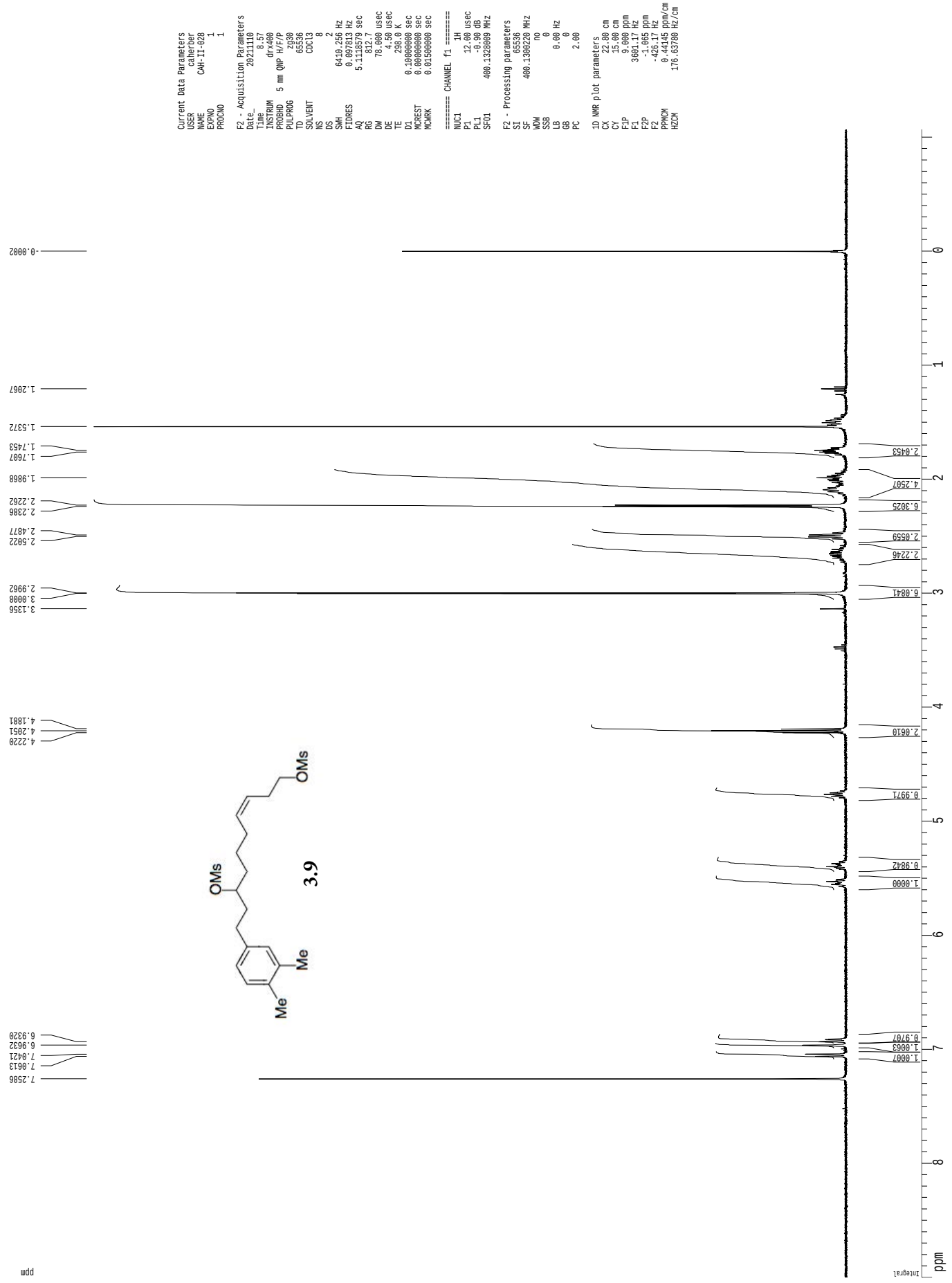

Z-restored spin-echo 13C spectrum with 1H decoupling
ppm
Current Data Parameters
USER Catherber
NAME CAH-II-024-full
EXPNO 2
PROCNO 1
F2 - Acquisition Parameters
Date_ 20211102
Time 15.06
INSTRUM cryo500
PROBHD 5 mm CPTCI 1H-
PULPROG SpinEchopg30gp2.prd
TD 65536
SOLVENT CDCl3
NS 520
DS 16
SWH 30303.031 Hz
FIDRES 0.462388 Hz
AQ 1.0813940 sec
RG 3251
DW 16.500 usec
DE 6.00 usec
TE 298.0 K
D1 0.25000000 sec
d11 0.03000000 sec
D16 0.00020000 sec
d17 0.00019600 sec
MCREST 0.00000000 sec
MCWRK 0.01500000 sec
P2 37.70 usec
======== CHANNEL f1 =======
NUC1 13C
P1 18.85 usec
P12 2000.00 usec
P20 500.00 usec
PL0 120.00 dB
PL1 -1.00 dB
SFO1 125.7942548 MHz
SP2 1.55 dB
SP4 1.55 dB
SPNAM2 Crp60comp.4
SPNAM4 Crp60,0.5,20.1
SPOFF2 0.00 Hz
SPOFF4 0.00 Hz
======== CHANNEL f2 =======
CPDPRG2 waltz16
NUC2 1H
PCPD2 100.00 usec
PL2 1.60 dB
PL12 22.00 dB
SFO2 500.2225011 MHz
===== GRADIENT CHANNEL ====
GPNAM1 SINE.100
GPNAM2 SINE.100
GPX1 0.00 %
GPX2 0.00 %
GPY1 0.00 %
GPY2 0.00 %
GPZ1 30.00 %
GPZ2 50.00 %
p15 500.00 usec
p16 1000.00 usec
F2 - Processing parameters
SI 65536
SF 125.7894076 MHz
WDW no
SSB 0
LB 0.00 Hz
GB 0
PC 2.00
1D NMR plot parameters
CX 22.80 cm
CY 15.65 cm
F1P 230.637 ppm
F1 29009.68 Hz
F2P -10.287 ppm
F2 -1293.96 Hz
PPMCM 10.56688 ppm/cm
HZCM 1329.10693 Hz/cm
38.22
37.93
33.06
31.40
31.37
31.33
30.57
29.95
22.20
19.91
19.45
17.57
68.24
77.42
77.16
76.91
75.65
96.58
92.15
139.70
136.56
133.97
129.98
129.93
129.72
125.93
125.88
OH
O
Me
Me
3.23
ppm
0
50
100
150
200


1H spectrum
ppm
Integral
OH
OH
Me
Me
3.24

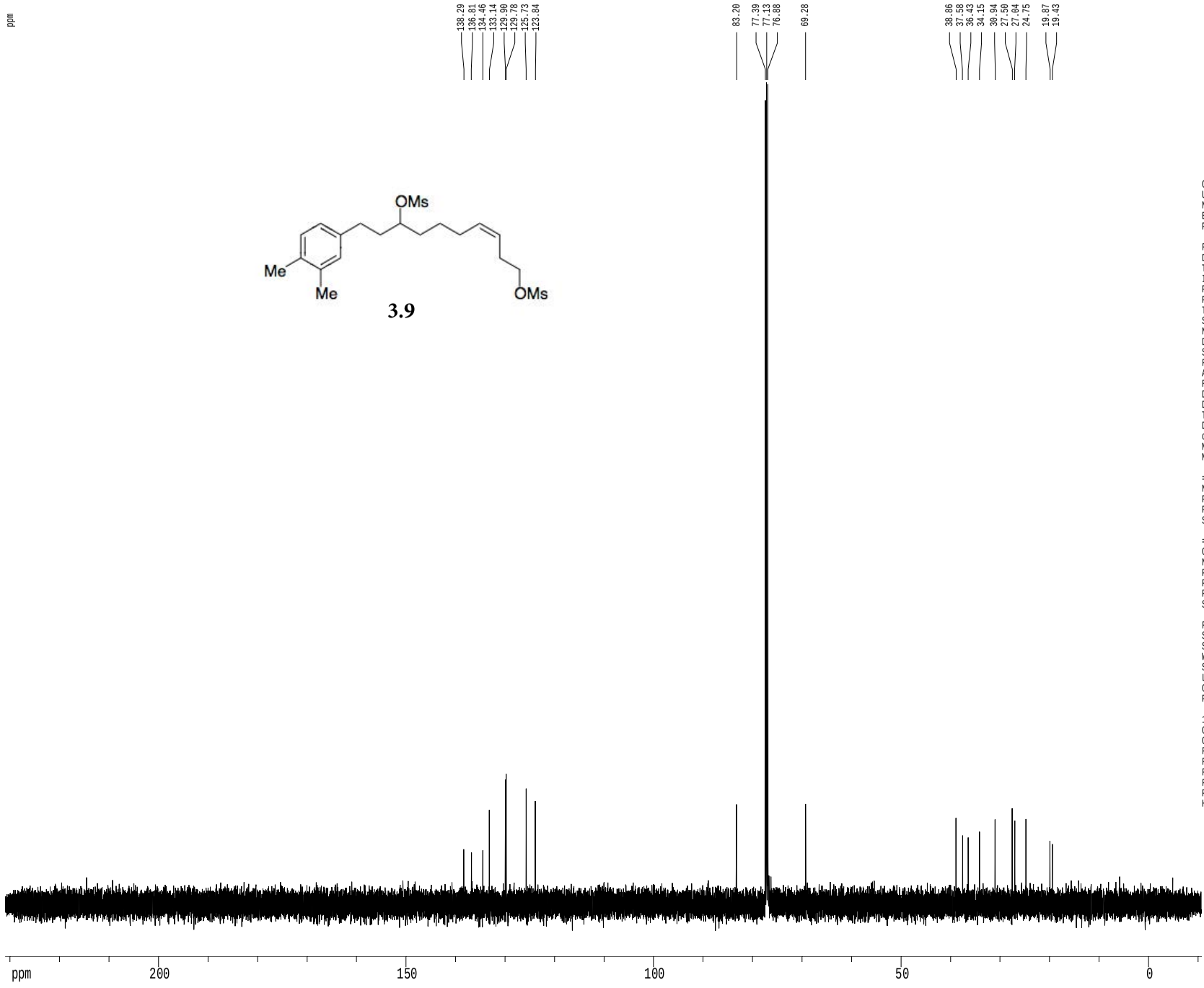
Z-restored spin-echo 13C spectrum with 1H decoupling



1H spectrum


Current Data Parameters
USER caliherber
NAME CAH-II-028
EXPNO 1
PROCNO 1
F2 - Acquisition Parameters
Date_ 20211110
Time 8.57
INSTRUM drx400
PROBHD 5 mm QNP H/F/P
PULPROG zg30
TD 65536
SOLVENT CDCl3
NS 8
DS 2
SWH 6410.256 Hz
FIDRES 0.097813 Hz
AQ 5.1118579 sec
RG 812.7
DW 78.000 usec
DE 4.50 usec
TE 298.0 K
D1 0.10000000 sec
MCREST 0.00000000 sec
MCWRK 0.01500000 sec
======== CHANNEL f1 ========
NUC1 1H
P1 12.00 usec
PL1 -0.90 dB
SFO1 400.1328009 MHz
F2 - Processing parameters
SI 65536
SF 400.1300220 MHz
WDW no
SSB 0
LB 0.00 Hz
GB 0
PC 2.00
1D NMR plot parameters
CX 22.80 cm
CY 15.00 cm
F1P 9.000 ppm
F1 3601.17 Hz
F2P -1.065 ppm
F2 -426.17 Hz
PPMCM 0.44145 ppm/cm
HZCM 176.63708 Hz/cm
0.0002
1.2067
1.5372
1.7453
1.7607
1.9868
2.2262
2.2386
2.4877
2.5022
2.9962
3.0008
3.1356
4.1881
4.2051
4.2220
6.9320
6.9632
7.0421
7.0613
7.2586
2.0453
4.2507
6.3025
2.0559
2.2246
6.0841
2.0610
0.9971
0.9842
1.0000
0.9707
1.0063
1.0007
OMs
OMs
Me
Me
3.9
integral
ppm

13C spectrum with 1H decoupling



Current Data Parameters
USER caherber
NAME CAH-II-029-13C
EXPNO 2
PROCNO 1

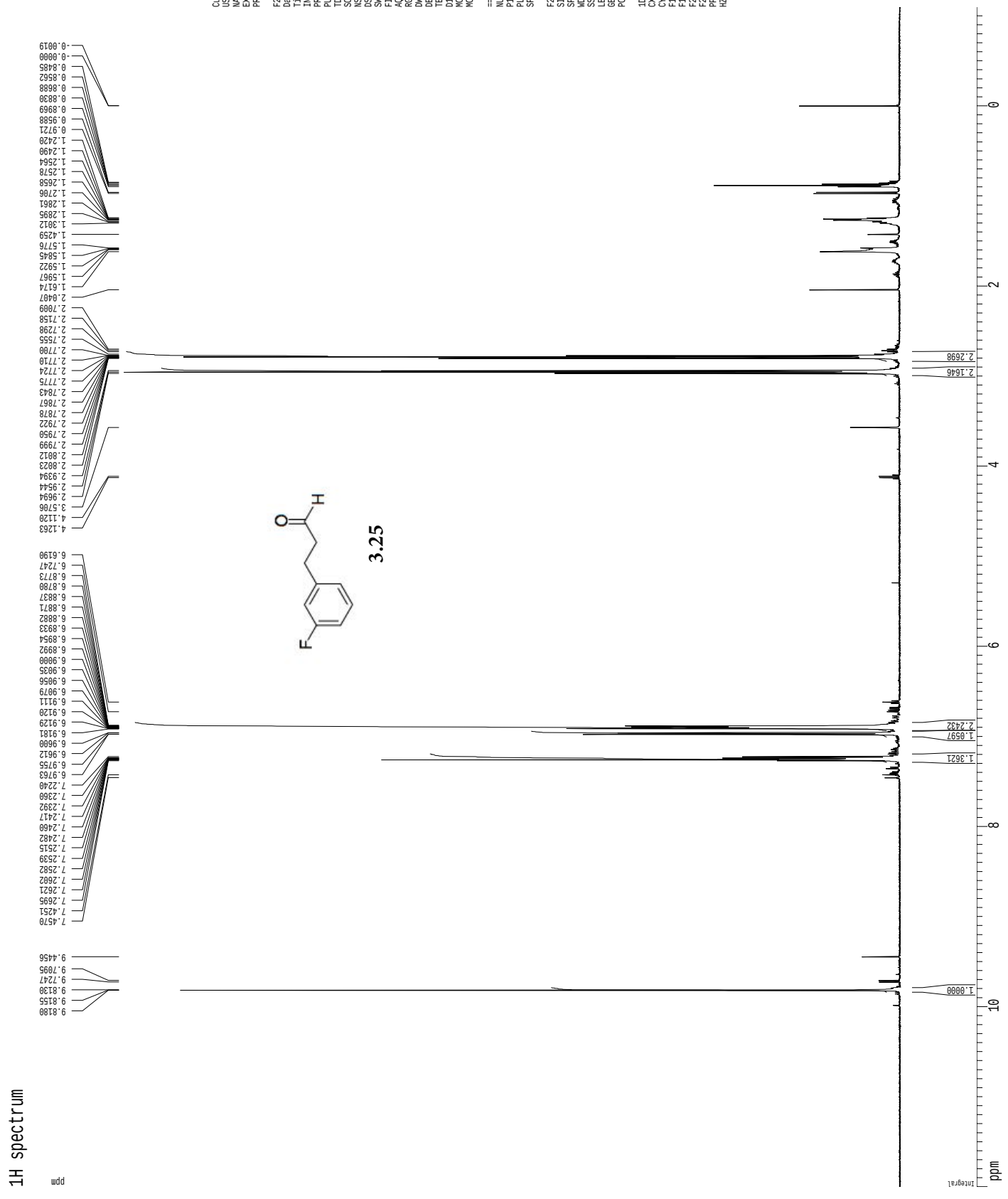
F2 - Acquisition Parameters
Date_ 20220114
Time 13.50
INSTRUM gn500
PROBHD 5 mm broadband
PULPROG zgdc30
TD 65536
SOLVENT CDCl3
NS 608
DS 4
SWH 30303.031 Hz
FIDRES 0.462388 Hz
AQ 1.0813940 sec
RG 46341
DW 16.500 usec
DE 6.00 usec
TE 293.1 K
D1 0.25000000 sec
d11 0.03000000 sec
MCREST 0.00000000 sec
MCWRK 0.01500000 sec

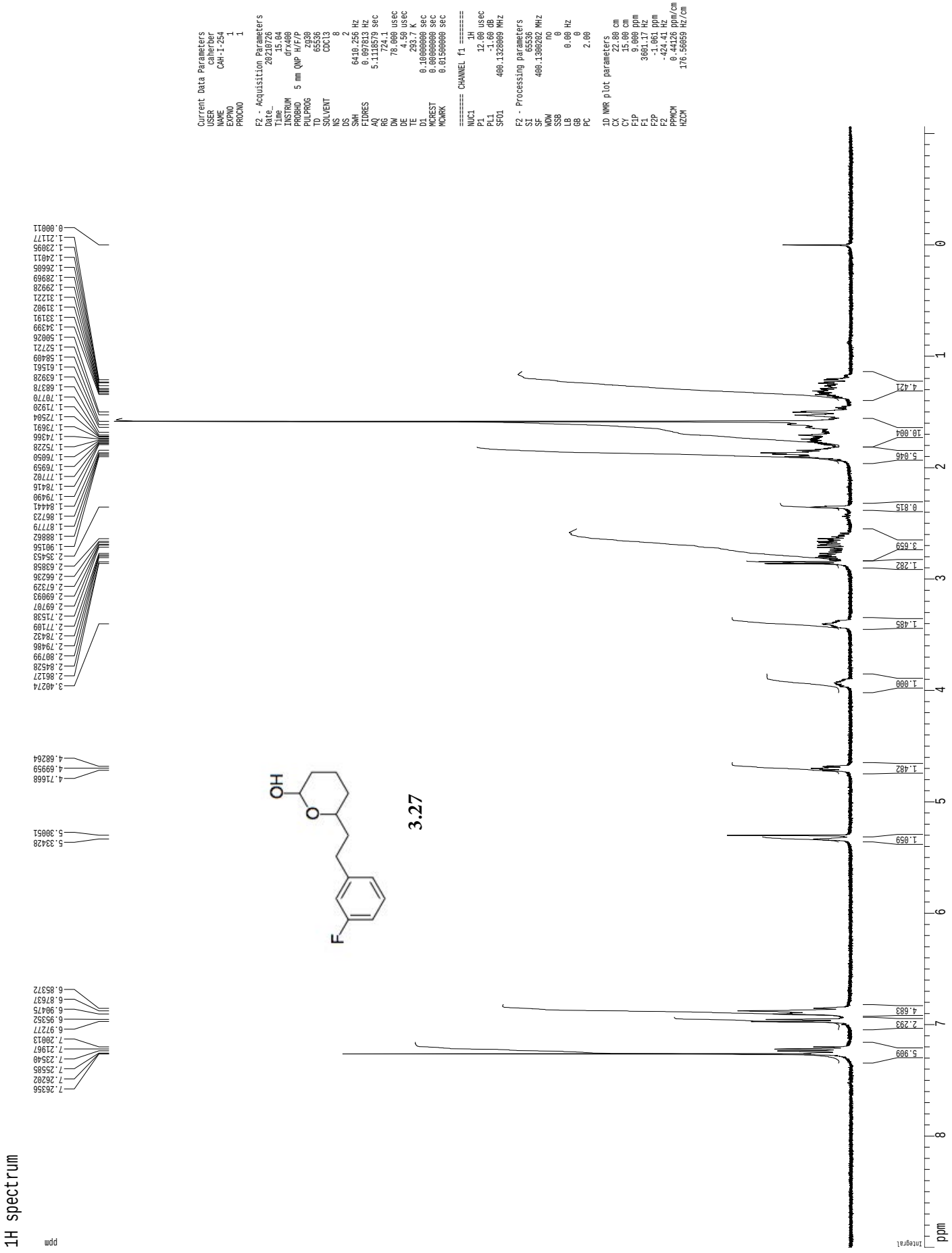
======== CHANNEL f1 ========
NUC1 13C
P1 14.20 usec
PL1 -6.00 dB
SFO1 125.3994349 MHz

======== CHANNEL f2 ========
CPDPRG2 waltz16
NUC2 1H
PCPD2 100.00 usec
PL2 -6.00 dB
PL12 12.30 dB
SFO2 498.6524933 MHz

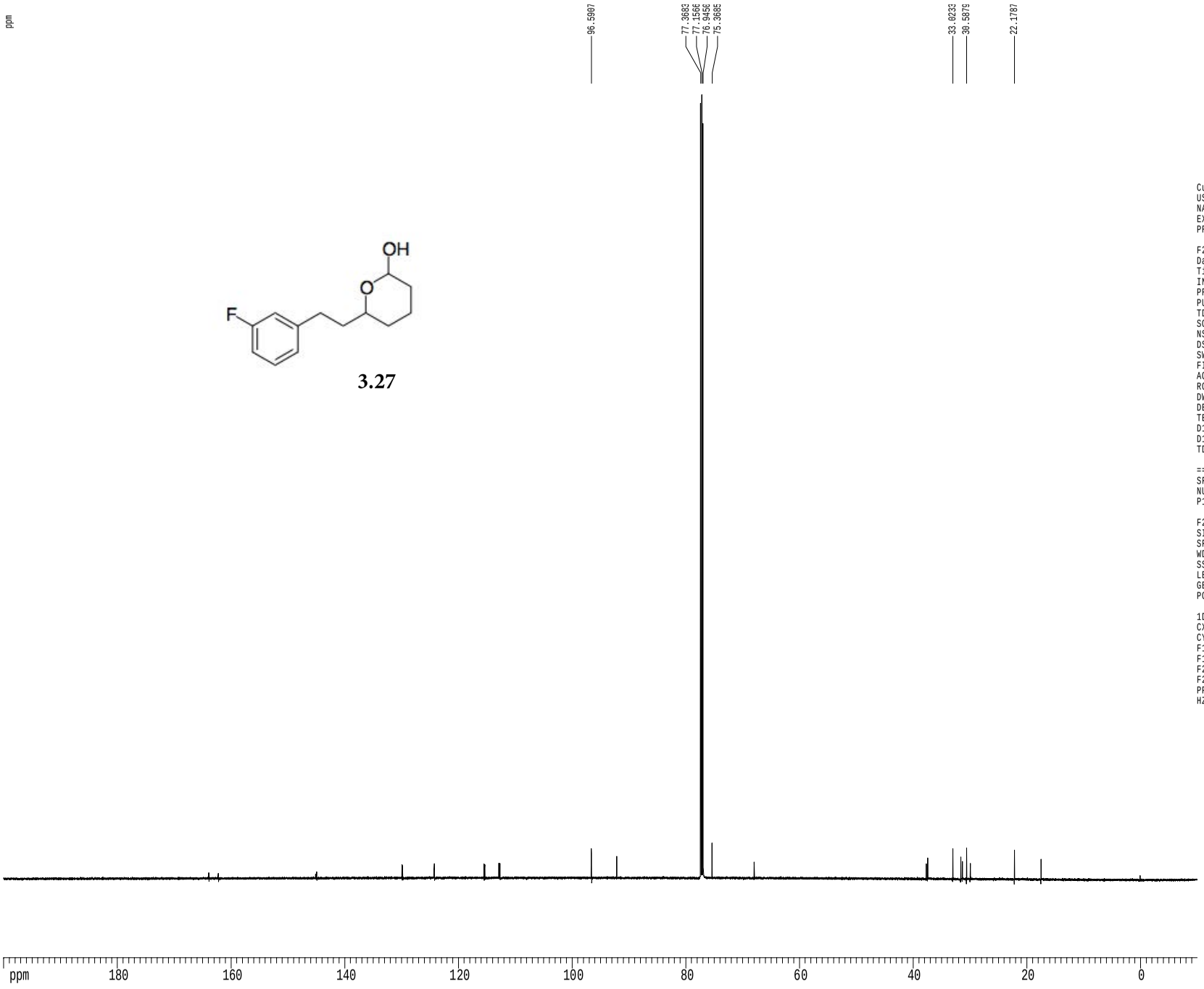
F2 - Processing parameters
SI 65536
SF 125.3856343 MHz
WDW no
SSB 0
LB 0.00 Hz
GB 0
PC 2.00

1D NMR plot parameters
CX 22.80 cm
CY 15.65 cm
F1P 230.956 ppm
F1 28958.52 Hz
F2P -10.723 ppm
F2 -1344.51 Hz
PPMCM 10.59994 ppm/cm
HZCM 1329.08032 Hz/cm


1H spectrum
Current Data Parameters
USER calherber
NAME CAH-I-250
EXPNO 1
PROCNO 1
F2 - Acquisition Parameters
Date_ 20210720
Time 15.44
INSTRUM spect
PROBHD 5 mm broadband
PULPROG zg30
TD 81728
SOLVENT CDCl3
NS 8
DS 2
SWH 8012.820 Hz
FIDRES 0.098043 Hz
AQ 5.0998774 sec
RG 574.7
DW 62.400 usec
DE 6.00 usec
TE 297.9 K
D1 0.10000000 sec
MCREST 0.00000000 sec
MCWRK 0.01500000 sec
======== CHANNEL f1 ========
NUC1 1H
P1 12.00 usec
PL1 -6.00 dB
SFO1 498.6534906 MHz
F2 - Processing parameters
SI 65536
SF 498.6500298 MHz
WDW no
SSB 0
LB 0.00 Hz
GB 0
PC 1.00
1D NMR plot parameters
CX 22.80 cm
CY 15.00 cm
F1P 12.000 ppm
F1 5983.80 Hz
F2P -1.093 ppm
F2 -544.82 Hz
PPMCM 0.57424 ppm/cm
HZCM 286.34293 Hz/cm
O
H
F
3.25
9.8180
9.8155
9.8130
9.7247
9.7095
9.4456
7.4570
7.4251
7.2695
7.2621
7.2602
7.2582
7.2539
7.2515
7.2482
7.2460
7.2417
7.2392
7.2360
7.2240
6.9763
6.9755
6.9612
6.9600
6.9181
6.9129
6.9120
6.9111
6.9079
6.9056
6.9035
6.9000
6.8992
6.8954
6.8933
6.8882
6.8871
6.8837
6.8780
6.8773
6.7247
6.6190
4.1263
4.1120
3.5706
2.9694
2.9544
2.9394
2.8023
2.8012
2.7999
2.7950
2.7922
2.7878
2.7867
2.7843
2.7775
2.7724
2.7710
2.7700
2.7555
2.7298
2.7158
2.7009
2.0407
1.6174
1.5967
1.5922
1.5845
1.5776
1.4259
1.3012
1.2895
1.2861
1.2706
1.2658
1.2578
1.2564
1.2490
1.2420
0.9721
0.9588
0.8830
0.8688
0.8562
0.8485
0.0000
0.0019
1.0000
2.2698
2.1646
2.2432
1.0597
1.3621
integral
ppm
0
2
4
6
8
10


1H spectrum
3.27
ppm

13C Spectrum



Current Data Parameters
USER caherber
NAME CAH-I-254-full
EXPNO 3
PROCNO 1

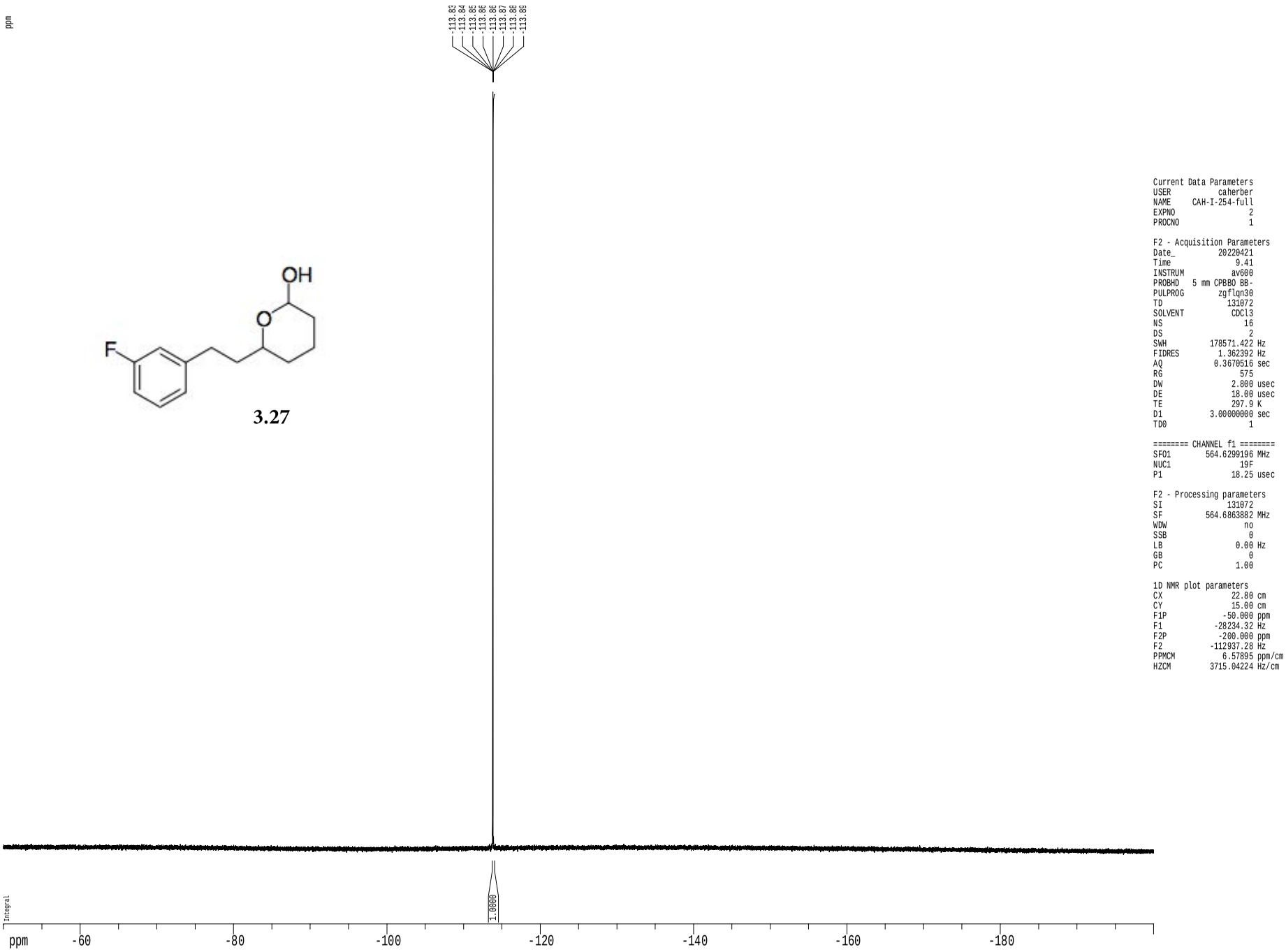
F2 - Acquisition Parameters
Date_ 20220421
Time 9.54
INSTRUM av600
PROBHD 5 mm CPBBO BB-
PULPROG zgdc30
TD 65536
SOLVENT CDCl3
NS 912
DS 4
SWH 36231.883 Hz
FIDRES 0.552855 Hz
AQ 0.9044468 sec
RG 2050
DW 13.800 usec
DE 19.63 usec
TE 298.0 K
D1 0.40000001 sec
D11 0.03000000 sec
TD0 1

======== CHANNEL f1 ========
SFO1 150.9194080 MHz
NUC1 13C
P1 10.10 usec

F2 - Processing parameters
SI 65536
SF 150.9027936 MHz
WDW no
SSB 0
LB 0.00 Hz
GB 0
PC 1.00

1D NMR plot parameters
CX 22.80 cm
CY 15.00 cm
F1P 200.000 ppm
F1 30180.56 Hz
F2P -9.950 ppm
F2 -1501.56 Hz
PPMCM 9.20835 ppm/cm
HZCM 1389.56641 Hz/cm

19F spectrum



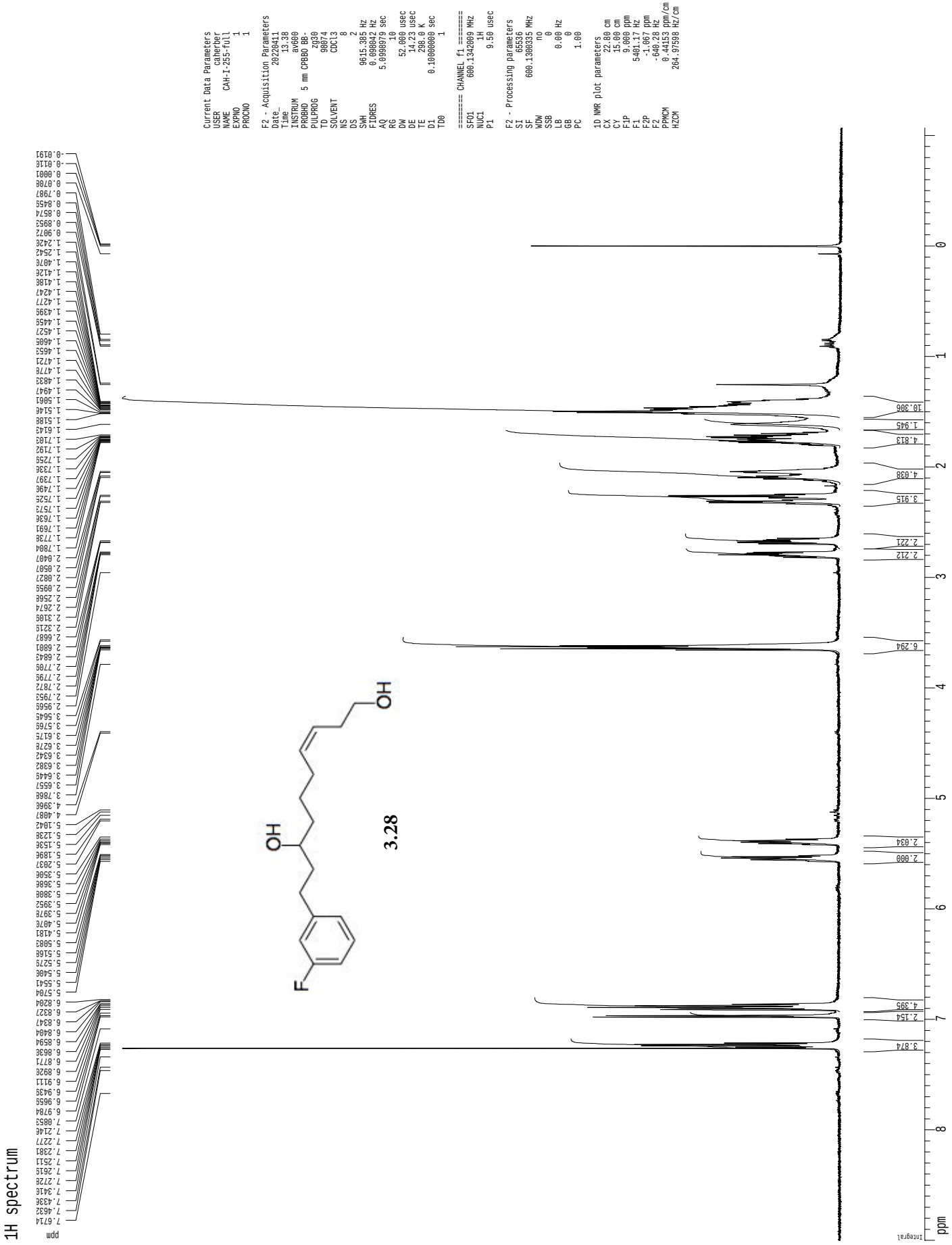

```
Current Data Parameters
USER            caherber
NAME      CAH-I-254-full
EXPNO                   2
PROCNO                  1

F2 - Acquisition Parameters
Date_            20220421
Time                9.41
INSTRUM            av600
PROBHD   5 mm CPBBO BB-
PULPROG         zgflqn30
TD                131072
SOLVENT             CDCl3
NS                     16
DS                      2
SWH           178571.422 Hz
FIDRES          1.362392 Hz
AQ              0.3670516 sec
RG                    575
DW                2.800 usec
DE                18.00 usec
TE                297.9 K
D1            3.00000000 sec
TD0                     1

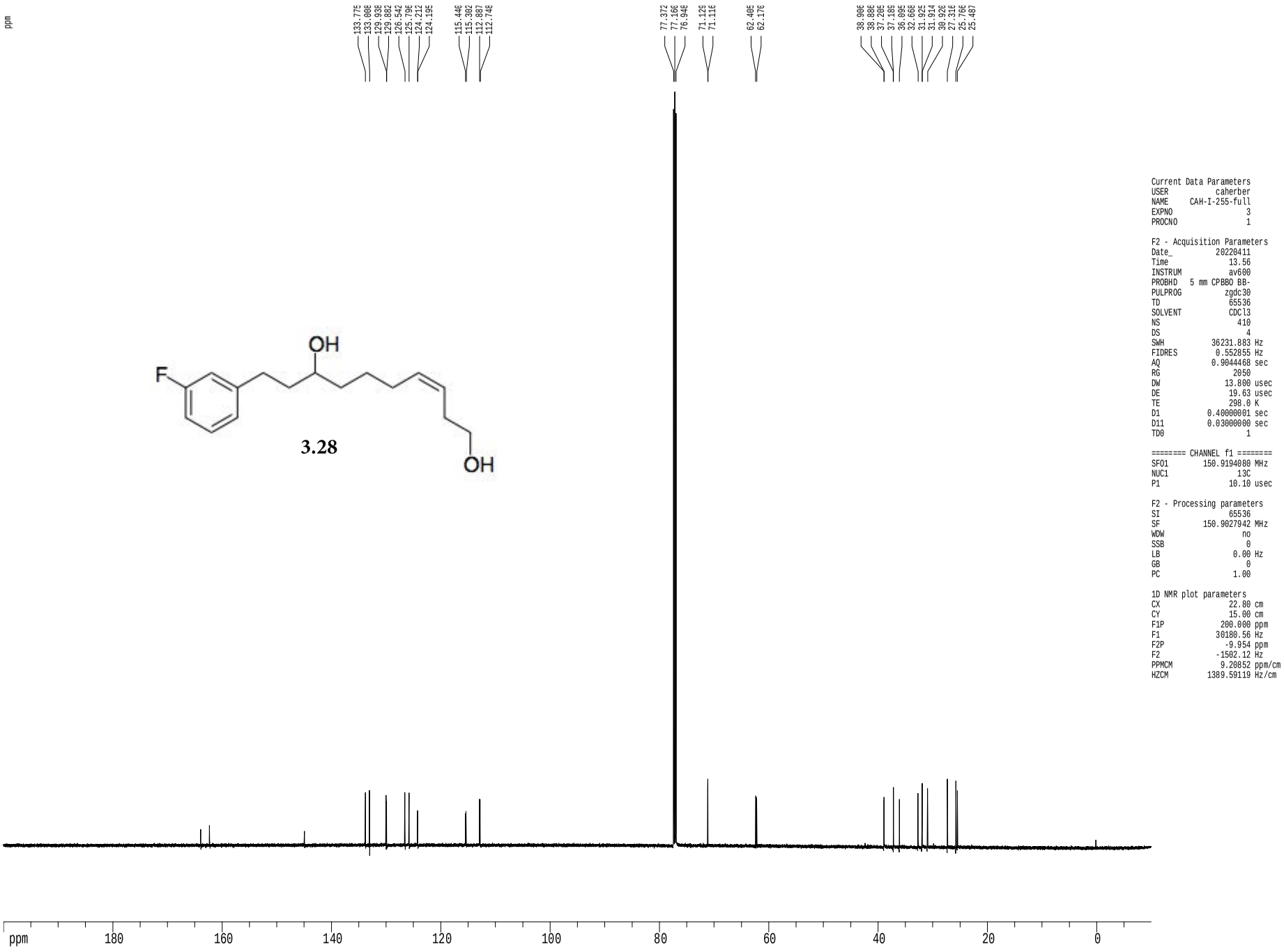
======== CHANNEL f1 ========
SFO1         564.6299196 MHz
NUC1                  19F
P1                 18.25 usec

F2 - Processing parameters
SI                 131072
SF           564.6863882 MHz
WDW                    no
SSB                     0
LB                 0.00 Hz
GB                      0
PC                 1.00

1D NMR plot parameters
CX                 22.80 cm
CY                 15.00 cm
F1P              -50.000 ppm
F1             -28234.32 Hz
F2P              -200.000 ppm
F2             -112937.28 Hz
PPMCM            6.57895 ppm/cm
HZCM          3715.04224 Hz/cm
```


1H spectrum
Current Data Parameters
USER caherber
NAME CAH-I-255-full
EXPNO 1
PROCNO 1
F2 - Acquisition Parameters
Date_ 20220411
Time 13.38
INSTRUM av600
PROBHD 5 mm CPBBO BB-
PULPROG 2d30
TD 98874
SOLVENT CDCl3
NS 2
DS 2
SWH 9615.385 Hz
FIDRES 0.098042 Hz
AQ 5.0998979 sec
RG 10
DW 52.000 usec
DE 14.23 usec
TE 298.0 K
D1 0.10000000 sec
TD0 1
======== CHANNEL f1 ========
SFO1 600.1342009 MHz
NUC1 1H
P1 9.50 usec
F2 - Processing parameters
SI 65536
SF 600.1300335 MHz
WDW no
SSB 0
LB 0.00 Hz
GB 0
PC 1.00
1D NMR plot parameters
CX 22.80 cm
CY 15.00 cm
F1P 9.000 ppm
F1 5401.17 Hz
F2P -1.067 ppm
F2 -640.28 Hz
PPMCM 0.44153 ppm/cm
HZCM 264.97598 Hz/cm
OH
OH
F
3.28
10.306
1.945
4.813
4.038
3.915
2.221
2.212
6.294
2.034
2.000
4.395
2.154
3.874
ppm
Integral

13C spectrum



Current Data Parameters
USER caherber
NAME CAH-I-255-full
EXPNO 3
PROCNO 1

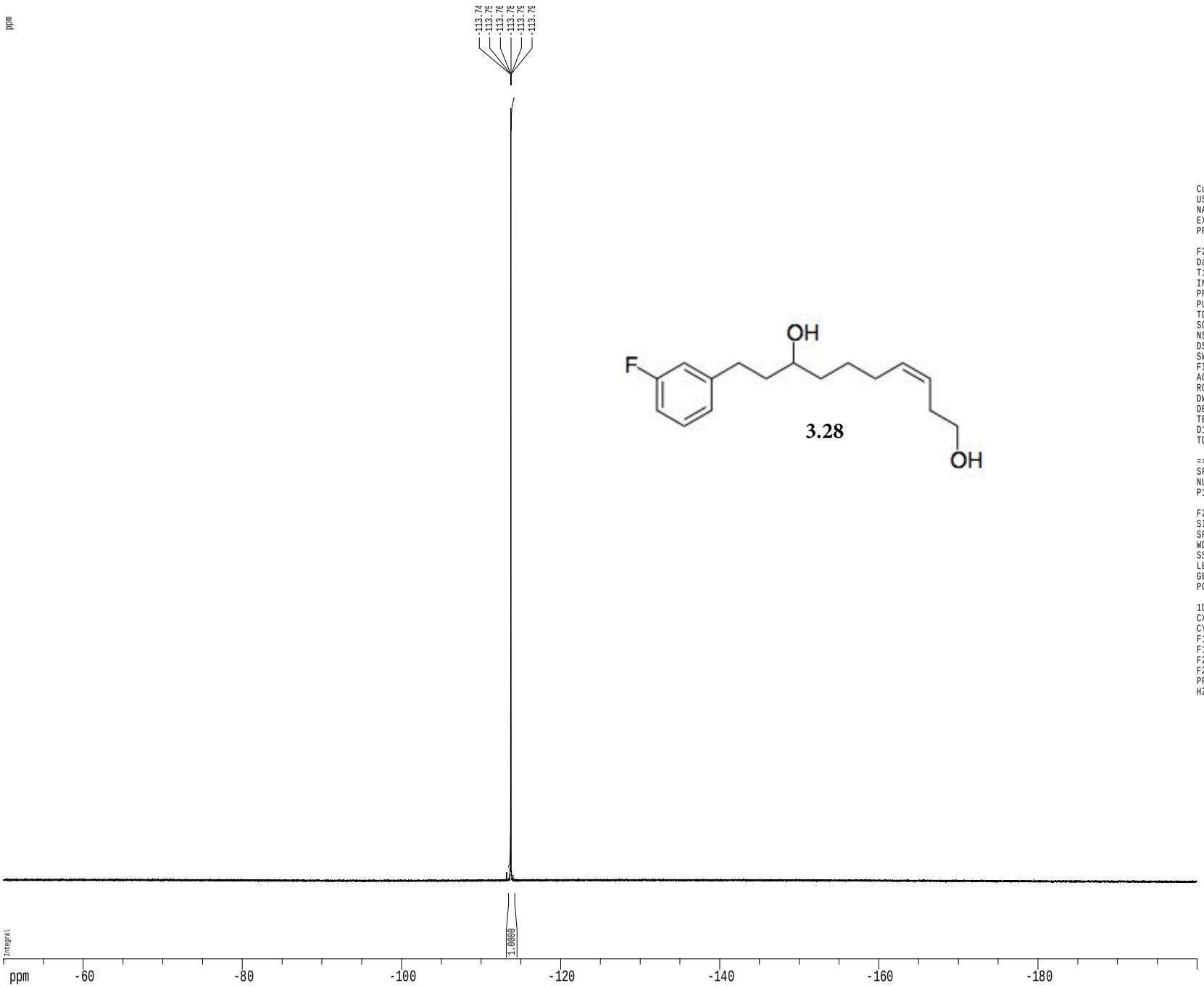
F2 - Acquisition Parameters
Date_ 20220411
Time 13.56
INSTRUM av600
PROBHD 5 mm CPBBO BB-
PULPROG zgdc30
TD 65536
SOLVENT CDCl3
NS 410
DS 4
SWH 36231.883 Hz
FIDRES 0.552855 Hz
AQ 0.9044468 sec
RG 2050
DW 13.800 usec
DE 19.63 usec
TE 298.0 K
D1 0.40000001 sec
D11 0.03000000 sec
TD0 1

======== CHANNEL f1 ========
SFO1 150.9194080 MHz
NUC1 13C
P1 10.10 usec

F2 - Processing parameters
SI 65536
SF 150.9027942 MHz
WDW no
SSB 0
LB 0.00 Hz
GB 0
PC 1.00

1D NMR plot parameters
CX 22.80 cm
CY 15.00 cm
F1P 200.000 ppm
F1 30180.56 Hz
F2P -9.954 ppm
F2 -1502.12 Hz
PPMCM 9.20852 ppm/cm
HZCM 1389.59119 Hz/cm

19F spectrum



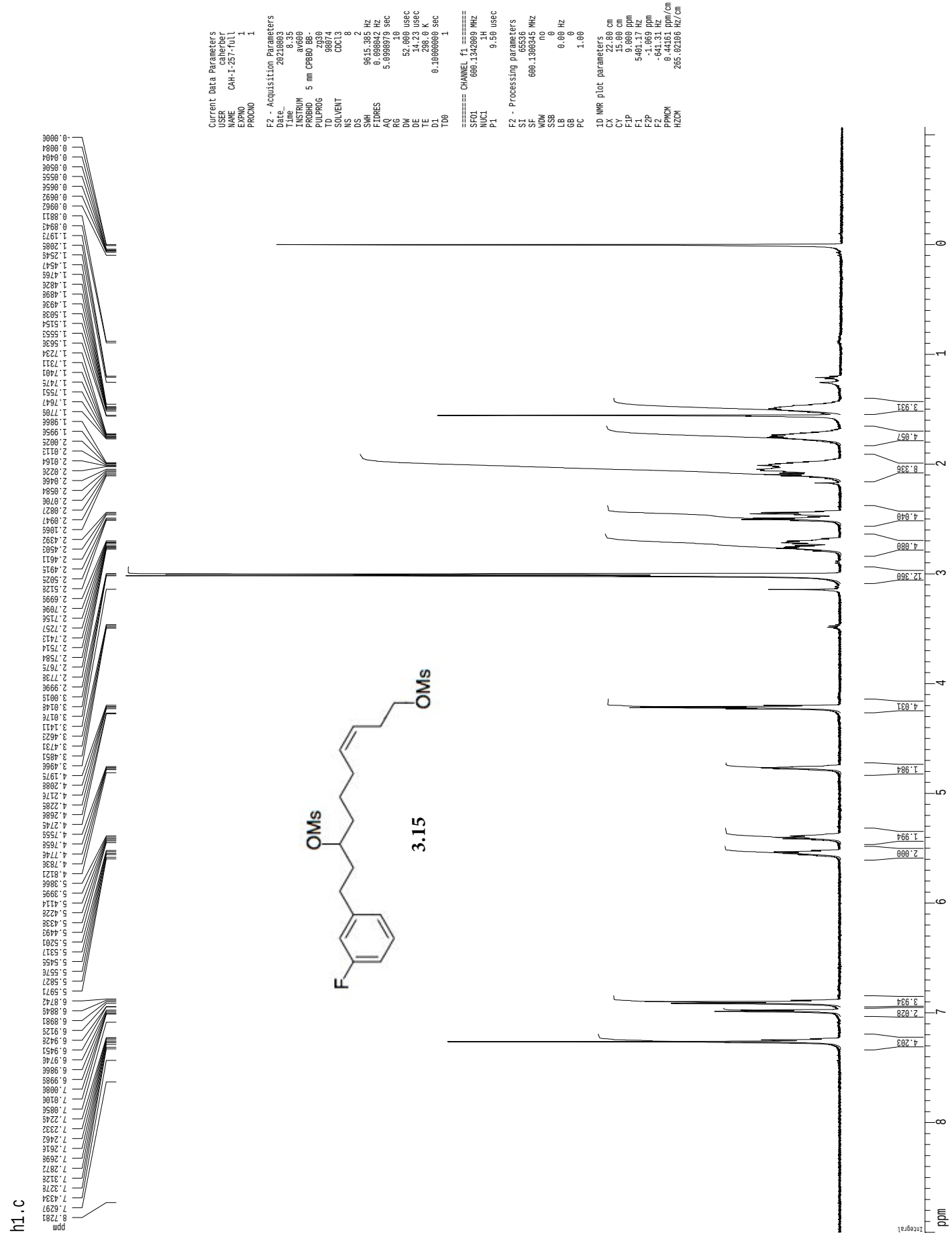

```
Current Data Parameters
USER            caherber
NAME      CAH-I-255-full
EXPNO                   2
PROCNO                  1

F2 - Acquisition Parameters
Date_            20220411
Time                13.44
INSTRUM             av600
PROBHD   5 mm CPBBO BB-
PULPROG          zgflqn30
TD                131072
SOLVENT             CDCl3
NS                     16
DS                      2
SWH           178571.422 Hz
FIDRES          1.362392 Hz
AQ             0.3670516 sec
RG                    575
DW                2.800 usec
DE                18.00 usec
TE                298.0 K
D1            3.00000000 sec
TD0                     1

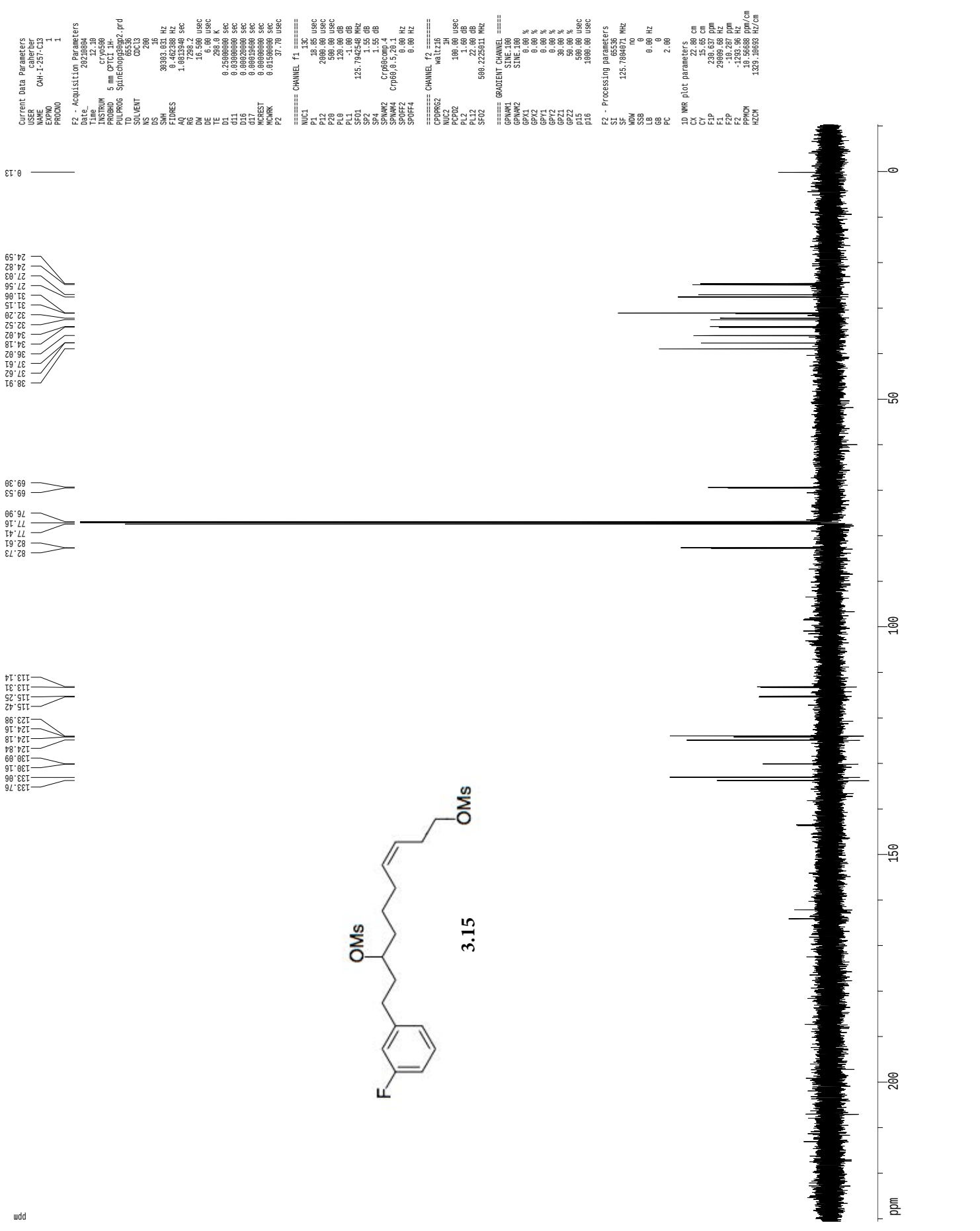
======== CHANNEL f1 ========
SFO1         564.6299196 MHz
NUC1                  19F
P1                 18.25 usec

F2 - Processing parameters
SI                 131072
SF           564.6863882 MHz
WDW                    no
SSB                     0
LB                 0.00 Hz
GB                      0
PC                 1.00

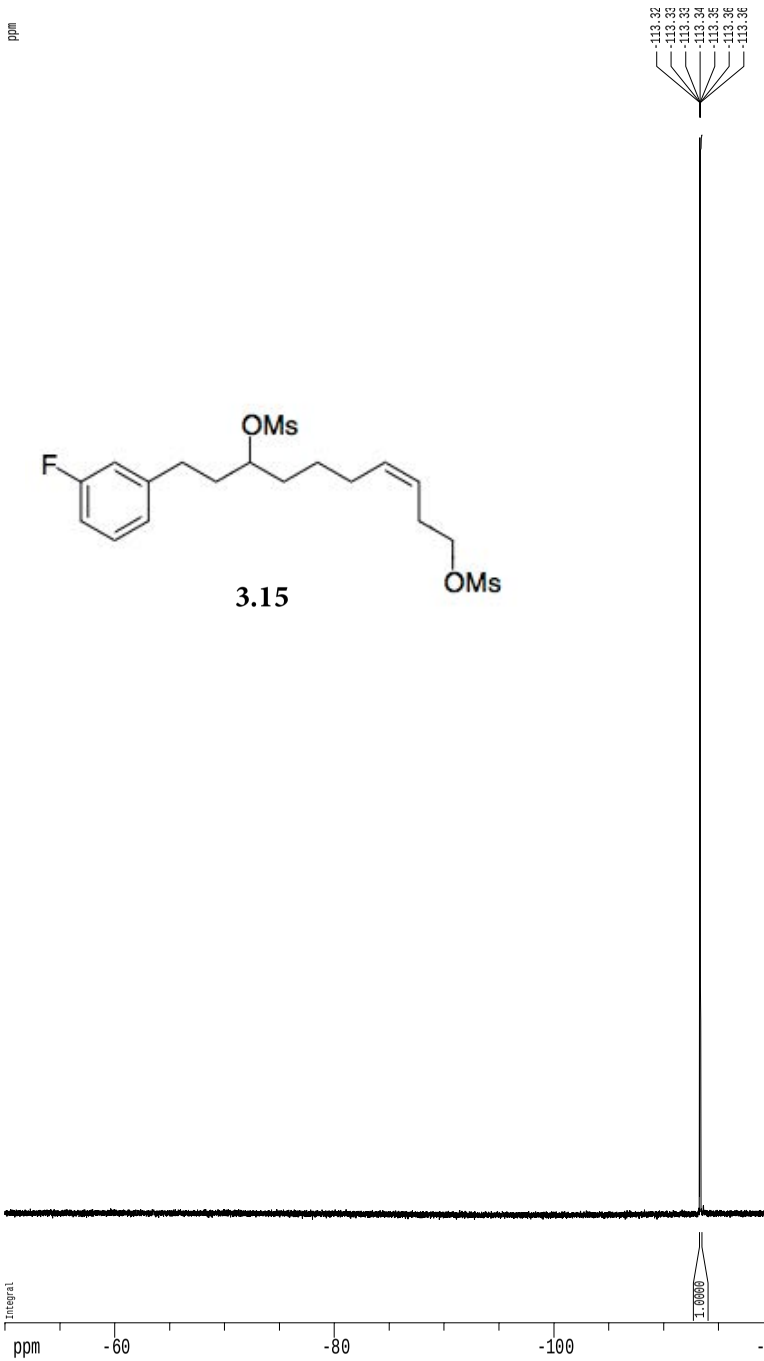
1D NMR plot parameters
CX                 22.80 cm
CY                 15.00 cm
F1P              -50.000 ppm
F1             -28234.32 Hz
F2P              -200.000 ppm
F2             -112937.28 Hz
PPMCM            6.57895 ppm/cm
HZCM          3715.04224 Hz/cm
```


h1.c
Current Data Parameters
USER caherber
NAME CAH-I-257-full
EXPNO 1
PROCNO 1
F2 - Acquisition Parameters
Date_ 20210803
Time 8.35
INSTRUM av600
PROBHD 5 mm CPBBO BB-
PULPROG 2d30
TD 98874
SOLVENT CDCl3
NS 2
DS 2
SWH 9615.385 Hz
FIDRES 0.098042 Hz
AQ 5.0998979 sec
RG 10
DW 52.000 usec
DE 14.23 usec
TE 298.0 K
D1 0.10000000 sec
TD0 1
======= CHANNEL f1 =======
SFO1 600.1342009 MHz
NUC1 1H
P1 9.50 usec
F2 - Processing parameters
SI 65536
SF 600.1300345 MHz
WDW no
SSB 0
LB 0.00 Hz
GB 0
PC 1.00
1D NMR plot parameters
CX 22.80 cm
CY 15.00 cm
F1P 9.000 ppm
F1 5401.17 Hz
F2P -1.069 ppm
F2 -641.31 Hz
PPMCM 0.44161 ppm/cm
HZCM 265.02106 Hz/cm
OMs
OMs
F
3.15
ppm
Integral
3.931
4.057
8.336
4.040
4.080
12.360
4.031
1.984
1.994
2.000
3.934
2.028
4.203

Z-restored spin-echo 13C spectrum with 1H decoupling



f19.c



Current Data Parameters
USER caherber
NAME CAH-I-257-full
EXPNO 3
PROCNO 1

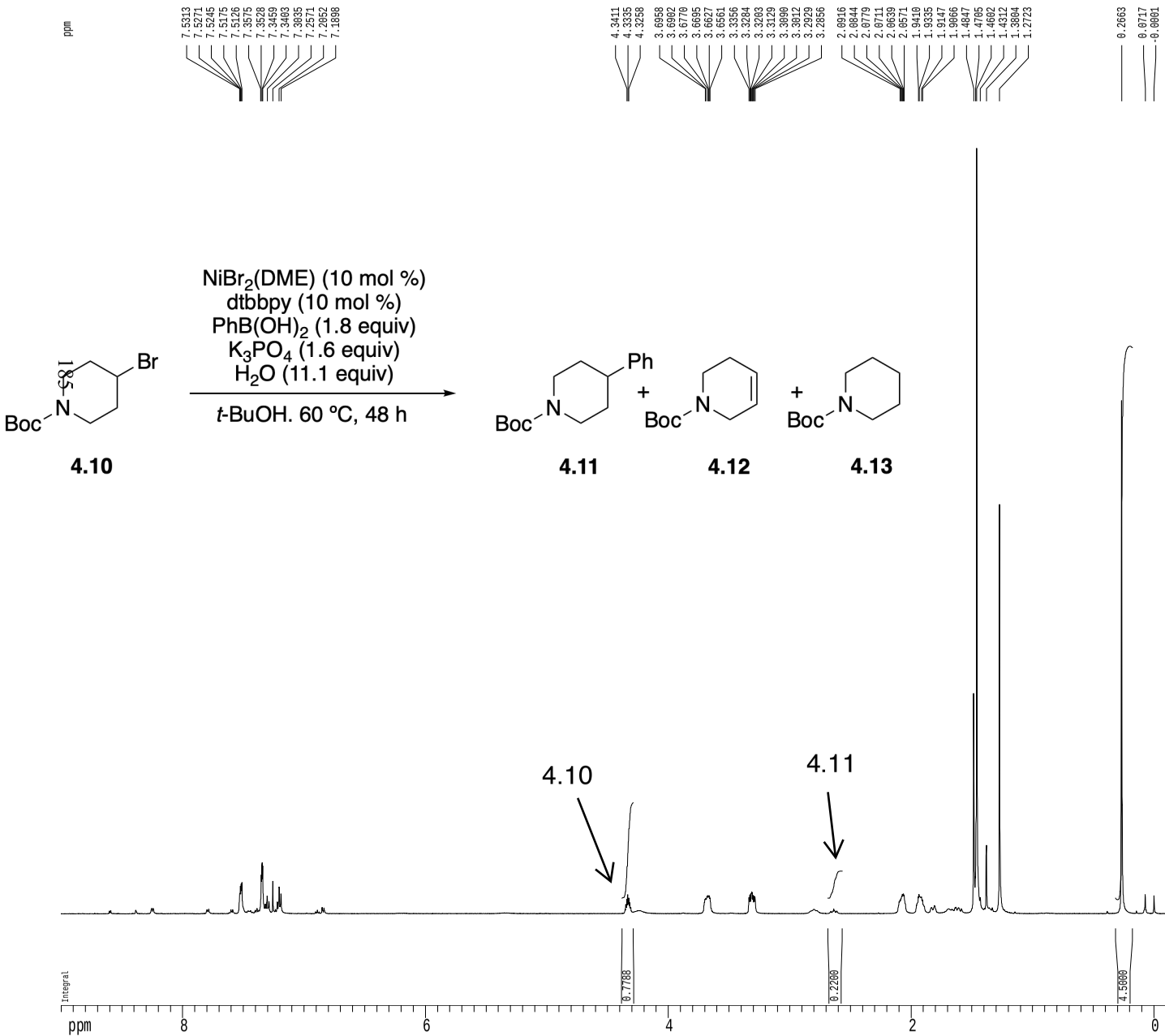
F2 - Acquisition Parameters
Date_ 20210803
Time 8.59
INSTRUM av600
PROBHD 5 mm CPBBO BB-
PULPROG zgflqn30
TD 131072
SOLVENT CDCl3
NS 16
DS 2
SWH 178571.422 Hz
FIDRES 1.362392 Hz
AQ 0.3670516 sec
RG 575
DW 2.800 usec
DE 18.00 usec
TE 298.0 K
D1 3.00000000 sec
TD0 1

======== CHANNEL f1 ========
SFO1 564.6299196 MHz
NUC1 19F
P1 18.25 usec

F2 - Processing parameters
SI 131072
SF 564.6863882 MHz
WDW no
SSB 0
LB 0.00 Hz
GB 0
PC 1.00

1D NMR plot parameters
CX 22.80 cm
CY 15.00 cm
F1P -50.000 ppm
F1 -28234.32 Hz
F2P -200.000 ppm
F2 -112937.28 Hz
PPMCM 6.57895 ppm/cm
HZCM 3715.04224 Hz/cm

1H spectrum




```
Current Data Parameters
USER            caherber
NAME      CAH-IV-065-A-CRUDE
EXPNO                  1
PROCNO                 1

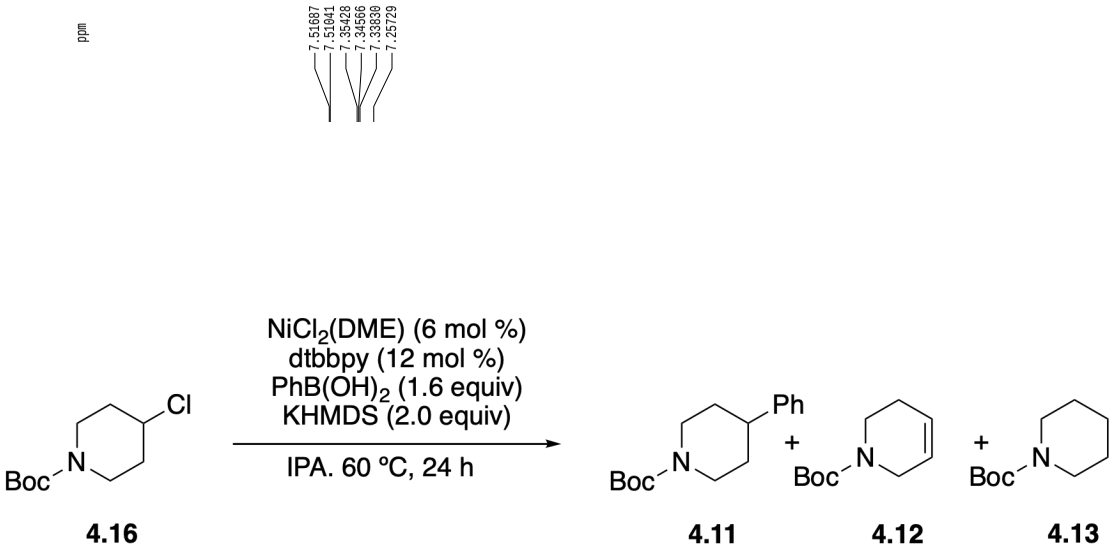
F2 - Acquisition Parameters
Date_           20240302
Time               15.14
INSTRUM            gn500
PROBHD   5 mm broadband
PULPROG             zg30
TD                 81728
SOLVENT            CDCl3
NS                     8
DS                     2
SWH             8012.820 Hz
FIDRES             0.098043 Hz
AQ              5.0998774 sec
RG                 143.7
DW                  62.400 usec
DE                   6.00 usec
TE                 298.0 K
D1              0.10000000 sec
MCREST          0.00000000 sec
MCWRK           0.01500000 sec

======== CHANNEL f1 ========
NUC1                   1H
P1                  12.00 usec
PL1                 -6.00 dB
SFO1          498.4534891 MHz

F2 - Processing parameters
SI                  65536
SF            498.4500317 MHz
WDW                    no
SSB                     0
LB                   0.00 Hz
GB                      0
PC                   1.00

1D NMR plot parameters
CX                  20.00 cm
CY                  12.50 cm
F1P                 9.000 ppm
F1                4486.05 Hz
F2P                -1.101 ppm
F2                -548.97 Hz
PPMCM              0.50507 ppm/cm
HZCM             251.75127 Hz/cm
```

1H spectrum




```
Current Data Parameters
USER            caherber
NAME      CAH-III-162-CRUDE
EXPNO                   1
PROCNO                  1

F2 - Acquisition Parameters
Date_          20230627
Time               8.29
INSTRUM          drx400
PROBHD   5 mm QNP H/F/P
PULPROG            zg30
TD                65536
SOLVENT           CDCl3
NS                    8
DS                    2
SWH            6410.256 Hz
FIDRES         0.097813 Hz
AQ             5.1118579 sec
RG                203.2
DW               78.000 usec
DE                4.50 usec
TE                298.1 K
D1            0.10000000 sec
MCREST        0.00000000 sec
MCWRK         0.01500000 sec

======== CHANNEL f1 ========
NUC1                 1H
P1                12.00 usec
PL1               -1.10 dB
SFO1         400.1328009 MHz

F2 - Processing parameters
SI                65536
SF          400.1300225 MHz
WDW                  no
SSB                   0
LB                 0.00 Hz
GB                    0
PC                 2.00

1D NMR plot parameters
CX                22.80 cm
CY                15.00 cm
F1P                9.000 ppm
F1              3601.17 Hz
F2P              -1.067 ppm
F2              -426.76 Hz
PPMCM           0.44152 ppm/cm
HZCM          176.66344 Hz/cm
```